COMSAT

Technical Review

Volume 20 Number 1, Spring 1990

COMSAT TECHNICAL REVIEW is published twice a year by the Communications Satellite Corporation (COMSAT). Subscriptions, which include the two issues published within a calendar year, are: one year, $20 U.S.; two years, $35; three years, $50; single copies, $12; article reprints, $3. Overseas airmail delivery is available at an additional cost of $18 per year. Make checks payable to COMSAT and address to Records Department, Communications Satellite Corporation, 22300 Comsat Drive, Clarksburg, MD 20871-9475, U.S.A.

ISSN 0095-9669

COMSAT TECHNICAL REVIEW

Volume 20 Number 1, Spring 1990

Effect of argon plasma cleaning on GaAs FET passivation

E. Y. CHANG, F. R. PHELLEPS, T. SMITH, P. LAUX, H. E. CARLSON, R. J. PORTER, T. C HO, AND K. PANDE

(Manuscript received December 11, 1989)

Abstract

Monolithic microwave integrated circuit (MMIC) chips are typically passivated with a dielectric film to improve their long-term environmental reliability. Improper passivation generally degrades chip performance, reducing wafer yield. Surface preparation of the field-effect transistor (FET) channel prior to dielectric passivation requires good control to reduce the native oxide and thus maintain the initial device performance. This paper describes a plasma process to etch the native oxide, coupled with silicon nitride passivation. Before nitride passivation, pulsed current/voltage measurement was used to study the effect of this etching process. It was found that argon plasma etching prior to passivation affects the channel surface differently, depending on the structure of the GaAs FET. For example, argon plasma etching using self-induced bias voltage in the plasma-enhanced chemical vapor deposition (PECVD) system is beneficial for GaAs metal-semiconductor FETs (MESFETs) that have a recess width approximately equal to the gate length. However, for delta-doped GaAs FETs with unrecessed gates, use of the plasma process before nitride passivation is likely to generate surface states and degrade FET performance.

Introduction

The passivation of GaAs field-effect transistors (FETs) and monolithic microwave integrated circuits (MMICs) using dielectric films, with varying degrees of success, has been reported in the past few years [1]–[5]. The preferred dielectric for passivation is silicon nitride, because devices passivated with this dielectric display significantly improved resistance to long-term burnout [4]. However, to maintain device performance after passivation, it is essential to control the interface states between the silicon nitride and the GaAs. For example, poor-quality passivation can degrade the breakdown voltage of power FETs and lead to a burnout problem, which has been attributed to the chemical instability of the GaAs native oxides [5].

This paper evaluates an *in situ* argon plasma etching process for removing the native oxide from the FET channel surface to control the interface prior to silicon nitride passivation. This technique was successfully applied to flat-profile power metal-semiconductor FET (MESFET) passivation, yielding FETs with excellent RF performance and device reliability. However, for delta-doped FETs with an unrecessed gate, use of the plasma process before nitride passivation was found to generate surface states and degrade FET performance. Thus it was determined that the usefulness of the plasma process during passivation depends on the device structure.

Experimental procedures

Device fabrication

Two types of device structures, one with a flat doping profile (regular MESFET) and the other delta-doped, were used for this study. Standard processing available at COMSAT Laboratories was used to fabricate both types of devices. The layers for the flat-doped MESFET were grown by vapor phase epitaxy (VPE), while molecular beam epitaxy (MBE) was used to grow the layers for the delta-doped FETs. Mesa etch was used for device isolation. The ohmic contacts to the device structure were formed by alloying Au/Ge/Ni/Ag/Au in a rapid thermal annealing system at 450°C. The COMSAT direct-write electron-beam (e-beam) lithography system was used to define the submicrometer gates, which were recessed using citric acid prior to Ti/Pt/Au metalization. The gate length of the MESFETs used in this study was 0.7 µm.

Passivation process

Two distinct processes were used to passivate the two types of MESFETs. In the first process, the surface of the GaAs wafer was cleaned in a dilute etch mixture containing sulfuric acid, and the wafer was immediately loaded onto the grounded electrode of the plasma-enhanced chemical vapor deposition (PECVD) system. The wafer was then etched lightly in argon plasma using self-

induced bias voltage in the PECVD system. The parameters for the argon plasma etch were as follows:

- Pressure: 600 mTorr
- Argon Flow: 1,000 sccm
- Temperature: 250°C
- Time: 30 s

In the second process, the GaAs channel surface was etched in the sulfuric acid mixture and immediately loaded onto the grounded electrode; however, the sample was not subjected to argon plasma etch.

In both cases, the nitride film was deposited at 250°C in the PECVD system. The reactant gases were ammonia and silane, with nitrogen as the carrier gas. The deposition conditions were as follows:

- Gas Flow Rate
  - Ammonia: 3.8 sccm
  - Nitrogen: 800 sccm
  - Silane: 10 sccm
- Power: 25 W
- Pressure: 600 mTorr

This nitride film exhibited stress of 10^9 dyne/cm^2 (tensile stress) as measured by a stress gauge; a refractive index of 2.0 as measured by an ellipsometer; and a silicon-nitrogen ratio of 0.75 as obtained by Auger analysis.

Current transient measurement

Current transient measurement was used to evaluate the passivation characteristics of the FETs. In this technique, the drain current transient measurement samples and records the drain current (I_{ds}) of a FET at various times following an abrupt change in gate voltage (usually reverse-biased near pinchoff voltage, *e.g.*, at -4 to +1 V). The drain voltage is stepped in even increments from V_{ds} (drain-to-source voltage) minimum (usually $V_{ds} = 0$) to V_{ds} maximum ($>V_{ds}$ knee), and the I_{ds} is measured and recorded for each V_{ds} increment. These data are then plotted in the form of an I/V curve (I_{ds} *vs* V_{ds}), with pulsed time as a parameter. If a drain current transient exists, the plotted data will be a family of curves showing the time-dependence of I_{ds}. Otherwise, the curves will overlay each other, providing a single trace (showing no time-dependence of I_{ds}).

Since GaAs FET performance is quantitatively related to the drain current, a large transient in the drain current usually indicates that significant surface states have been generated as a result of the plasma passivation process. A small transient, as indicated by the drain current curves being superimposed on each other, usually indicates low interface states in the passivated channel, unless the "access length" (the length from the recessed wall to the gate) is small [6].

Experimental results and discussion

The I_{ds} transient measurement was used to evaluate the passivation process. This measurement is performed both before and after nitride passivation, and the difference in the transient amplitude* before and after passivation is used to determine whether the surface states created by the PECVD process will adversely affect large-signal performance. In these experiments, small changes in the process chemistry were found to affect the amplitude of the transients. Before passivation, GaAs FETs usually show a certain amount of transient in the I_{ds} pulse measurement. The amplitude of this transient increases relative to the amount of time the FET channel surface is exposed to the air prior to passivation. This increase in I_{ds} transient amplitude before nitride passivation is believed to be due to oxidation of the GaAs surfaces.

Results on passivation for flat-profile MESFETs and delta-doped MESFETs are described below.

Flat-profile MESFET passivation

Flat-profile MESFETs have a recess width of 1.8 µm. Figure 1 shows a cross section of the recessed gate configuration. To examine the effect of argon plasma cleaning, a flat-profile MESFET wafer was cleaved into halves. One half was treated with a wet chemical etch before passivation. A typical I_{ds} transient measurement taken on this sample prior to nitride passivation is shown in Figure 2a. The MESFETs exhibited a transient amplitude of 0.8 ± 0.3 mA (the average of four measurements) in this piece. The sample was then etched in a sulfuric-acid-based solution and passivated with silicon nitride film. Figure 2b shows the I_{ds} measurement of the same FET as in Figure 2a, after nitride passivation. The transient amplitude increases after passivation (4.2 ± 0.1 mA for four measurements on the same devices). The difference between I_{dss} at $t = 0$ and $t \rightarrow \infty$ is about 3.4 mA in this case.

* Defined as the difference in saturation current curves between time $t = 0$ and $t = \infty$.

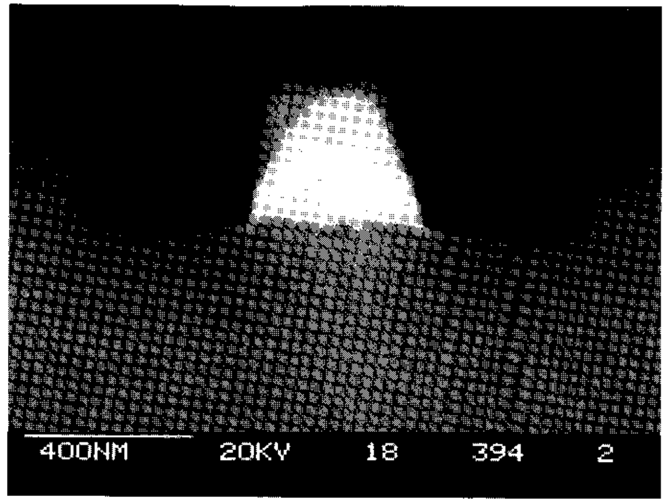

Figure 1. *SEM Micrograph of a Cross Section of the Flat-Profile MESFET*

The other half of the wafer was passivated using both a wet chemical etch and a plasma etching process. Figure 3a shows the I_{ds} pulse measurement for the MESFET that was plasma etched before nitride passivation. A typical MESFET in this case shows a transient amplitude of about 0.8 ± 0.3 mA (four measurements) before nitride passivation. The same FET then is etched in a sulfuric-acid-based solution, loaded into the chamber, etched with argon plasma using a self-induced bias voltage in the PECVD system, and finally passivated with silicon nitride film. Figure 3b shows the transient measurement of this device after passivation. The amplitude of the transient in the I_{ds} measurement decreased (0.2 ± 0.1 mA for four measurements on the same devices) after nitride passivation as a result of the plasma etching. This indicates that both the plasma etching and PECVD processes did not induce significant surface states or damage to the device.

To compare the surface composition differences between the plasma etching and non-plasma etching processes, samples of passivated devices from each process were subjected to SIMS analysis. A comparison of the interface regions of the two samples reveals that the oxygen peak at the interface of the plasma etched sample is a factor of 4 lower than that of the chemically etched sample, while the oxygen level in the bulk of the films is nearly the same. Figure 4 shows the surface oxygen composition for plasma etched and wet chemically etched surfaces as observed by SIMS. For a plasma etched surface,

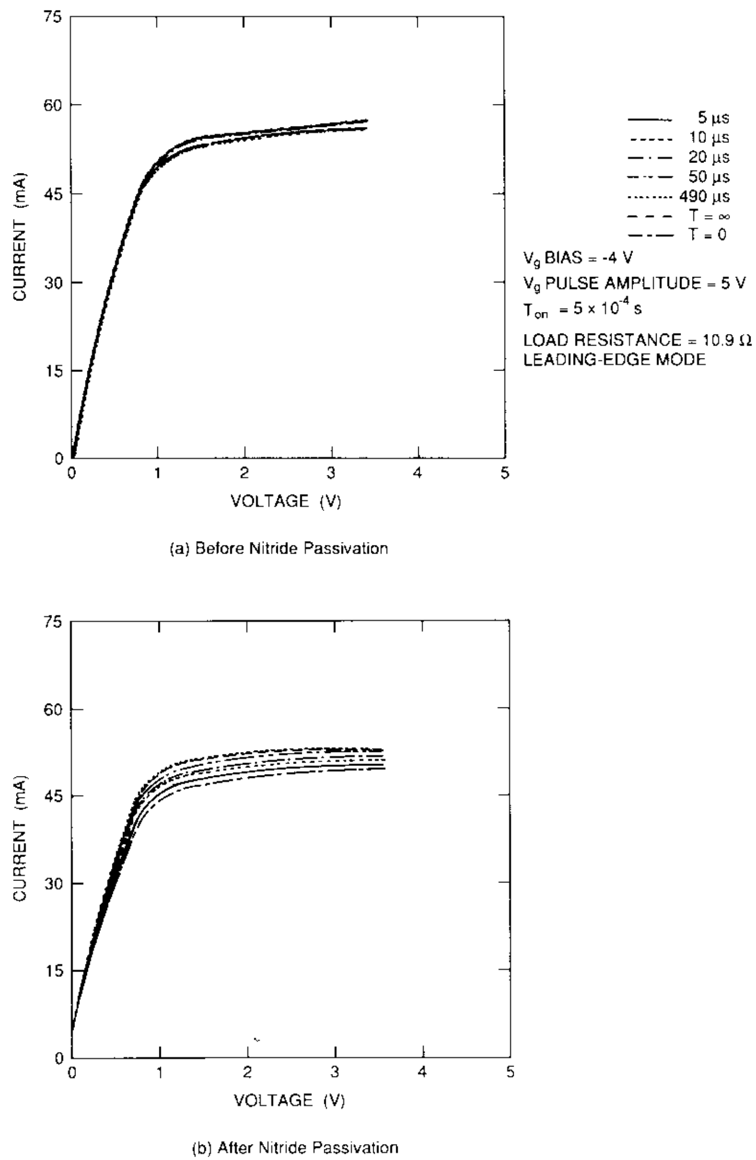

Figure 2. *I_{ds} Transient Measurement Data for the Wet Chemically Etched Flat-Profile MESFET*

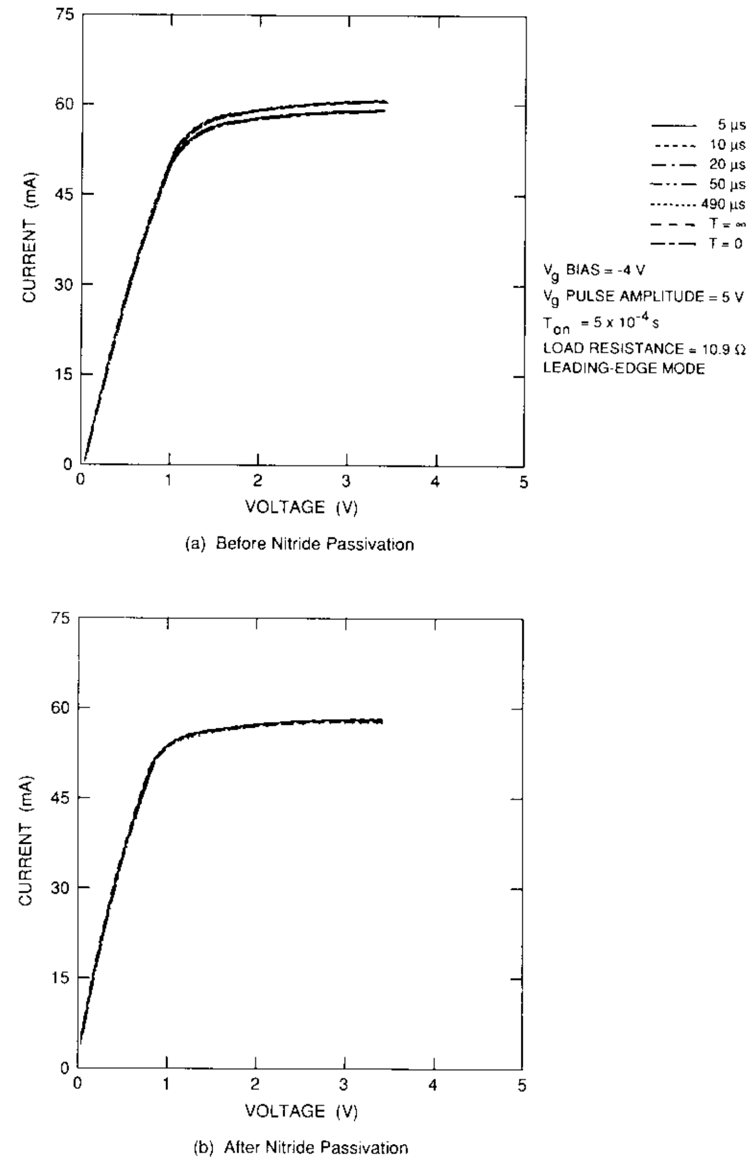

Figure 3. *I_{ds} Transient Measurement Data for the Plasma Etched Flat-Profile MESFET*

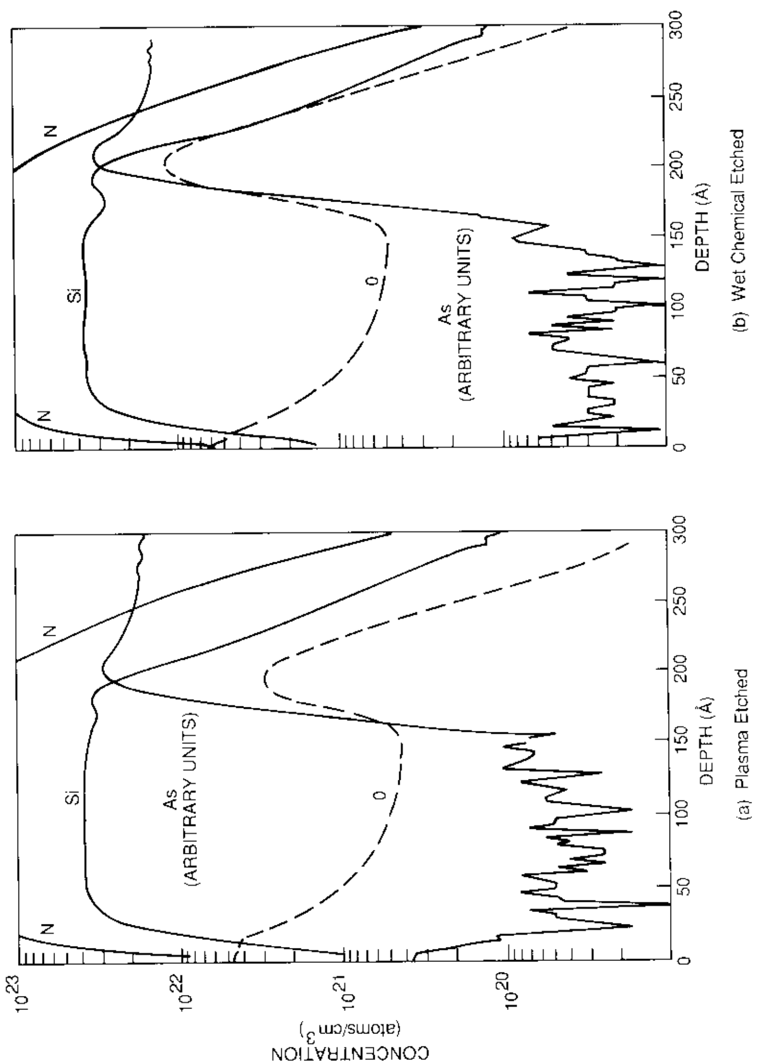

Figure 4. *SIMS Spectrum of the Etched Surfaces*

the oxygen concentration is around 2 x 10^{21} atom/cm^3 at the interface region (where the arsenic concentration begins to increase). For a wet chemically etched surface, the oxygen concentration is around 10^{22} atom/cm^3 at the interface region. The light argon plasma etch reduces the surface oxide thickness and results in less transient in I_{ds} measurement, as shown in Figure 3.

Table 1 compares the electrical parameters before and after nitride passivation for both argon plasma etched and wet chemically etched channels in MESFETs. The changes in drain-to-source saturation current, I_{dss}, transconductance, G_m, and pinchoff voltage, V_p, before and after nitride passivation are within 5 percent of each other. For plasma etched MESFETs, the shift in the breakdown voltage before and after nitride passivation is 0.8 V. For wet chemically etched MESFETs in the same wafer, the shift is around 1.5 V. Evidence of surface oxides reducing the breakdown voltage of GaAs devices has been reported previously [1]. The smaller voltage drop in the plasma etched MESFET is due to the removal of the surface oxides.

Table 1. Electrical Parameters Before and After Nitride Passivation for Flat-Profile MESFETs

FET PARAMETERS	V_p (V)	I_{dss} (mA/mm)	G_m (mS/mm)	V_{br} (V)
Argon Plasma Etch				
• Before Passivation	2.8 ± 0.3	199 ± 34	177 ± 15	15.0 ± 0.4
• After Passivation	2.6 ± 0.4	214 ± 28	184 ± 9	14.2 ± 0.7
Wet Chemical Etch				
• Before Passivation	2.6 ± 0.5	141 ± 46	158 ± 12	15.5 ± 0.2
• After Passivation	2.5 ± 0.3	145 ± 33	165 ± 33	14.0 ± 0.4

To test the reliability of the plasma etched wafer, the plasma etched sample was heated at 300°C for 72 hours. Figure 5 shows the I_{ds} transient measurement for the device shown in Figure 3a, following 72-hr heating. The amplitude of the current transient does not change. Table 2 gives the parameter shift after heating. As can be seen, the pinchoff and breakdown voltages remain the same after a heating cycle, while the I_{dss} and transconductance decrease (however, the change is within 5 percent). Meanwhile, for the wet chemically etched sample after the same thermal cycle, the parameter shifts are a little higher (around 10 percent) and there is a larger I_{ds} transient amplitude change, indicating that the surface chemistry of the sample has changed due to thermal stress.

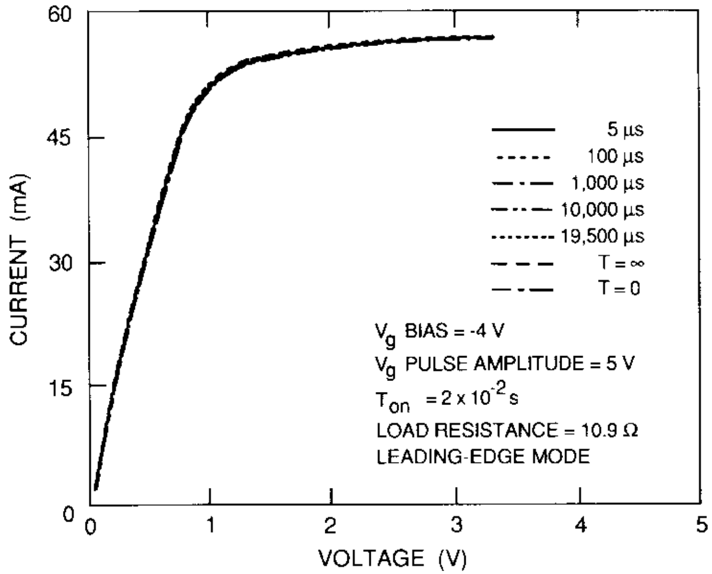

Figure 5. *I_{ds} Transient Measurement Data for the Plasma Etched Flat-Profile MESFET Sample of Figure 3 After 300°C, 72-hr Heating*

TABLE 2. ELECTRICAL PARAMETER SHIFT AFTER 300°C, 72-hr HEATING FOR PLASMA ETCHED MESFET

FET PARAMETERS	V_p (V)	I_{dss} (mA/mm)	G_m (mS/mm)	V_{br} (V)
After Passivation	2.6 ± 0.4	214 ± 28	184 ± 9	14.2 ± 0.7
After Heating (300°C, 72 hr)	2.6 ± 0.5	197 ± 33	179 ± 11	14.1 ± 0.7

MESFETs passivated using the plasma etching process have demonstrated excellent RF performance. In the MMIC chips, 0.25-µm MESFETs of 400-µm gate width, passivated using the plasma etching process, have demonstrated an output power of 21.6 dBm at the 1-dB compression point, and 5.8-dB small-signal gain at 32 GHz, as shown in Figure 6. This is state-of-the-art performance for a power FET.

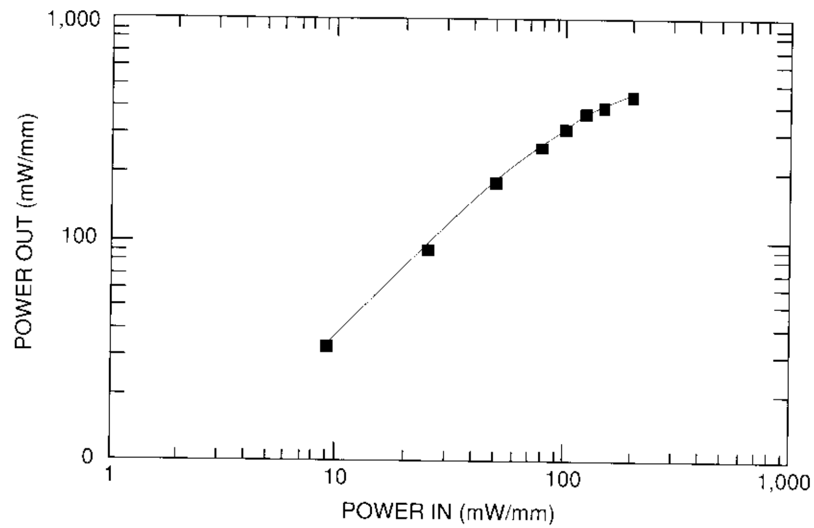

(a) 32-GHz Power Out vs Power In

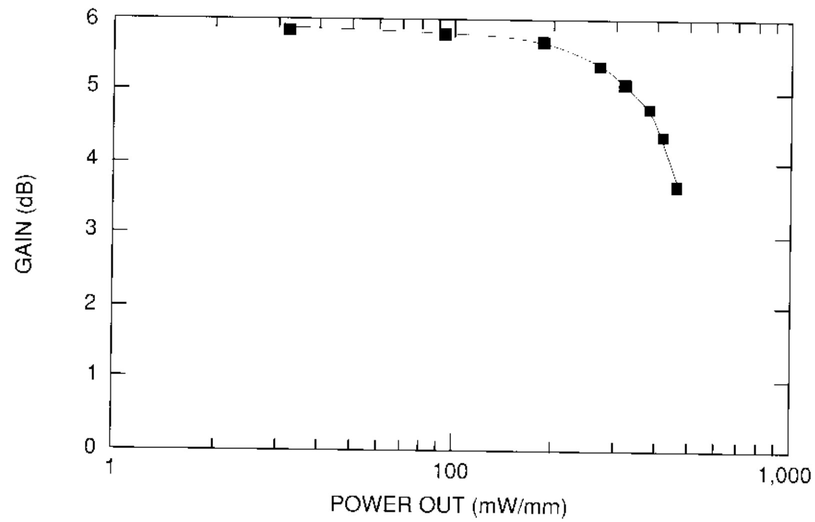

(b) 32-GHz Gain vs Output Power

Figure 6. *RF Performance of a 0.25 x 400-µm Flat-Profile MESFET*

Delta-doped MESFET passivation

The structure of the delta-doped FETs is shown in Figure 7. These MESFETs have a gate length of 0.7 µm and source-to-drain spacing of 3 µm. The gate region of these devices is not recessed.

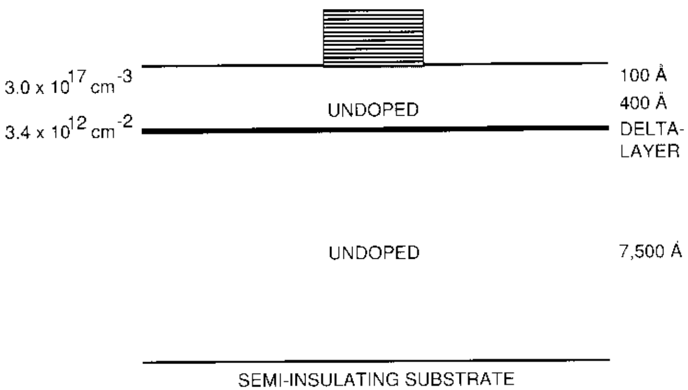

Figure 7. *Structure of the Delta-Doped FET*

To examine the effect of plasma etching, a delta-doped wafer was cleaved into halves. One half was passivated after plasma etching, and the other was passivated after wet chemical etching. Table 3 compares the DC parameters of the two pieces. Before passivation, the two halves exhibit similar DC characteristics; however, after passivation, the wet chemically etched sample demonstrates both higher breakdown voltage and higher transconductance.

TABLE 3. ELECTRICAL PARAMETERS BEFORE AND AFTER NITRIDE PASSIVATION FOR DELTA-DOPED MESFETs

FET PARAMETERS	V_p (V)	I_{dss} (mA/mm)	G_m (mS/mm)	V_{br} (V)
Plasma Etch	1.4 ± 0.2	214 ± 14	134 ± 14	16 ± 1
Wet Chemical Etch	1.2 ± 0.1	242 ± 16	145 ± 10	19 ± 1

Figures 8 and 9 compare the I-V characteristics and breakdown voltage before and after passivation for plasma etched and wet chemically etched delta-doped MESFETs. The plasma etched device (Figure 8) shows a kink in the breakdown voltage curve after passivation, which is not seen in the wet chemically etched MESFET (Figure 9). It appears that the plasma etching

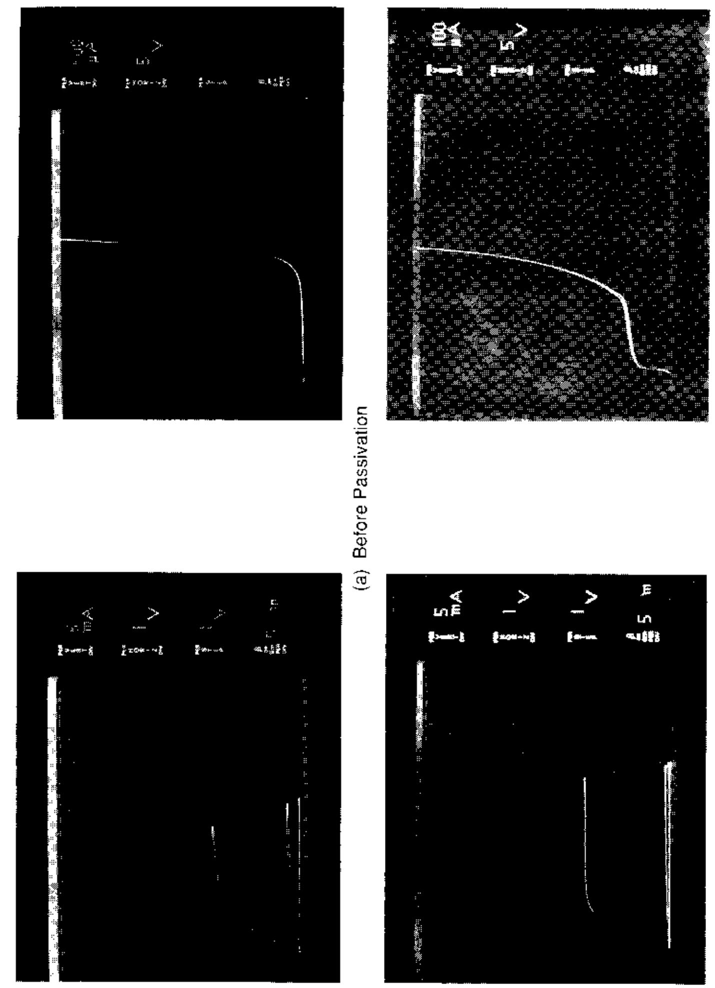

(a) Before Passivation

(b) After Passivation

Figure 8. *I-V Characteristics and Breakdown Voltage for the Plasma Etched Delta-Doped MESFET*

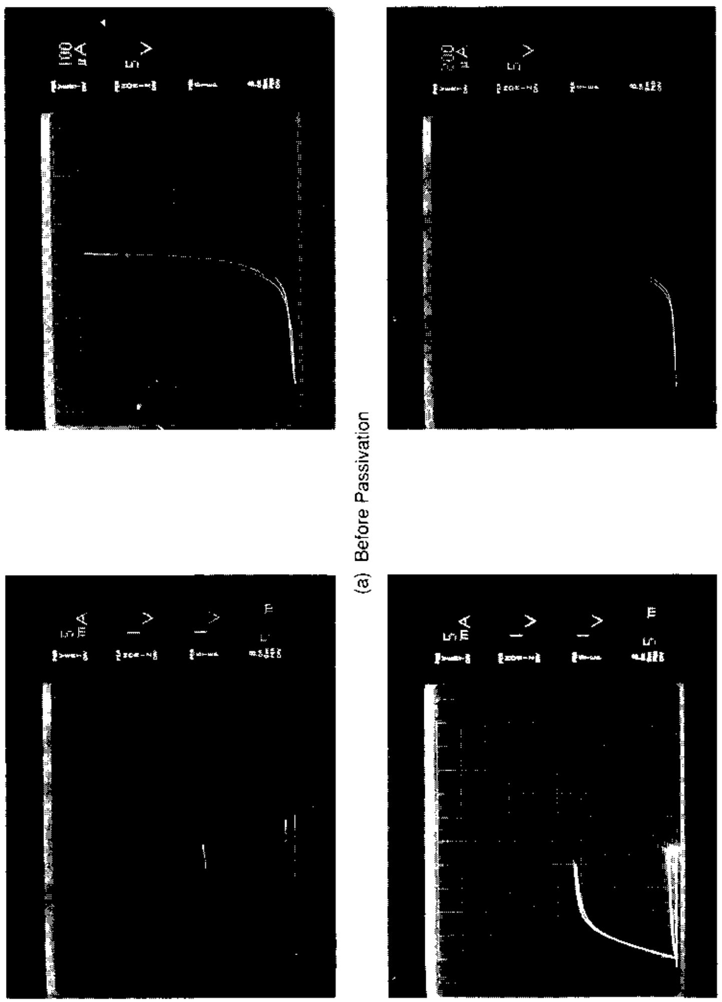

(a) Before Passivation

(b) After Passivation

Figure 9. *I-V Characteristics and Breakdown Voltage for the Wet Chemically Etched Delta-Doped MESFET*

process generates surface states, which induce leakage current through the surface region.

The increase in surface states due to the plasma etching process is supported by data from I_{ds} transient measurement. Figure 10 shows a comparison of the I_{ds} current transient measurements for the two etching processes. For the wet chemical etching process (Figure 10a), the amplitude of the I_{ds} transient is quite small, indicating that very few surface states are generated during the passivation process. However, for the plasma etching process (Figure 10b), the amplitude of the I_{ds} transient is large, indicating that much damage has been done to the surface region of the delta-doped FET. Since the area of the channel region may determine the total number of the surface states, there are likely to be more surface states for the unrecessed sample with wider channel area than for the recessed flat-profile sample.

Conclusions

It has been demonstrated that channel surface treatment prior to passivation is critical to achieving stable device passivation. Depending on the device structure selected and the geometry of the gate region, it is possible to use a light argon plasma to etch the GaAs native oxide prior to silicon nitride passivation. In a flat-profile MESFET with narrow recess width, this process results in devices with improved RF performance and excellent reliability under thermal stress. However, this dry etching process must be applied with care; otherwise, depending on the structure and geometry of the FET, it could have a detrimental effect on device performance, as was found to be the case with unrecessed delta-doped MESFETs.

Acknowledgments

The authors would like to thank H. Huang for his encouragement and support, and D. Mullinex for RF measurements. Thanks are also due to D. Wilcox for SEM and to E. Sparks for SIMS analysis.

References

[1] E. Y. Chang, G. T. Cibuzar, and K. P. Pande, "Passivation of GaAs FETs With PECVD Silicon Nitride Films of Different Stress States," *IEEE Transactions on Electron Devices*, Vol. 35, No. 9, September 1988, pp. 1412–1419.

[2] E. Y. Chang, G. T. Cibuzar, J. M. Vanhole, R. M. Nagarajan, and K. P. Pande, "GaAs Passivation Using Sputtered Silicon Nitride," *Applied Physics Letters*, Vol. 53, No. 17, October 1988, pp. 1638–1640.

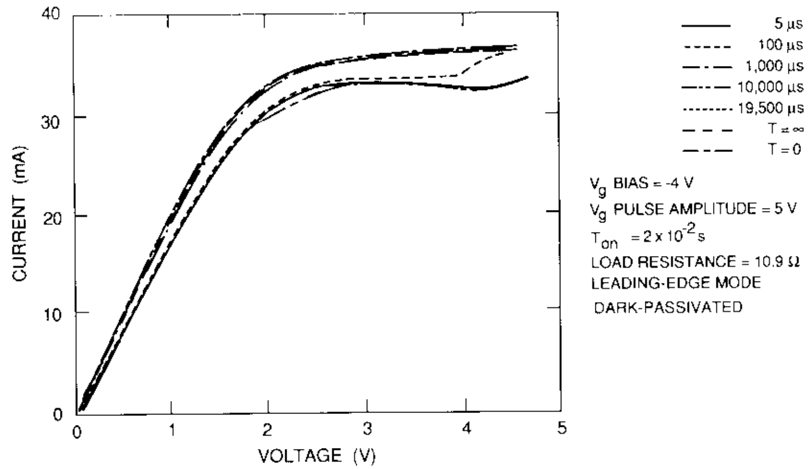

(a) Wet Chemical Etched

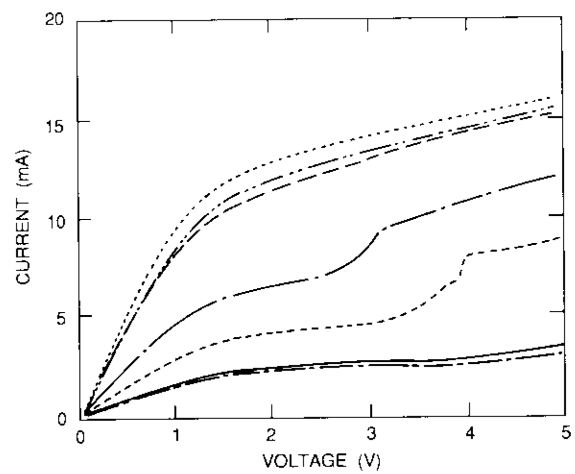

(b) Plasma Etched

Figure 10. *I_{ds} Transient Measurement Data for the Delta-Doped MESFET*

[3] R. L. Van Tuyl, V. Kumar, D. C. D'Avanzo, T. W. Taylor, V. E. Peterson, D. P. Hornbuckle, R. A. Fisher, and D. B. Estreich, "A Manufacturing Process for Analog and Digital Gallium Arsenide Integrated Circuits," *IEEE Transactions on Electron Devices*, Vol. ED-29, No. 7, July 1982, pp. 1031–1038.

[4] J. G. Tenedorio and P. A. Terizian, "Effects of Si_3N_4, SiO, and Polyimide Surface Passivations on GaAs MESFET Amplifier RF Stability," *IEEE Electron Device Letters*, Vol. EDL-5, No. 6, June 1984, pp. 199–202.

[5] S. H. Wemple, W. C. Niehouse, H. Fukui, J. C. Irving, H. M. Cox, J. C. M. Huang, J. V. Delorenzo, and W. O. Schlosser, "Long Term and Instantaneous Burnout in GaAs Power FET's: Mechanism and Solutions," *IEEE Transactions on Electron Devices*, Vol. ED-28, No. 7, July 1981, pp. 834–840.

[6] S. R. Blight, R. H. Wallin, and H. Thomas, "Surface Influence on Conductance DLTS Spectra of GaAs MESFETs," *IEEE Transactions on Electron Devices*, Vol. ED-33, No. 10, October 1986, pp. 1447–1453.

Edward Y. Chang received a B.S. in materials science from the National Tsing-Hua University, Taiwan, in 1977, and a Ph.D. in materials science from the University of Minnesota in 1985. He is currently working in the Microelectronics Division at COMSAT Laboratories, where his activities focus on high-performance GaAs MMIC devices, as well as process research and development. Prior to joining COMSAT, he worked for the GaAs Research Group at Unisys Corporation, Eagan, Minnesota, from 1985 to 1988. Dr. Chang is a member of the IEEE Electron Device Society and the Components, Hybrids, and Manufacturing Technology Society.

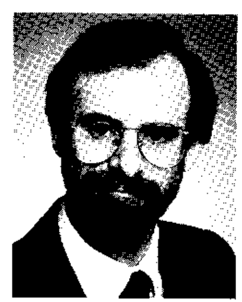

Fred R. Phelleps received a B.S. in physics from Bethany College in 1979, and an M.S.E.E. from George Washington University in 1985. He joined COMSAT Laboratories in 1980 and is Associate Manager of the MMIC Production Department. He has made major contributions in the areas of reactive sputtering, plasma-enhanced chemical vapor deposition, dry-etch processing, and deep-ultraviolet optical resist technology. He is a member of IEEE and the American Vacuum Society.

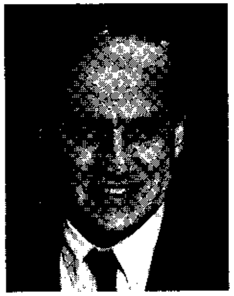

Thane Smith received a B.S. in physics from the Massachusetts Institute of Technology in 1962, and an M.S. and Ph.D. from Carnegie-Mellon University in 1964 and 1968, respectively. He joined COMSAT Laboratories in 1975 and is currently Senior Scientist in the Microelectronics Division. His responsibilities include the design and modeling of GaAs FETs, varactors, and other devices for both internally and externally funded programs. As the first Manager of MMIC Fabrication at COMSAT, he guided the initial development of MMIC capabilities. He has also been involved in research and development of novel GaAs devices (AMP and SAMP) and epitaxial growth of GaAs. Dr. Smith is a member of Sigma Xi and a Senior Member of IEEE. He has coauthored many technical papers, presentations, and reports. He shares with P. L. Fleming the patent for the SAMP device. His concept for optical wafer probing has lead to a patent application with H. Huang and C. Lee.

Paul E. Laux received a B.S. in ceramic engineering from the University of Illinois in 1988. While at Illinois, he worked for the University Microelectronics Group. He joined COMSAT Laboratories in 1988 as a Thin-Films Process Technician in the Microelectronics Division, and is currently working in the Advanced Device Research Group. He is also pursuing his M.S. in electrical engineering at the Johns Hopkins University.

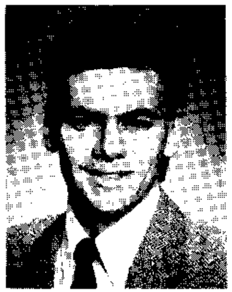

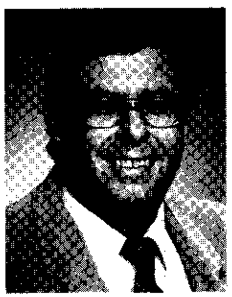

Henry E. Carlson joined COMSAT Laboratories in 1968 and participated in the Beacon and ATS-F programs as a member of the Reliability and Quality Assurance Department. He received a B.S. in electrical engineering from the Johns Hopkins University in 1976. He is currently a Senior Member of the Technical Staff in the Microelectronics Evaluation and Assembly Department and is responsible for on-wafer DC/RF testing, product reliability assessment, and statistical process control database management. Mr. Carlson is a member of Tau Beta Pi and Eta Kappa Nu.

Richard J. Porter joined COMSAT Laboratories in 1969 and participated in the Beacon and ATS-F programs as a member of the Reliability and Quality Assurance Department. He received a diploma in electronic technology from Maryland Technical Institute, and in general education from Catonsville Community College. He is currently an Associate Staff Member in the Microelectronics Materials Department, where he is responsible for materials and device DC and RF testing and evaluation. Mr. Porter has authored internal papers on semiconductor characterization and computer-controlled data acquisition systems.

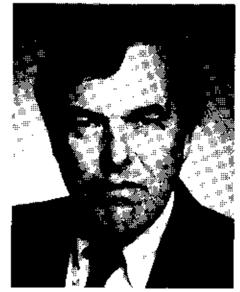

Thomas C. Ho received a B.S.E.E. from Chung Cheng Institute of Technology, Taiwan, in 1970; an M.S.E.E. from the University of California, Los Angeles, in 1975; and a Ph.D. from Cornell University in 1984. He is currently Manager of the MMIC Evaluation and Assembly Department in the Microelectronics Division at COMSAT Laboratories, where he is involved in the research and development of monolithic components and subsystems. His responsibilities include the design, module integration, and testing of high-reliability microwave and millimeter-wave hardware. Prior to joining COMSAT in 1988, he was with Chung Shan Institute of Science and Technology, Taiwan. Dr. Ho is a Senior Member of IEEE and of the Chinese Institute of Electrical Engineering. He is also a member of Eta Kappa Nu and Tau Beta Pi.

Krishna Pande received a Ph.D. in solid-state physics from the Indian Institute of Technology in 1973. He is currently Associate Executive Director at COMSAT Laboratories, where he is managing a divisional effort to develop and produce gallium arsenide MMICs and related subsystems. He is also involved with the marketing of MMIC and subsystem technology to DoD agencies and aerospace systems companies. He has been a Program Manager on a number of defense R&D contracts in these areas. Prior to joining COMSAT, Dr. Pande was Director at Unisys Semiconductor Operations in St. Paul, Minnesota, and Research Manager at Bendix Aerospace Technology Center in Columbia, Maryland. He also

provided consulting services to the Air Force Wright Avionics Laboratory in the area of gallium arsenide device passivation.

Dr. Pande has authored more than 60 research papers and has secured two patents. He has won special recognition and inventors awards from Allied-Signal Corporation, and the Outstanding Contributions Award from Sperry (now Unisys) Semiconductor Operations. He is a Fellow of IEEE and a member of the American Physical Society, the New York Academy of Sciences, and the Electromagnetic Academy.

Index: satellite communication, intersatellite links, digital transmission, data transmission, multiplexing

RF/optical interface design for optical intersatellite links

R. K. GARLOW AND S. J. CAMPANELLA

(Manuscript received July 5, 1990)

Abstract

Future data acquisition satellites will be required to multiplex a number of independent data streams of widely varying rates, and exhibiting Doppler variations between low and geosynchronous altitude satellites, into a single, continuous, high-rate data stream. Forward links in these systems will contain commands, and return links will handle data from low earth orbit satellites. This study addresses the flexibility of these links in handling varying missions and data rates to 1 Gbit/s, with a focus on requirements for the NASA Tracking and Data Acquisition System.

Five system components are described: the return link multiplexer, the return link transmultiplexer, the forward link multiplexer, the forward link demultiplexer, and operation of a frontside/backside switch. Ping-pong buffers provide rate buffering for each input data stream, and justification bits handle variations due to Doppler shift and local oscillator variation. The time-division multiplexed streams consist of a unique synchronization word for frame synchronization, and control words associated with each data burst to identify the presence or absence of a justification bit. Redundant data paths are described for both forward and return data streams.

Introduction

Throughout its history, NASA has depended on a network of ground stations for telemetry, tracking, and command (TT&C) support of earth-orbiting satellites. While continuous contact is possible at synchronous altitude, direct communication between an earth station and low-orbit satellites is generally limited to a few minutes up to a 20-minute period. Gaps in coverage of several hours may occur. Even with the extensive NASA earth station network, contact with an earth station is typically possible only about 15 percent of the time. On-board recording equipment is often required to store data during the gaps for later playback during an earth station contact. Due to the short contact time, these data must frequently be played back at a high rate, which further limits the amount of data that can be acquired by the satellite.

Satellites such as NASA's Tracking and Data Relay Satellite (TDRS) provide communications links between a single earth station and one or more low earth orbit (LEO) satellites. Their use has greatly improved worldwide connectivity between LEO satellites and the earth over what was previously possible with worldwide networks of earth stations alone. Two TDRSs in synchronous earth orbit provide forward and return links between LEO satellites and the earth station, increasing the direct contact time to 85 percent. The earth stations and LEO satellites both communicate with the data relay satellites. Figure 1a depicts communications with two TDRSs. Continuous communications are possible except for the period when a low-orbiting spacecraft is in a region where neither relay satellite is visible. This is shown as the zone of exclusion (ZOE).

The NASA Tracking and Data Acquisition System (TDAS) program was created to study future replacements for the TDRSs. The program added an intersatellite link (ISL) between the data relay satellites so that two of these satellites at proper orbital positions provide nearly continuous contact between the low-orbit satellites through a single earth station located at White Sands, New Mexico. Figure 1b illustrates communications for the TDAS. The ZOE for this system is considerably smaller, and earth stations can be located over a much larger area.

This paper discusses systems and implementational aspects of the digital RF/optical interface design, as well as multiplexing requirements for an optical ISL between the two relay satellites. Included is part of a report submitted to NASA for the proposed TDAS program [1]. The first part of the COMSAT Laboratories' study covers optical communications aspects. Marshalek [2] and Paul [3] have reported results on portions of the optical link design. Herein is addressed work on multiplexing and system engineering. The rates used in this design were specified by NASA; however, the techniques described here can be applied to other systems and missions as well. The interfaces in the data relay satellites that support digital communications with the LEO satellites and the earth stations are also described.

Communications between LEO satellites, data relay GEO (geosynchronous earth orbit) satellites, and an earth station are illustrated in Figure 1b. Two relay satellites are located in the geosynchronous equatorial plane orbit with a separation of 160°. One of these satellites, the "frontside" satellite, is visible from White Sands and has continuous communications with one or more earth

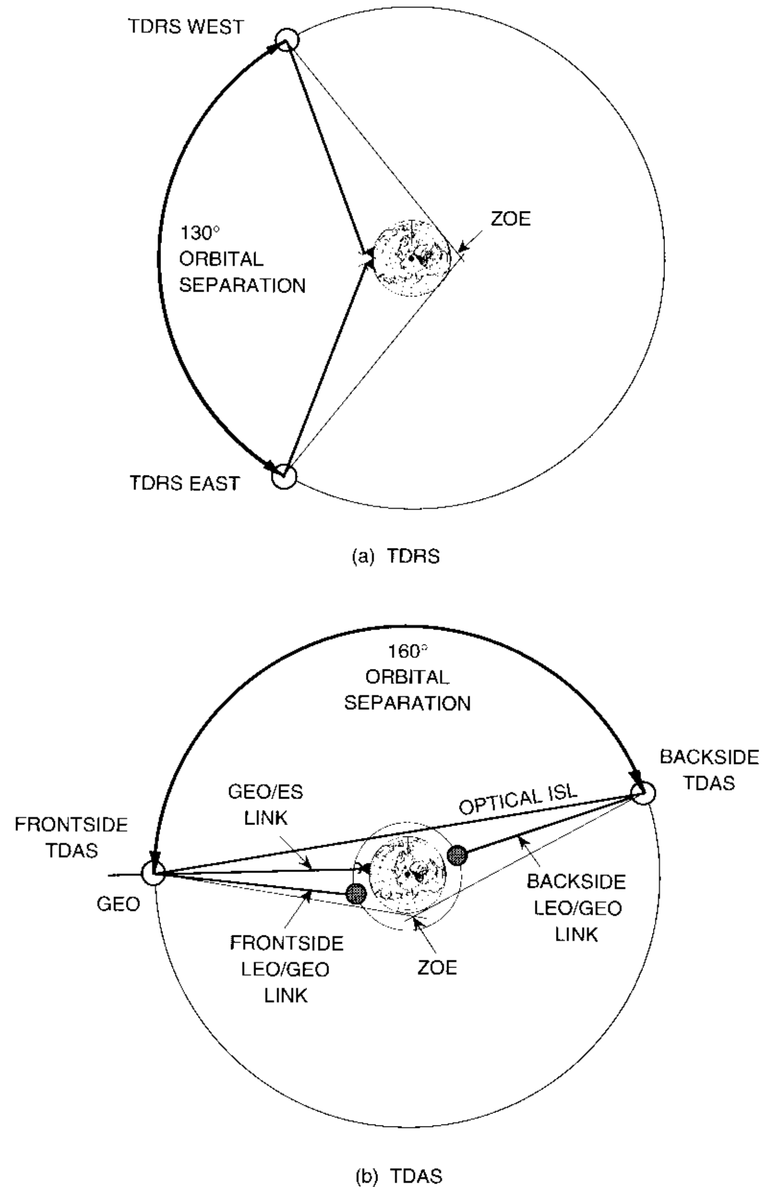

Figure 1. *Orbital Positions for TDRS and TDAS*

stations. An ISL provides continuous communications between the frontside and "backside" relay satellites. When the frontside relay satellite is visible from the LEO satellite, both the forward and return links between the earth station and the LEO satellite can function through the the frontside satellite. However, when only the backside relay satellite is visible from the LEO satellite, the forward and return links must be routed over the ISL. This combination permits nearly continuous communications between the earth station and the LEO satellite.

The channels and linkages supported by the system are illustrated in Figure 2. The table shown in the figure lists the forward and return channel types used for this study, the number of each type, and the symbol rate (high and low limits) per channel. The actual operating rate for a channel can be any value between the high and low limits. Each channel is given a three-letter name. The first letter indicates the frequency used between a LEO satellite and a TDAS satellite: L is a laser link, K and S are microwave frequencies, and W is undefined. The second and third letters indicate the access mode: SA is single access, while MA is multiple access. Each channel is demodulated to a baseband digital signal at the relay satellite. The cumulative rate in each direction is tallied in the bottom row. The maximum forward composite rate totals 103.63 Mbit/s, and the return rate totals 2,524.51 Mbit/s. Several LEO satellites can be served by this arrangement. It is unlikely that the maximum rates on all channels would combine simultaneously on the backside relay satellite; rather they would be distributed between the backside and frontside relay satellites. For this reason, the return intersatellite crosslink can be scaled to a lower number. For this study, the maximum capacity for the return crosslink is 2,000 Mbit/s, and the capacity for the forward link is 110 Mbit/s. The frontside satellite provides forward and return links for up to nine U.S. earth stations.

The principal objective of this study was to design the digital RF/optical interfaces needed on the frontside and backside relay satellites for switching and carrying the wide variety of digital channel rates to serve the needs of several orbiting LEO satellites. Another objective was to define a number of component building blocks that can be applied repetitively to the design. The communications techniques and design considerations for these building-block components are described, followed by a discussion of how they were used to design the major components for the return and forward links on the GEO relay satellites.

The design approach identifies a number of circuit elements that can be implemented using large-scale integration (LSI) or very large-scale integration (VLSI) techniques.

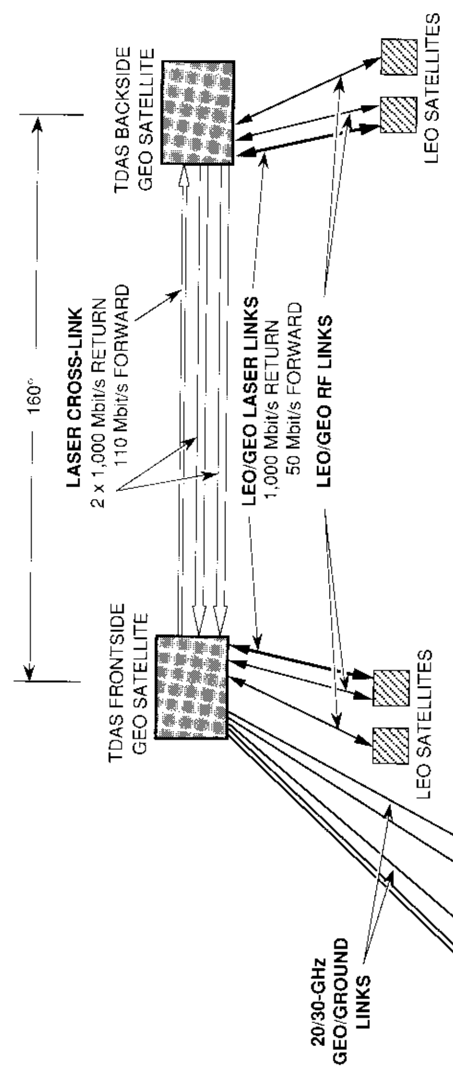

LEO Ch	Return			Forward		
	No.	Max Rate (MHz)	Min Rate (kHz)	No.	Max Rate (MHz)	Min Rate (kHz)
LSA	1	1,000	10,000	1	50	1,000
KSA	2	300	1	2	25	1
WSA	3	300	1	3	1	1
SSA	2	12	0.1	2	0.3	0.1
SMA	10	0.05	0.1	2	0.01	0.1
TT&C	1	0.01	10	1	0.01	10
Total	19	2,524.51	10,016.2	11	103.63	1,015.4

Figure 2. *TDAS Overview*

RF/optical digital interface design

The design of the RF/optical digital interface must take into consideration a number of factors. First, the fact that the links are between geostationary relay satellites and rapidly moving LEO satellites creates variations in the data rate on the links between the relay satellites and the LEO satellites which must be accommodated at the interface. The second factor concerns the impact of combining a number of streams from LEO satellites into a single high-rate stream in the relay satellite. The third consideration is the wide range of input rates necessary to accommodate the various channel rates, which must be changed as a function of LEO location and mission requirements. This requires a highly flexible time-division multiplexer (TDM) that can easily be reconfigured by ground command.

This section discusses the general techniques needed to address some of these design challenges. These include multiplexing sources with rate variations caused by Doppler motion, combining channels that have different rates, and the factors to be considered in selecting frame periods. Techniques for frame synchronization and the detection of smoothing bits are then described. The operation of buffers that can perform the required multiplexer and demultiplexer functions is also discussed. In later sections, the techniques described here will be used to develop specific multiplexer designs for the forward and return links.

Multiplexing data sources of varying Doppler effects

Transmissions arriving at a relay satellite from various LEO satellites are received on-board and multiplexed into a single high-rate data stream for transmission to the other relay satellite or to the earth. One requirement for an optical intersatellite data link is to multiplex a number of independent data streams (of widely differing rates and exhibiting Doppler variations typical of LEO/GEO paths) from arbitrarily located LEO platforms into a single, continuous, high-rate data stream. The maximum peak-to-peak rate variation caused by the effect of Doppler on the transmission from LEO to GEO satellites is $\pm 2.5 \times 10^{-5}$. A combination of data buffers and variable-rate TDMs provides the control and adjustment needed to handle these variations. These multiplexers permit the number of bits used per frame to be adjusted over a small number of justification bits in order to accommodate the rate variations of the individual channels when they are multiplexed on a constant-rate transmission path.

Multiplexing variable-rate data channels

A second problem is posed by the range of operating data rates for each LEO/GEO channel. Each of these channels is described by maximum and minimum rates. Since the sum of the individual streams at maximum rates is larger than the available TDAS backside-to-frontside intersatellite data links, the TDM burst time format should be programmable to accommodate changes in the operational modes for the LEO/GEO links. A technique to provide highly efficient operation at the maximum rates is considered first, followed by a simple modification for operation at the minimum rates.

Figure 3 illustrates the basic method for interpolating data channels from differing sources onto a common-rate channel. In a frame of duration, T_F, and containing N_F bits, the various channels to be accommodated are assigned a range of bits varying from a minimum, m_i, to a maximum, n_i, for the ith channel. The difference, D_i, between n_i and m_i must be selected to encompass the variations in channel data rate that result from the combined variations due to Doppler effect and source clock. D_i is typically referred to as the number of justification bits and is determined by the procedure given below.

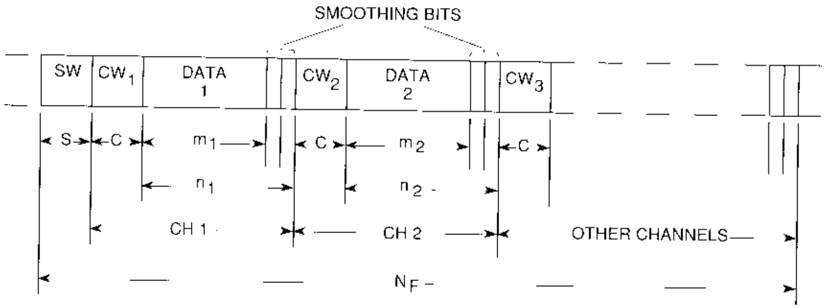

N_F = Frame period
m_i = Min bits used for channel i = $R_i T_F - 1$
n_i = Max bits used for channel i = $R_i T_F + 1$
Nominal rate for channel i = R_i
Max rate for channel i = $R_i + \frac{1}{T_F}$
Min rate for channel i = $R_i - \frac{1}{T_F}$
Number of bits per frame = $N_F = S + kC + \sum_{i=1}^{k} n_i$

Figure 3. *Optical Link Multiplex Frame*

If the Doppler rate variation coefficient is d_i and the channel's nominal data rate is R_i, then the data rate can vary over the range

$$R_i(1-d_i) < R_i < R_i(1+d_i) \quad (1)$$

and the number of bits per frame can vary over the range

$$m_i < T_F R_i(1-d_i) < T_F R_i < T_F R_i(1+d_i) < n_i \quad (2)$$

The variables m_i and n_i must be selected so that they bound the range needed to accommodate the Doppler coefficient, d_i. Hence, the value of D_i must be an integer (since there are no fractions of bits) that is greater than the peak-to-peak difference given by equation (2). Thus,

$$D_i = \lceil 2T_{Fmax} R_i d_i \rceil \quad (3)$$

where $\lceil \ldots \rceil$ indicates rounding up to the nearest integer. For the multiplexers recommended for TDAS, $D_i = 2$ has been selected, since it results in the simplest overall design.

As illustrated in Figure 3, the data channels from various sources are time-division multiplexed into a single stream. Each channel (identified by index i) is allocated a share of the frame capacity sufficient to accommodate a control word, CW_i, containing C bits to carry interpolation control information, and a group of data bits to carry the actual data transmitted. For channel i, the number of data bits actually used during each frame varies from a minimum, m_i, to a maximum, n_i (a range of $D_i = n_i - m_i = 2$ bits) to accommodate the rate variation; however, the maximum value (n_i) must always be provided. In a given frame, the actual number of bits used by the data must be signaled in CW_i to the receiving demultiplexer in order to eliminate the non-data bits. A frame synchronization word, SW, of length S is used to establish frame synchronization.

Frame period selection

For each channel rate, R_i, to be accommodated, there exists a maximum frame period, T_{Fmax}, determined by equation (3) and the number of justification bits per frame, D_i. The maximum frame length is the minimum of the values calculated for each channel. If a longer frame is used, bit justification corresponding to $D_i = 2$ will not cover the desired range of Doppler variation for all channels. However, shorter frames increase the Doppler variation range and reduce the size of the channel-forming buffers. The disadvantages of shortening the frame are reduced frame efficiency and increased symbol jitter in the recovered data stream. Thus, a tradeoff must be made between buffer size and frame efficiency, while maintaining low jitter in the recovered bit stream. At the high speeds used for the TDAS, it is clearly desirable that the buffer size be confined to a few hundred bits to stay within the expected bounds of GaAs technology.

For a given frame period, T_F, the range of transmission rates provided for channel i is

$$\frac{m_i}{T_F} \le R_i \le \frac{n_i}{T_F} \quad (4)$$

Corresponding to the choice of $D_i = 2$, the values of n_i and m_i necessary to accommodate a nominal rate of R_i are

$$n_i = R_i T_F + 1 \quad (5a)$$

$$m_i = R_i T_F - 1 \quad (5b)$$

and the maximum and minimum channel transmission rates are

$$R_i - \frac{1}{T_F} \le \text{Channel rate} \le R_i + \frac{1}{T_F} \quad (6)$$

For any value of T_F up to the maximum, the number of bits per frame is determined by equation (5a). This choice results in the use of three values for the number of data bits per channel. The number of bits carried in each frame is indicated by the control word, CW_i, as given in Table 1.

TABLE 1. MULTIPLEX FRAME PARAMETERS

DATA BURST LENGTH	NO. OF BITS	CONTROL WORD	RATE
Minimum	$R_i T_F - 1$	00	$R_i - \frac{1}{T_F}$
Nominal	$R_i T_F$	01	R_i
Maximum	$R_i T_F + 1$	11	$R_i + \frac{1}{T_F}$

Fraction of frames using other than nominal rate

By choosing T_F to be equal to or less than the minimum T_{Fmax}, all the channel rates will be appropriately accommodated. Thus, in operation, the instantaneous minimum and maximum rates (provided by deleting or adding 1 bit) will be more than sufficient to accommodate the variation encountered on the channel. Most of the time the nominal rate will be used, and occasionally the maximum rate (add 1 bit) will be used to accommodate the effect of up-Doppler, or the minimum rate (delete 1 bit) to accommodate the effect of down-Doppler. It will be demonstrated below that the fraction of frames using the maximum and minimum rates, rather than the nominal rate, for a frequency variation coefficient, d_i, is

$$e_i = d_i R_i T_F \tag{7}$$

and consequently only one in e_i^{-1} frames will use other than the nominal rate R_i (*i.e.*, will carry other than $R_i T_F$ bits per frame).

To demonstrate the development of the above expression, consider the following. Over a time interval sufficient to contain a large number of frames, assume that p frames occur at the nominal rate R_i, and q at the maximum rate $R_i + 1/T_F$. The average rate during the time interval is the weighted average of the nominal and maximum-rate frames, which must equal the rate presented on the LEO/GEO link. Thus,

$$\frac{pR_i + q\left(R_i + \frac{1}{T_F}\right)}{p+q} = R_i\left(1 + d_i\right) \tag{8}$$

Solving for the fraction of frames that use the high rate,

$$e_i = \frac{q}{p+q} = d_i R_i T_F \tag{9}$$

This development pertains whether d_i is positive or negative. Of course, when it is negative, the fraction of frames calculated is for the low rate.

Synchronization and control words

The function of the frame synchronization word, SW, of S bits in length, is to produce a synchronization pulse at the instant of correlation (corresponding to perfect alignment) between itself and a replica stored in a correlator, and to produce small deviations (±1) around a mean value of $S/2$ when the alignment is not perfect. The operation of such a correlator is shown in Figure 4. Figure 4a shows that the output of the correlator as a stream containing the

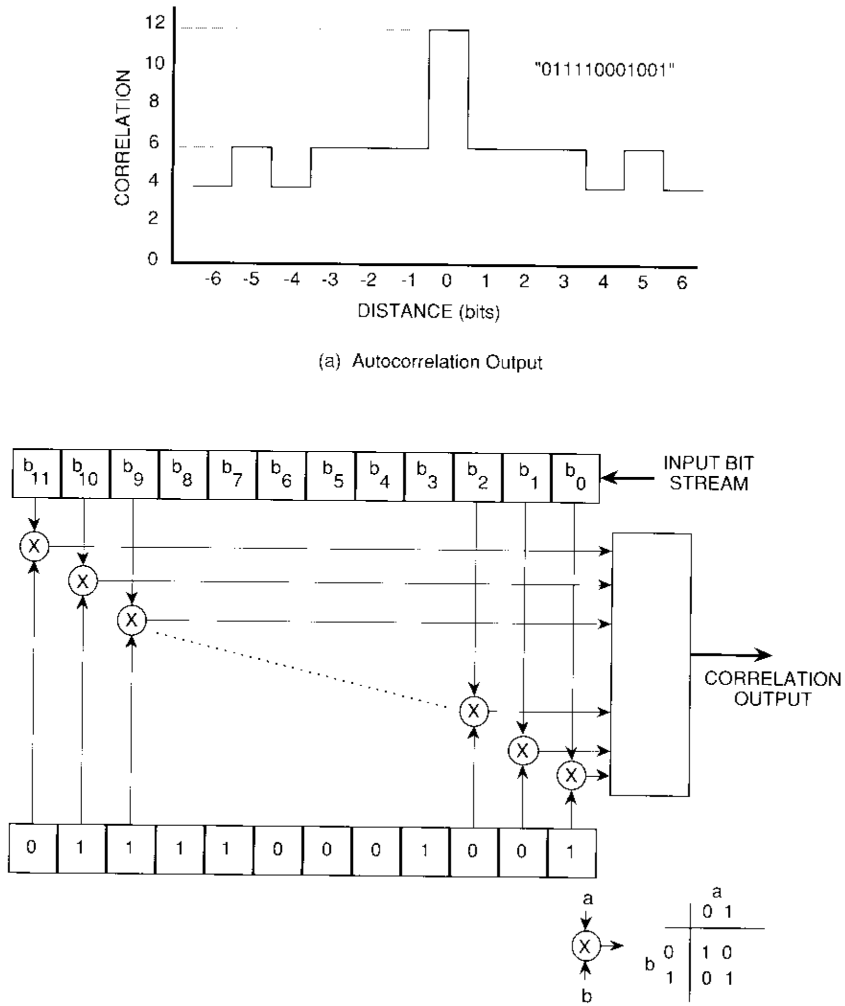

Figure 4. *Synchronization Word Correlation*

synchronization word is shifted 1 bit at a time through a register, and compared at each shift with a replica of the synchronization word. At each shift, the output is the number of bits that agree. At the instant of correlation, the output reaches a maximum value equal to the length of the synchronization word. The bit sequence of the synchronization word must be chosen to achieve these correlation properties.

A 12-bit word that has been used very successfully for time-division multiple access (TDMA) implementation, 011110001001, is used to implement the subject multiplexer. Figure 4b shows one implementation of the correlator. The false-alarm and miss probabilities of this word for gated and non-gated operation have been described by Campanella and Schaefer [4]. Non-gated operation is recommended during the search for the synchronization word, and gated operation during maintenance of synchronization.

The function of the control word is to signal when the group of bits in the frame is less than nominal, nominal, or greater than nominal. These three states require at least 2 bits to signal them. The control bits are extremely important for restoration at the receiver. An error in detecting the correct control word introduces both a clock and a data error. Therefore, error correction coding is mandatory. For this application, two different techniques were considered. One uses eightfold majority logic coding to yield 16 bits for the control channel. Up to three errors can occur in the 16-bit word without an error decision, or approximately one error in 5 bits.

A second option uses a control word only 8 bits long, but with similar properties. Use of this shorter control word will improve efficiency for low-rate channels by taking advantage of the fact that only three states are needed to represent the number of justification bits. The previous method allows four states to be decoded because 2 bits are used in each of the eight copies. If two errors are allowed to occur in the 8-bit control word, then the acceptable error rate is one error in 4 bits. To achieve this, at least five codes for the number of justification bits in the burst must be transmitted in the control word. With two bit errors, at least three of the codes must still agree so that the number of justification bits can be determined.

To determine the minimum number of bits in the control word, let Q be the code representing the number of justification bits in the frame and let $Q = \{0, 1, 2\}$ represent the nominal, n_j, and m_j lengths, respectively. The minimum-length control word can be constructed by forming a new word containing five instances of the code Q raised to successive powers of 3, as

$$CW = p_0 + Q3^0 + Q3^1 + Q3^2 + Q3^3 + Q3^4 \qquad (10)$$

The control word values corresponding to $Q = 0, 1, 2$ and $p_0 = 0$ are $CW = 0, 121, 242$. This range requires an 8-bit control word. The next step is to evaluate the effects of all possible combinations of one and two errors. The corrupted control word is then decoded to determine if three valid codes can be obtained with two errors.

The value of p_0 can range from 0 to 13 without overflowing an 8-bit word. Each of these values for p_0 was evaluated with error patterns consisting of 0, 1, and 2 errors. The evaluation showed that two values for p_0 are acceptable: $p_0 = 2$ or 11. For the other values, there were one or more instances where two errors in the control word caused three of the coefficients to be corrupted. The two sets of 8-bit control words that meet the requirements for coding three buffer-length states in the presence of two errors in the 8-bit word are $CW = \{2, 123, 244\}$ and $\{11, 132, 253\}$. For either of these sequences, three distinct sets of numbers exist corresponding to the three values for Q in the presence of 0, 1, or 2 errors. These sets can be stored in memory and used to quickly decode a control word.

Composite transmission rate and frame efficiency

Referring again to the frame structure shown in Figure 3, the total number of bits carried in one frame containing k channels of various sizes, n_i, is seen to be

$$N_F = S + kC + \sum_{i=1}^{k} n_i \qquad (11)$$

and hence the composite transmission rate is

$$R_c = \frac{N_F}{T_F} = \frac{S + kC}{T_F} + \sum_{i=1}^{k} R_i \qquad (12)$$

where R_i is the rate of incoming channel i.

The frame efficiency is the ratio of channel data payload per frame to N_F, which is

$$\eta = \frac{1}{N_F} \sum_{i=1}^{k} n_i = \frac{N_F - (S + kC)}{N_F} \qquad (13)$$

It is obvious that, as the frame period is shortened, the number of bits contained in the synchronization word and the control words becomes an increasingly large fraction, thus reducing efficiency. Figure 5 shows the efficiency for various numbers of channels as a function of N_F. These curves are for a control word of length $C = 8$ bits and a synchronization word of $S = 12$ bits. A

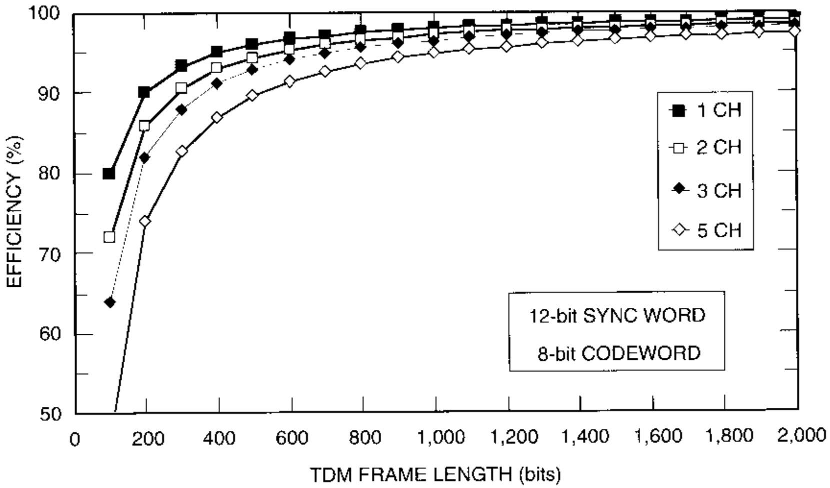

Figure 5. *Multiplexer Efficiency*

frame length of approximately 1,000 bits, yielding an efficiency of better than 90 percent assuming five channels, is a reasonable choice. Thus, for a 1-Gbit/s ISL transmission rate, the frame duration is approximately $T_F = 1$ µs.

Multiplexer implementation

Figure 6 is a block diagram of an implementation of the TDAS optical data link multiplexer which illustrates the implementation details for two channels. Each channel's digital bit stream is presented to the multiplexing buffer, which performs the joint functions of formatting frame sub-bursts and compensating for rate variations in the data flow. Each buffer has a pair of buffer memories, designated B_i and $\overline{B_i}$, respectively, that exchange function in a ping-pong fashion from frame to frame. Thus, if during one frame B_i is read and $\overline{B_i}$ is written, in the next frame $\overline{B_i}$ is read and B_i is written. The ping-pong action is implemented by exchanging the read and write clocks on alternating frames. By this means, data from the input channel are continuously formatted into data bursts transmitted at the proper frame location.

The data are written into each buffer using a clock derived directly from the channel data stream. They are read from each buffer by bursts of clock pulses generated by a master clock operating at the rate of the TDAS-multiplexed transmission link, namely N_F/T_F. A frame timing unit generates frame period pulses, F, which control the administration of the buffer read and

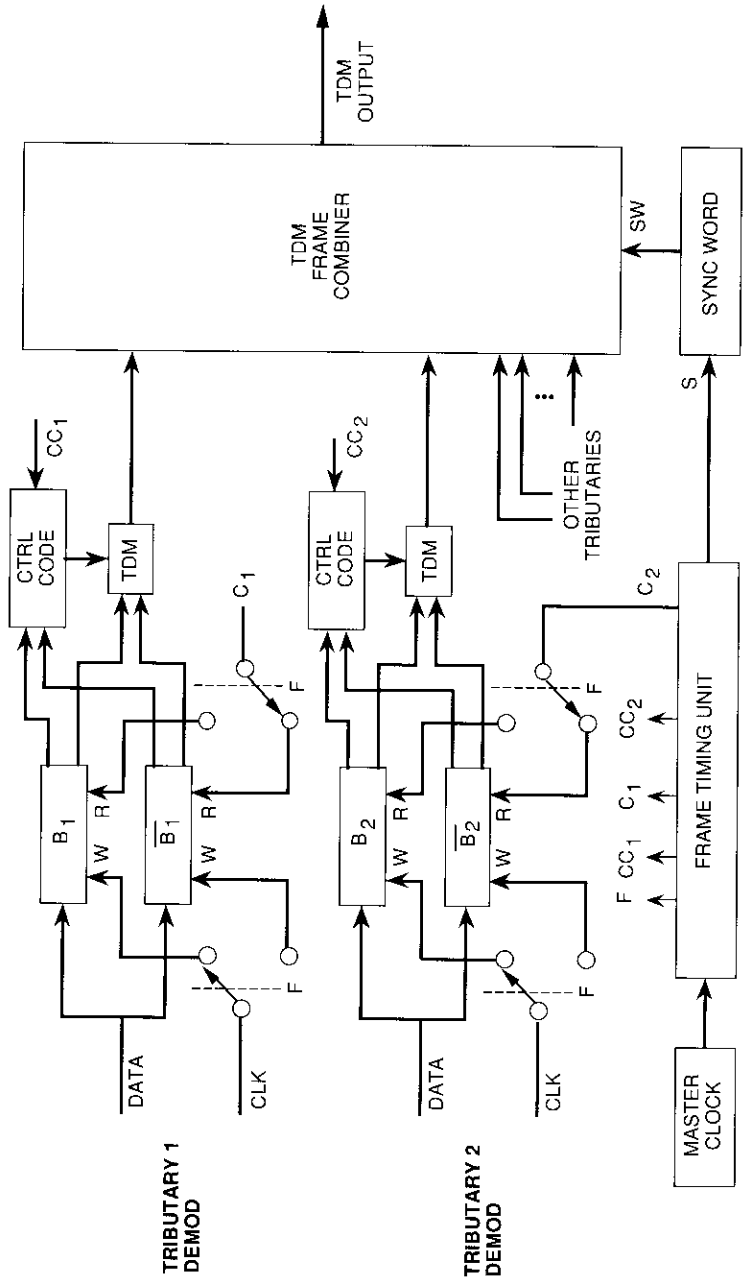

Figure 6. *Optical Link Multiplexer Circuit Elements*

write clocks, and bursts of clock pulses of the proper number and frame location to format the multiplexed stream. For buffer $B_i / \overline{B_i}$, the bursts of read clock pulses are designated as C_i. The variable C_i comprises n_i clock pulses (the maximum possible) which occur at a time in the frame that precisely locates the read $B_i / \overline{B_i}$ bits at their assigned location in the TDM frame. All n_i bits are always read; however, the number actually written may be n_i, $n_i - 1$, or $n_i - 2$, depending on the accidents of alignment at the input to the buffer in filling the buffer. The burst thus formed is said to be "bit justified."

Figure 7 is a timing diagram that illustrates the buffer operation. The primary requirement is that the read and write periods for a buffer must never overlap. Writing n_i bits causes the write period to shift to the right (delay), while writing m_i bits causes the write period to shift to the left (advance). It is this action that accommodates the variable rates occurring on individual channels. This buffer fill condition is sensed at the end of each write cycle in a

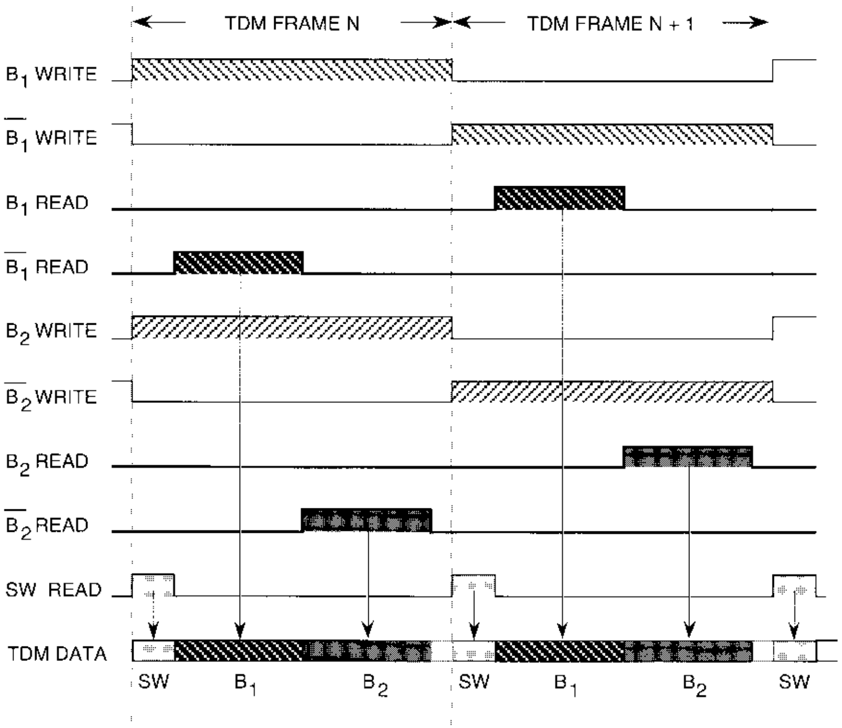

Figure 7. *Optical Link Multiplexer Timing*

buffer and sets the state of the control buffer to one of the three fill states. This state is read in CW_i, just before the data bits are read, by using the clock pulses designated as CC_i generated by the frame timing unit. This process is repeated for each channel carried in the frame.

To generate the synchronization word bits that mark the beginning of each multiplex frame, the frame timing unit generates a set of clock pulses, S, that read the contents of the synchronization (sync) word buffer at the start of each frame. Other channel bursts are generated in the same manner using appropriately timed outputs from the frame timing unit.

Demultiplexer implementation

Figure 8 depicts the implementation of the demultiplexer, while Figure 9 shows its timing. The multiplex stream comprises the sequence of bit-justified data sub-bursts (one for each origin channel generated by the multiplexer) and is supplied as input after demodulation from the optical receiver. To establish the timing of clock pulses necessary to accomplish the demultiplexing, the clock rate of the transmission link must be recovered and the instant of synchronization word correlation detected. Based on these signals, the frame timing unit generates the following timing symbols:

- F — Frame timing signal that marks the start instant of each frame.
- C_i — A sequence of n_i clock pulses that occur at the received clock rate N_F / T_F and at the proper time to write the n_i bits of channel i's sub-burst into the demultiplexing buffer, B_i or $\overline{B_i}$.
- CC_i — A sequence of clock pulses that occur at the time in the frame needed to write the control word for channel i (CW_i) into the output smoothing buffer. The information is used during the frame following the frame in which it is received.
- CT_i — A sequence of clock pulses that occur at the smoothed rate, R_i, used to read the contents of the demultiplexing buffer, B_i or $\overline{B_i}$. The number of pulses is either m_i, $n_i - 1$, or n_i, as determined by the control word received from the previous block. The smoothed clock generator uses the control words and frame timing unit to generate the smoothed clock at rate R_i.

The demultiplexer restores the signal to the same rates and format found at the input to the multiplexer. Two functions are required: the additional justification bits inserted into the bit stream at the multiplexer input must be removed, and the average input clock rate, R_i, must be regenerated.

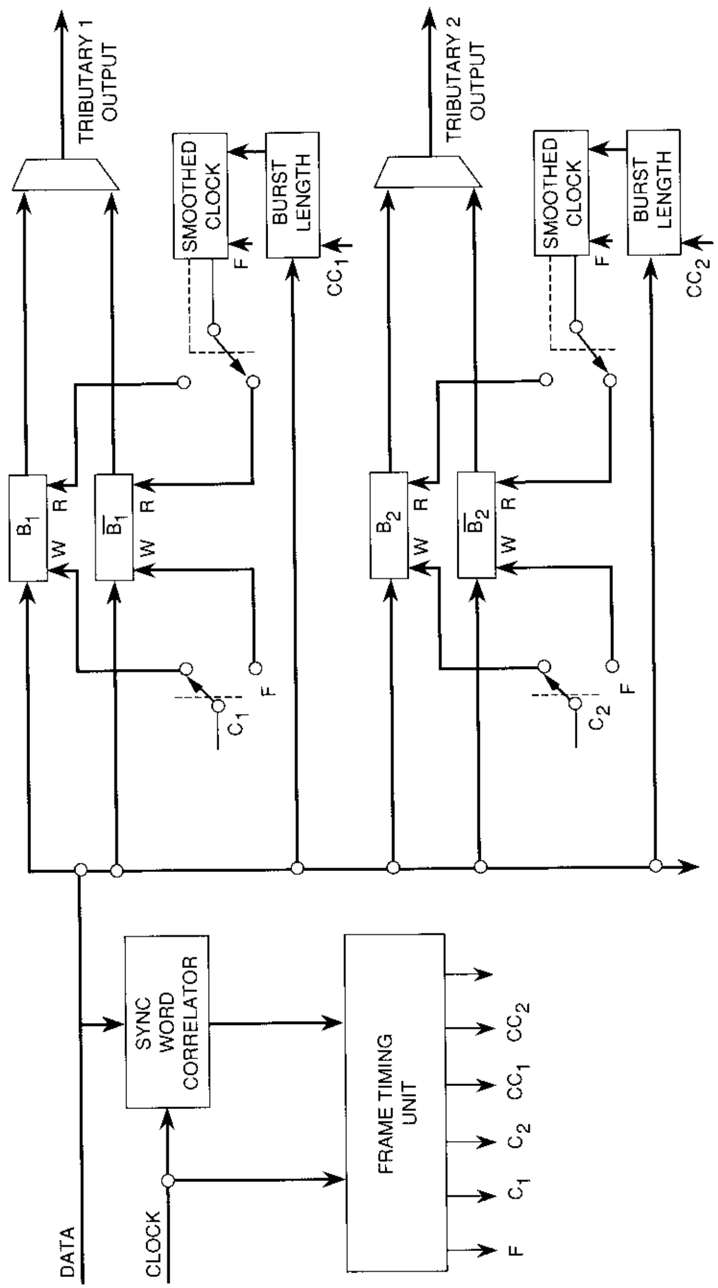

Figure 8. *Optical Link Demultiplexer Circuit Elements*

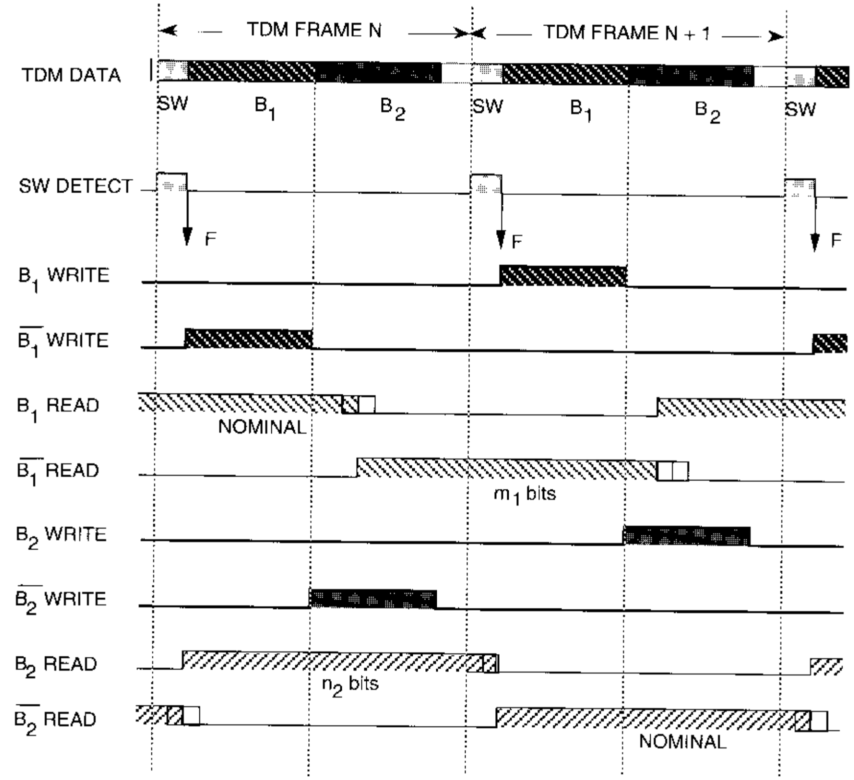

Figure 9. *Optical Link Demultiplexer Timing*

The clock signal corresponding to the multiplexed stream is used to write n_i bits in each frame into the ping-pong buffers B_i and $\overline{B_i}$. At this point, the stored signal still contains the justification bits. These bits must be eliminated and the rate adjusted to recover the channel stream. To accomplish this, the read clock rate is adjusted to recover the average rate, as follows. When the rate on the LEO/GEO link is high or low by a fraction d_{im}, the number of frames between frames that carry other than $n_i - 1$ bits is e_{im}^{-1}, which is obtained by substituting d_{im} into equation (7). Thus, the number of bits over which the retiming clock is high or low is

$$L = (R_i T_F d_{im})^{-1} = e_{im}^{-1} \tag{14}$$

When the transmission rate over the link is at the nominal rate corresponding to R_i, each frame will contain $R_i T_F = n_i - 1$ bits (T_F and R_i referenced to the transmit end). When this is the case, the write and read clocks are the same. For this condition to be maintained, the read clock must operate at a rate $[(n_i - 1)/T_F]$ (T_F referenced to the receive end). When the transmission rate is high, such that a frame carrying n_i information bits occurs once every L frames to accommodate the extra bit, the next read pointer is retarded by one address. The buffer must recover from this state by advancing the phase of the read clock by one bit period over a time interval, LT_F. This requires that the clock frequency of the read clock be increased to

$$\text{High read clock frequency} = \left(\frac{n_i - 1}{T_F}\right)\left(1 + \frac{L}{n_i - 1}\right) = R_i\left(1 + d_{im}\right) \quad (15)$$

This clock rate is maintained until the read clock phase advances by one bit period—a condition that is sensed by return of the alignment buffer to the normal state.

When the transmission rate is low, such that a frame carrying $n_i - 2$ bits occurs once every L frames to accommodate the loss of 1 bit, the read vector is advanced by one address of the buffer. The buffer must recover from this state by retarding the phase of the read clock by one bit period over a time interval, LT_F. This requires that the frequency of the read clock be reduced to

$$\text{Low read clock frequency} = \left(\frac{n_i - 1}{T_F}\right)\left(1 - \frac{L}{n_i - 1}\right) = R_i\left(1 - d_{im}\right) \quad (16)$$

It is also necessary to accommodate corrections that can be caused by the drift of the smoothing clock itself. The smoothing clock always attempts to maintain the normal state in the read buffer. If, due to its own drift, it advances the clock rate to either the plus or minus state, the clock frequency will be decreased or increased in the same manner described above to correct for the drift, and the frequency correction will occur in the same way as for a rate change on the channel. Because these corrections are in addition to those needed to compensate for the bit justification corrections, both may occasionally occur simultaneously in the same direction, causing a shift of two addresses rather than one. Consequently, the buffer needs to accommodate either two leading or two lagging corrections. For such double address changes, the frequency must be increased or decreased by twice the amount used for a single address change. At the rates defined for this study, there is ample margin for this alignment.

Return link design

The intersatellite return link must accommodate data from a large number of LEO/GEO digital up-links from different LEO platforms. The return link is the path from the LEO satellites to the GEO data relay satellite. The table in Figure 2 lists 19 separate channels to be handled by the two data relay satellites. These satellites function in either the backside or frontside role. The backside satellite functions are shown in Figure 10. The backside satellite collects data from the LEO satellites, forms these data into two 1-Gbit/s streams, and transmits the data to the frontside satellite using the optical ISLs. As shown in Figure 11, the frontside GEO satellite receives data directly from the LEO satellites, as well as from the backside GEO satellite. It then transmits a number of data streams to the earth stations.

One objective of this study was to develop a common design for the frontside and backside satellite roles. Since the functions of the two satellites differ, some of the equipment may not be used for both roles; however, a common design allows economies in terms of the number of spare satellites needed, and may be important for restoring service after partial failure in an orbiting spacecraft. Functions that must be performed by both the frontside and backside relay satellites include up-links and down-links to the LEO satellites. These are the Space/Space MW (microwave) link and the Space/Space Optical links shown on both figures. Functions that differ in the two spacecraft roles are those associated with the optical ISL and with the Space/Ground microwave links in the frontside satellite.

The table specifies maximum and minimum data rates for each return link channel, since each can vary over a wide range. Although the aggregate data rate for the 18 data streams can exceed the 2-Gbit/s capacity of the return optical ISL if all streams are at their maximum values, this would seldom occur in actual operation. During each LEO satellite orbit, communications alternate between the frontside and backside relay satellites. Therefore, only a portion of each of these links is active at any point in time. Three design considerations focus on a flexible multiplexer to maximize data collection, a design with redundancy to minimize the impact of component failure, and eventual implementation with space-qualified components capable of operation at gigabit-per-second rates. The number of building blocks used for each channel should be minimized.

These design considerations led to the following features in the return link design. First, each LEO data channel should be capable of transmission over either of the two optical ISLs. Second, as much flexibility in data rates as possible must be provided to accommodate changes in traffic demand over the

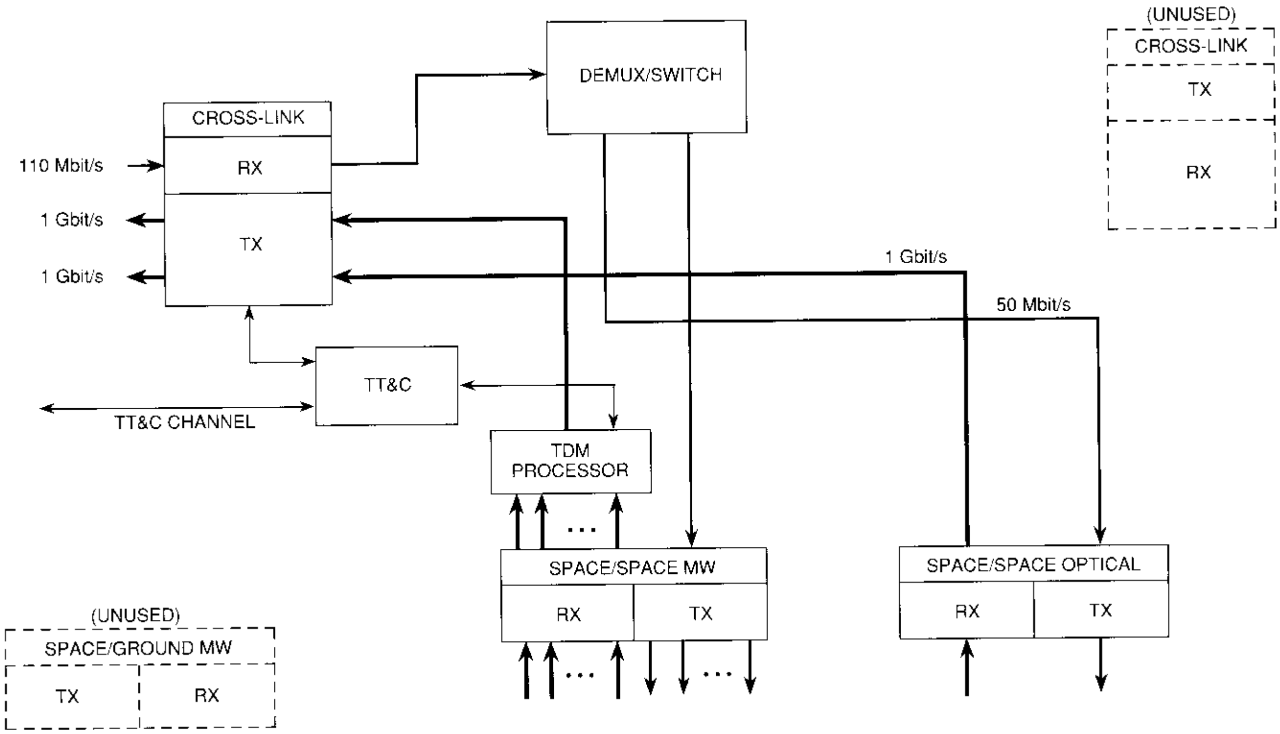

Figure 10. *Backside Operation*

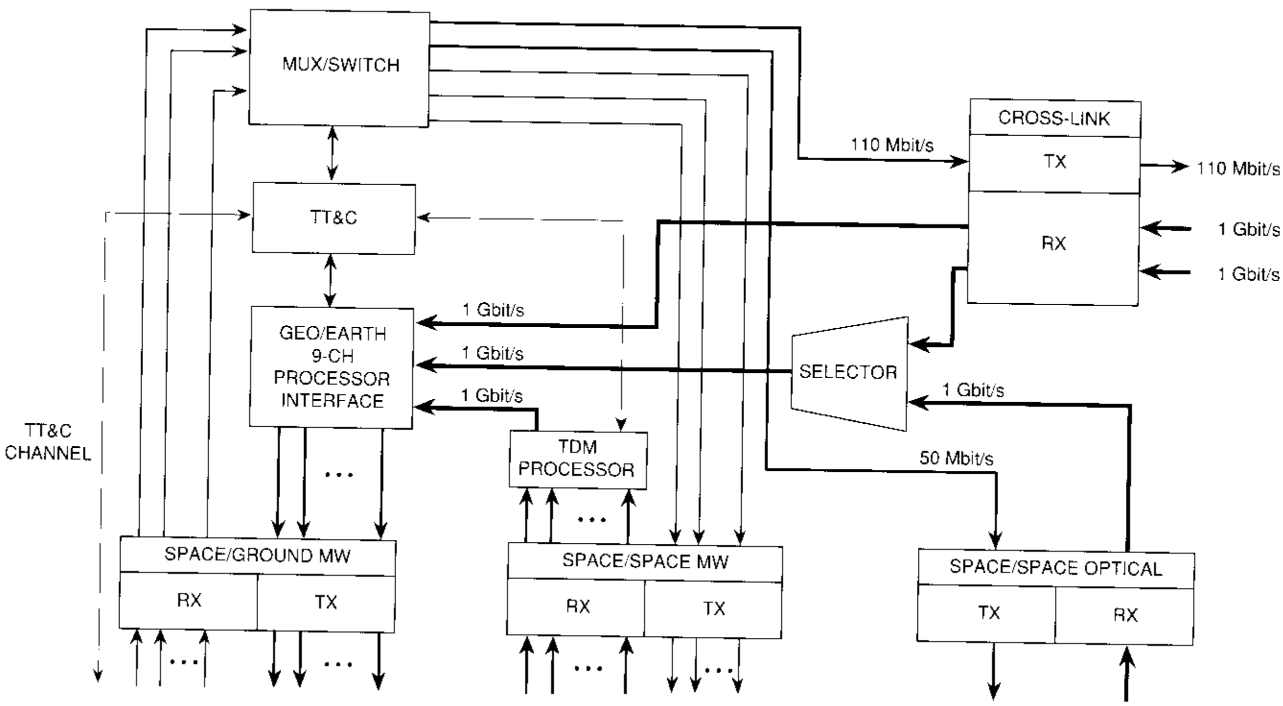

Figure 11. *Frontside Operation*

satellite's lifetime. Finally, the design should provide simple controls for on-orbit operation.

Return link multiplexer design considerations

A return link multiplexer was designed which operates at 1 Gbit/s and also adapts to wide changes in the nominal rate for each channel without changing the topology of the data paths. The return link channels can be considered in three groups. First, most of the data are provided by six channels: the LSA channel operating at 1 Gbit/s, and the WSA and KSA channels operating at 300 Mbit/s each. Second, there are two channels with maximum operating rates of 12 Mbit/s. Third, there are 10 channels operating at 50 kbit/s, and the TT&C channel at 10 kbit/s. The approach was to design a multiplexer suitable for the maximum data rates for each channel, and then modify the clock signals to attain efficient operation at lower rates.

Suitable frame periods must first be determined for the first two groups. For the highest group, three 300-Mbit/s channels can be combined using a multiplexer similar to the one shown in Figure 6. Figure 5 shows the efficiency achieved when several streams of equal rate are combined, and suggests that the frame length should be at least 600 bits, with 1,000 bits being desirable. Three channels with a frame period, T_F, of 1 μs can be transmitted with an efficiency greater than 95 percent using an 8-bit control word. An alternative mode might combine five channels at 200 Mbit/s. A frame length of approximately 1,000 bits was selected as a reasonable choice for the primary multiplexer frame length. Therefore, the corresponding multiplexer primary frame period, T_F, is 1 μs. However, the 1-μs frame period will lead to very low efficiencies for the two 12-Mbit/s channels. A longer "superframe" is needed that is a multiple of the primary frame length. Superframes ranging from 10 to perhaps 30 frames in length provide efficiencies in the range of 85 to 95 percent for two channels, as shown in Figure 5.

The next decision involves the topology of the multiplexer design for the selected frame and superframe periods. One method often used to combine channels of widely differing rates is a hierarchical multiplexer structure. Lower-rate channels are first combined to form higher-rate channels, which are then combined with other high-rate channels. The high-rate frames repeat at a constant rate, and there are multiple frames in each superframe. If the data rates for each channel are constant, a hierarchical organization provides efficient data transmission and minimizes buffer size. One problem with a hierarchical multiplexer structure is the variation in tributary rates for this application. For example, the KSA and WSA channel rates can be as high as

300 Mbit/s or as low as 1 kbit/s. At the higher rates, the signal should be connected to a high-rate input, while at the lower rates it should be connected to a low-rate input. The need for alternative paths between high and low rates is a significant complication to the design of the multiplexer, and maintaining efficient operation over a range of rates becomes difficult.

An alternative to a hierarchical topology is to change the generation of clock signals to the ping-pong buffers. At high data rates, a ping-pong buffer is written and read during a frame period. At low rates, it is written and read during a superframe. Channels operating in the superframe mode are assigned one or more bits in each superframe. High-rate LEO channels operate in the frame mode at high data rates, and can be switched to the superframe mode at lower data rates. Moderate-rate LEO channels could operate in the superframe mode at all times, but the number of bits assigned in the primary frame is reduced as the data rate becomes lower. Burst slots in the TDM are dynamically assigned during orbital operation to accommodate the changing LEO missions. Figure 12 is a block diagram of this multiplexer. Each input labeled B is connected to a ping-pong buffer of the type shown in Figure 6.

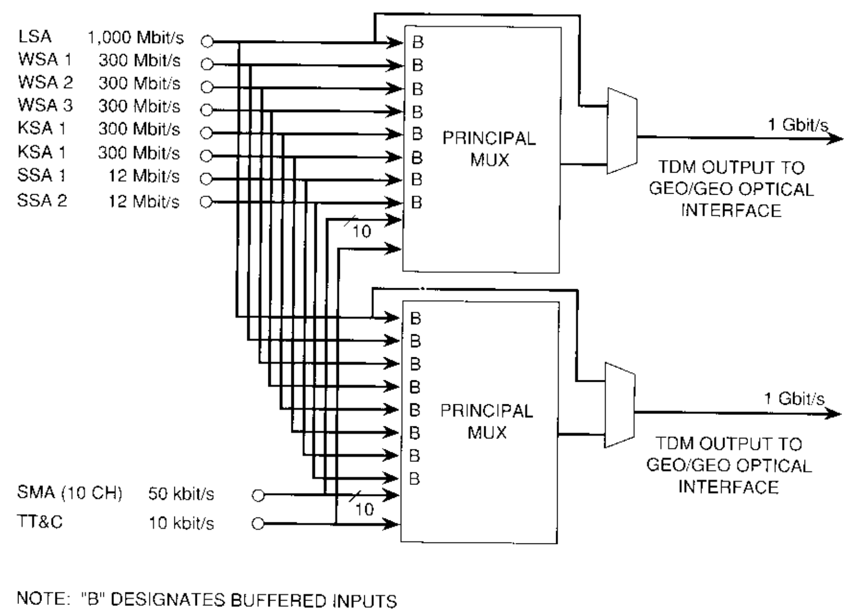

Figure 12. *Return Link Multiplexer*

The advantage of the above approach is that the design is modular and the circuit components are the same for all buffered channels. Only the control signals change. For each channel carried in a superframe, a codeword is sent once each superframe. A value of $D_i = 2$ is also used for justifying the bits carried in each superframe. The same control word is used to indicate the number of justification bits in the superframe burst.

Assuming that a superframe consists of J_i TDM primary frames, a superframe channel will be assigned k_i bits in each primary frame. The length of a superframe mode burst is simply J_i x k_i. The number of bits required in the superframe, N_s, for these channels is

$$N_s = C + n_i = C + R_i J_i T_F + 1 \tag{17}$$

and the number of bits in each primary frame becomes

$$k_i = \left\lceil R_i T_F + \frac{1 + C}{J_i} \right\rceil \tag{18}$$

The remaining group of channels consists of the 10 SMA channels with maximum rates of 50 kHz, and the 10-kHz TT&C channel. These channels do not require much bandwidth, but represent a significant number of paths. If they are handled the same as the previous channels, then 11 additional buffers would be required and a third level of frame period would be needed. An alternative is to recognize that the superframe and frame rates are much higher than the bit rate from any of these channels; therefore, these channels can be transmitted by simply sampling the bit stream and sending 1 bit per sample. Although this is very inefficient in terms of transmission, the circuitry required in the multiplexer becomes trivial.

The above design now meets all of the design objectives. Efficient transmission of data at high rates has been achieved; the design is flexible and can be programmed after launch or in orbit; the design can be implemented using a few building blocks that are simply replicated for each channel; and redundant data paths have been provided in the optical ISL. The next section describes some on-orbit applications for this multiplexer design.

Return link multiplexer operation

Referring to the block diagram of Figure 12, it can be seen that two symmetric multiplexers are connected to the two ISLs. Each multiplexer can be programmed independently of the other. A 1-μs principal TDM frame length is used for these examples. Since a very large number of rate combinations is possible, the examples of TDM frame time plans will be limited to the following:

- An LSA channel directly connected to an ISL channel.
- An LSA channel connected to an ISL channel using bit justification.
- Three WSA channels, two SSA channels, and the remaining low-rate channels.
- Two KSA channels and the remaining low-rate channels.
- Four WSA and KSA channels at reduced rates, plus all other low-rate channels.

Figure 13 shows frame structures for each of the above examples. The first is for a directly connected LSA channel operating at 1-Gbit/s. It simply comprises 1,000 bits of the LSA stream, where the bit rate is driven by the arrival rate on the LEO/GEO up-link, with no attempt to eliminate the Doppler effect. In this case, there is no need for either a frame synchronization burst or a codeword.

The second example is for the LSA connected to the 1-Gbit/s ISL channel. To carry precisely 1 Gbit/s, the actual link rate must exceed 1 Gbit/s by a small amount in order to accommodate the synchronization word and the codeword needed to control the demultiplexing clock. Thus, the frame must contain 1,022 bits and operate at 1,022 Gbit/s. Note that 1 bit in the frame is assigned to TT&C. This provides 1 Mbit/s, which exceeds the actual TT&C rate of 10 kbit/s by 100 times. Although this represents a minute inefficiency (0.1 percent), it is extremely simple to implement and provides an opportunity for higher rates and redundancy encoding.

Figures 13c and 13d show other frame configurations for carrying various mixes of 300-Mbit/s WSA and KSA, 12-Mbit/s SSA, and 50-kbit/s SMA channels. Each 300-Mbit/s WSA or KSA channel is bit-justified, using 301 data bits per channel plus an 8-bit codeword. Each 12-Mbit/s SSA is bit-justified using 13 data bits plus an 8-bit codeword, which represents a channel usage efficiency of 57 percent. Figure 13e shows four WSA or KSA channels operating at 230 Mbit/s, as well as all lower-rate channels.

The SMA channels are treated differently because of their relatively lower rate (50 kbit/s). Each SMA channel is assigned 1 bit in the frame, thus oversampling the channel by 20 times. Each of these channels can be sent using a self-clocking code such as RZ (return to zero), NRZ (nonreturn to zero), or biphase [5]. Doppler compensation can easily be accomplished by a Doppler buffer having a range of ±20 ms, which is sufficient to accommodate

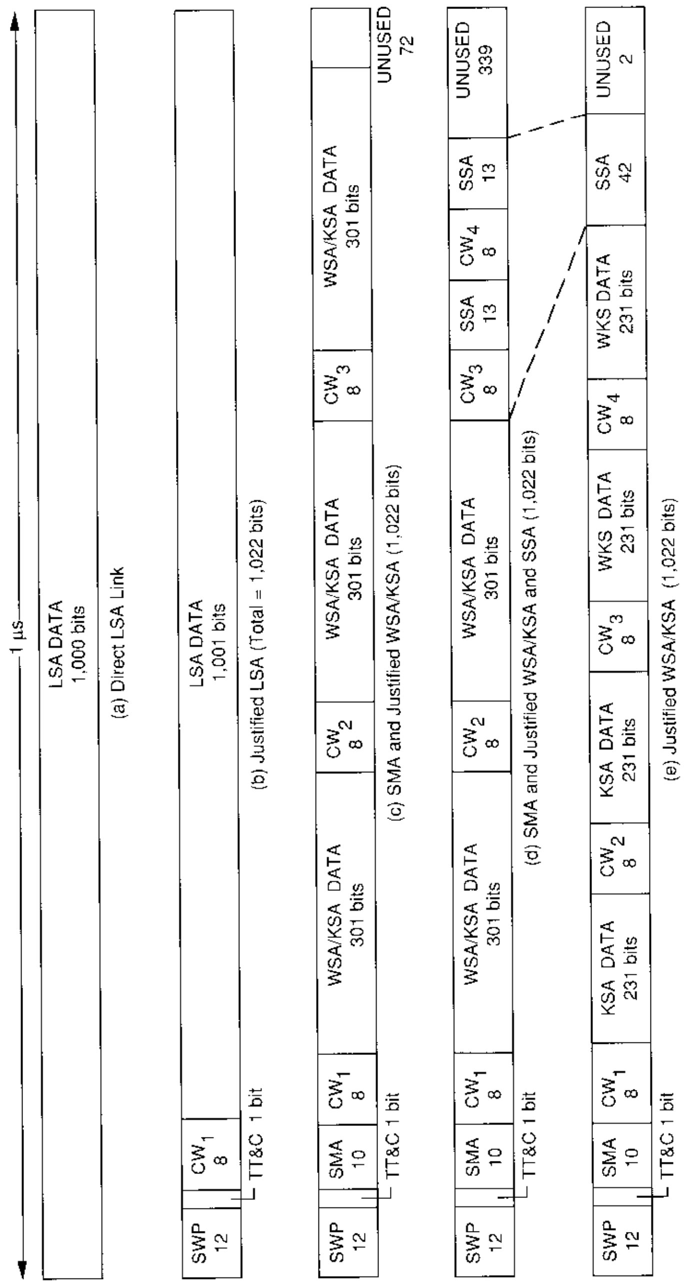

Figure 13. Return Link Multiplex Frame Structure

changes in the GEO/LEO range and can be implemented with a maximum memory size of 4 kbit/s.

The channel efficiency for the SSA channels (12 Mbit/s) can be improved by operation in a superframe. From equation (15), it is seen that for a codeword of size C, the superframe should have a length $J_i = C + 1$. A superframe length $J_i = 9$ allows 1 bit for the codeword plus the justification bit in each primary frame. This is a superframe period of 9 μs. For these values, equation (15) yields a k_i value of 13 bits per primary frame to carry the entire SSA channel. This corresponds to a superframe length of $n_i = 217$ to carry 108 SSA channel bits, and hence improves the channel usage efficiency to 92 percent. The frame time plan for this case is shown in Table 2.

TABLE 2. EXAMPLE OF RETURN LINK MULTIPLEXER BURST ASSIGNMENT

TDM CHANNEL	k_i	J_i	R_i (Mbit/s)
Synchronization Word	12	1	
TT&C	1	1	0.01
WSA/KSA Ch 1	317	1	300
WSA/KSA Ch 2	317	1	300
WSA/KSA Ch 3	317	1	300
SSA Ch 1	13	9	12
SSA Ch 2	13	9	12
Reserved for SMA Channels	10	–	0.5
Total	1,000		924.51

k_i = number of bits from a superframe mode buffer transmitted in each frame.
J_i = number of frames in a superframe.
R_i = channel data rate.

Return link demultiplexer

The frontside relay satellite receives data from LEO satellites that are in a position to communicate with it, as well as multiplexed LEO data from the backside relay satellite. This unit, called the GEO/Earth Nine-Channel Processor in Figure 11, accepts data streams that may be received at either of the two relay satellites and provides nine output streams for transmission to the White Sands earth station. Each of the nine GEO/Earth streams is defined to have a 200-Mbit/s capacity. Therefore, the GEO/Earth processor must demultiplex signals from the optical ISL and then select the active stream, if any, from each of the 18 data channels. If the data for a channel are being received from the backside relay satellite, they must be taken from the optical ISL. If the data are being received by the frontside satellite, they are taken from the appropriate LEO satellite receiver.

The number of active channels, the data rates for each channel, and the relay satellite receiving the data vary according to the orbits and mission programming of each LEO satellite. However, these factors are known at any moment in time and can be used to efficiently and dynamically program the GEO/Earth processor. Each input stream can be described by a form of burst time plan that changes according to a set of prescribed plans. The GEO/Earth processor can be programmed to select data from the correct relay satellite, to operate at the data rate currently in use, and to select of one of the GEO/Earth channels.

The 18 streams are processed for transmission to an earth station. Data streams with rates higher than 200 Mbit/s must be separated into two or more streams for transmission to the earth, while channels with lower data rates may be combined with other streams. The 12 low-rate streams can always be combined into a single stream. Both TT&C (telemetry) channels are sent to the earth station, and may be sent over more than one link to ensure reliable transmission of this important data. The GEO/Earth processor must combine 20 channels to form nine separate streams for transmission to the earth station.

Two different approaches to the design of the GEO/Earth processor have been considered. One is to demultiplex the streams received from the backside relay satellite, rate-buffer the data to remove the effects of LEO/GEO Doppler variation and restore the original transmission rate, separate the higher-rate streams, and combine these with the lower-rate streams. In the second approach, the blocks formed for multiplexing signals for the ISL are retained and the rate-smoothing buffers are implemented at the earth station.

In the first approach, two demultiplexers operate on the composite signals from the 1-Gbit/s ISLs, as shown in Figure 14. Since each link can handle a number of different signals, the rate buffers can receive signals from either of the two return ISLs. The smoothing buffers shown here are detailed in Figure 8. Seven rate buffers are needed for the WSA, KSA, and SSA channels. The 10 SMA channels and the TT&C channels are recovered by simply clocking the corresponding bits at the primary multiplex frame rate. Each smoothing buffer is connected to both ISL buffers. An input selector switch (not shown in Figure 8) connects the smoothing buffer to the link containing the data.

Each smoothing buffer consists of a ping-pong buffer and a clock regeneration circuit, operating in the manner described previously. As was determined for typical LEO orbiters, $d_{im} = 2.5 \times 10^{-5}$. To recover from a 1-bit correction in

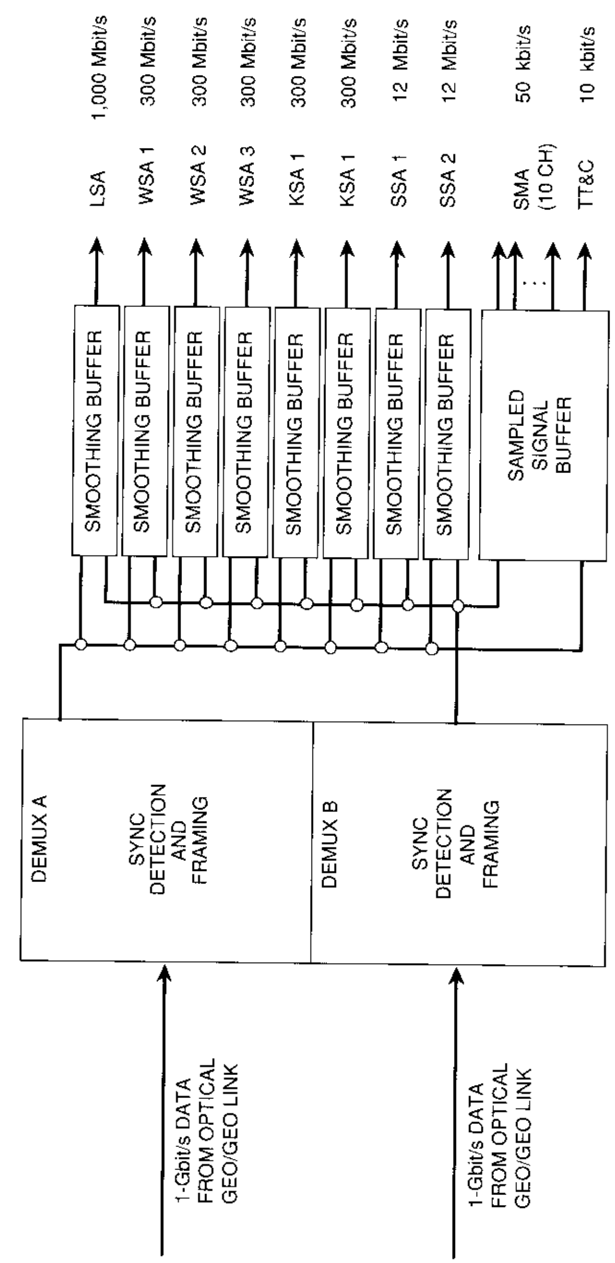

Figure 14. Return Link Demultiplexer

the minimum time between corrections, the recovered clock rate for channel i must run high at a rate $R_i(1 + 2.5 \times 10^{-5})$ or low at $R_i(1 - 2.5 \times 10^{-5})$ every time a high or low rate correction is signaled by the control word associated with the channel. Otherwise, the rate is R_i, which is the rate recovered from the received digital stream. The correction rate will last for an interval sufficient to contain d_{im}^{-1} bits.

Each smoothing buffer must operate over the range of clock speeds given in the table in Figure 2. The demultiplexer's framing section is programmed to match the time-division plan used by the return link multiplexer. The outputs of the smoothing buffers must then be processed to form nine channels, each with rates under 200 Mbit/s. Two of the 300-Mbit/s channels can be separated into three 200-Mbit/s channels for transmission to the earth station. Similarly, a 1,000-Mbit/s data channel is separated into five 200-Mbit/s streams. These are the approaches required at the maximum rates for the six channels with the highest rates. Since these channels have a minimum rate of only 1 kbit/s, it is also possible that two or more of these signals could be multiplexed and sent in a single GEO/Earth link, instead of being separated into two or more GEO/Earth links. The remaining signals total less than 25 Mbit/s, even if all are at the maximum rates. These can be multiplexed into a single stream, with care being taken to accommodate the rate variation that may occur. The processing required is similar to that needed for the ISL. Since each of the 18 data streams has rate variations due to the GEO/LEO orbits, buffering is needed when signals are being combined.

The second approach to the design of the GEO/Earth nine-channel processor retains the blocks of data formed in the backside satellite. Two factors make this desirable. First, while the processing has removed most of the data stream variations due to Doppler effect, the smoothing buffers shown in Figure 8 tend to restore these variations. If the GEO/Earth links operate at the same rate as the data channels, this is of little concern. When two of the high-rate channels are separated and then combined into three GEO/Earth channels, the effects of Doppler variation in the data rates must again be considered. The second factor is the principle of minimizing the processing of data in a satellite. This is served by retaining the data blocks once they have been formed, and transferring functions to the earth station where possible.

To separate the high-rate data channels, it is necessary to form blocks of data in buffers. These blocks are then used to change the transmission rate to match the GEO/Earth channel rate of 200 Mbit/s. Since buffering of the signal in the backside satellite compensates for rate variations due to Doppler effect, it can also be used to simplify timing in the GEO/Earth processor. The data blocks (a codeword followed by a block of data) form the basis for a simple data packet, needing only the addition of a sequence number to ensure that the streams can be properly reformed at the earth station.

If the frontside and backside satellites are identical in design, then one approach is to process incoming LEO data in the frontside satellite in the same manner as data are processed in the backside satellite. The burst time plans for the 1-Gbit/s streams in the frontside satellite can be identical to those used in the backside satellite. This reduces the effect of Doppler variations in the data rates for signals received directly by the frontside satellite from LEO satellites. In addition, the frontside satellite TDM processor shown in Figure 11 can be phase-locked to the signal received via the ISL from the backside satellite TDM processor shown in Figure 10. Corresponding streams from the frontside and backside relay satellites can then be presented to the GEO/Earth processor. Blocks of data are then selected from the appropriate stream according to a predetermined plan. Figure 15 is a block diagram of this approach.

The set of nine TDM streams is then formed from the 1-Gbit/s streams from the frontside and backside TDM processors. The functions required to implement these new streams can be identical to those shown in Figure 6 and used in the TDM processors. The primary additions are circuits to select blocks of data from the appropriate stream, and storage for the burst time plans for the input and output streams. The smoothing buffers shown in Figure 8 can be moved to the earth station if necessary. In some cases, signals received from the frontside relay satellite may be recorded for later processing, and could be recorded with the inserted codewords intact. The codewords could easily be removed during the processing steps, and the smoothing buffers would not be needed since the signal is not displayed in real time.

The optimum benefit of the second approach is attained if the frontside and backside satellites share a common design. In this case, the TDM multiplexer is available for LEO satellite channels received directly at the frontside satellite. In addition, the GEO/Earth TDM streams can be formed using the same types of circuits used for other functions. This approach becomes less attractive when the two relay satellites do not have a common design, or when the GEO/Earth channels have the same bandwidth as the LEO/GEO channels.

The first approach is desirable when the GEO/Earth channel bandwidths match the LEO channel bit rates, when a number of earth stations receive and process the data from a channel, and when a simple earth station design is desired. The second approach becomes desirable when the GEO/Earth channel bandwidths are different than the LEO channel bit rates, or when the spacecraft design should be as simple as possible. The smoothing buffers are relatively complex due to the wide range of operating rates that could be required, and should preferably be located at an earth station.

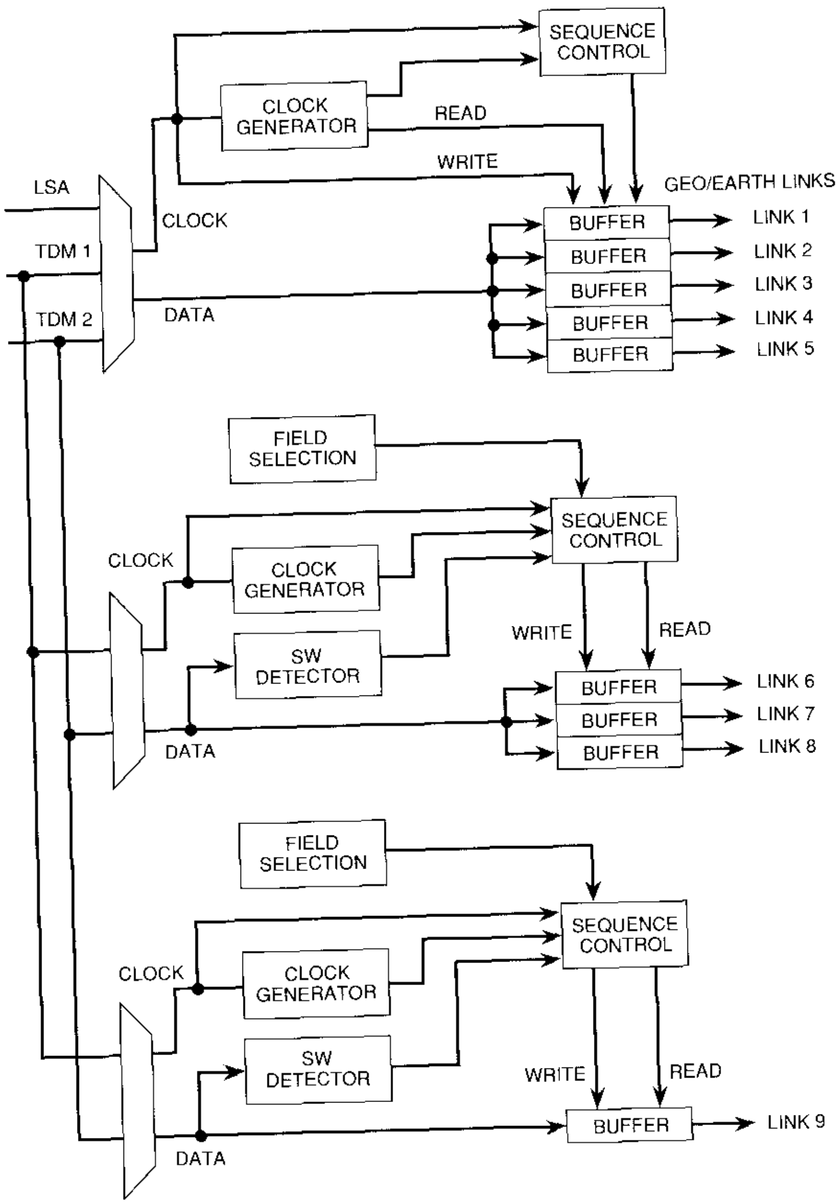

Figure 15. *GEO/Earth Nine-Channel Processor (220-Mbit/s links)*

Forward link design

The forward link must accommodate a number of low-bit-rate carriers of various data rates arriving on up-links from the nine earth station locations. The table in Figure 2 lists the forward channels used for the TDAS program, totalling 103.63 Mbit/s. The carriers will have differing values of Doppler variation caused by orbital motion relative to the earth terminals.

Figure 11 showed some of the signal paths for forward link operations. Signals from the ground stations, received by the frontside satellite, are sent to the forward path switch/multiplexer. The 50-Mbit/s LSA link and the two 25-Mbit/s KSA links dominate the design.

The switch/multiplexer unit connects the nine earth-to-GEO up-link receivers, the 10 GEO/LEO links, and the forward link GEO/GEO optical ISL. Signals to be sent to LEO satellites in view of the frontside relay satellite are sent directly, without the need for multiplexing. Signals for LEO satellites in the view of the backside relay satellite are routed to an on-board forward link multiplexer, where they are combined onto a single TDM channel at a higher composite bit rate and transmitted to the backside satellite over an optical ISL. On-board the backside satellite, the composite TDM channel is demultiplexed to the original channel rates, and selected channels are sent to the LEO satellites in the view of the backside satellite.

Provision must be made on-board both relay satellites to serve either the frontside or backside role by switching the GEO/LEO down-links to either the output of the up-link interface for frontside operation, or to the optical link demultiplexer for backside operation. Also, to accommodate frontside operation, it is necessary to include a switch to connect the output of the up-link interface either directly to the GEO/LEO down-links for serving LEO satellites in the view of the frontside relay satellite, or to the input of the optical link multiplexer for serving LEO satellites in the view of the backside TDAS.

Forward link multiplexer

The forward link multiplexer must combine earth-to-GEO up-link channels of differing bit rates, origins, and Doppler rates onto a common TDM channel for transmission over the frontside-to-backside ISL. A suitable multiplexer design is shown in Figure 16. This multiplexer employs a hierarchical organization. All of the up-link channels expected to be carried on the forward link are identified in the figure. The highest bit rate channels (one LSA at 50 Mbit/s and two KSA at 25 Mbit/s) determine the principal multiplexer frame period. Other channels operate in the superframe mode or in the sampling mode.

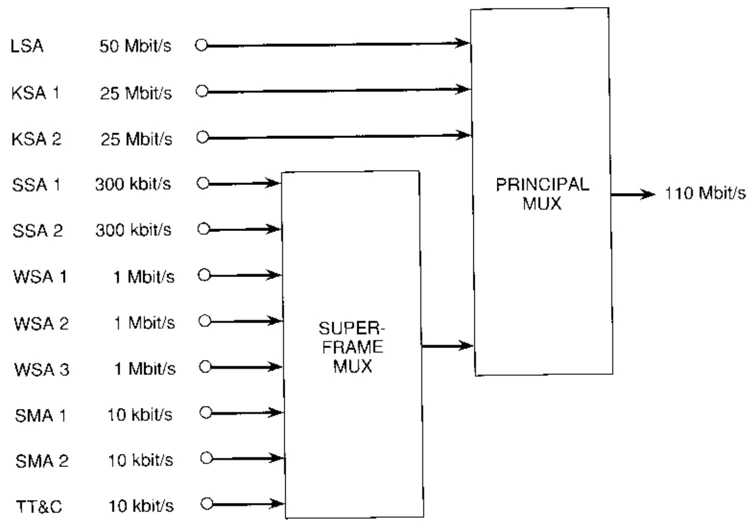

Figure 16. *Forward Link Multiplexer*

The principal multiplex frame plan is described in Table 3 and shown in Figure 16. It is assembled using the multiplexer design shown in Figure 8. The primary TDM frame is 10 µs and has a superframe length of 18 primary frames. Each primary frame contains 1,107 bits and has a length of 10 µs. The structure shown in Figure 16 accommodates one 50-Mbit/s channel using 517 bits ($n_i = 501$), and two 25-Mbit/s channels, each using 267 bits ($n_i = 251$). Each WSA channel uses 197 bits ($n_i = 181$) in the superframe mode, and each SSA channel uses 71 bits ($n_i = 55$) in the superframe mode. The TT&C and SMA channels are each assigned 1 bit in the primary frame and operate in the sampled signal mode. A synchronization word uses 12 bits. The length of the primary TDM frame is 1,107 bits and requires a 110.7-Mbit/s ISL. The efficiency of the link with all signals at the maximum rate is 94 percent.

This forward link design employs the same basic building blocks used by the return link. Flexibility is provided by using the same design for 8 of the 11 channels, which can operate over a wide variety of rates without changes to the basic structure. The three low-rate channels (the TT&C channel and the SMA channels) operate in the sampled signal mode. Although this represents a 10:1 oversampling at the maximum rate, these three channels contribute only 3 bits to the TDM frame. The advantages are that no adjustments to the multiplexer design on the relay satellites are needed for bit rate variations from maximum down to minimum, and the ping-pong buffers are eliminated. A processor will be needed at the ground to recover the signal from the set of samples.

TABLE 3. EXAMPLE OF RETURN LINK MULTIPLEXER BURST ASSIGNMENT

TDM CHANNEL	k_i	J_i	R_i (Mbit/s)
Synchronization Word	12	1	
TT&C	1	–	0.01
LSA Channel	517	1	50
KSA Ch 1	267	1	25
KSA Ch 2	267	1	25
WSA Ch 1	11	18	1
WSA Ch 2	11	18	1
WSA Ch 3	11	18	1
SSA Ch 1	4	18	0.3
SSA Ch 2	4	18	0.3
SMA Ch 1	1	–	0.01
SMA Ch 2	1	–	0.01
Total	1,107		103.63

k_i = number of bits from a superframe mode buffer transmitted in each frame.
J_i = number of frames in a superframe.
R_i = channel data rate.

Forward link demultiplexer

The demultiplexer for the forward link will operate on the composite channel rate of 110.7 Mbit/s. Each relay satellite will have the demultiplexer, but it will be used only when serving in the backside role. The demultiplexer design is shown in Figure 17. It must synchronize to the principal frame synchronization word every 10 µs and then distribute the TDM channels to expansion buffers, followed by retiming buffers operating in the manner described previously, in order to recover the original channel data streams.

The variations encountered on the earth-to-GEO up-link channels due to Doppler shift should be no worse than $\pm 10^{-8}$, and those due to originating clock variation no worse than $\pm 10^{-6}$; however, they could be less, depending on the clock specification. These values are much less than those encountered on the LEO/GEO links, which are $\pm 2.5 \times 10^{-5}$ due to much greater Doppler effect. In the design of the forward link demultiplexer, the clock variation will be assumed to be no worse than $\pm 10^{-6}$. To recover from addition or subtraction

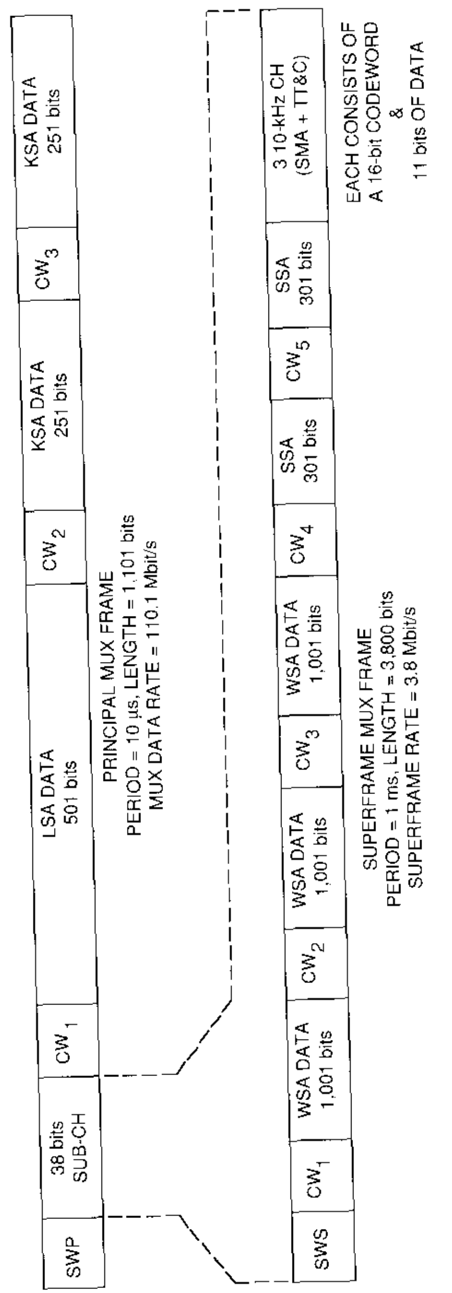

Figure 17. *Forward Link Multiplex Frame Structure*

of 1 bit in the minimum time between corrections, the retiming clock of the alignment buffer must run high, at a rate of $R_i(1 + 10^{-6})$, or low, at $R_i(1 - 10^{-6})$, respectively, and the rate will last for an interval sufficient for 10^{-6} bits to occur.

Forward link switch

The forward link signals are received at the frontside relay satellite and transmitted to the backside relay satellite over a 110-Mbit/s optical link. Thus, both satellites have available the data to be sent to the LEO satellite. Since only one of the relay satellites should transmit this data, a frontside/backside switch is included in each satellite to control data routing. Each channel will have a different switching time for each LEO satellite. The switching can be activated by an on-board timer or by real-time command from the controlling earth station.

A "break before make" design is suggested. There should be no period when both relay satellites can forward data on the same channel. When control is to pass from the frontside to the backside relay satellite, the frontside switch will be disabled before the backside switch is enabled. The gap will include the time required for transmission between the frontside and backside satellites, as well as the time for operation of the switch. When control is to pass from the backside to the frontside relay satellite, the frontside satellite will forward the command to disable the backside switch, then wait an appropriate amount of time before enabling its corresponding switch. This switch should gate the demultiplexer output and switch components in the RF section. The interface to the RF components should be clock, data, and an enable signal.

Conclusions

A design approach for the RF/optical link interface for a data relay satellite has been described. The two GEO data relay satellites are assumed to be connected by a pair of 1-Gbit/s optical links. This provides sufficient capacity to handle the number of TDAS return link data streams specified by NASA. Each GEO satellite has a number of links to LEO satellites. The frontside GEO role also includes links to nine earth stations.

The return link path may at times be from a LEO satellite to an earth station via the backside GEO satellite, and at other times via the frontside LEO satellite. A flexible multiplexer was described that can be programmed to support of a wide range of missions. The design includes techniques to deal with Doppler shifts caused by the varying high velocity of LEO satellites relative to GEO satellites, and with local oscillator frequency variations. Design equations were provided which described the range of nominal and allowable variations in oscillator frequency. The forward link path is from an earth station to a LEO satellite through either the frontside GEO satellite, or through both the frontside and backside GEO satellites. For the forward link, provisions were included to ensure that signals from the earth station to the LEO spacecraft are relayed by only one of the spacecraft.

The design approach identified a number of circuit elements that can be implemented using LSI or VLSI techniques.

Acknowledgments

The authors would like to acknowledge the assistance of D. Paul of COMSAT Laboratories; R. Marshalek, formerly of COMSAT Laboratories and currently with Ball Aerospace Systems Division; R. Nelson of Ball Aerospace Systems Division; and L. Caudill and M. Fitzmaurice at NASA Goddard Space Flight Center. Thanks are also due to G. Koepf, formerly of COMSAT Laboratories and currently with Ball Aerospace. It is noted with gratitude that related efforts were funded by COMSAT World Systems Division's INTELSAT Satellite Services (J. Martin, Project Manager).

This paper covers part of the "TDRS Laser ISL Communications Study" performed for Ball Aerospace Systems Division under NASA/GSFC contract NAS 5-29128 and incorporated into the Final Report by Ball to NASA/GSFC (NASA Contract Report No. CR-183419), "Tracking and Data Acquisition System Laser ISL Communication Study." The first part of the COMSAT Laboratories study covers the optical communications aspects. This paper covers the work of S. Campanella on multiplexing and of R. K. Garlow on system engineering under this contract.

References

[1] COMSAT Laboratories, "TDAS Laser Intersatellite Communications Study," performed for Ball Aerospace Systems Division under Subcontract 01232 and NASA GSFC Contract No. NAS5-29128, July 1986. Incorporated into the Final Report by Ball to NASA GSFC, Contract Report No. CR-183419, July 1986.

[2] R. G. Marshalek, "Comparison of Optical Technologies for Intersatellite Link Payloads, Part I: Mass, Prime Power, and Volume Estimates," *COMSAT Technical Review*, Vol. 18, No. 2, Fall 1988, pp. 191–214.

[3] D. K. Paul, "Comparison of Optical Technologies for Intersatellite Link Payloads, Part II: Impact of Reliability Considerations on Technology Selection," *COMSAT Technical Review*, Vol. 18, No. 2, Fall 1988, pp. 215–238.

[4] S. J. Campanella and D. Schaefer, "Time-Division Multiple-Access Systems (TDMA)," K. Feher, *Digital Communications, Satellite/Earth Station Engineering*, Ch. 8, Englewood Cliffs, New Jersey: Prentice-Hall, 1983.

[5] W. L. Morgan and G. D. Gordon, *Communications Satellite Handbook*, New York: Wiley, 1989, pp. 581–582.

Ronald K. Garlow received a B.S.E.E. from Kansas State University in 1960. He joined COMSAT Laboratories in 1969 and is currently a Senior Scientist in the Network Technology Division, performing system analysis and design of satellite networks. Previously, as manager of the Image Processing Department, he was involved with the design of digital television transmission codecs, and the design of a prototype system for direct-broadcast television. Prior to joining COMSAT, Mr. Garlow was with the Astro-Electronics Division of RCA, where he designed television cameras for use in the Nimbus, Ranger, and TIROS satellites. He is a member of IEEE, Phi Kappa Phi, Sigma Tau, and Eta Kappa Nu.

S. Joseph Campanella received a B.S.E.E. from the Catholic University of America in 1950, an M.S.E.E. from the University of Maryland in 1956, and a Ph.D. in electrical engineering from Catholic University in 1965. He is currently Chief Scientist and Vice President of COMSAT Laboratories. Previously, he served as Executive Director of the Communications Technology Division. He has contributed significantly to technologies for TDMA network control, satellite-switched TDMA, and TDMA terminal development, and has been responsible for the research and development of numerous other satellite communications innovations such as echo cancellers, digital speech interpolation, demand-assigned TDMA, and synchronous burst time plan control. Most recently, his efforts have been devoted to advanced satellite communications concepts involving on-board baseband processing, multiple hopping beams, and intersatellite links. Dr. Campanella is a Fellow of IEEE and AAAS, and an Associate Fellow of AIAA. He received the 1990 IEEE Behn Medal for International Communications. He teaches at George Washington University and holds numerous patents in digital processing techniques.

Index: modems, coding, digital transmission, distortion

140-Mbit/s COPSK modem laboratory tests and transatlantic field trials

D. H. LAYER, J. M. KAPPES, AND C. B. COTNER

(Manuscript received December 14, 1989)

Abstract

Results of laboratory and transatlantic field tests conducted using a 140-Mbit/s information rate, coded octal phase shift keying (COPSK) modem are presented. Laboratory testing included modem bit error rate (BER) performance as a function of receive IF level and frequency variations, as well as introduced IF linear slope, parabolic group delay, and linear amplitude distortion. These tests were performed in linear (back-to-back) and nonlinear (satellite simulator) channel environments. Under nominal conditions, the 140-Mbit/s COPSK system provided a BER of 1×10^{-6} at a lower E_b/N_o than would be required of an uncoded 120-Mbit/s quadrature phase shift keying (QPSK) modem. Laboratory test results also showed that this system is more sensitive to channel distortion than uncoded 120-Mbit/s QPSK; however, performance is dramatically improved by using a transversal equalizer.

Field tests were conducted between INTELSAT Standard-A earth stations in France, the United States, and the United Kingdom, using zone beam transponders on an INTELSAT V-A satellite at 332.5°E longitude. The approach to conditioning the earth station and establishing the optimum operating points of its high-power amplifiers and satellite transponders is described, and the results of the conditioning are presented. The BER measurements are compared with the expected performance, and the results demonstrate performance consistent with current CCIR recommendations. These tests have particular historical significance, since they comprise the first transoceanic digital transmission at 140-Mbit/s information rate via any medium.

Introduction

This paper presents results from laboratory and field testing of the 140-Mbit/s coded octal phase shift keying (COPSK) system (Figure 1) developed by COMSAT Laboratories to accommodate single-transponder global trunking, satellite restoration of transoceanic fiber optic cables, and other high-data-rate applications. Two units of the COPSK system have been built: one for the Intelsat Satellite Services (ISS) division of COMSAT, and the other for INTELSAT. Laboratory tests discussed include linear channel performance (back-to-back) as a function of IF input level and frequency offset. Further tests held the IF input level and frequency offset constant, while introducing added linear and parabolic delay and linear amplitude distortion. During the portion of the laboratory tests involving added distortion, the effect of an IF transversal equalizer on improving performance was demonstrated. Also presented are nonlinear channel laboratory measurements made in conjunction with the INTELSAT V satellite simulator. Field test results demonstrate the performance of both units operated in back-to-back, earth station and satellite loopback, and satellite cross-connect configurations.

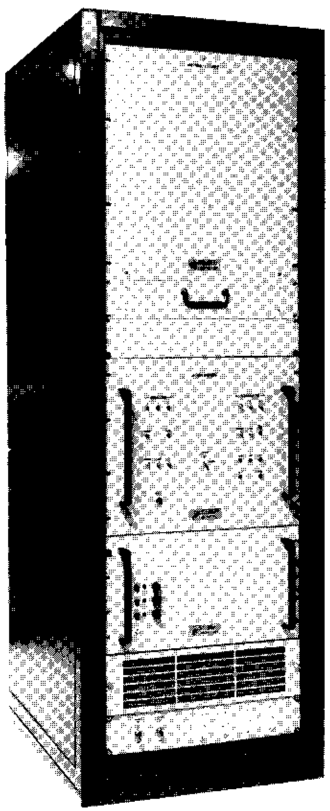

Figure 1. *COPSK System*

(COMSAT Laboratories has previously published the results of research activity in the area of bandwidth- and power-efficient coded modulation systems, in particular those utilizing COPSK. References 1 and 2 present information on the background and theory of this general class of system.)

Satellite testing of the COPSK unit was performed in a two-phase transatlantic field trial. These tests were carried out in cooperation with American Telephone and Telegraph (AT&T), British Telecom International (BTI), France Telecom (DTRE), and INTELSAT, and have historical significance in that they represent the first transatlantic transmission of data at a 140-Mbit/s information rate over any medium, including fiber optic cable. For each phase, similar test plans were followed which included earth station equalization, high-power amplifier (HPA) and satellite traveling wave tube amplifier (TWTA) calibration, earth station and satellite loopback bit error rate (BER) measurement, and one- and two-way (simultaneous) transatlantic BER measurements. Measurements were also made of the spectral spreading of the COPSK signal and the resulting out-of-band emissions (OBEs), and of BER with co-channel interference (CCI).

The COPSK system achieved a BER of better than 1×10^{-7} through a 72-MHz transponder, with an energy-per-bit to noise-power density ratio (E_b/N_o) comparable to or lower than that required for uncoded 120-Mbit/s quadrature phase shift keying (QPSK) [3]. A comparison with 120-Mbit/s QPSK is particularly appropriate for a number of reasons. Both systems use identical data-shaping filters [4], and consequently have identical spectral occupancy. Both systems were designed specifically for use in 72-MHz transponders with 80-MHz spacings and are subject to the same types of adjacent channel interference (ACI) and CCI. Also, because the INTELSAT procedures and specifications for link equalization of 120-Mbit/s QPSK [5] were followed in equalizing the links used during the COPSK tests, the link characteristics should be the same for either type of signal, and thus a valid comparison is possible.

Additional satellite tests of the COPSK system have been conducted [6] as part of digital high-definition television (HDTV) transmission experiments between the U.S. and Japan. During these tests, the BER performance of the COPSK system over a link employing small-aperture earth stations was demonstrated, as was its suitability for use in digital HDTV transmission.

Laboratory testing

Laboratory tests of the two COPSK units were conducted to verify the functionality of each unit and to characterize the performance of the hardware. This testing was undertaken in two stages, with each stage including both linear channel (back-to-back) and nonlinear channel (satellite simulator) tests. In the first stage, system performance was measured *vs* variations in receive IF amplitude and frequency offset. In the second stage, nominal receive IF signal conditions were maintained, while linear slope and parabolic group delay distortions and linear slope amplitude distortions were introduced into the channel. A transversal equalizer was used during the second stage to determine its effect on performance in the distorted channel. The data and discussions which follow on laboratory measurements apply to the ISS unit; however, similar testing was done on the INTELSAT unit, with similar results.

Measurements vs receive IF variations

Figure 2 shows the laboratory test setup for the COPSK unit. Linear channel testing, for the first stage of laboratory tests, was accomplished using the path indicated by the dashed line. BER was measured under combinations of receive IF amplitude and frequency offset extremes, with the amplitude varying from its nominal value to +2 and -10 dB, and the input frequency offset varying from zero to ±25 kHz (the allowable ranges specified for the COPSK unit, corresponding to the INTELSAT requirements in Reference 4). Since the modem is constrained to lock up in two (of eight possible) ambiguity states, the BER was measured in both of these states and then averaged, with the averaged data being presented. Figure 3a shows COPSK performance with no frequency offset over maximum input level variations. The worst-case performance occurs at an input level offset of -10 dB. Figure 3b depicts the effect of frequency offset at this worst-case level.

These measurements demonstrate that the COPSK system is capable of providing a BER of 1×10^{-6} at an E_b/N_o of 10.5 dB under nominal conditions of input level and frequency offset in a back-to-back configuration. This compares favorably with uncoded QPSK, which requires approximately 11.5 dB [3] to achieve the same error rate performance under the same operating conditions but is transmitting only 120 Mbit/s, as compared to the 140-Mbit/s COPSK rate.

Nonlinear channel testing of the system was performed next, using the laboratory setup shown in Figure 2, but this time employing the INTELSAT V satellite simulator. A 72-MHz Ku-band transponder was used. Data were taken for combinations of receive IF level and frequency offset extremes (as in

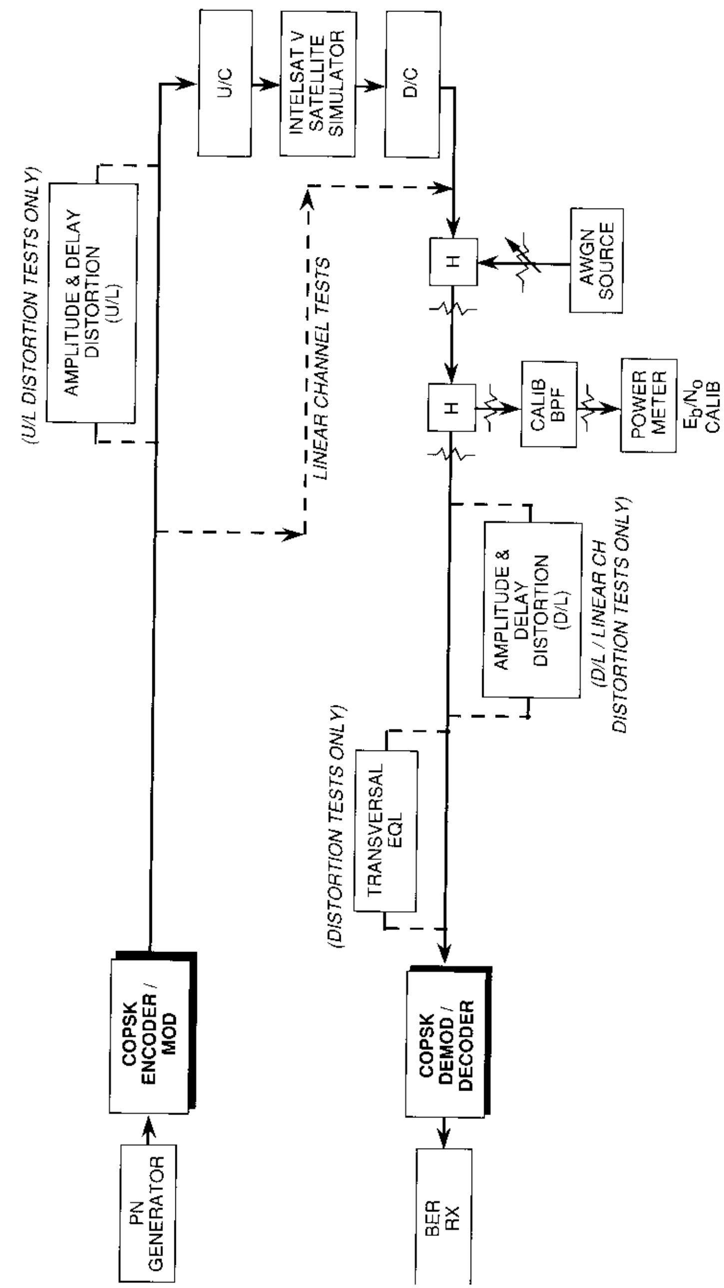

Figure 2. *Laboratory Test Setup*

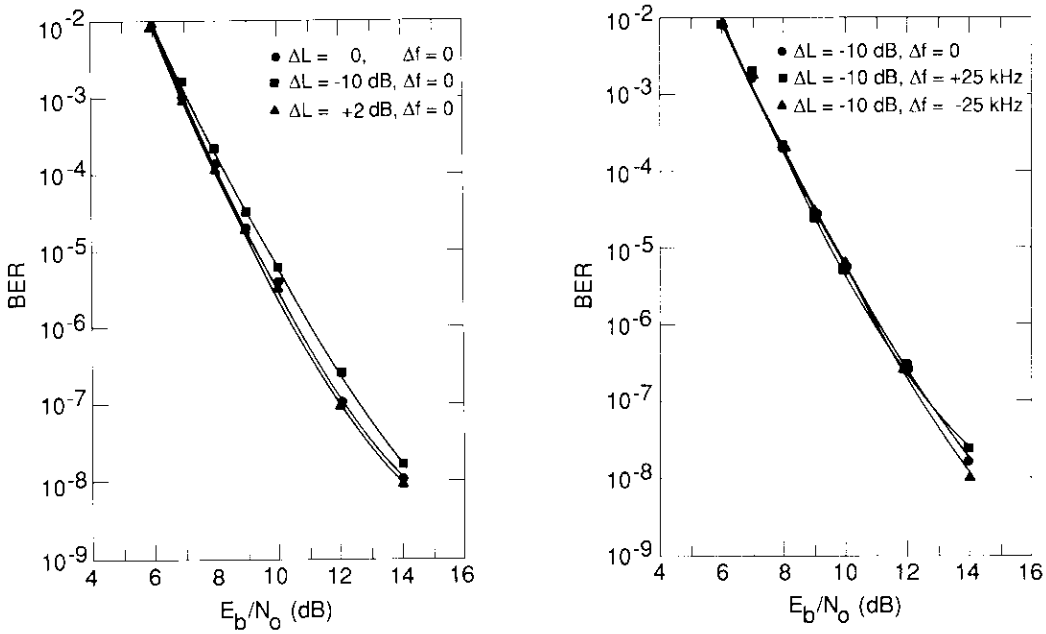

(a) With Input-Level Variation (no frequency offset)

(b) With Frequency-Offset Variation at Minimum Input Level

Figure 3. *Linear Channel BER Performance Parametric in Receive IF Signal Variations*

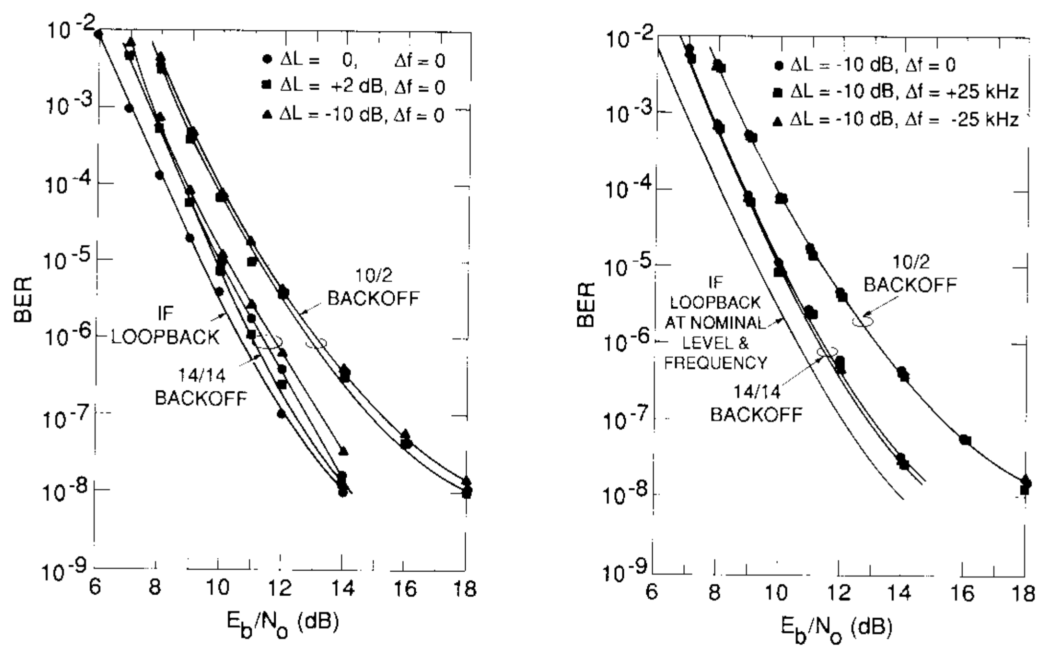

(a) With Input-Level Variation (no frequency offset)

(b) With Frequency-Offset Variation at Minimum Input Level

Figure 4. *Nonlinear Channel BER Performance Parametric in Receive IF Signal Variations and Transponder IBOs*

the linear channel case), and for two values of HPA/TWTA input backoff (IBO) (14/14 and 10/2), in each case with the results from the two (allowed) ambiguity states being averaged. The two backoff combinations were selected to approximate a linear channel (14/14) for the purpose of test setup verification, and in the case of 10/2, to approximate the typical operating conditions of an actual satellite channel.

Figure 4a shows the COPSK performance with no frequency offset over maximum input level variations for the cases of IF loopback (*i.e.*, linear channel), 14/14 backoff, and 10/2 backoff. The performance in the 14/14 case is degraded by approximately 1 dB at a BER of 1×10^{-6} with respect to the IF loopback case (on the average), despite the fact that the TWTA and HPA are being operated in the linear region. This is due to the amplitude and group delay characteristics of the satellite simulator which, while they meet INTELSAT specifications, are more restrictive (*i.e.*, band-limiting) than those of the linear channel setup, and hence introduce a small amount of intersymbol interference. With the backoff set at 10/2, the effect of nonlinear operation of the TWTA becomes apparent, degrading the performance at 1×10^{-6} by an additional 1.5 to 2 dB. Figure 4b illustrates the effect of frequency offset at the worst-case input level of -10 dB from nominal for the 14/14- and 10/2-dB backoff cases.

These nonlinear channel results demonstrate that the COPSK system is capable of providing a BER of 1×10^{-6} at an E_b/N_o of 13 dB under nominal operating conditions with the simulator configured for 10/2-dB HPA/TWTA IBO. As in the linear channel case, this performance compares favorably with uncoded 120-Mbit/s QPSK, which requires approximately 13.5 dB [7] to achieve the same error rate.

Measurements vs introduced IF distortion

Performance of the COPSK system was characterized with IF group delay and amplitude distortions present, for both linear and nonlinear channels, under nominal receive IF level and frequency conditions. During these measurements, a three-tap transversal equalizer was placed in the channel and adjusted to cancel out as much of the introduced distortion as possible. This effort was motivated primarily by the improvement obtained through similar efforts with 120-Mbit/s QPSK operation [8].

The distortion types used for these measurements are listed in Table 1, with only one type of distortion being placed into the channel at a time. The procedure followed for each measurement was to add the distortion, measure the BER performance with no transversal equalizer, then measure the performance again after adjusting the transversal equalizer for best BER.

TABLE 1. DISTORTION TYPES USED IN LABORATORY TESTING OF COPSK SYSTEM

DISTORTION	VALUE*
Linear Group Delay	(2, 4, 6) ns Positive Slope (4, 8, 10, 12) ns Negative Slope
Parabolic Group Delay	(5, 9) ns Concave Up (4, 8, 12, 14) ns Concave Down
Linear Amplitude	(2, 4, 6) dB Positive Slope (2, 4, 6) dB Negative Slope

* Over a ±36-MHz frequency span.

Refer again to Figure 2 for a block diagram of the test setup used for linear channel distortion measurements. The measurement results for the linear channel case are summarized in Figure 5. In each graph, the upper and lower curves represent system performance without and with the transversal equalizer, respectively. It appears that the unequalized response of the system to linear group delay slope is not symmetrical about the 0-ns point, but is instead symmetrical about approximately -2 ns. This skewing of the response is the result of a +2-ns delay slope inherent in the equalizer used for these measurements. Symmetry is observed about the -2-ns point on the curve, since this amount of introduced distortion cancels out the residual distortion of the equalizer.

Compared to similar data obtained with 120-Mbit/s QPSK [8], and taking the residual skew of the equalizer into account, the COPSK system appears (on the average) to be about twice as sensitive (*i.e.*, experiences twice as much degradation, in dB, at a BER of 1×10^{-7}) to all three types of distortion tested, with no transversal equalizer present. However, in spite of this increased sensitivity, the transversal equalizer is able to bring the system performance to within approximately 0.5 dB of that achieved with no added distortion, which represents a greater improvement than that experienced with QPSK.

For the nonlinear channel, two different cases were considered, namely introduced up-link and down-link distortion. In each case, the TWTA in the simulator was operated at 2-dB IBO, which approximates the operating point used in an actual link. Refer again to Figure 2 for a block diagram of the nonlinear channel test setup. The results of the down-link distortion tests are shown in Figure 6. The test results for this case, for all distortion types, were similar to those obtained in the linear channel case. The skew in the linear group delay slope distortion case previously discussed is again apparent.

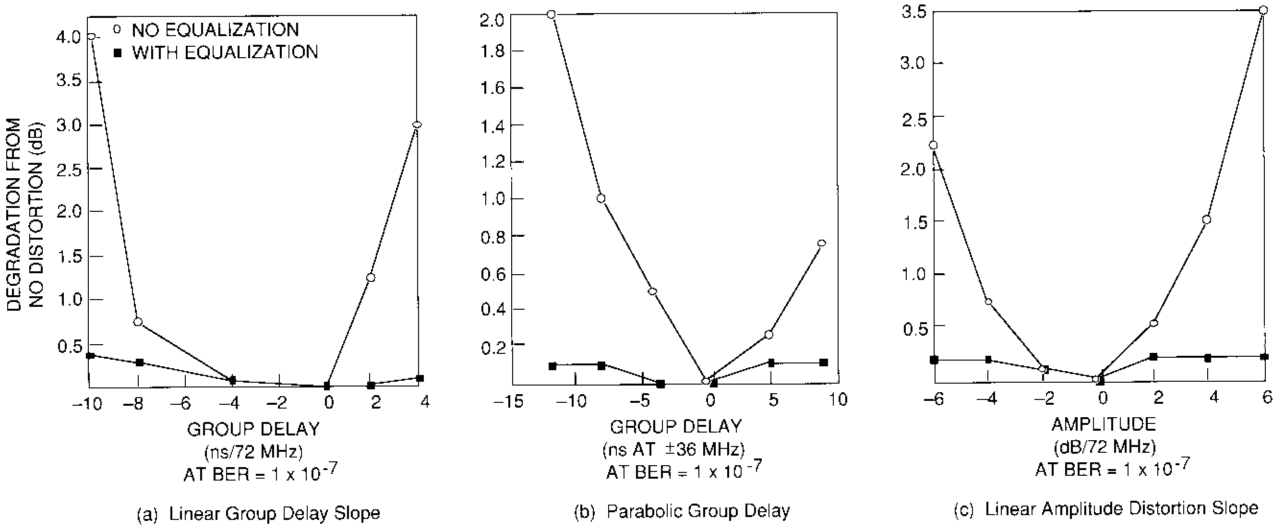

Figure 5. *Linear Channel Performance Degradation vs Group Delay and Amplitude Distortion*

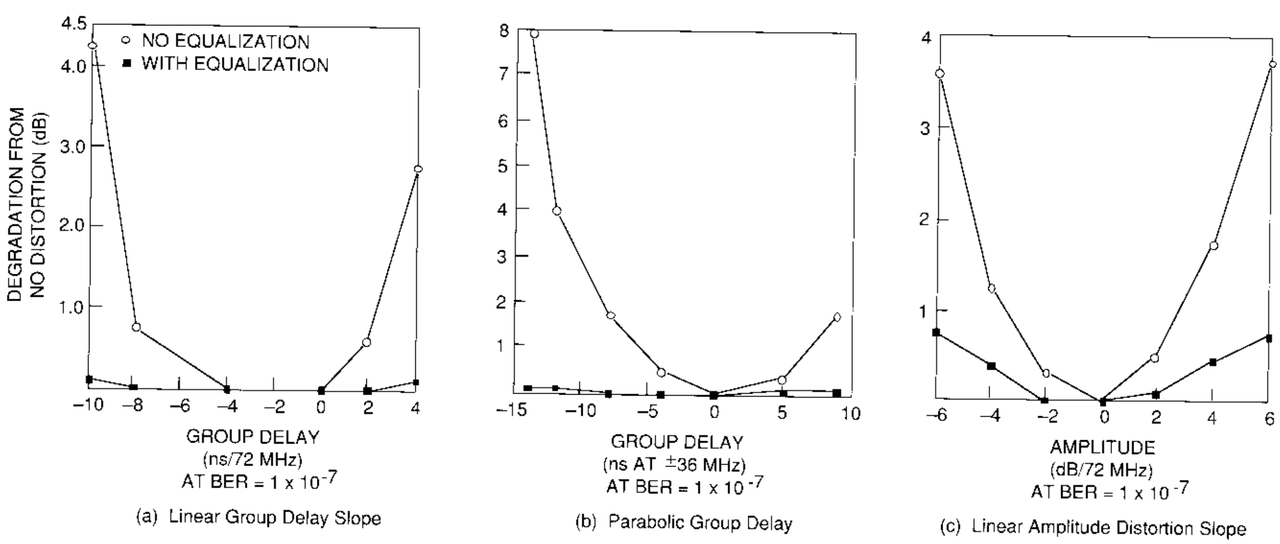

Figure 6. *Nonlinear Channel Performance Degradation vs Down-Link Group Delay and Amplitude Distortion*

Figure 7 shows the results of the up-link distortion tests. In this case, the transversal equalizer is not as effective in improving the performance as it was for the nonlinear channel down-link and linear channel setups. As discussed in Reference 8, this is to be expected due to the nonlinearity between the distortion element and the equalizer.

A comparison of the nonlinear channel results with those obtained for QPSK [8] reveals that, on the average, in the case of down-link distortion, the COPSK system is two to three times as sensitive to both types of group delay slope, and is equally sensitive to amplitude slope. Also, as was true for QPSK, the transversal equalizer provides significant improvement over the unequalized performance. For up-link distortion, COPSK is about five times more sensitive to linear group delay slope, three times more sensitive to parabolic delay slope, and one to two times as sensitive to linear amplitude distortion slope. However, the transversal equalizer appears to be more effective at improving this performance than it was for QPSK, particularly in the parabolic group delay and linear amplitude distortion cases.

Transatlantic field trials

Field testing of the COPSK system through an INTELSAT V-A satellite across the Atlantic Ocean proceeded in two phases. The first involved transmission between the Roaring Creek (Bloomsburg, Pennsylvania, USA) and Goonhilly (Helston, Cornwall, UK) earth stations, and the second between the Roaring Creek and Pleumeur-Bodou (Pleumeur-Bodou, FR) earth stations. For phase I, the ISS unit was shipped to Roaring Creek and the INTELSAT unit to Goonhilly. For phase II, the INTELSAT unit was moved to Pleumeur-Bodou.

After appropriate station equalization, loopback testing was performed at all earth stations in back-to-back, station loopback, and satellite loopback configurations. This was followed by one-way and simultaneous transmission transatlantic testing. Equalization was performed according to INTELSAT TDMA earth station requirements for up- and down-links [5]. The OBE characteristics of the COPSK signals were checked at all three locations for compliance with INTELSAT specifications. The effects of CCI on BER were measured in the satellite loopback configuration at Roaring Creek and Pleumeur-Bodou, and in the transatlantic configuration from Goonhilly to Roaring Creek and Roaring Creek to Pleumeur-Bodou, by inserting a 120-Mbit/s QPSK interferer in the down-link.

The parameters of the three earth stations are listed in Table 2. The equivalent isotropically radiated power (e.i.r.p.) values given in this table are those actually measured during the transatlantic transmission, and correspond to the

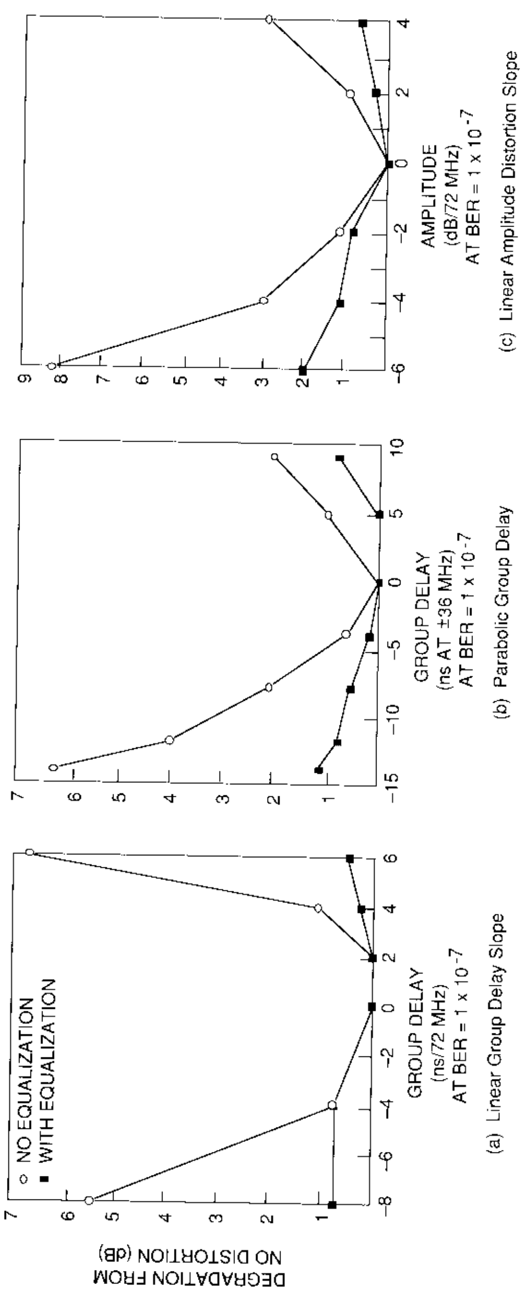

Figure 7. Nonlinear Channel Performance Degradation vs Up-Link Group Delay and Amplitude Distortion

TABLE 2. EARTH STATION PARAMETERS

PARAMETER	ROARING CREEK	GOONHILLY	PLEUMEUR-BODOU
Location	Bloomsburg, PA (USA)	Helston, Cornwall (UK)	Pleumeur-Bodou (France)
INTELSAT Standard Class	A	A	A
INTELSAT Earth Station Code	RCK-1	GHY-1	PB-3
Antenna Diameter (m)	32	25.9	30
Transmit Gain (dB)	64.5	61.5	64.2
Elevation Angle	21.0°	27.9°	29.0°
e.i.r.p. (for TWTA 2-dB IBO) (dBW)	83.9	82.8	80.2
Earth Station *G/T* (dB/K)	41.4–41.6	40.7	40.7
HPA Type	3-kW Klystron	3-kW TWTA	3-kW TWTA
Output Backoff Used	8 dB	3 dB	(Linear)*

*Saturation point of HPA not measured.

values required to achieve approximately 2-dB IBO at the satellite TWTA. The difference in e.i.r.p. values measured at Goonhilly and Pleumeur-Bodou was not resolved, but was most likely due to calibration errors. Time constraints did not permit recalibration of the net coupling loss. The elevation angles given are required for determining the OBE specification point. Satellite parameters are given in Table 3, and were the same for both phases of the field test.

Link performance calculations

To estimate the performance expected during the field tests of the 140-Mbit/s COPSK system, as well as for general operation, link budgets were prepared. First, upper bounds on expected performance were calculated using pre-launch e.i.r.p. data. These data were about 1.5 dB better than the specified performance for the transponders [42/52, West-Zone/East-Zone (WZ/EZ)] and the particular satellite involved (INTELSAT V-A, F-11). The upper performance bounds assume only thermal noise contributions. Performance in the direction of the participating earth stations was estimated from coverage patterns given in the *INTELSAT Earth Station Standards* (IESS) [9]. Perfect earth station antenna pointing was assumed. These link budgets are contained in the "Upper Bound" column of Table 4.

TABLE 3. SATELLITE PARAMETERS FOR THE TRANSATLANTIC FIELD TESTS

PARAMETER	VALUE
Satellite	INTELSAT V-A, F-11, 332.5°E Longitude
Transponder	Ch. 3-4 Zone Beam (42 + 52)
Up-Link Frequency	6050 MHz (RHCP)
Down-Link Frequency	3825 MHz (LHCP)

Note that, at the desired operating point of the transponders, some considerable suppression of up-link thermal noise (and other up-link impairments) was expected. Because the transponders used TWTAs, approximately 8.0-dB small-signal suppression and 3.7-dB compression (based on actual TWTA measurements [10] of large and small unmodulated signals) were assumed at the operating point. Consequently the upper bound on one-way link performance was established as 24.2-dB E_b/N_o from the United States to Europe and 24.5-dB E_b/N_o from Europe to the United States.

Having established the upper bounds, interference and other impairments were introduced into the link budgets. For these budgets, satellite e.i.r.p. from the IESS [11] was assumed, with slightly less satellite pattern advantage to account for the locations of other earth stations relative to the satellite. An allowance of 0.5 dB was introduced for earth station antenna pointing tolerance.

The carrier-to-interference ratio *(C/I)* for ACI was taken as 30 dB, based on earlier work [12] for a similar COPSK carrier in one adjacent transponder bank. (A transponder bank consists of the two co-frequency hemi-beam transponders and the two co-frequency zonal-beam transponders.) An allowance of 0.7 dB was made for adjacent satellite interference, corresponding to 15 percent of the link noise (in accordance with CCIR Recommendation 523).

CCI was estimated by assuming three interference entries, each 30-dB down from the two geographically isolated and one oppositely polarized transponders in the bank. An earth station antenna axial ratio of 1.06 was also assumed. Therefore, the net *C/I* is 24.1 dB on both the up- and down-links. Assuming a 60-MHz noise bandwidth, this equates to a co-channel *C/I* noise density entry of 101.9 dB-Hz.

With the interference contributors given above, and using a more conservative value for satellite e.i.r.p. performance, the expected link performance is an E_b/N_o of 16.5 to 16.7 dB, taking into account the small-signal suppression

TABLE 4. LINK BUDGETS FOR 140-Mbit/s COPSK OPERATION*

PARAMETER	UPPER BOUND		NOMINAL EXPECTED	
	TO EUROPE	TO USA	TO EUROPE	TO USA
Earth Station e.i.r.p. (dBW)	82.4	82.3	82.9	82.8
Up-Link Path Loss (dB)	200.1	200.0	200.1	200.0
Pointing Error (dB)	–	–	0.5	0.5
Satellite G/T (dB/K)	-4.0	-4.0	-4.0	-4.0
Boltzmann's Constant (dBW/HzK)	-228.6	-228.6	-228.6	-228.6
Up-Link Thermal (dB-Hz)	106.9	106.9	106.9	106.9
Co-Channel Int. (dB-Hz)	–	–	101.9	101.9
Adjacent Channel Int. (dB-Hz)	–	–	107.8	107.8
Up-Link C/kT (dB-Hz) Transponder Input	106.9	106.9	99.9	99.9
G, 1 m^2 (dB)	37.1	37.1	37.1	37.1
Operating Flux Density (dBW/m^2)	-80.6	-80.6	-80.6	-80.6
Satellite Flux Density (dBW/m^2)	-78.6	-78.6	-78.6	-78.6
Input Backoff (dB)	2.0	2.0	2.0	2.0
Output Backoff (dB)	0.3	0.3	0.3	0.3
Sat. Saturation e.i.r.p. (dBW)	34.2	33.9	32.0	32.0
Operating e.i.r.p. (dBW)	33.9	33.6	31.7	31.7
Intermodulation (dB-Hz)	–	–	–	–
Down-Link Path Loss (dB)	196.0	196.1	196.0	196.1
Pointing Error (dB)	–	–	0.5	0.5
Earth Station G/T (dB/K)	40.7	41.5	40.7	41.5
Down-Link Thermal (dB-Hz)	107.2	107.6	104.5	105.2
Co-Channel. Int. (dB-Hz)	–	–	101.9	101.9
Adjacent Channel Int. (dB-Hz)	–	–	107.8	107.8
Down-Link C/kT (dB-Hz)	107.2	107.6	99.3	99.5
Up-Link C/kT (dB-Hz) Transponder Output	111.2	111.2	102.9	102.9
Net Link C/kT (dB-Hz)	105.7	106.0	97.7	97.9
Adj. Sat. and Terrestrial Int. (dB)	–	–	0.7	0.7
Available C/kT (dB-Hz)	105.7	106.0	97.0	97.2
Available E_b/N_o (dB)	24.2	24.5	15.5	15.7

*For an INTELSAT V-A satellite at 332.5°E with zonal transponders.

and gain compression on the up-link, when signal noise and interference are referred to the output of the transponder. To be conservative, slightly less small-signal suppression (7.3 dB) and slightly more gain compression (4.3 dB) than had been measured on a different space TWTA were assumed. The link budgets for nominal expected operation are given in the "Nominal Expected" column of Table 4.

Using laboratory data obtained on the COPSK equipment (see Figure 4a), and with the E_b/N_o expected for the link (including a quasi-linear TWTA representing an earth station HPA, and a second TWTA driven to 2.0-dB IBO), a BER of about 5 x 10^{-8} to 8 x 10^{-8} was the expected clear-sky performance for 140-Mbit/s COPSK with all four transponders in a bank handling the same type of E_b/N_o signal. A margin of 0.5 to 1.0 dB to a BER of 1 x 10^{-7} appeared to be available. Note that the link is primarily interference-limited, not thermal noise-limited.

The analysis also showed that a 21- to 22-dB C/I is a good choice for investigating the effects of CCI on the overall link.

Earth station equalization and loopback testing

Figure 8 is a simplified block diagram typical of the setups used at each earth station. Indicated on the diagram are the interconnections between the various pieces of earth terminal equipment, as well as the test equipment configurations and signal paths used for equalization and loopback testing. Path A was used for back-to-back testing of the COPSK system BER, which was performed upon arrival at the earth station to ensure proper equipment operation. The vane attenuator and power meter shown connected to the HPA input and output, respectively, were used to determine the HPA power transfer characteristic and saturation point at each site.* During this procedure, the vane attenuator was calibrated with respect to both HPA backoff and station e.i.r.p. so that it would then be possible to set or confirm the station operation point by simply reading the setting of the vane.

Up-link equalization was performed from the COPSK transmit output to the diplexer input. The frequency response of the up-link was measured using a microwave link analyzer (MLA) and a broadband down-converter, in accordance with INTELSAT TDMA equalization procedures [5]. During equalization, the HPA was operated well backed-off to ensure linear response. Fixed and/or adjustable equalizers were added, as shown, to flatten the up-link

*The saturation point was not measured at Pleumeur-Bodou, since linear operation during the test was ensured by virtue of the low loss between the HPA output and the antenna feed.

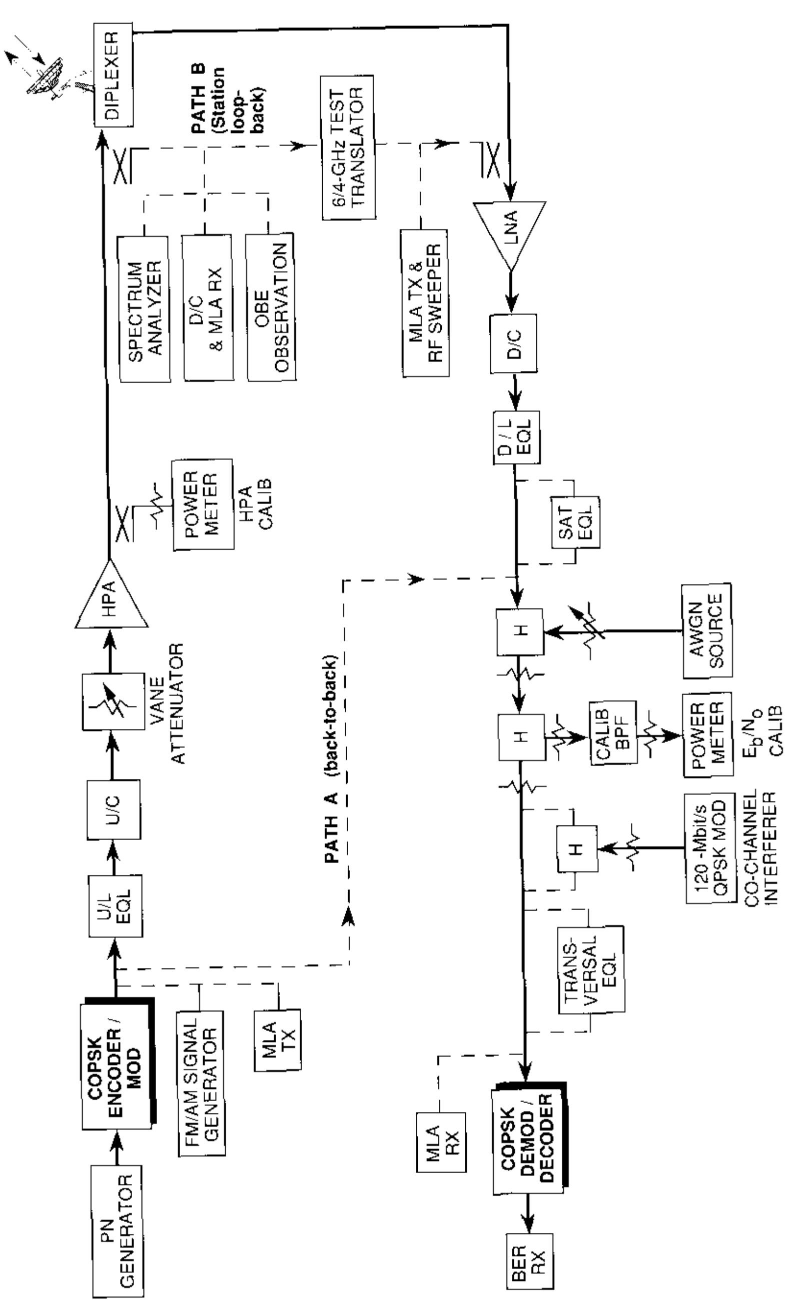

Figure 8. *Simplified Block Diagram of Earth Station Configuration for the Transatlantic Field Tests*

amplitude and group delay characteristics. At Roaring Creek, it was possible to bring this response within the masks specified in Reference 4; however, due in large part to the time constraints of the field tests, the responses at Goonhilly and Pleumeur-Bodou were left slightly out-of-spec. In a similar manner, the down-link was equalized from the diplexer output to the COPSK receive input. After equalization, the Roaring Creek and Pleumeur-Bodou responses were within the INTELSAT masks [4], while the Goonhilly response was left out-of-spec by a small amount, again because of scheduling considerations.

Station loopback BER testing was performed using path B* of Figure 8. For this test, two HPA operating points were used, one well within the linear region and the other corresponding to that required for 2-dB IBO of the satellite TWTA. This second operating point was established by measuring TWTA saturation while the satellite was configured in a loopback mode. Table 5 lists the HPA operating points measured. The lower backoff values (and thus higher HPA drive levels) at Goonhilly are a result of the lower antenna gain at that site (refer to Table 2). Nonlinear operation of the Goonhilly HPA is indicated by the fact that a 3.6-dB change in the HPA input drive was required in order to effect a 2-dB change in the TWTA drive level. At Roaring Creek and Pleumeur-Bodou, the corresponding changes in input drive were 2.2 and 2.0 dB, respectively.

TABLE 5. HPA OPERATING POINTS

EARTH STATION	SATELLITE TWTA SATURATION		SATELLITE TWTA 2-dB IBO	
	HPA IBO (dB)	e.i.r.p. (dBW)	HPA IBO (dB)	e.i.r.p. (dBW)
Roaring Creek	9.5	85.9	11.7	83.9
Goonhilly	6.0	84.8	9.6	82.8
Pleumeur-Bodou	–	82.2	–	80.2

Figure 9 depicts the station loopback BER performance curves for Roaring Creek, Goonhilly, and Pleumeur-Bodou. The performance compares favorably with back-to-back measurements made on the COPSK system (Figure 3); and at Goonhilly, for the linear HPA case, the performance is actually better. This may be due to the difference in the amplitude and group delay characteristics of the two configurations. When operated for TWTA saturation,

*At Goonhilly, it was not possible to connect the output of the test translator to the low-noise amplifier (LNA) input due to the equipment arrangement at the antenna site. Instead, a point accessible at the LNA output was used.

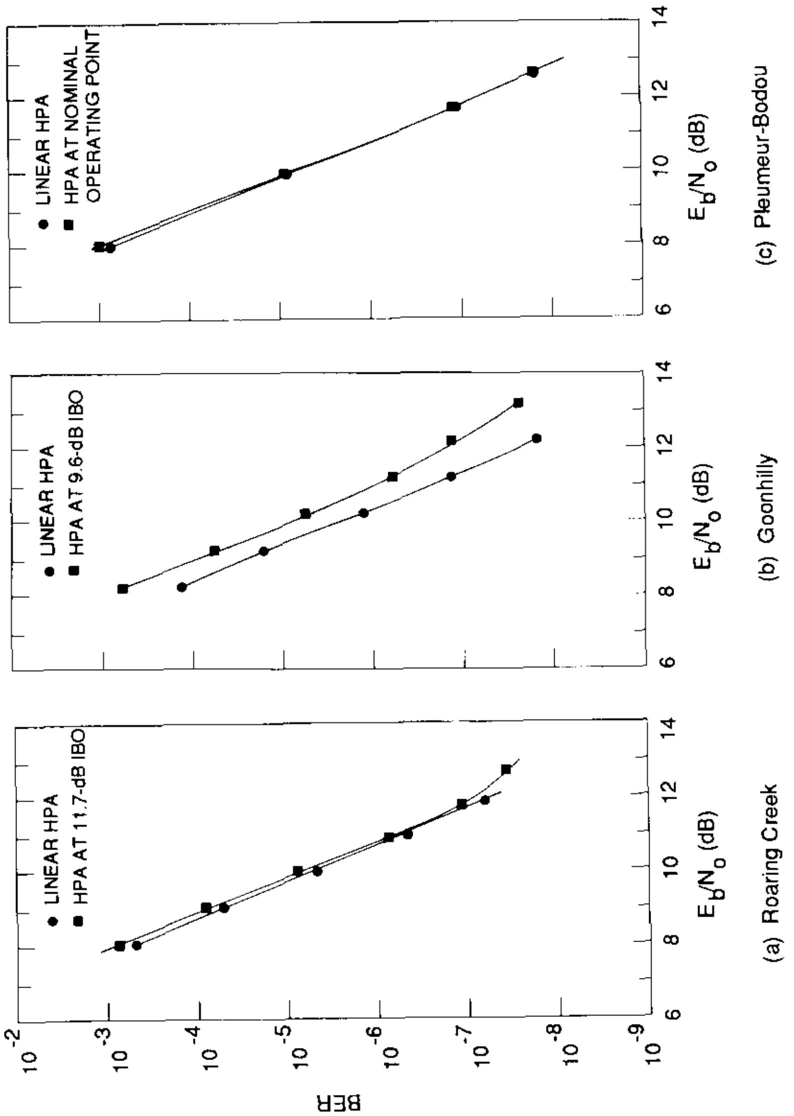

Figure 9. *Earth Station Loopback BER vs* E_b/N_o

however, the Goonhilly performance is degraded due to the nonlinear HPA operating point discussed earlier. This effect can also be seen in the Roaring Creek data, but to a lesser extent. The BER performance at Pleumeur-Bodou is nearly identical at the two HPA operating points, indicating basically linear HPA operation.

HPA spectral spreading

Observations were made at the antenna feed couplers at each site (see Figure 8), with the HPA operating point set for satellite TWTA 2-dB IBO,* to establish the amount of spectral regrowth experienced by the COPSK signals and to verify that these signals were not violating INTELSAT requirements regarding OBEs [4]. The HPA output spectrum observed at Roaring Creek is shown in Figure 10 and is typical of that seen at all three sites. In addition to spectral regrowth, discrete frequency components are also visible due to the 1, 0 pattern used in the system preamble.

Based on the antenna elevation angle for each site (refer to Table 2), the allowable signal power at ±44 MHz from the center frequency of each signal was calculated with respect to the resolution bandwidth used to observe the output spectra (10 kHz for Roaring Creek and Pleumeur-Bodou; 1 MHz for Goonhilly) and is given in Table 6. From the known e.i.r.p. value corresponding to each site's spectrum, the spectral density of each signal was then calculated at the ±44-MHz specification point, assuming a signal bandwidth of 60 MHz, and again relative to the resolution bandwidth of the particular observation. The e.i.r.p. and calculated spectral density values are given in Table 6, along with the margins relative to the INTELSAT specification. In each case, the signal spectrum was within the specified limits.

Satellite loopback equalization and testing

A satellite loopback configuration was established at each earth station to measure BER *vs* E_b/N_o. Prior to making this measurement, additional equalization was required in order to compensate for the output multiplex filter onboard the spacecraft, in accordance with INTELSAT procedures. The characteristics of this equalizer are specified by INTELSAT; no further adjustments were made to the earth station equalization.**

*At Goonhilly, two observations were made at operating points corresponding to satellite TWTA IBO values of 1.2 and 5.8 dB.

**At Goonhilly, an additional equalizer was added to compensate for the LNA and associated waveguide, which were not part of the station loopback (as previously discussed).

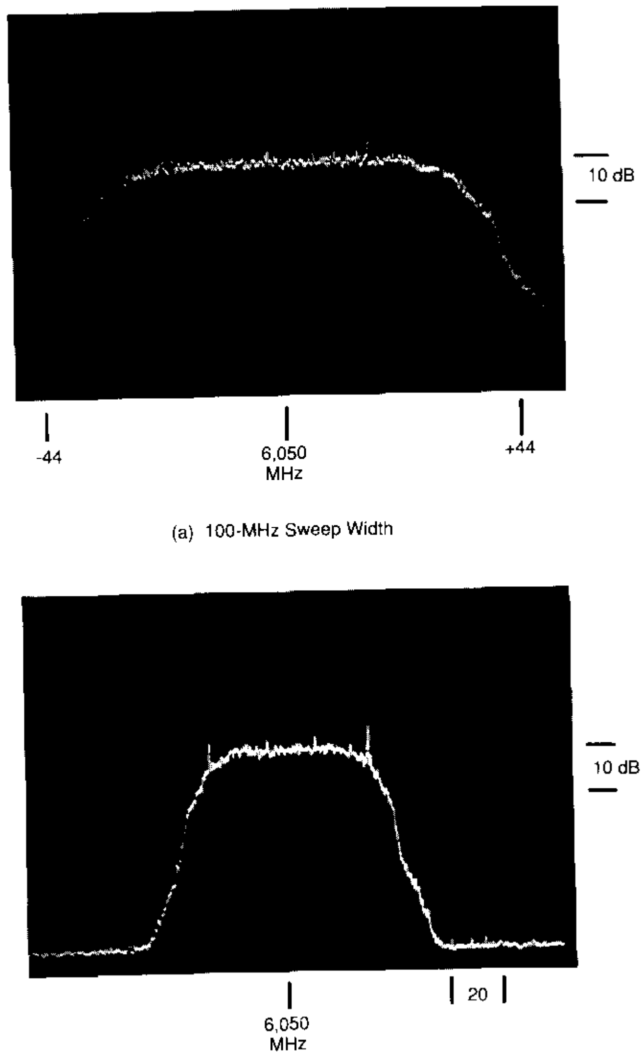

(a) 100-MHz Sweep Width

(b) 200-MHz Sweep Width

Figure 10. *HPA Output Spectrum for the Roaring Creek Earth Station*

TABLE 6. OUT-OF-BAND EMISSION PERFORMANCE

EARTH STATION	OBE SPECIFICATION	OPERATING POINT		SPECTRAL DENSITY AT ±44 MHz *	MARGIN (dB)
		SATELLITE TWTA IBO (dB)	e.i.r.p. (dBW)		
Roaring Creek	26.8 dBW/10 kHz	2.0	83.9	20 dBW/10 kHz	+6.8
Goonhilly	46.6 dBW/1 MHz	1.2	83.6	46 dBW/1 MHz	+0.6
		5.8	79.0	34 dBW/1 MHz	+12.6
Pleumeur-Bodou	26.6 dBW/10 kHz	2.0	80.2	7.4 dBW/10 kHz	+19.2

* Assumes signal bandwidth R_s = 60 MHz.

With the satellite equalizer in place, a frequency sweep of each satellite loopback link was performed using the MLA, and the results were compared with the INTELSAT satellite link response specifications [5]. In each case, the group delay responses did not meet the specifications at the band edges. The specification calls for less than 15 ns of group delay distortion at ±36 MHz. At Roaring Creek, this value was 27 ns at the low band edge and 21 ns at the high band edge. At Pleumeur-Bodou, only the low band edge did not meet specifications and was approximately 17 ns. However, the center portions of both group delay responses were quite flat over a large portion of the band. At Goonhilly, the differential group delay was approximately 20 ns across the band, and the responses indicated some type of interference, which was later identified as relatively low cross-polarization isolation in the antenna feed.

Next, the optimum satellite TWTA operating point was determined by injecting a fixed quantity of white noise into the receive signal at the downconverter output to establish an arbitrary value of BER (approximately 1 x 10^{-6} was used), and then varying the transmit e.i.r.p. with the vane attenuator so as to minimize the BER. Figure 11 shows a plot of the BER *vs* the satellite TWTA

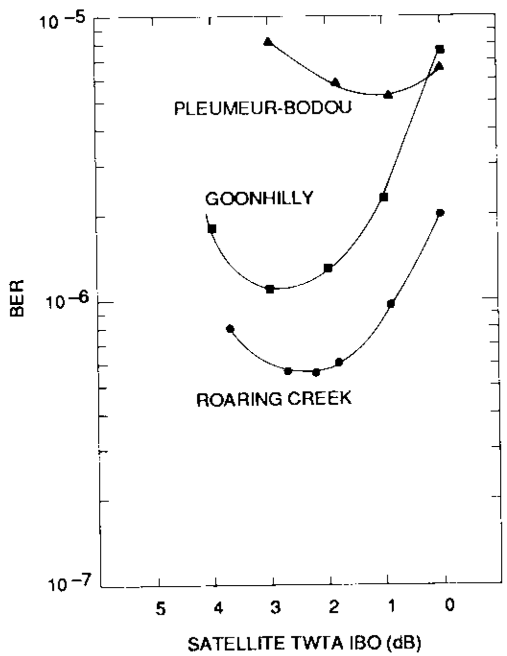

Figure 11. *BER vs Satellite TWTA Operating Point in Satellite Loopback*

operating point for each station. Since the noise added at each station was arbitrary and the E_b/N_o was not measured, the absolute value of the different BER performance curves is not significant.

Based on these data, the satellite transponder operating point for each site was selected. For Roaring Creek and Pleumeur-Bodou, a 2-dB IBO was chosen, partly as a result of discussions held with the various participants during the test plan development. It was decided that 2 dB should be used if the data indicated that the optimum operating point was within 1 dB of the nominal 2-dB operating point of the INTELSAT TDMA system. At Goonhilly, the optimum operating point was found to be 3-dB IBO, and this value was used for satellite loopback measurements. This larger value of backoff is presumed to be due to the predominance of nonlinearity over thermal noise, since the HPA at Goonhilly is operating close to saturation.

With the optimum satellite operating points established, the BER *vs* E_b/N_o was measured, and the results are presented in Figure 12. At Goonhilly and Pleumeur-Bodou, the performance was initially degraded. However, by placing a transversal equalizer in the down-link (in addition to the equalizers

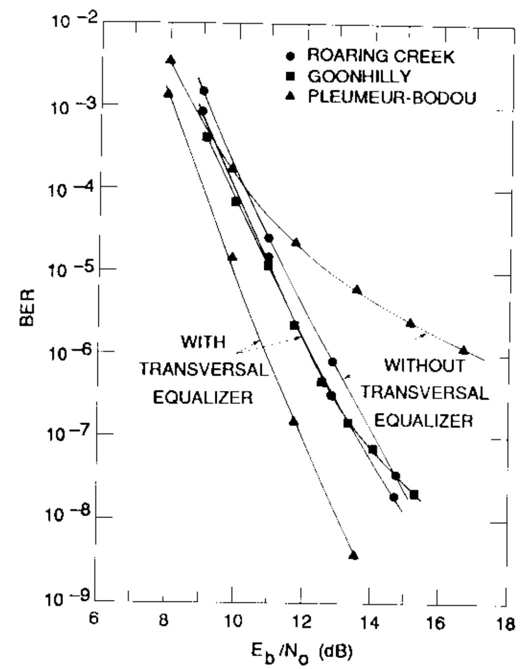

Figure 12. *Satellite Loopback Performance*

already present for station equalization), performance was significantly improved in both cases. A similar effort at Roaring Creek resulted in only about 0.5 dB of improvement at a BER of 1 x 10^{-7}.

It is unclear why the transversal equalizer had such a significant effect on BER performance at Goonhilly and Pleumeur-Bodou. One possibility is that the clock/data relationship within the COPSK demodulator/decoder is being affected by the satellite channel, and the transversal equalizer is compensating for this effect. Further measurements will be necessary to characterize this behavior. Note that the magnitude of improvement obtained with the transversal equalizer in these field measurements is consistent with that experienced in laboratory tests involving IF distortion, but in this case the source of the degradation is unknown.

It is likely that the link to Goonhilly experienced significant down-link interference because of relatively low polarization isolation in the feed. The E_b/N_o performance did not approach the calculated upper bound nearly as closely as it did at Roaring Creek. For instance, the mean E_b/N_o among the three loopback and two transatlantic measurements made at Goonhilly was 19.2 dB; whereas, the bounding link analysis had predicted an E_b/N_o of up to 24.2 dB. In contrast, among the two loopback and two transatlantic measurements made at Roaring Creek, the mean E_b/N_o obtained was 24.8 dB, compared to a predicted upper bound of 24.5 dB, and among the two loopback and two one-way transatlantic measurements made at Pleumeur-Bodou, the mean E_b/N_o obtained was 24.4 dB compared to a predicted upper bound of 24.2 dB.

The values of E_b/N_o used in the above analyses are given in Table 7. It was clearly possible to achieve E_b/N_o values which would produce a BER much lower than 1 x 10^{-7}; however, a primary purpose of the field tests was to demonstrate that 1 x 10^{-7} could be achieved. The time available for the tests was limited, and obtaining meaningful data at very low BERs (even at 140-Mbit/s) is difficult. Therefore, the E_b/N_o range over which measurements were made was purposely limited by injecting noise on the receive side of the links.

Transatlantic equalization and testing

After satellite loopback measurements were completed, the satellite was reconfigured for transatlantic operation. During each phase of the field trial, BER performance was measured with each earth station transmitting in turn, and then with simultaneous transmission from both stations. Additionally, BER performance was measured at Roaring Creek and Pleumeur-Bodou with CCI added on the down-link.

TABLE 7. VALUES OF LINK E_b/N_o EXPERIENCED DURING THE COPSK FIELD TESTS

DATE	DESCRIPTION	LINK E_b/N_o (dB)
3/14/88	RCK–GHY	17.7
3/15/88	Satellite Loopback–GHY	20.2
3/18/88	Satellite Loopback–GHY	19.5
3/20/88	RCK–GHY	19.2
3/22/88	Satellite Loopback–GHY	19.4
5/16/88	Satellite Loopback–RCK	21.1
5/17/88	Satellite Loopback–RCK	26.3
5/18/88	PBD–RCK	26.6
5/19/88	PBD–RCK	25.1
5/16/88	Satellite Loopback–PBD	25.3
5/17/88	Satellite Loopback–PBD	23.4
5/18/88	RCK–PBD (single-carrier transmission)	24.1
5/19/88	RCK–PBD (with PBD carrier transmitting)	22.6
5/19/88	RCK–PBD (single-carrier transmission)	24.7

First, the optimum operating point for each transatlantic link was determined in a manner similar to that used for satellite loopback. BER was then measured with a fixed amount of noise added on the down-link. The satellite TWTA operating point was varied by changing the earth station e.i.r.p. using the vane attenuator. The optimum point for the Roaring Creek-to-Goonhilly link was 2-dB IBO, while for the reverse link it was approximately 4-dB IBO. For the link between Roaring Creek and Pleumeur-Bodou, the optimum operating point was 2.5-dB IBO, and for the reverse link it was 3 dB. It appears from these data that the HPA backoff required at Goonhilly, because of the tradeoff regarding antenna size during the station design, was influencing the BER, and thus contributed to the selection of the optimum operating point. At Roaring Creek and Pleumeur-Bodou, the HPAs were nearly linear for the range of TWTA operating points tested.

As with satellite loopback testing, a satellite equalizer was added to the station down-link at all locations to compensate for the group delay distortion of the transponder output multiplex filter, in accordance with the INTELSAT *Satellite System Operating Guide* for TDMA/digital speech interpolation (DSI) operations [5]. No further adjustments were made to the earth station at Roaring Creek. At Goonhilly and Pleumeur-Bodou, it was again necessary to use the transversal equalizer to obtain satisfactory BER performance.

The amplitude and group delay responses from Goonhilly to Roaring Creek are shown in Figure 13 at 14- and 2-dB IBO of the satellite TWTA, and are typical of those obtained from all sites. The responses are relatively flat over most of the band, but do not quite meet the INTELSAT requirements at the band edges. For the link response from Pleumeur-Bodou to Roaring Creek, the group delay again does not meet the specification at the band edges, but is quite flat over most of the band. The Roaring Creek-to-Pleumeur-Bodou link experienced less group delay distortion at the band edges, and consequently the response just met the INTELSAT requirements for 120-Mbit/s TDMA.

Transatlantic BER measurement results

The BER *vs* E_b/N_o performance curves for the Roaring Creek-Goonhilly transatlantic link are shown in Figure 14a. As can be seen, BER performance from Roaring Creek to Goonhilly was actually better than that observed over the reverse link, even though it was necessary to add a transversal equalizer on the Goonhilly down-link to achieve good performance. A transversal equalizer was also added at Roaring Creek; however, no significant improvement was observed and the equalizer was removed.

The value of interference introduced at Roaring Creek by the outgoing 140-Mbit/s COPSK transmission was measured to be a C/I of 31 dB. This is in good agreement with the 30-dB figure used in the link analysis for one spatially isolated co-frequency transponder. The single simultaneous transmission had little effect on the Goonhilly-to-Roaring Creek BER, as can be seen in the figure.

The BER *vs* E_b/N_o performance curves for the Roaring Creek-to-Pleumeur-Bodou transatlantic link with one-way and simultaneous transmission are shown in Figure 14b. Transversal equalizers were employed for these measurements at both locations. A BER of 4×10^{-10} was achieved on the Roaring Creek-to-Pleumeur-Bodou link at an E_b/N_o of approximately 17 dB. It is interesting to note that, as with the Goonhilly link, it was necessary to add the transversal equalizer to obtain reasonable performance; yet with the equalizer in use, the performance was actually better than that of the reverse link.

Although it appears from the curves of Figure 14b that the simultaneous transmission performance from Roaring Creek to Pleumeur-Bodou was superior to the one-way performance, the difference is actually the result of taking the data for these curves on different days. As mentioned above, this is one

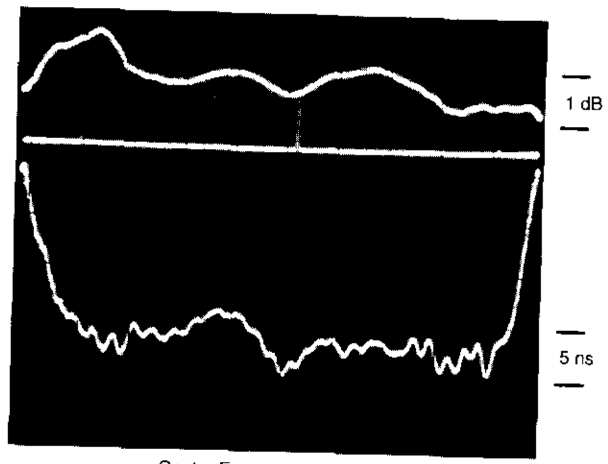

Center Frequency = 140 MHz
Markers at ±30 MHz

(a) At 14-dB IBO

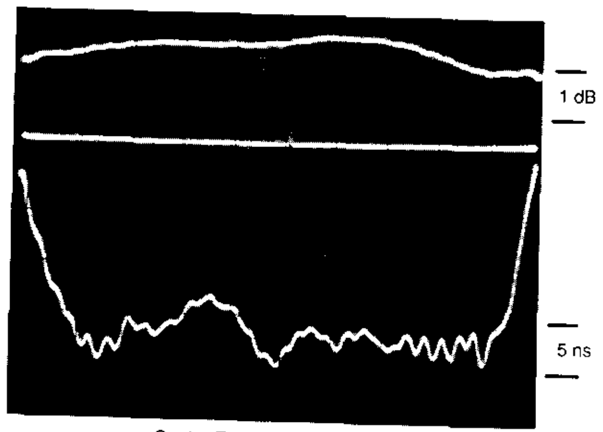

Center Frequency = 140 MHz
Markers at ±30 MHz

(b) At 2-dB IBO

Figure 13. *Goonhilly-to-Roaring Creek Amplitude and Group Delay Swept Response*

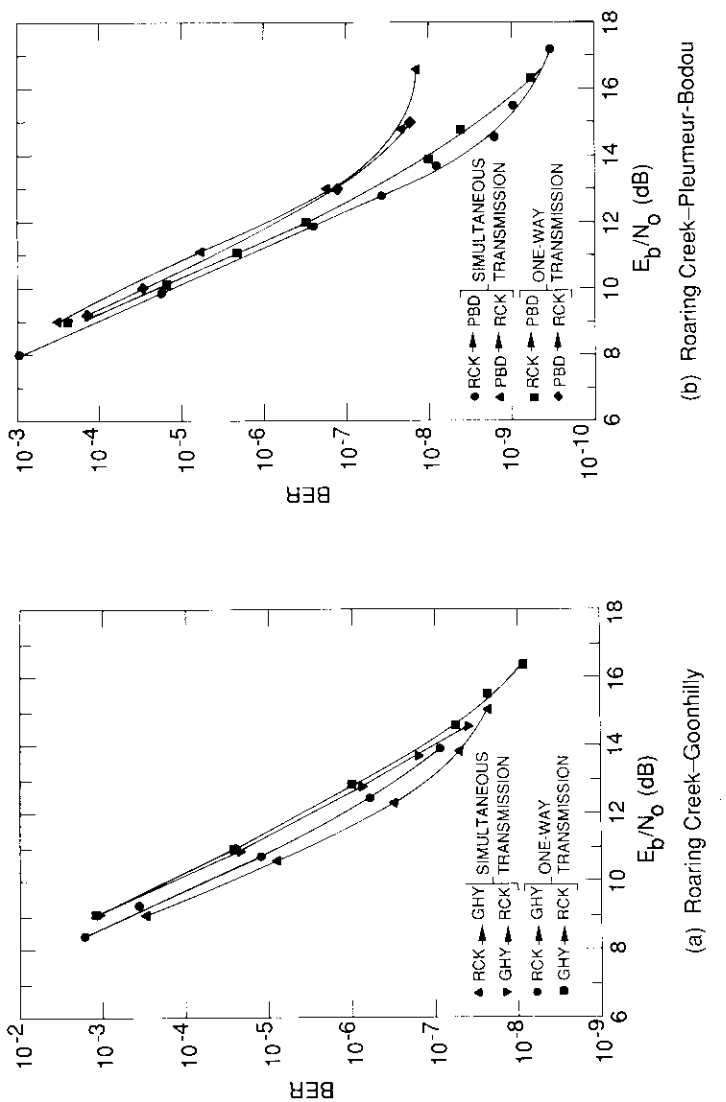

Figure 14. *Transatlantic BER Performance*

indication of the repeatability of these measurements from one day to the next. To validate this, a single point was compared with one-way and simultaneous transmission, and there was approximately 0.1 dB of degradation for simultaneous transmission at 1×10^{-7} BER.

The effects on BER performance of CCI added on the down-link at Pleumeur-Bodou were also measured. Figure 15 summarizes these data at *C/I* values of 18, 21, and 24 dB.

Summary

Extensive laboratory and field testing of the COPSK system have demonstrated the feasibility of 140-Mbit/s data rate transmission through a 72-MHz-wide satellite transponder, in a manner which compares very favorably with that of 120-Mbit/s QPSK. In the laboratory, undistorted linear and nonlinear

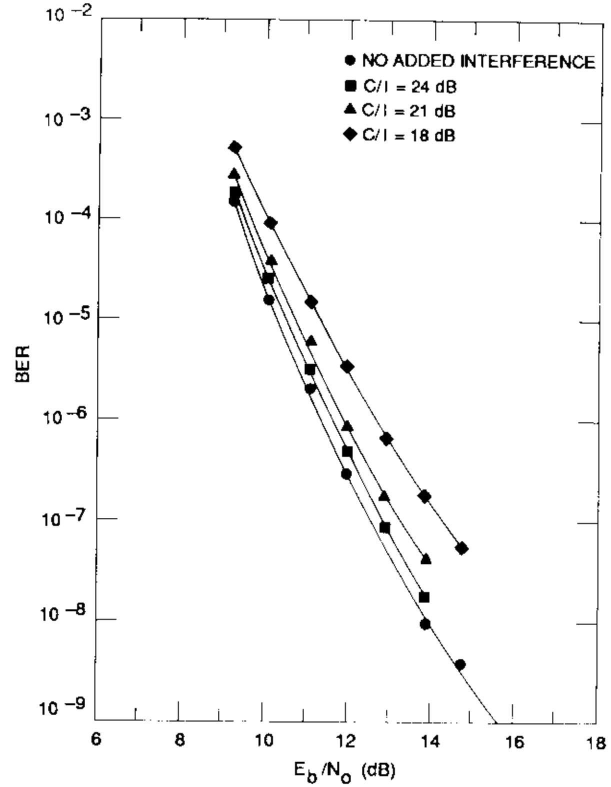

Figure 15. *Roaring Creek-to-Pleumeur-Bodou BER Performance With CCI*

channel performance was shown to be better than that obtained with uncoded 120-Mbit/s QPSK at comparable values of E_b/N_o. Greater sensitivity to linear slope, parabolic group delay distortion, and linear amplitude slope distortion than that experienced with QPSK was demonstrated, but was effectively canceled out when a transversal equalizer was placed in the receive signal path.

During the field trials, a BER of 1×10^{-7} or better was achieved for transatlantic two-way operation in both phases of testing, at E_b/N_o values ranging from 12.4 to 14.3 dB. Comparison with the expected nominal link performance shows that more than 1-dB margin should be available for the link to a BER of 1×10^{-7}. This is somewhat better than the performance of the (uncoded) 120-Mbit/s QPSK TDMA system currently in use. For the Roaring Creek-to-Pleumeur-Bodou link, BER was measured down to 4×10^{-10}. Compared to what was actually observed during these tests (Table 7), the E_b/N_o from the expected nominal link performance budgets (Table 4) seems quite conservative. However, for the planning of service, a conservative approach is probably warranted. The OBE characteristics of the COPSK signal were shown to be well within INTELSAT specifications, even with an HPA operating in the nonlinear region.

A transversal equalizer was required at both the Goonhilly and Pleumeur-Bodou earth stations in order to obtain good performance; however, the reason for this is unclear. It is possible that some characteristic of the INTELSAT COPSK unit (as opposed to the ISS unit) requires a transversal equalizer when operated over a satellite link, since this same unit required the equalizer at two different earth stations.

Another important result of the field tests is the relatively stable performance demonstrated by the COPSK system. IF loopback data taken at various times during the field trials revealed almost identical performance. After initial alignment at the earth stations, no adjustments were made to the equipment at Roaring Creek and Goonhilly, and only one adjustment was made to the INTELSAT modem after it was shipped from Goonhilly to Pleumeur-Bodou.

Acknowledgments

Laboratory testing of the COPSK units was carried out through the combined efforts of many persons, including J. Miller, M. Hutchins, D. Lee, and R. Eicher, all of the Communications Technology Division at COMSAT Laboratories.

The field trials were conducted under the direction of the COMSAT ISS Division and with the assistance of INTELSAT, AT&T (USA), BTI (UK), and DTRE (France). The tests were organized and managed by J. Snyder of COMSAT Laboratories. Testing at the earth stations was performed with the assistance of J. Miller and M. Hutchins of COMSAT, and M. Robusto and S. Lange of INTELSAT. N. Becker of COMSAT assisted in setting up the codec at the Goonhilly earth station. J. Weaver, R. Mansell, and T. Jacobs of AT&T; D. Prouse, R. Oppenshaw, and F. Trevaskis of BTI; and G. Marc and M. Mille of DTRE provided essential support at their respective earth stations.

References

[1] S. A. Rhodes, R. J. Fang, and P.Y. Chang, "Coded Octal Phase Shift Keying in TDMA Satellite Communications," *COMSAT Technical Review*, Vol. 13, No. 2, Fall 1983, pp. 221–258.

[2] F. Hemmati and R. J. F. Fang, "Low-Complexity Coding Methods for High-Data-Rate Channels," *COMSAT Technical Review*, Vol. 16, No. 2, Fall 1986, pp. 425–447.

[3] C. J. Wolejsza, J. S. Snyder, and J. M. Kappes, "120-Mbit/s TDMA Modem and FEC Codec Performance," *COMSAT Technical Review*, Vol. 15, No. 2B, Fall 1985, pp. 423–465.

[4] INTELSAT, "INTELSAT TDMA/DSI System Specifications," *INTELSAT Earth Station Standards*, Document IESS-307 and Rev. A, December 1987.

[5] INTELSAT, *Satellite System Operating Guide*, Vol. 3, Book 2, Sec. 3 and 7, October 1986.

[6] S. Matsumoto, M. Saito, E. Faine, M. Mikulicz, and A. Meyers, "First International HDTV Digital Transmission via INTELSAT Satellite," Pacific Telecommunications Conference, January 1990, *Proc.*, pp. 53–61.

[7] M. E. Jones, "Laboratory Hardware Simulation Measurements of 120-Mbit/s QPSK/TDMA Transmission Performance in the INTELSAT V System," 6th International Conference on Digital Satellite Communications, Phoenix, Arizona, September 1983, *Proc.*, pp. I-A-1–I-A-8.

[8] J. M. Kappes, "An Adaptive Equalizer for 120-Mbit/s QPSK Transmission," *COMSAT Technical Review*, Vol. 17, No. 1, Spring 1987, pp. 55–86.

[9] INTELSAT, "INTELSAT VA Satellite Characteristics," *INTELSAT Earth Station Standards*, Document IESS-406, Rev. 3, June 1989.

[10] J. R. Potukuchi, F. T. Assal, and R. C. Mott, "A Computer-Controlled Satellite Communications Monitoring System for Time Division Multiple Access," *COMSAT Technical Review*, Vol. 14, No. 2, Fall 1984, pp. 391–430.

[11] INTELSAT, "INTELSAT Space Segment Leased Transponder Definitions and Associated Operating Conditions," *INTELSAT Earth Station Standards*, Document IESS-410, June 1989.

[12] G. Robinson, O. Shimbo, and R. Fang, "PSK Signal Power Spectrum Spread Produced by Memoryless Nonlinear TWTs," *COMSAT Technical Review*, Vol. 3, No. 2, Fall 1973, pp. 227–256.

David H. Layer received a B.S.E.E. from the University of Maryland, College Park, in 1981, and an M.S.E.E. from Purdue University in 1984. He is a Senior Member of the Technical Staff in the Transmission Processing Department at COMSAT Laboratories, and has recently been working in the areas of high-speed modem development and broadband IF equalizers for digital transmission. Another current area of interest is differential GPS, in particular the distribution of DGPS correction signals by satellite. Since joining the Transmission Processing Department in 1985, Mr. Layer has been involved in the design and development of a number of medium-rate PSK modems for TDM/TDMA applications, utilizing both digital and analog implementations.

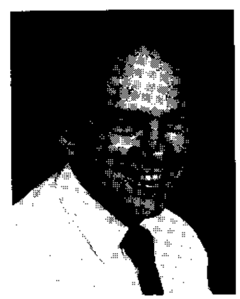

Mark Kappes received a B.S.E.E. and an M.S.E.E. from the University of Illinois in 1971. Since joining COMSAT Laboratories in 1979, he has been involved with the design of high-bit-rate modems and satellite link equalization equipment. As Manager of the Transmission Processing Department, he is responsible for ongoing work in satellite modem technology and associated transmission link equipment. Previously, Mr. Kappes was employed by the Watkins-Johnson Company, where he was responsible for the design of low-noise, high-dynamic-range receivers and special-purpose demodulators.

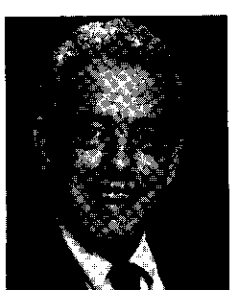

Calvin B. Cotner received a B.S. in electrical engineering, Cum Laude, from Princeton University in 1962, and an M.S.E.E. from Cornell University in 1964. He has been with COMSAT since 1967 and is currently Director of Technical Liaison and Analysis with COMSAT's Intelsat Satellite Services (ISS). His primary technical interests are earth station design, transmission analysis, and high-power amplifiers. He has held several technical management positions in COMSAT Laboratories, COMSAT General, and COMSAT ISS, including representing the U.S. Signatory on the INTELSAT Board of Governors' Technical Advisory Committee for 5 years. He is a colonel in the Signal Corps, U.S. Army Reserve, and a Commandant's List Graduate of the U.S. Army Command and General Staff College. He is a Senior Member of AIAA.

CTR Notes

Results of a 12-GHz radiometric site diversity experiment at Atlanta, Georgia

D. V. ROGERS AND J. E. ALLNUTT

(Manuscript received May 2, 1990)

Introduction

The increasing use of 14/11- and 14/12-GHz satellite communications systems has highlighted the need for accurate prediction methods for estimating the path attenuation caused by rainfall. At frequencies above 10 GHz, rain attenuation can cause unacceptable service outages on some paths. In regions where rain effects are severe, techniques for reducing the impact of rain impairments will be required for some links. One such technique is site diversity, wherein interconnected earth terminals are spaced sufficiently far apart to reduce the probability of joint occurrence of intense rain on the separate paths. Since many factors can affect the performance of such a system, INTELSAT has sponsored a series of site diversity measurements worldwide to study these effects. This note reports the results of a two-site site diversity experiment conducted near Atlanta, Georgia, USA.

Experimental configuration

Passive Dicke-switched radiometers operating at 12 GHz, along with tipping-bucket rain gauges, were deployed at two sites (Atlanta and Cobb County, Georgia) separated by 37.5 km, as shown in Figure 1. The radiometers and rain gauges were identical to those used in earlier INTELSAT experiments, and the same automatic and manual calibration procedures were employed [1].

David V. Rogers, formerly Manager of the Propagation Studies Department at COMSAT Laboratories, is currently with the Communications Research Center, Department of Communications, Government of Canada.

Jeremy E. Allnutt is with the International Telecommunications Satellite Organization (INTELSAT).

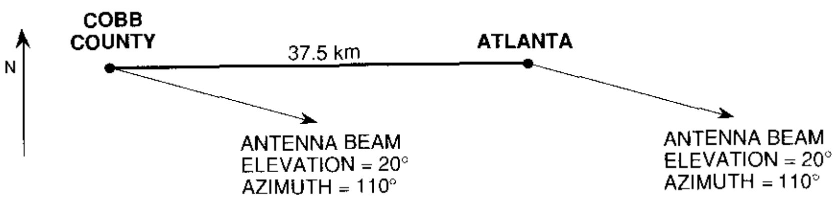

Figure 1. *Configuration of the 12-GHz Site Diversity Measurement Near Atlanta, Georgia*

The data were recorded locally on chart recorders, with time markers, and were later digitized and automatically transferred to magnetic tape for computer analysis.

The data collection period covered the interval from April 1979 through October 1980. However, for a variety of reasons (including occasional equipment malfunctions and a requirement to relocate some of the Cobb County equipment midway through the measurement to accommodate another experiment), joint operation of the two sites was not continuous (see Table 1). The resulting impact on the statistics is discussed later.

Atlanta is located in the southern foothills of the Appalachian mountains at a latitude of 33°39' N and longitude of 84°26' W. It is characterized by a moderately severe rain climate, with an average annual rainfall, M, of 1,236 mm and a convectivity ratio, ß, of 0.30, where ß is defined by Rice and Holmberg [2]. The ß factor is intended to correspond to the fraction of annual rainfall contributed by convective (thunderstorm) activity. That is, on average, 30 percent of the annual rainfall accumulation at Atlanta is presumed to arise from convective rain.

TABLE 1. DETAILS OF THE DATA COLLECTION PERIOD

SITE	TOTAL EQUIPMENT UP-TIME				MEASURED RAINFALL (NORMALIZED TO ANNUAL)
	RADIOMETER		RAIN GAUGE		
	(hr)	(%)	(hr)	(%)	(mm)
Atlanta	10,525	76	11,770	85	1,427
Cobb County	7,564	55	6,875	50	1,055
Joint Distribution	6,232	45	6,232	45	

Measurement results

RAIN RATE STATISTICS

The Rice-Holmberg rain rate model [2] is widely used to predict rain rate statistics. Using the derived ß value of 0.30 and the normalized annual rainfall for the two sites (computed from the measured accumulations of Table 1), rainfall rate statistics were predicted for each location. In Figure 2, these results are compared to the measured rain rate data. Within the accuracy limits of the rain gauge the agreement is quite good, which indicates that the several (presumably random) data gaps did not appreciably alter the cumulative statistics. A similar condition is assumed to prevail for the derived attenuation statistics.

DERIVED ATTENUATION STATISTICS

Attenuation statistics were derived in the standard way, from the measured sky noise data, by applying the well-known relation

$$A = 10 \log [T_m/(T_m - T_s)] \qquad \text{(dB)} \qquad (1)$$

where T_m (K) is the equivalent temperature of the propagation medium (assumed to be 280 K) and T_s (K) is the measured sky noise temperature increase caused by rain, which is obtained by normalizing to the nominal clear-sky noise level prior to rain events. Noise samples were digitized at approximately 1-minute intervals (a sampling rate which has been found sufficient for annual statistics). Due to logarithmic saturation, the accuracy of the attenuation values derived from equation (1) decreases as T_s increases. The error in derived attenuation is estimated to be within ±0.5 dB for levels up to about 6 dB, increasing to about ±1.0 dB for computed rain fades of 10 dB.

Cumulative distributions of attenuation for the individual paths and for the diversity configuration (*i.e.*, the joint path statistics obtained by selecting the lesser of the two single-path attenuations for each sample in the time series) are displayed in Figure 3. These results are based on those periods when both radiometers were operating simultaneously (a total of 6,232 hours).

The curves of Figure 3 can be converted to a useful performance criterion called *diversity gain* [3], which is defined as the difference (in dB) between the average single-site and joint attenuation distributions for a specified time percentage. In Figure 4, the derived diversity gain is plotted *vs* the mean single-site attenuation, as well as *vs* the diversity gain predicted using an empirical model developed by Hodge [3], that predicted by the authors' model (for CCIR rain zone M) [4], and the "ideal" diversity gain representing

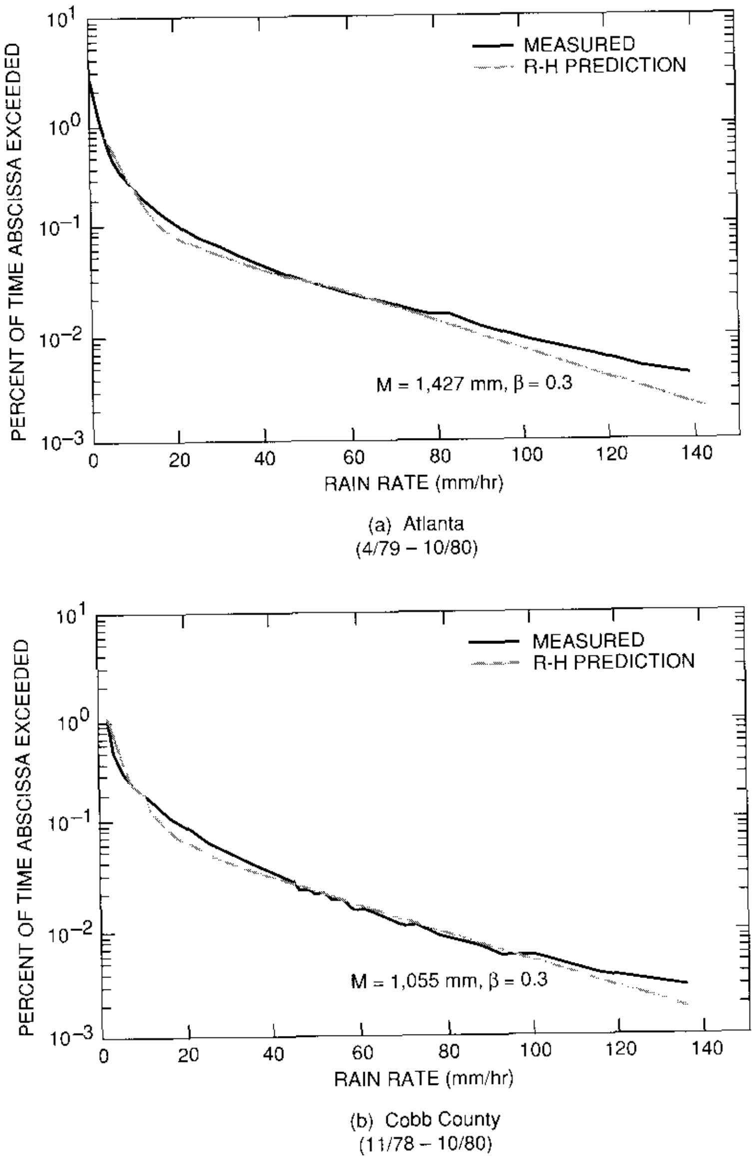

Figure 2. *Measured and Predicted Rain Rate Statistics*

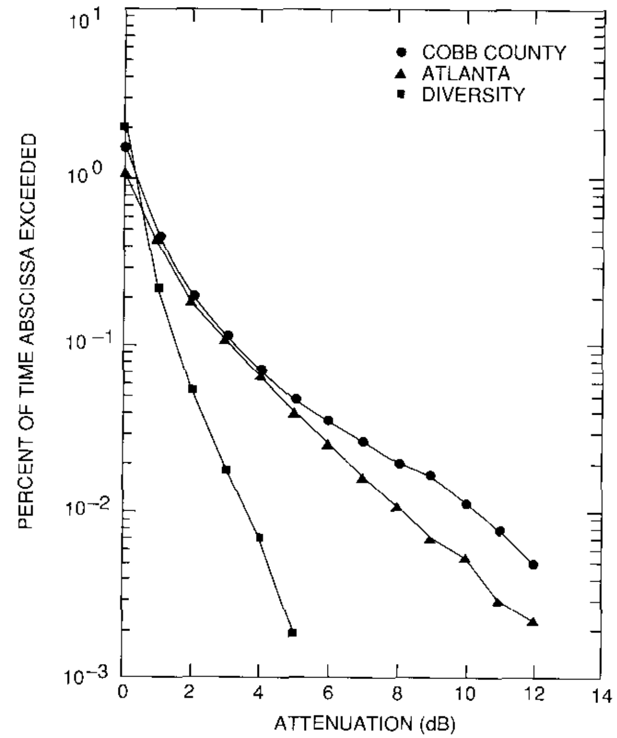

Figure 3. *Measured Cumulative 12-GHz Attenuation Statistics for Atlanta, Cobb County, and the Joint Distribution (4/79–10/80, based on joint experiment time only)*

decorrelated fading on the two paths. Hodge's model is based on rms curve fits to a sequence of diversity parameters, and should replicate average diversity gain behavior very well. Both predicted gains agree rather well with the measured gain; however, a comparison of the measured and predicted gains for many of the available data sets reveals that the performance of Hodge's model is superior overall [5].

Diversity gain for a given location has been demonstrated to be relatively insensitive to single-path fading characteristics, year-to-year variations in slant path impairments, and the length of the experimental period [6]. Figure 4 should therefore represent nominal site diversity performance for the Atlanta locale. The fact that the measured gain curve agrees well with Hodge's model, based on empirical fitting to data, supports this conclusion.

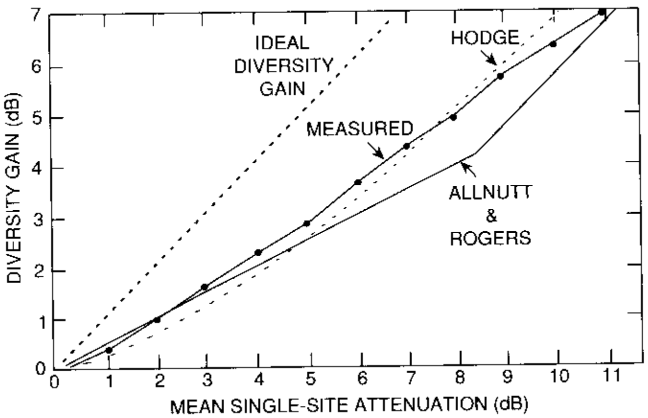

Figure 4. *Measured and Predicted Diversity Gain vs Mean Single-Site Attenuation*

It is instructive to compare the observed diversity gain with corresponding time percentages for the cumulative distributions of single-path attenuation of Figure 3. For example, it can be deduced that diversity gain exceeds 1 dB only for time percentages below about 0.2 percent (*i.e.*, for 99.8 percent of the year, the gain is expected to be less than 1 dB), although site diversity is not, of course, designed for such relatively unimpaired time percentages. At smaller time percentages, the gain is substantial (almost 3-dB gain for a single-site attenuation of 5 dB). Because the dynamic range of radiometers is limited to about 10 to 12 dB due to the saturation effect, it is not possible to deduce diversity gain for higher fades. This limitation is common to much of the diversity site data, and presents a particular difficulty in the testing available site diversity data, and presents a particular difficulty in the testing of site diversity models. The joint attenuation never exceeded 5 dB during the measurement period, and it would be reasonable to assume a fairly linear extension of the measured gain curve of Figure 4 to higher attenuations.

Conclusions

Cumulative statistics for rain rate, single-site attenuation, and site diversity attenuation have been presented for a 12-GHz radiometric measurement conducted near Atlanta, Georgia. The diversity gain results are judged to be representative for the measurement location and configuration, and agree well with the predictions of an empirical site diversity model. Such results are needed for the design of site diversity systems and the development of predictive models.

Acknowledgments

This paper is based on work performed under the sponsorship of the International Telecommunications Satellite Organization (INTELSAT). Views expressed are not necessarily those of INTELSAT. The authors gratefully acknowledge the substantial data processing contributions of P. Kumar.

References

[1] D. V. Rogers, "Diversity- and Single-Site Radiometric Measurements of 12-GHz Rain Attenuation in Different Climates," *IEE Conference Publication No. 195*, Pt. 2, 1981, pp. 118–123.

[2] P. L. Rice and N. R. Holmberg, "Cumulative Time Statistics of Surface-Point Rainfall Rates," *IEEE Transactions on Communications*, Vol. COM-21, No. 10, October 1973, pp. 1131–1136.

[3] D. B. Hodge, "An Improved Model for Diversity Gain on Earth-Space Propagation Paths," *Radio Science*, Vol. 17, No. 6 , November–December 1982, pp. 1393–1399.

[4] D. V. Rogers and J. E. Allnutt, "Evaluation of a Site Diversity Model for Satellite Communications Systems," *Proc. IEE* , Vol. 131, Pt. F, 1984, pp. 501–506.

[5] J. E. Allnutt, *Satellite-to-Ground Radiowave Propagation*, Ch. 4., London: Peter Peregrinus, 1989.

[6] J. E. Allnutt, "Nature of Space Diversity in Microwave Communications via Geostationary Satellites: A Review," *Proc. IEE* , Vol. 125, 1978, pp. 369–376.

Geostationary satellite log for year-end 1989

L. W. KEMP

(Manuscript received January 10, 1990)

Since the last revision of the Geostationary Satellite Log in 1988, more than 40 new satellites have been launched into geosynchronous orbit. Hundreds more are in the planning stage, and industry analysts anticipate an upturn in the number of satellites launched over the next 5 years [1],[2].

This increased activity is taking place in a more complex world environment—one marked by the proliferation of both rival operators and advanced applications. Among the new satellites are the first separate systems authorized to compete with INTELSAT, as well as some of the first privately owned ventures to appear outside the United States. At the same time, markets ancillary to the traditional telecommunications offerings in the Fixed Satellite Service are developing as a result of additions such as direct broadcast satellites, remote sensing, and commercial mobile satellite services. Indeed, the trend toward hybridization of the Insat or Hispasat variety is blurring the customary divisions among categories of spacecraft. These realities are reflected in the updated Satellite Log, which covers all satellites in the geostationary arc. Alternative uses and prospective relocations are noted where known, as are details of system ownership.

Table 1 (see p. 108) lists in-orbit satellites through December 1989. Proposed satellites are listed in Table 2 (see p. 156) at their currently planned orbital positions. The primary source for both tables is the *List of Geostationary Space Stations* [3] compiled by the International Frequency Registration Board (IFRB). This has been supplemented with data from the IFRB's weekly circulars and other documents published by the Federal Communications Commission [4]. Wherever possible, actual subsatellite longitude is derived from NASA situation reports [5],[6], while a variety of secondary sources

---

Louis W. Kemp is a Research Analyst with COMSAT's Intelsat Satellite Services, Marketing and Sales Support.

were consulted to verify technical parameters and other information pertaining to usage and operation [7]–[11].

Inevitably, reliance on the IFRB lists introduces distortions to the data. Delays associated with the registration procedure contribute to a situation in which satellites no longer operative—or in the case of planned systems, no longer under consideration—are still in the ITU process. For clarity, these systems have been retained, but with their current status indicated in the footnotes accompanying each table.

Table 3 (see p. 210) provides an index of the frequency codes used in Tables 1 and 2. Bands of operation are those defined in the Table of Frequency Allocations contained in the *ITU Radio Regulations*. Several common abbreviations are used to denote categories of service, as follows:

FSS	Fixed Satellite Service
BSS	Broadcasting Satellite Service
MSS	Mobile Satellite Service
MMSS	Maritime Mobile Satellite Service
LMSS	Land Mobile Satellite Service
AMSS	Aeronautical Mobile Satellite Service
RNS	Radionavigation Satellite Service
SRS	Space Research Service
EES	Earth Exploration Service
MetSat	Meteorological Satellite Service

The deployment and use of satellites in the geostationary orbit represents a continuous series of changes, punctuated by new launches, reassignments, and the passage of older satellites reaching the end of their stationkeeping lifetimes. The tables below are intended to offer only a snapshot of that process and may contain data that have already become outdated by the time of publication. The author invites both comments and corrections and would welcome additional information for future updates.

Acknowledgments

Special thanks are given to M. Clark, O. Efremov, and S. Fox. The author also wishes to thank C. Schmitt, compiler of previous editions of the Geostationary Satellite Log, for providing a solid base from which to begin.

References

[1] C. H. Schmitt, "Geostationary Satellite Log for Year End 1987," *COMSAT Technical Review, Vol. 18, No. 1, Spring 1988, pp. 65–134.*

[2] M. Giget, ed., *World Space Industry Survey: Ten Year Outlook*, Euroconsult, Paris, 1989, pp. 2–3.

[3] International Frequency Registration Board, *List of Geostationary Space Stations (List A/List B)*, International Telecommunication Union, Geneva, June 1989.

[4] "1990 FCC Authorized Orbital Assignments," Staff Working Paper, Federal Communications Commission, Washington, D.C., March 1990.

[5] National Aeronautics and Space Administration, Goddard Space Flight Center, Project Operations Branch, "Satellite Situation Report," Vol. 29, No. 2, June 1989.

[6] National Aeronautics and Space Administration, Goddard Space Flight Center, Project Operations Branch, Code 513, "Geosynchronous Satellite Report," January 1990.

[7] M. Long, *The 1990 World Satellite Annual*, MLE, Inc., Winter Beach, Florida, 1989.

[8] R. Turnhill, ed., *Jane's Spaceflight Directory*, London: Jane's Publishing, 1989.

[9] W. L. Pritchard, *Satellite Systems Digest*, Satellite Systems Engineering, Bethesda, Maryland, 1988.

[10] R. Stanyard, *World Satellite Survey*, Lloyd's Aviation Department, London, 1987.

[11] D. H. Martin, *Communication Satellites 1958–1988*, Aerospace Corporation, El Segundo, California, 1986.

TABLE 1. IN-ORBIT GEOSTATIONARY COMMUNICATIONS SATELLITES FOR YEAR-END 1989

SUBSATELLITE LONGITUDE[1] (deg)	LAUNCH DATE/ INTERNATIONAL CATALOG NUMBER[2]	SATELLITE DESIGNATION[3]	COUNTRY OR ORGANIZATION	SERVICE FREQUENCY CODE UP/DOWN-LINK (GHz)	ORBIT PARAMETERS[4]	REGISTRATION SPECIAL SECTION NUMBERS
5.1E	11 May 78 1978-44-A 10855	OTS[5] OTS-2	ESA	FSS 14a/11,12a	P 1436.3 r_a 35805 r_p 35776 i 5.6 n -0.0523	IFRB: 5.0E SPA-AA/90/1194
5.6E	2 Apr 89 1989-27-A 19919	TELE-X NOTELSAT	Sweden, Norway	FSS,BSS 14a,17,20a/ 12c,12d,12e,12f	P 1436.1 r_a 35915 r_p 35658 i 0.1 n -0.0009	IFRB: 5.0E AR11/A/27/1535 AR11/C/733/1674
6.0E	11 Dec 88 1988-109-A 19687	SKYNET-4B	UK	FSS,MSS 0.2,0.3a,0.3b, 8a,44/ 0.3a,0.3b,7b	P 1436.1 r_a 35800 r_p 35773 i 2.6 n -0.0009	IFRB: 6.0E AR11/A/22/1531 AR11/C/183/1611 -ADD1/1652
7.0E	4 Aug 84 1984-81-A 15158	EUTELSAT 1-2 EUTELSAT I-F2 ECS 2	Eutelsat	FSS 14a/11,12c,12d	P 1436.1 r_a 35815 r_p 35758 i 0.2 n -0.0009	IFRB: 13.0E SPA-AA/278/1426 SPA-AJ/328/1492 SPA-AJ/330/1492 SPA-AJ/433/1516 AR11/C/445/1644
10.0E	21 Jul 88 1988-63-B 19331	EUTELSAT 1-2 EUTELSAT I-F5 ECS 5[6]	Eutelsat	FSS 14a/11,12c	P 1436.1 r_a 35809 r_p 35763 i 0.2 n +0.0055	IFRB: 13.0E AR11/A/61/1578 -ADD1/1582 -ADD2/1589 -ADD3/1593 AR11/C/1078/1789
10.0E	6 Mar 89 1989-20-B 19876	METEOSAT S1 METEOSAT-4 MOP-1	ESA	MetSat,SRS,EES 2/1.6f,1.6g,0.4g	P 1436.3 r_a 35798 r_p 35783 i 1.0 n -0.0523	IFRB: 10.0E AR11/A/414/1815 AR11/C/1606/1892
11.0E	18 Jan 85 1985-7-A 15484	STATSIONAR-27[7] GORIZONT 11	USSR	FSS 6b,14a/4a,11	P 1436.2 r_a 35794 r_p 35781 i 2.7 n -0.0137	IFRB: 12.0E AR11/A/392/1799 -CORR1/1822 AR11/C/1593/1888
13.0E	16 Sep 87 1987-78-B 18351	EUTELSAT 1-4 EUTELSAT I-F4 ECS 4[6]	Eutelsat	FSS 14a/11,12c	P 1436.1 r_a 35952 r_p 35620 i 0.0 n +0.0055	IFRB: 16.0E AR11/A/218/1685 AR11/C/874/1737 AR11/C/1080/1789
15.6E	16 Jun 83 1983-58-A 14128	EUTELSAT-1 EUTELSAT I-F1 ECS 1[6]	Eutelsat	FSS 14a/11	P 1436.1 r_a 35802 r_p 35769 i 0.1 n +0.0119	IFRB: 10.0 SPA-AA/229/1370 SPA-AJ/327/1492 SPA-AJ/329/1492 SPA-AJ/432/1516 AR11/A/60/1578 -ADD1/1582 -ADD2/1589

TABLE 1. IN-ORBIT GEOSTATIONARY COMMUNICATIONS SATELLITES FOR YEAR-END 1989

SUBSATELLITE LONGITUDE[1] (deg)	LAUNCH DATE/ INTERNATIONAL CATALOG NUMBER[2]	SATELLITE DESIGNATION[3]	COUNTRY OR ORGANIZATION	SERVICE FREQUENCY CODE UP/DOWN-LINK (GHz)	ORBIT PARAMETERS[4]	REGISTRATION SPECIAL SECTION NUMBERS
						-ADD3/1593 AR11/C/230/1617 AR11/C/444/1644
19.2E	8 Feb 85 1985-15-A 15560	ARABSAT 1-A[8] ARABSAT F1 ARABSAT 1	Arab League	FSS,BSS 6b/2.5a,4a	P 1436.1 r_a 35814 r_p 35758 i 0.1 n +0.0055	IFRB: 19.0E SPA2-3-AA/7/1347 SPA-AA/210/1347 SPA-AJ/172/1388 RES33/C/1/1597
19.2E	11 Dec 88 1988-109-B 19688	GDL-6 ASTRA 1A	Luxembourg— Societe Europeene des Satellites	FSS,BSS 14a/11	P 1436.1 r_a 35790 r_p 35783 i 0.1 n -0.0009	IFRB: 19.2E AR11/A/94/1594 -ADD1/1708 -ADD2/1747 AR11/C/614/1657 AR11/C/1283/1827
21.0E	22 Jun 84 1984-63-A 15057	STATSIONAR-19[9] RADUGA 15	USSR	FSS 6a,6b,8a/4a,7b	P 1437.3 r_a 35825 r_p 35794 i 3.4 n -0.2962	IFRB: 23.0E AR11/A/221/1686 AR11/A/239/1693 AR11/C/914/1750 -CORR1/1812 AR11/C/916/1752 -CORR1/1756
21.4E	13 Dec 73 1973-100-B 06974	USGCSS PH2[10] DSCS II F-4[11] DSCS 1-B OPS 9434	US	FSS 8a/7b	P 1436.1 r_a 35794 r_p 35778 i 10.2 n +0.0055	
24.0E	5 Jun 89 1989-41-B 20041	DFS-1 DFS KOPERNIKUS	West Germany	FSS 14a,30a/ 11,12c,12d,20b	P 1436.1 r_a 35865 r_p 35708 i 0.1 n -0.0009	IFRB: 23.5E AR11/A/40/1556 -ADD1/1611 -ADD2/1828 AR11/C/695/1760 -ADD1/1877
26.8E	18 Jun 85 1985-48-C 15825	ARABSAT 1-B[8] ARABSAT F2	Arab League	FSS,BSS 6b/2.5a,4a	P 1436.1[12] r_a 35833 r_p 35740 i 0.1 n -0.0009	IFRB: 26.0E SPA2-3-AA/8/1347 SPA-AA/211/1347 SPA-AJ/173/1388 RES33/C/2/1597
34.7E	20 Oct 88 1988-95-A 19596	STATSIONAR-D3 RADUGA 22	USSR	FSS 6a,6b,8a/4a,7b	P 1436.1 r_a 35833 r_p 35739 i 0.9 n +0.0055	IFRB: 35.0E SPA-AA/340/1480 AR11/C/29/1561 AR11/A/195/1675 AR11/C/1170/1796 -CORR1/1894
40.0E	28 Dec 79 1979-105-A 11648	STATSIONAR-12 GORIZONT 3	USSR	FSS 6b/4a	P 1436.3 r_a 35799 r_p 35782 i 7.5 n -0.0523	IFRB: 40.0E SPA-AA/271/1425 SPA-AJ/304/1469

TABLE 1. IN-ORBIT GEOSTATIONARY COMMUNICATIONS SATELLITES FOR YEAR-END 1989

SUBSATELLITE LONGITUDE[1] (deg)	LAUNCH DATE/ INTERNATIONAL CATALOG NUMBER[2]	SATELLITE DESIGNATION[3]	COUNTRY OR ORGANIZATION	SERVICE FREQUENCY CODE UP/DOWN-LINK (GHz)	ORBIT PARAMETERS[4]	REGISTRATION SPECIAL SECTION NUMBERS
44.4E	25 Oct 86 1986-82-A 17046	STATSIONAR-D4 RADUGA 19	USSR	FSS 6a,6b,8a/4a,7b	P 1436.0 r_a 35787 r_p 35783 i 1.2 n +0.0184	IFRB: 45.0E SPA-AA/154/1262 SPA-AJ/112/1335 AR11/A/196/1675 AR11/C/1171/1796 -CORR1/1894
45.4E	15 Dec 89 1989-98-A 20367	STATSIONAR-D4 RADUGA 24	USSR	FSS 6a,6b,8a/4a,7b	P 1436.0 r_a 35805 r_p 35763 i 1.3 n +0.0312	IFRB: 45.0E SPA-AA/154/1262 SPA-AJ/112/1335 AR11/A/196/1675 AR11/C/1171/1796 -CORR1/1894
48.9E	21 Jun 89 1989-48-A 20083	STATSIONAR-24 RADUGA 1-1	USSR	FSS 6a,6b,8a/4a,7b	P 1436.4 r_a 35815 r_p 35768 i 1.4 n -0.0651	IFRB: 49.0E AR11/A/314/1740 -ADD1/1798 -ADD2/1826 AR11/A/411/1806 -CORR1/1822 AR11/C/1497/1878
50.4E	26 Dec 80 1980-104-A 12120	STATSIONAR-T2[9] EKRAN 6[11]	USSR	FSS,BSS 6a,6b/4a	P 1436.5 r_a 35819 r_p 35769 i 7.1 n -0.0972	IFRB: 99.0E SPA2-3-AA/10/1426 SPA2-3-AJ/7/1469
52.7E	26 Jan 89 1989-4-A 19765	STATSIONAR-5 GORIZONT 17	Intersputnik	FSS 6b,14a/4a,11	P 1436.2 r_a 35789 r_p 35786 i 1.1 n -0.0137	IFRB: 53.0E SPA-AA/93/1197 SPA-AA/150/1271 AR11/C/1114/1793 AR11/C/1200/1809
53.1E	22 Apr 84 1984-41-A 14940	STATSIONAR-5[13] GORIZONT 9	Intersputnik	FSS 6b,14a/4a,11	P 1435.5 r_a 35783 r_p 35766 i 3.4 n +0.1532	IFRB: 53.0E SPA-AA/93/1197 SPA-AA/150/1271 AR11/C/769/1678 AR11/C/889/1743 -ADD1/1800
55.2E	25 Oct 85 1985-102-A 16199	CSDRN[14] COSMOS 1700	USSR	FSS,SRS 14b,14f/11,13c	P 1436.6 r_a 35811 r_p 35781 i 2.0 n -0.1229	IFRB: 95.0E SPA-AA/341/1484 SPA-AA/342/1484 AR11/C/69/1570
56.0E	25 Aug 77 1977-80-A 10294	SIRIO[15] SIRIO-1	Italy	FSS 17/11	P 1436.6 r_a 35862 r_p 35728 i 5.9 n -0.1100	IFRB: 15.0W SPA-AA/73/1174 SPA-AA/102/1204 SPA-AJ/65/1282
57.4E	23 Nov 74 1974-94-A 07547	SKYNET-2B[10]	UK	FSS 8a/7b	P 1437.7 r_a 35838 r_p 35798 i 9.0 n -0.4054	

TABLE 1. IN-ORBIT GEOSTATIONARY COMMUNICATIONS SATELLITES FOR YEAR-END 1989

SUBSATELLITE LONGITUDE[1] (deg)	LAUNCH DATE/ INTERNATIONAL CATALOG NUMBER[2]	SATELLITE DESIGNATION[3]	COUNTRY OR ORGANIZATION	SERVICE FREQUENCY CODE UP/DOWN-LINK (GHz)	ORBIT PARAMETERS[4]	REGISTRATION SPECIAL SECTION NUMBERS
59.5E	30 Oct 82 1982-106-A 13636	USGCSS PH2 INDOC DSCS II F-15	US	FSS 8a/7b	P 1436.1 r_a 35793 r_p 35777 i 3.8 n +0.0184	IFRB: 60.0E SPA-AA/140/1253
60.0E	27 Jan 89 1989-6-A 19772	INTELSAT5A INDOC1[16] INTELSAT V-A IND 1 INTELSAT V-A F-15	Intelsat	FSS 6b,14a/ 4a,11, 12a,12c,12d[17]	P 1436.1 r_a 35804 r_p 35769 i 0.0 n -0.0009	IFRB: 60.0E AR11/A/67/1580 AR11/C/462/1646
62.9E	28 Sep 82 1982-97-A 13595	INTELSAT5 INDOC1 INTELSAT V IND 1 INTELSAT MCS INDOC A INTELSAT V F-5	Intelsat	FSS,MMSS 1.6b,6b,14a/ 1.5b,4a,11[18]	P 1436.0 r_a 35807 r_p 35765 i 0.0 n +0.0055	IFRB: 63.0E SPA-AA/134/1250 SPA-AJ/58/1279 SPA-AA/214/1348 SPA-AJ/176/1389 AR11/C/1095/1791
66.0E	19 Oct 83 1983-105-A 14421	INTELSAT5 INDOC4 INTELSAT V IND 4 INTELSAT MCS INDOC D INTELSAT V F-7	Intelsat	FSS,MMSS 1.6b,6b,14a/ 1.5b,4a,11[18]	P 1436.1 r_a 35803 r_p 35771 i 0.0 n -0.0073	IFRB: 66.0E SPA-AA/253/1419 SPA-AA/275/1425 SPA-AJ/353/1500 SPA-AJ/375/1511 AR11/C/857/1735
67.9E	25 Jun 81 1981-61-A 12564	STATSIONAR-T2[9] EKRAN 7[11]	USSR	FSS,BSS 6a,6b/4a	P 1436.9 r_a 35846 r_p 35757 i 6.8 n -0.1935	IFRB: 99.0E SPA2-3-AA/10/1426 SPA2-3-AJ/7/1469
68.6E	8 Apr 83 1983-28-A 13974	STATSIONAR-20[9] RADUGA 12	USSR	FSS 6a,6b,8a/4a,7b	P 1436.1 r_a 35795 r_p 35778 i 4.5 n -0.0009	IFRB: 70.0E AR11/A/316/1740 -CORR1/1760 AR11/A/387/1798 -ADD1/1826 AR11/C/1193/1804 -CORR1/1822 AR11/C/1499/1878
69.1E	15 Nov 85 1985-107-A 16250	STATSIONAR-20[19] RADUGA 17	USSR	FSS 6a,6b,8a/4a,7b	P 1436.2 r_a 35792 r_p 35786 i 2.0 n -0.0330	IFRB: 70.0E AR11/A/316/1740 -CORR1/1760 AR11/A/387/1798 -ADD1/1826 AR11/C/1193/1804 -CORR1/1822 AR11/C/1499/1878
70.0E	30 Sep 83 1983-100-A 14377	STATSIONAR-T2[9] EKRAN 11	USSR	FSS,BSS 6a,6b/4a	P 1436.9 r_a 35807 r_p 35797 i 4.9 n -0.1999	IFRB: 99.0E SPA2-3-AA/10/1426 SPA2-3-AJ/7/1469

TABLE 1. IN-ORBIT GEOSTATIONARY COMMUNICATIONS SATELLITES FOR YEAR-END 1989

SUBSATELLITE LONGITUDE[1] (deg)	LAUNCH DATE/ INTERNATIONAL CATALOG NUMBER[2]	SATELLITE DESIGNATION[3]	COUNTRY OR ORGANIZATION	SERVICE FREQUENCY CODE UP/DOWN-LINK (GHz)	ORBIT PARAMETERS[4]	REGISTRATION SPECIAL SECTION NUMBERS
72.3E	4 May 79 1979-38-A 11353	FLTSATCOM INDOC FLTSATCOM F-2 FLTSATCOM 2 OPS 6392	US	FSS,MSS 0.3a,8a/0.3a,7b	P 1436.1 r_a 35848 r_p 35723 i 6.1 n +0.0119	IFRB: 72.0E SPA-AA/87/1186 SPA-AJ/169/1382 AR11/A/338/1762
72.4E	10 Jun 76 1976-53-A 08882	MARISAT-INDOC[20] MARISAT F-2 MARISAT 2	US— Comsat General	FSS,MSS,MMSS 0.3a,1.6b,6b/ 0.3a,1.5b,4a[21]	P 1436.2 r_a 35806 r_p 35768 i 6.7 n -0.0073	IFRB: 72.5E SPA-AA/125/1237 SPA-AA/131/1243 SPA-AJ/56/1277 SPA-AJ/57/1277
72.7E	31 Aug 84 1984-93-C 15236	FLTSATCOM-A INDOC SYNCOM IV-2 LEASESAT F-2 LEASAT 2	US— Hughes Communications	FSS,MSS 0.3a,8a/0.3a,7b	P 1436.1 r_a 35792 r_p 35781 i 1.1 n -0.0009	IFRB: 77.0E AR11/A/100/1605 -ADD1/1652 AR11/A/336/1762 -ADD1/1794 -ADD2/1802
74.2E	31 Aug 83 1983-89-B 14318	INSAT-1B	India	FSS,BSS, MetSat,EES 0.4b,6b/2.5a,4a	P 1436.1 r_a 35800 r_p 35774 i 0.0 n -0.0073	IFRB: 74.0E SPA-AA/208/1344 SPA-AJ/231/1429
79.5E	2 Mar 84 1984-22-A 14783	STATSIONAR-13 COSMOS 1540[22]	USSR	FSS 6b,14a/4a,11	P 1436.0 r_a 35797 r_p 35773 i 4.0 n +0.0184	IFRB: 80.0E SPA-AA/276/1426 AR11/C/598/1655 -ADD1/1737 AR11/A/271/1707 -CORR1/1728 AR11/C/1048/1779
80.3E	18 Aug 88 1988-71-A 19397	STATSIONAR-13 GORIZONT 16	Intersputnik	FSS 6b,14a/4a,11	P 1436.2 r_a 35808 r_p 35768 i 0.6 n -0.0201	IFRB: 80.0E SPA-AA/276/1426 AR11/A/271/1707 AR11/C/1048/1779 AR11/C/1124/1793
80.4E	1 Oct 87 1987-84-A 18384	STATSIONAR-13 COSMOS 1888[22]	Intersputnik	FSS 6b,14a/4a,11	P 1436.0 r_a 35805 r_p 35763 i 0.2 n +0.0312	IFRB: 80.0E SPA-AA/276/1426 AR11/A/271/1707 AR11/C/1048/1779 AR11/C/1124/1793
81.1E	5 Jul 89 1979-62-A 11440	STATSIONAR-13[9] GORIZONT 2[11]	USSR	FSS 6b/4a	P 1435.7 r_a 35788 r_p 35767 i 7.8 n +0.1146	IFRB: 80.0E SPA-AA/276/1426 SPA-AJ/305/1469
81.7E	17 May 82 1982-44-A 13177	STATSIONAR-13[9] COSMOS 1366[22]	USSR	FSS 6b/4a	P 1436.1 r_a 35797 r_p 35774 i 5.7 n +0.0119	IFRB: 80.0E SPA-AA/276/1426 SPA-AJ/310/1469 AR11/C/598/1655 -ADD1/1737

TABLE 1. IN-ORBIT GEOSTATIONARY COMMUNICATIONS SATELLITES FOR YEAR-END 1989

SUBSATELLITE LONGITUDE[1] (deg)	LAUNCH DATE/ INTERNATIONAL CATALOG NUMBER[2]	SATELLITE DESIGNATION[3]	COUNTRY OR ORGANIZATION	SERVICE FREQUENCY CODE UP/DOWN-LINK (GHz)	ORBIT PARAMETERS[4]	REGISTRATION SPECIAL SECTION NUMBERS
84.5E	15 Feb 84 1984-16-A 14725	STATSIONAR-3 RADUGA 14	USSR	FSS 6a,6b,8a/4a,7b	P 1436.1 r_a 35810 r_p 35761 i 3.7 n +0.0119	IFRB: 85.0E SPA-AA/77/1179 SPA-AJ/27/1251 SPA-AA/155/1262 SPA-AJ/113/1335
85.3E	19 Mar 87 1987-28-A 17611	STATSIONAR-D5 RADUGA 20	USSR	FSS 6a,6b,8a/4a,7b	P 1436.1 r_a 35793 r_p 35779 i 1.3 n +0.0055	IFRB: 85.0E SPA-AA/155/1262 SPA-AJ/113/1335 AR11/A/197/1675 AR11/C/1172/1796 -CORR1/1894
87.2E	9 Oct 81 1981-102-A 12897	STATSIONAR-3[9] RADUGA 10	USSR	FSS 6a,6b,8a/4a,7b	P 1435.9 r_a 35792 r_p 35771 i 6.5 n +0.0633	IFRB: 85.0E SPA-AA/77/1179 SPA-AJ/27/1251 SPA-AA/155/1262 SPA-AJ/113/1335
87.6E	7 Mar 88 1988-14-A 18922	CHINASAT-1 DFH2-A1 PRC 22	China	FSS 6b/4a	P 1436.1 r_a 35794 r_p 35778 i 0.1 n +0.0055	IFRB: 87.5E AR11/A/255/1702 -ADD1/1712 AR11/C/1027/1778
88.0E	20 Sep 77 1977-92-A 10365	STATSIONAR-T[9] EKRAN 2[11]	USSR	FSS,BSS 6a,6b/4a	P 1436.6 r_a 35967 r_p 35624 i 9.2 n -0.1165	IFRB: 99.0E SPA2-3-AA/2/1153
89.7E	18 Nov 86 1986-90-A 17083	STATSIONAR-6 GORIZONT 13	USSR	FSS 6b,14a/4a,11	P 1436.3 r_a 35795 r_p 35784 i 1.0 n -0.0394	IFRB: 90.0E SPA-AA/108/1210 SPA-AJ/30/1251 SPA-AA/151/1261 SPA-AJ/86/1318 AR11/C/1116/1793
93.4E	21 Jul 88 1988-63-A 19330	INSAT-1C	India	FSS,BSS, MetSat,EES 0.4b,6b/2.5a,4a	P 1436.2 r_a 35790 r_p 35784 i 0.1 n -0.0073	IFRB: 93.5E AR11/A/191/1673 -CORR1/1688 AR11/C/851/1708
95.1E	26 Nov 87 1987-96-A 18575	CSDRN[14] COSMOS 1897	USSR	FSS,SRS 14b,14f/11,13c	P 1436.1 r_a 35812 r_p 35761 i 0.1 n -0.0009	IFRB: 95.0E SPA-AA/341/1484 SPA-AA/342/1484 AR11/C/69/1570
96.2E	5 Jul 89 1989-52-A 20107	STATSIONAR-14 GORIZONT 18	USSR	FSS 6b,14a/4a,11	P 1436.1[12] r_a 35807 r_p 35774 i 1.3 n -0.0523	IFRB: 96.5E SPA-AA/272/1425 SPA-AJ/306/1469 AR11/A/272/1707 -CORR1/1728 AR11/C/1050/1779 AR11/C/1181/1802

TABLE 1. IN-ORBIT GEOSTATIONARY COMMUNICATIONS SATELLITES FOR YEAR-END 1989

SUBSATELLITE LONGITUDE[1] (deg)	LAUNCH DATE/ INTERNATIONAL CATALOG NUMBER[2]	SATELLITE DESIGNATION[3]	COUNTRY OR ORGANIZATION	SERVICE FREQUENCY CODE UP/DOWN-LINK (GHz)	ORBIT PARAMETERS[4]	REGISTRATION SPECIAL SECTION NUMBERS
96.5E	15 Mar 82 1982-20-A 13092	STATSIONAR-14 GORIZONT 5	USSR	FSS 6b,14a/4a,11	P 1436.3 r_a 35933 r_p 35647 i 6.1 n -0.0458	IFRB: 96.5E SPA-AA/272/1425 SPA-AJ/306/1469 AR11/A/272/1707 -CORR1/1728 AR11/C/1050/1779
98.9E	6 May 88 1988-36-A 19090	STATSIONAR-T2 EKRAN 18	USSR	FSS,BSS 6a,6b/4a	P 1436.2 r_a 35793 r_p 35784 i 0.6 n -0.0265	IFRB: 99.0E SPA2-3-AA/10/1426 SPA2-3-AJ/7/1469
99.1E	8 Dec 88 1988-108-A 19683	STATSIONAR-T2 EKRAN 19	USSR	FSS,BSS 6a,6b/4a	P 1436.0 r_a 35792 r_p 35776 i 0.9 n +0.0312	IFRB: 99.0E SPA2-3-AA/10/1426 SPA2-3-AJ/7/1469
99.4E	27 Dec 87 1987-109-A 18715	STATSIONAR-T2 EKRAN 17	USSR	FSS,BSS 6a,6b/4a	P 1436.1 r_a 35793 r_p 35777 i 0.2 n +0.0184	IFRB: 99.0E SPA2-3-AA/10/1426 SPA2-3-AJ/7/1469
99.7E	4 Sep 87 1987-73-A 18328	STATSIONAR-T2 EKRAN 16	USSR	FSS,BSS 6a,6b/4a	P 1436.1 r_a 35804 r_p 35767 i 1.3 n +0.0119	IFRB: 99.0E SPA2-3-AA/10/1426 SPA2-3-AJ/7/1469
101.5E	1 Feb 86 1986-10-A 16526	STW-2[23] PRC 18	China	FSS 6b/4a	P 1435.8 r_a 35785 r_p 35776 i 0.8 n +0.0761	IFRB: 103.0E AR11/A/245/1695 -ADD1/1712 AR11/C/1023/1777
103.0E	11 May 87 1987-40-A 17969	STATSIONAR-21[24] GORIZONT 14	USSR	FSS 6b,14a/4a,11	P 1436.2 r_a 35792 r_p 35785 i 2.8 n -0.0265	IFRB: 103.0E AR11/A/243/1694 AR11/A/244/1694 AR11/C/905/1748 -ADD1/1752 -ADD2/1765 AR11/C/966/1766
108.1E	18 Jun 83 1983-59-C 14134	PALAPA-B1 PALAPA B-1	Indonesia	FSS 6b/4a	P 1436.3 r_a 35792 r_p 35787 i 0.0 n -0.0394	IFRB: 108.0E SPA-AA/197/1319 SPA-AJ/185/1397
109.8E	12 Feb 86 1986-16-A 16597	BS-2 BS-2B YURI 2B[25]	Japan	FSS,BSS 14a/12e	P 1436.2 r_a 35805 r_p 35770 i 0.0 n -0.0137	IFRB: 110.0E SPA-AA/305/1459 SPA-AA/362/1512 AR11/C/10/1556

TABLE 1. IN-ORBIT GEOSTATIONARY COMMUNICATIONS SATELLITES FOR YEAR-END 1989

SUBSATELLITE LONGITUDE[1] (deg)	LAUNCH DATE/ INTERNATIONAL CATALOG NUMBER[2]	SATELLITE DESIGNATION[3]	COUNTRY OR ORGANIZATION	SERVICE FREQUENCY CODE UP/DOWN-LINK (GHz)	ORBIT PARAMETERS[4]	REGISTRATION SPECIAL SECTION NUMBERS
110.0E	23 Jan 84 1984-5-A 14659	BS-2 BS-2A YURI 2A[26]	Japan	FSS,BSS 14a/12e	P 1436.4 r_a 35800 r_p 35782 i 0.6 n -0.0586	IFRB: 110.0E SPA-AA/305/1459 SPA-AA/362/1512 AR11/C/10/1556
110.4E	22 Dec 88 1988-111-A 19710	CHINASAT-2 DFH2-A2 PRC 25	China	FSS 6b/4a	P 1436.1 r_a 35788 r_p 35786 i 0.1 n -0.0073	IFRB: 110.5E AR11/A/256/1702 AR11/C/1034/1778
113.1E	20 Mar 87 1987-29-A 17706	PALAPA-B2 PALAPA B-2P	Indonesia	FSS 6b/4a	P 1436.2 r_a 35791 r_p 35786 i 0.1 n -0.0265	IFRB: 113.0E SPA-AA/198/1319 SPA-AJ/187/1397 SPA-AJ/201/1407
124.7E	8 May 85 1985-35-B 15678	TELECOM-1B[27]	France	FSS 6b,8a,14a/ 4a,7b,12c,12d[28]	P 1434.6 r_a 35767 r_p 35746 i 1.3 n +0.3843	IFRB: 5.0W SPA-AA/269/1425 SPA-AJ/472/1612 AR11/C/128/1593 -ADD1/1619 AR11/C/186/1611 AR11/C/391/1628
127.6E	10 Dec 87 1987-100-A 18631	STATSIONAR-D6 RADUGA 21	USSR	FSS 6a,6b,8a/4a,7b	P 1436.3 r_a 35793 r_p 35788 i 0.3 n -0.0523	IFRB: 128.0E AR11/A/198/1675 AR11/A/247/1695 AR11/C/919/1753 AR11/C/1173/1796
128.0E	4 Feb 83 1983-6-A 13782	CS-2A SAKURA 1	Japan	FSS 6b,30a/ 4a,20a,20b	P 1436.1 r_a 35791 r_p 35781 i 1.8 n +0.0055	IFRB: 132.0E[29] SPA-AA/256/1421 SPA-AJ/323/1490 SPA-AJ/359/1505
128.0E	5 Aug 83 1983-81-A 14248	CS-2B SAKURA 2	Japan	FSS 6b,30a/ 4a,20a,20b	P 1436.1 r_a 35791 r_p 35783 i 1.1 n -0.0073	IFRB: 136.0E[29] SPA-AA/257/1421 SPA-AJ/325/1490 SPA-AJ/368/1508
129.9E	23 Feb 77 1977-14-A 09852	ETS-2[30] KIKU 2	Japan	MetSat,SRS 2/0.1c,1.7a	P 1436.1 r_a 35790 r_p 35783 i 8.0 n -0.0009	IFRB: 130.0E SPA-AA/91/1194
131.9E	19 Feb 88 1988-12-A 18877	CS-3A SAKURA 3A	Japan	FSS 6b,30a/ 4a,20a,20b	P 1436.2 r_a 35793 r_p 35784 i 0.1 n -0.0265	IFRB: 132.0E AR11/A/212/1680 AR11/C/1128/1794 -ADD1/1805 -CORR1/1810 -CORR2/1835

TABLE 1. IN-ORBIT GEOSTATIONARY COMMUNICATIONS SATELLITES FOR YEAR-END 1989

SUBSATELLITE LONGITUDE[1] (deg)	LAUNCH DATE/ INTERNATIONAL CATALOG NUMBER[2]	SATELLITE DESIGNATION[3]	COUNTRY OR ORGANIZATION	SERVICE FREQUENCY CODE UP/DOWN-LINK (GHz)	ORBIT PARAMETERS[4]	REGISTRATION SPECIAL SECTION NUMBERS
135.8E	27 Aug 87 1987-70-A 18316	ETS-5[30] EMSS-C	Japan	FSS,MMSS,AMSS 1.6b,1.6d,6b/ 1.5b,1.5d,5a	P 1436.2 r_a 36010 r_p 35565 i 0.0 n -0.0137	IFRB: 150.0E AR11/A/217/1685 AR11/C/920/1754 AR11/C/923/1754
135.9E	16 Sep 88 1988-86-A 19508	CS-3B SAKURA 3B	Japan	FSS 6b,30a/ 4a,20a,20b	P 1436.2 r_a 35791 r_p 35785 i 0.0 n -0.0201	IFRB: 136.0E AR11/A/213/1680 AR11/C/1145/1794 -ADD1/1805 -CORR1/1835
137.8E	2 Aug 84 1984-80-A 15152	GMS-3[31] HIMAWARI 3	Japan	MetSat,SRS,EES 2/0.4g,1.6f,1.6g	P 1436.2 r_a 35789 r_p 35787 i 1.0 n -0.0201	IFRB: 140.0E AR11/A/54/1563 AR11/C/474/1648 -ADD1/1887
150.0E	6 Mar 89 1989-20-A 19874	JCSAT-1 JC-SAT 1	Japan– Japan Communications Satellite	FSS 14a/12b,12c,12d	P 1436.2 r_a 35792 r_p 35784 i 0.0 n -0.0201	IFRB: 150.0E AR11/A/253/1700 AR11/C/946/1763 -CORR1/1813 -CORR2/1860 -ADD1/1860
154.0E	31 Dec 89 1990-1-B 20402	JCSAT-2 JC-SAT 2	Japan– Japan Communications Satellite	FSS 14a/12b,12c,12d	P 1436.2 r_a 35794 r_p 35782 i 0.0 n -0.0201	IFRB: 154.0E AR11/A/254/1700 AR11/C/953/1763 -CORR1/1813 -CORR2/1860 -ADD1/1860
154.0E	26 Nov 82 1982-113-A 13669	STATSIONAR-2[9] RADUGA 11	USSR	FSS 6a,6b,8a/4a,7b	P 1473.8 r_a 36688 r_p 36355 i 4.7 n -9.4398	IFRB: 35.0E SPA-AA/76/1179 SPA-AJ/26/1251 SPA-AA/340/1480 AR11/C/29/1561 AR11/C/109/1578
156.0E	27 Nov 85 1985-109-C 16275	AUSSAT-2 AUSSAT A2 AUSSAT K-2	Australia	FSS,BSS 14a/12b, 12c,12d,12g,12h	P 1436.2 r_a 35793 r_p 35783 i 0.0 n -0.0201	IFRB: 156.0E SPA-AA/300/1456 SPA-AA/373/1575 AR11/C/305/1624
157.9E	5 Jun 89 1989-41-A 20040	SUPERBIRD-A	Japan— Space Communications Corporation	FSS 14a,30a/ 12b,12c,20a,20b	P 1436.1 r_a 35802 r_p 35768 i 0.1 n +0.0184	IFRB: 158.0E AR11/A/340/1762 AR11/C/1303/1836 -CORR1/1865
159.6E	5 Sep 89 1989-70-A 20217	GMS-160E[31] GMS-4	Japan	MetSat,SRS,EES 2/0.4g,1.6f,1.6g	P 1436.2[12] r_a 35854 r_p 35720 i 1.6 n -0.0073	IFRB: 160.0E SPA-AA/72/1173 AR11/C/8/1555 -ADD1/1887 AR11/A/423/1821 -ADD1/1833 AR11/C/1464/1875 -CORR1/1886

TABLE 1. IN-ORBIT GEOSTATIONARY COMMUNICATIONS SATELLITES FOR YEAR-END 1989

SUBSATELLITE LONGITUDE[1] (deg)	LAUNCH DATE/ INTERNATIONAL CATALOG NUMBER[2]	SATELLITE DESIGNATION[3]	COUNTRY OR ORGANIZATION	SERVICE FREQUENCY CODE UP/DOWN-LINK (GHz)	ORBIT PARAMETERS[4]	REGISTRATION SPECIAL SECTION NUMBERS
160.0E	27 Aug 85 1985-76-B 15993	AUSSAT-1 AUSSAT A1 AUSSAT K-1	Australia	FSS,BSS 14a/12b, 12c,12d,12g,12h	P 1436.2 r_a 35795 r_p 35780 i 0.0 n -0.0137	IFRB: 160.0E SPA-AA/299/1456 SPA-AA/372/1575 AR11/C/296/1624
164.0E	16 Sep 87 1987-78-A 18350	AUSSAT-3 AUSSAT A3 AUSSAT K-3	Australia	FSS,BSS 14a/12b, 12c,12d,12g,12h	P 1436.1 r_a 35796 r_p 35777 i 0.1 n -0.0009	IFRB: 164.0E SPA-AA/301/1456 SPA-AA/374/1575 AR11/C/314/1624
167.6E	14 Jul 77 1977-65-A 10143	GMS-140E[9,31] GMS-1[11] HIMAWARI 1	Japan	MetSat,SRS,EES 2/0.4g,1.6f,1.6g	P 1436.0 r_a 36139 r_p 35432 i 7.1 n +0.0119	IFRB: 140.0E SPA-AA/72/1173 SPA-AJ/95/1329
171.6E	31 Oct 80 1980-87-A 12046	FLTSATCOM W PAC FLTSATCOM F-4 FLTSATCOM 4	US	FSS,MSS 0.3a,8a/0.3a,7b	P 1436.2 r_a 35794 r_p 35781 i 5.4 n -0.0137	IFRB: 172.0E SPA-AA/86/1186 SPA-AJ/167/1382
174.0E	15 Dec 81 1981-119-A 12994	INTELSAT5 PAC1[32] INTELSAT V PAC 1 INTELSAT V F-3	Intelsat	FSS 6b,14a/4a,11	P 1436.2 r_a 35805 r_p 35772 i 0.2 n -0.0265	IFRB: 174.0E SPA-AA/254/1419 SPA-AJ/376/1511
175.2E	21 Nov 79 1979-98-A 11621	USGCSS PH2 W PAC DSCS II F-13 DSCS 2-D OPS 9443	US	FSS 8a/7b	P 1436.2 r_a 35790 r_p 35785 i 5.6 n -0.0137	IFRB: 175.0E SPA-AJ/403/1514
176.1E	14 Oct 76 1976-101-A 09478	MARISAT-PAC[20] MARISAT F-3 MARISAT 3	US— Comsat General	FSS,MSS,MMSS 0.3a,1.6b,6b/ 0.3a,1.5b,4a[21]	P 1436.1 r_a 35791 r_p 35782 i 8.2 n -0.0009	IFRB: 176.5E SPA-AA/3/1101 SPA-AA/6/1101 SPA-AJ/25/1244
177.0E	23 May 81 1981-50-A 12474	INTELSAT5 PAC2 INTELSAT V PAC 2 INTELSAT V F-1	Intelsat	FSS 6b,14a/4a,11	P 1436.2 r_a 35804 r_p 35773 i 1.2 n -0.0265	IFRB: 177.0E SPA-AA/225/1419 SPA-AJ/377/1511 AR11/A/81/1588 AR11/C/590/1652 -ADD1/1660 AR11/C/681/1668 -ADD1/1802
177.5E	14 Dec 78 1978-113-B 11145	USGCSS PH2 W PAC-2 DSCS II F-12[33] DSCS 2-C OPS 9442	US	FSS 8a/7b	P 1436.1 r_a 35792 r_p 35779 i 5.9 n +0.0119	IFRB: 180.0E AR11/A/405/1805

TABLE 1. IN-ORBIT GEOSTATIONARY COMMUNICATIONS SATELLITES FOR YEAR-END 1989

SUBSATELLITE LONGITUDE[1] (deg)	LAUNCH DATE/ INTERNATIONAL CATALOG NUMBER[2]	SATELLITE DESIGNATION[3]	COUNTRY OR ORGANIZATION	SERVICE FREQUENCY CODE UP/DOWN-LINK (GHz)	ORBIT PARAMETERS[4]	REGISTRATION SPECIAL SECTION NUMBERS
177.9E	20 Dec 81 1981-122-A 13010	MARECS PAC1 MARECS PAC OC 1 MARECS A MAREC 1	ESA	FSS,MMSS 1.6b,6b/1.5b,4a	P 1436.1 r_a 35803 r_p 35773 i 3.2 n -0.0201	IFRB: 178.0E SPA-AA/219/1353 SPA-AJ/241/1432
179.0E	29 Aug 85 1985-76-D 15995	FLTSATCOM-A[10] SYNCOM IV-4[34] LEASESAT F-4 LEASAT 4	US— Hughes Communications	FSS,MSS 0.3a,8a/0.3a,7b	P 1440.4 r_a 36519 r_p 35233 i 0.3 n -1.1502	
180.0E (180.0W)	3 Mar 84 1984-23-A 14786	INTELSAT5 PAC3 INTELSAT V PAC 3 INTELSAT MCS PAC A INTELSAT V F-8	Intelsat	FSS,MMSS 1.6b,6b,14a/ 1.5b,4a,11[18]	P 1436.1 r_a 35800 r_p 35774 i 0.0 n -0.0073	IFRB: 180.0E SPA-AA/255/1419 SPA-AA/332/1476 SPA-AJ/455/1535 SPA-AJ/469/1599 AR11/C/682/1668 -ADD1/1805 AR11/C/692/1669 AR11/C/859/1735
183.9E (176.1W)	9 Feb 78 1978-16-A 10669	FLTSATCOM-A W PAC FLTSATCOM F-1 FLTSATCOM 1 OPS 6391	US	FSS,MSS 0.3a,8a/0.3a,7b	P 1436.0 r_a 35793 r_p 35775 i 7.5 n +0.0312	IFRB: 177.0W AR11/A/99/1605 -ADD1/1652 AR11/A/335/1762 -ADD1/1794
185.4E (174.6W)	21 Nov 79 1979-98-B 11622	USGCSS PH2 W PAC-2[9] DSCS II F-14[35] DSCS 2-E OPS 9444	US	FSS 8a/7b	P 1436.0 r_a 35792 r_p 35777 i 5.6 n +0.0247	IFRB: 180.0E AR11/A/405/1805
188.8E (171.2W)	29 Sep 88 1988-91-B 19548	TDRS WEST TDRS-3 TDRS-C	US	FSS,SRS 2.1,6b,14f/ 2,2.2,4a,13c	P 1436.3 r_a 35798 r_p 35781 i 0.5 n -0.0394	IFRB: 171.0W SPA-AA/232/1381 AR11/C/47/1568 -ADD1/1595
190.5E (169.5W)	17 Jan 86 1986-7-A 16497	STATSIONAR-D2 RADUGA 18[36]	USSR	FSS 6a,6b,8a/4a,7b	P 1426.1 r_a 35752 r_p 35427 i 2.0 n +2.5290	IFRB: 170.0W SPA-AA/156/1262 SPA-AJ/114/1335 AR11/A/194/1672 AR11/C/1169/1796 -CORR1/1894
191.0E (169.0W)	1 Aug 84 1984-78-A 15144	STATSIONAR-10[37] GORIZONT 10	USSR	FSS 6b,14a/4a,11	P 1436.3 r_a 35808 r_p 35772 i 3.1 n -0.0458	IFRB: 170.0W SPA-AA/97/1197 SPA-AJ/52/1276 SPA-AJ/64/1280
212.9E (147.1W)	20 Oct 82 1982-103-A 13624	STATSIONAR-26 GORIZONT 6[9,38]	USSR	FSS 6b,14a/4a,11	P 1435.6 r_a 35782 r_p 35771 i 5.3 n +0.1275	IFRB: 155.0W AR11/A/385/1797 -ADD1/1803 -CORR1/1813 AR11/C/1313/1836

TABLE 1. IN-ORBIT GEOSTATIONARY COMMUNICATIONS SATELLITES FOR YEAR-END 1989

Subsatellite Longitude[1] (deg)	Launch Date/ International Catalog Number[2]	Satellite Designation[3]	Country or Organization	Service Frequency Code Up/Down-Link (GHz)	Orbit Parameters[4]	Registration Special Section Numbers
217.0E (143.0W)	28 Oct 82 1982-105-A 13631	US SATCOM-5 RCA SATCOM 5 SATCOM V AURORA 1	US— Alascom	FSS 6b/4a	P 1436.1 r_a 35788 r_p 35786 i 0.0 n -0.0073	IFRB: 143.0W AR11/A/7/1524 AR11/C/414/1630
221.1E (138.9W)	11 Apr 83 1983-30-A 13984	US SATCOM 1-R GE SATCOM 1-R SATCOM F1R SATCOM IR	US— RCA Americom[39]	FSS 6b/4a	P 1436.1 r_a 35793 r_p 35780 i 0.0 n -0.0009	IFRB: 139.0W AR11/A/6/1524 -ADD1/1548 AR11/C/337/1625
223.9E (136.1W)	28 Apr 83 1983-41-A 14050	GOES WEST GOES-6[40]	US	MetSat,SRS,EES 0.4b,2/ 0.4g,1.6f,1.6g	P 1436.0 r_a 35793 r_p 35779 i 1.3 n +0.0055	IFRB: 135.0W SPA-AA/28/1147 SPA-AJ/367/1508
225.1E (134.9W)	30 Oct 82 1982-106-B 13637	USGCSS PH3 E PAC DSCS III F-1 DSCS III-A1 PSCS 16	US	FSS,MSS 0.3a,8a/0.3a,7b[41]	P 1436.1 r_a 35802 r_p 35772 i 0.1 n -0.0073	IFRB: 135.0W SPA-AA/248/1413 SPA-AJ/344/1499 AR11/C/405/1629
225.9E (134.1W)	28 Jun 83 1983-65-A 14158	USASAT-11D HUGHES GALAXY 1 GALAXY I	US— Hughes Communications	FSS 6b/4a	P 1436.2 r_a 35789 r_p 35786 i 0.0 n -0.0137	IFRB: 134.0W AR11/A/120/1615 AR11/C/821/1696
228.9E (131.1W)	14 Dec 78 1978-113-A 11144	USGCSS PH2 E PAC-2 DSCS II F-11 DSCS 2-B OPS 9441	US	FSS 8a/7b	P 1436.4 r_a 35801 r_p 35784 i 6.0 n -0.0779	IFRB: 130.0W AR11/A/404/1805
229.1E (130.9W)	21 Nov 81 1981-114-A 12967	US SATCOM 3-R GE SATCOM 3-R SATCOM F3R SATCOM IIIR	US— RCA Americom[39]	FSS 6b/4a	P 1436.1 r_a 35795 r_p 35779 i 0.1 n -0.0073	IFRB: 131.0W SPA-AA/329/1476 AR11/C/347/1625 AR11/C/348/1625
229.9E (130.1W)	16 Jun 78 1978-62-A 10953	GOES WEST[9] GOES-3[42]	US	MetSat,SRS,EES 0.4b,2/ 0.4g,1.6f,1.6g	P 1436.2 r_a 35820 r_p 35756 i 6.1 n -0.0201	IFRB: 135.0W SPA-AA/28/1147 SPA-AJ/367/1508
231.4E (128.6W)	3 Nov 71 1971-95-B 05588	USGCSS PH2[10] DSCS II F-2[11]	US	FSS 8a/7b	P 1435.1 r_a 35782 r_p 35751 i 10.7 n +0.2559	

TABLE 1. IN-ORBIT GEOSTATIONARY COMMUNICATIONS SATELLITES FOR YEAR-END 1989

SUBSATELLITE LONGITUDE[1] (deg)	LAUNCH DATE/ INTERNATIONAL CATALOG NUMBER[2]	SATELLITE DESIGNATION[3]	COUNTRY OR ORGANIZATION	SERVICE FREQUENCY CODE UP/DOWN-LINK (GHz)	ORBIT PARAMETERS[4]	REGISTRATION SPECIAL SECTION NUMBERS
232.3E (127.7W)	27 Aug 85 1985-76-C 15994	ASC-1 CONTEL ASC-1	US— American Satellite Co.	FSS 6b,14a/4a,12a	P 1436.1 r_a 35796 r_p 35776 i 0.0 n -0.0055	IFRB: 128.0W AR11/A/202/1676 AR11/A/301/1723 -ADD1/1801 AR11/C/1066/1784 AR11/C/1106/1792
234.6E (125.4W)	22 Apr 76 1976-35-A 08808	SATCOM PHASE-3[9] NATO III-A NATO 3A	NATO	FSS 8a/7b	P 1436.2 r_a 35806 r_p 35770 i 7.4 n -0.0201	IFRB: 18.0W SPA-AA/144/1247 SPA-AJ/137/1355
234.9E (125.1W)	19 Jun 85 1985-48-D 15826	USASAT-20A TELSTAR 3D[43] TELSTAR 303	US— AT&T	FSS 6b/4a	P 1436.1 r_a 35794 r_p 35779 i 0.0 n -0.0009	IFRB: 126.0W AR11/A/304/1730 AR11/C/968/1769
237.0E (123.0W)	8 Sep 88 1988-81-B 19484	USASAT-10A STLC 2 SBS-5	US— Satellite Transponder Leasing Corp.[44]	FSS 14a/12a	P 1436.1 r_a 36008 r_p 35566 i 0.1 n -0.0073	IFRB: 122.0W AR11/A/4/1567 AR11/A/10/1525 -ADD1/1548 AR11/A/105/1609 AR11/C/616/1658 AR11/C/883/1741
237.5E (122.5W)	9 Jun 82 1982-58-A 13269	WESTAR-5 WU WESTAR 5 WESTAR V	US— Western Union[45]	FSS 6b/4a	P 1436.2 r_a 35793 r_p 35782 i 0.0 n -0.0137	IFRB: 123.0W AR11/A/5/1524 -ADD1/1548 AR11/C/284/1623
239.6E (120.4W)	16 Oct 75 1975-100-A 08366	GOES[9] GOES-1[42]	US	MetSat,SRS,EES 0.4b,2/ 0.4g,1.6f,1.6g	P 1436.8 r_a 35802 r_p 35797 i 8.9 n -0.1678	IFRB: 140.0W SPA-AA/28/1147
240.0E (120.0W)	23 May 84 1984-49-A 14985	SPACENET-1 GTE SPACENET I	US— GTE Spacenet	FSS 6b,14a/4a,12a	P 1436.2 r_a 35794 r_p 35781 i 0.0 n -0.0137	IFRB: 120.0W AR11/A/10/1525 -ADD1/1548 AR11/C/616/1658 -ADD1/1682 AR11/C/833/1699
241.7E (118.3W)	8 Aug 85 1985-70-A 15946	STATSIONAR-9[9] RADUGA 16[11]	USSR	FSS 6a,6b,8a/4a,7b	P 1435.3 r_a 35777 r_p 35764 i 2.3 n +0.2046	IFRB: 45.0E SPA-AA/96/1197 SPA-AA/154/1262 SPA-AJ/51/1276 SPA-AJ/63/1280 SPA-AJ/112/1335 AR11/C/1472/1876

TABLE 1. IN-ORBIT GEOSTATIONARY COMMUNICATIONS SATELLITES FOR YEAR-END 1989

SUBSATELLITE LONGITUDE[1] (deg)	LAUNCH DATE/ INTERNATIONAL CATALOG NUMBER[2]	SATELLITE DESIGNATION[3]	COUNTRY OR ORGANIZATION	SERVICE FREQUENCY CODE UP/DOWN-LINK (GHz)	ORBIT PARAMETERS[4]	REGISTRATION SPECIAL SECTION NUMBERS
243.2E (116.8W)	27 Nov 85 1985-109-B 16274	MORELOS 2 MORELOS II MORELOS-B	Mexico	FSS 6b,14a/4a,12a	P 1436.1 r_a 35792 r_p 35782 i 0.0 n -0.0073	IFRB: 116.5W AR11/A/30/1540 -ADD1/1555 AR11/C/387/1628
245.1E (114.9W)	12 Nov 82 1982-110-C 13652	ANIK C-3 TELESAT 5	Canada— Telesat Canada	FSS,BSS 14a/12a,12e	P 1436.0 r_a 35790 r_p 35780 i 0.0 n +0.0184	IFRB: 117.5W SPA-AA/138/1252 SPA-AJ/69/1302 SPA-AA/357/1500 SPA-AJ/450/1533 AR11/C/42/1567 AR11/C/245/1620 AR11/C/447/1645
246.0E (114.0W)	16 Jun 77 1977-48-A 10061	GOES[9] GOES-2[11]	US	MetSat,SRS,EES 0.4b,2/ 0.4g,1.6f,1.6g	P 1436.0 r_a 35813 r_p 35756 i 7.2 n +0.0247	IFRB: 140.0W SPA-AA/28/1147
246.6E (113.4W)	17 Jun 85 1985-48-B 15824	MORELOS 1 MORELOS I MORELOS-A	Mexico	FSS 6b,14a/4a,12a	P 1436.1 r_a 35795 r_p 35779 i 0.0 n -0.0073	IFRB: 113.5W AR11/A/28/1539 -ADD1/1555
248.4E (111.6W)	3 Nov 71 1971-95-A 05587	USGCSS PH2[10] DSCS II F-1[11] OPS 9431	US	FSS 8a/7b	P 1436.3 r_a 35803 r_p 35776 i 10.8 n -0.0394	
249.5E (110.5W)	9 Nov 84 1984-113-B 15383	ANIK D-2[46] ANIK D II	Canada— Telesat Canada	FSS 6b/4a	P 1436.1 r_a 35792 r_p 35782 i 0.0 n -0.0073	IFRB: 110.5W SPA-AA/358/1500 AR11/C/716/1673 AR11/C/960/1764 -CORR1/1770 AR11/C/961/1764 -CORR1/1770
250.0E (110.0W)	18 Jun 83 1983-59-B 14133	ANIK C-2 TELESAT 7	Canada— Telesat Canada	FSS,BSS 14a/12a,12e	P 1436.1 r_a 35792 r_p 35783 i 0.0 n -0.0137	IFRB: 110.0W SPA-AA/138/1252 SPA-AJ/347/1500 SPA-AJ/451/1533 SPA-AJ/466/1569 AR11/C/646/1666 -ADD1/1690 AR11/C/730/1674 -ADD1/1690 AR11/C/829/1698
250.7E (109.3W)	21 Feb 85 1985-16-A 15574	STATSIONAR-13[9] COSMOS 1629[22]	USSR	FSS 6b,14a/4a,11	P 1435.0 r_a 35779 r_p 35749 i 2.8 n +0.2880	IFRB: 80.0E SPA-AA/276/1426 AR11/C/598/1655 -ADD1/1737 AR11/A/271/1707 -CORR1/1728 AR11/C/1048/1779

TABLE 1. IN-ORBIT GEOSTATIONARY COMMUNICATIONS SATELLITES FOR YEAR-END 1989

SUBSATELLITE LONGITUDE[1] (deg)	LAUNCH DATE/ INTERNATIONAL CATALOG NUMBER[2]	SATELLITE DESIGNATION[3]	COUNTRY OR ORGANIZATION	SERVICE FREQUENCY CODE UP/DOWN-LINK (GHz)	ORBIT PARAMETERS[4]	REGISTRATION SPECIAL SECTION NUMBERS
252.7E (107.3W)	13 Apr 85 1985-28-B 15642	ANIK C-1	Canada— Telesat Canada	FSS,BSS 14a/12a,12e	P 1436.0 r_a 35862 r_p 35779 i 0.0 n -0.4375	IFRB: 107.5W SPA-AA/357/1500 SPA-AJ/434/1516 AR11/C/569/1649 -ADD1/1665 AR11/C/728/1674 AR11/C/832/1698 -ADD1/1709
255.0E (105.0W)	28 Mar 86 1986-26-A 16649	GSTAR-2 GTE GSTAR2 GSTAR-A2	US— GTE Spacenet	FSS 14a/12a	P 1436.2 r_a 35794 r_p 35781 i 0.0 n -0.0137	IFRB: 105.0W AR11/A/15/1525 -ADD1/1548 AR11/C/1075/1784
255.5E (104.5W)	26 Aug 82 1982-82-A 13431	ANIK D-1 ANIK D I TELESAT 6	Canada— Telesat Canada	FSS 6b/4a	P 1436.1 r_a 35797 r_p 35776 i 0.0 n -0.0009	IFRB: 104.5W SPA-AA/279/1426 SPA-AJ/427/1515 -ADD1/1664 SPA-AJ/465/1568 AR11/C/31/1565 AR11/C/43/1567 -ADD1/1612 AR11/C/105/1576 -ADD1/1600 AR11/C/151/1597 AR11/C/587/1651 AR11/C/651/1666
255.6E (104.4W)	12 Apr 85 1985-28-C 15643	FLTSATCOM-A EAST PAC SYNCOM IV-3 LEASESAT F-3 LEASAT 3	US— Hughes Communications	FSS,MSS 0.3a,8a/0.3a,7b	P 1436.1 r_a 35847 r_p 35727 i 0.7 n -0.0073	IFRB: 105.0W AR11/A/98/1605 -ADD1/1652
255.7E (104.3W)	5 Dec 86 1986-96-A 17181	FLTSATCOM-B EAST PAC[47] FLTSATCOM F-7	US	FSS,MSS 0.3a,8a,44/ 0.3a,7b,20e,20f	P 1436.1 r_a 35863 r_p 35709 i 3.0 n +0.0055	IFRB: 100.0W AR11/A/50/1561 -ADD1/1587
257.0E (103.0W)	29 Apr 85 1985-35-A 15677	GSTAR-1 GTE GSTAR 1 GSTAR-A1	US— GTE Spacenet	FSS 14a/12a	P 1436.2 r_a 35859 r_p 35717 i 0.0 n -0.0201	IFRB: 103.0W AR11/A/14/1525 -ADD1/1548 AR11/C/1073/1784 AR11/C/1074/1784
260.8E (99.2W)	15 Nov 80 1980-91-A 12065	USASAT-6A SBS F3 SBS-1[48]	US— Satellite Business Systems[49]	FSS 14a/12a	P 1436.1 r_a 35793 r_p 35780 i 1.3 n -0.0009	IFRB: 97.0W AR11/A/34/1553 AR11/C/325/1624
260.9E (99.1W)	24 Sep 81 1981-96-A 12855	USASAT-6C SBS F1 SBS-2[48]	US— Satellite Business Systems[49]	FSS 14a/12a	P 1436.1 r_a 35792 r_p 35783 i 1.3 n -0.0137	IFRB: 95.0W AR11/A/35/1553 AR11/C/331/1624

TABLE 1. IN-ORBIT GEOSTATIONARY COMMUNICATIONS SATELLITES FOR YEAR-END 1989

Subsatellite Longitude[1] (deg)	Launch Date/ International Catalog Number[2]	Satellite Designation[3]	Country or Organization	Service Frequency Code Up/Down-Link (GHz)	Orbit Parameters[4]	Registration Special Section Numbers
261.1E (98.9W)	26 Feb 82 1982-14-A 13069	WESTAR-4 WU WESTAR 4 WESTAR IV	US— Western Union[45]	FSS 6b/4a	P 1436.2 r_a 35798 r_p 35777 i 0.1 n -0.0137	IFRB: 99.0W AR11/A/4/1524 -ADD1/1548 AR11/C/272/1623
262.5E (97.5W)	26 Feb 87 1987-22-A 17561	GOES EAST GOES-7[50]	US	MetSat,SRS,EES 0.1a,0.2,0.4b,2/ 0.4g,1.6f,1.6g	P 1436.1 r_a 35815 r_p 35756 i 0.0 n +0.0119	IFRB: 75.0W SPA-AA/28/1147 SPA-AJ/366/1508
264.0E (96.0W)	28 Jul 83 1983-77-A 14234	TELSTAR-3A TELSTAR 3A TELSTAR 301	US— AT&T	FSS 6b/4a	P 1436.2 r_a 35796 r_p 35779 i 0.0 n -0.0137	IFRB: 97.0W AR11/A/8/1524 -ADD1/1548 AR11/C/879/1738
265.0E (95.0W)	11 Nov 82 1982-110-B 13651	USASAT-6B SBS F2 SBS-3	US— Satellite Business Systems[49]	FSS 14a/12a	P 1436.1 r_a 35795 r_p 35779 i 2.0 n -0.0073	IFRB: 99.0W SPA-AA/124/1235 SPA-AJ/61/1280
266.5E (93.5W)	21 Sep 84 1984-101-A 15308	USASAT-12B HUGHES GALAXY 3 GALAXY III	US— Hughes Communications	FSS 6b/4a	P 1436.1 r_a 35793 r_p 35780 i 0.0 n -0.0009	IFRB: 93.5W AR11/A/122/1615 AR11/C/824/1697
267.0E (93.0W)	8 Sep 88 1988-81-A 19483	USASAT-16A GSTAR-3 GTE GSTAR 3 GSTAR-A3	US— GTE Spacenet	FSS,AMSS 1.6a,14a/12a[52]	P 1186.3[51] r_a 36073 r_p 25414 i 1.9	IFRB: 93.0W AR11/A/222/1687 AR11/C/998/1772
268.9E (91.1W)	30 Aug 84 1984-93-B 15235	USASAT-9A STLC 1 SBS-4	US— Satellite Business Systems[49]	FSS 14a/12a	P 1436.1 r_a 35791 r_p 35782 i 0.0 n -0.0009	IFRB: 91.0W AR11/A/101/1609 AR11/C/818/1696
269.0E (91.0W)	10 Aug 79 1979-72-A 11484	WESTAR-3 WU WESTAR 3 WESTAR III	US— Western Union[45]	FSS 6b/4a	P 1436.2 r_a 35792 r_p 35783 i 1.5 n -0.0137	IFRB: 91.0W SPA-AA/37/1152 SPA-AJ/197/1406 SPA-AJ/198/1406
272.9E (87.1W)	11 Mar 88 1988-18-A 18951	SPACENET-3 GTE SPACENET III SPACENET 3R	US— GTE Spacenet	FSS,AMSS 1.6a,6b,14a/ 4a,12a[52]	P 1436.2 r_a 35790 r_p 35784 i 0.0 n -0.0073	IFRB: 88.5W AR11/A/13/1525 AR11/C/834/1699
274.9E (85.1W)	1 Sep 84 1984-93-D 15237	USASAT-3C TELSTAR 3C TELSTAR 302	US— AT&T	FSS 6b/4a	P 1436.0 r_a 35795 r_p 35778 i 0.0 n -0.0009	IFRB: 86.0W AR11/A/9/1524 AR11/C/246/1620 AR11/C/1084/1790

TABLE 1. IN-ORBIT GEOSTATIONARY COMMUNICATIONS SATELLITES FOR YEAR-END 1989

SUBSATELLITE LONGITUDE[1] (deg)	LAUNCH DATE/ INTERNATIONAL CATALOG NUMBER[2]	SATELLITE DESIGNATION[3]	COUNTRY OR ORGANIZATION	SERVICE FREQUENCY CODE UP/DOWN-LINK (GHz)	ORBIT PARAMETERS[4]	REGISTRATION SPECIAL SECTION NUMBERS
275.0E (85.0W)	12 Jan 86 1986-3-B 16482	USASAT-9C GE SATCOM K-1 SATCOM KU1	US— RCA Americom[39]	FSS 14a/12a	P 1436.2 r_a 35794 r_p 35783 i 0.0 n -0.0265	IFRB: 85.0W AR11/A/103/1609 AR11/C/1052/1780 -CORR1/1922
277.9E (82.1W)	16 Jan 82 1982-4-A 13035	USASAT-7B GE SATCOM 4 SATCOM F4 SATCOM IV	US— RCA Americom[39]	FSS 6b/4a	P 1436.1 r_a 35798 r_p 35776 i 0.0 n -0.0073	IFRB: 83.0W SPA-AA/327/1474 AR11/C/188/1612 -ADD1/1626
279.0E (81.0W)	28 Nov 85 1985-109-D 16276	USASAT-9D GE SATCOM K-2 SATCOM KU2	US— RCA Americom[39]	FSS 14a/12a	P 1436.2 r_a 35794 r_p 35782 i 0.0 n -0.0201	IFRB: 81.0W AR11/A/104/1609 AR11/C/1053/1780 -CORR1/1922
280.7E (79.3W)	5 Apr 83 1983-26-B 13969	TDRS CENTRAL TDRS-1[53] TDRS-A	US	FSS,SRS 2.1,6b,14f/ 2,2.2,4a,13c[54]	P 1440.6 r_a 35882 r_p 35867 i 3.6 n -1.1310	IFRB: 79.0W SPA-AA/233/1381 AR11/C/48/1568 AR11/C/773/1679
284.0E (76.0W)	22 Jul 76 1976-73-A 09047	COMSTAR D-2[55] COMSTAR 2	US— Comsat General	FSS 6b/4a	P 1436.1 r_a 35789 r_p 35786 i 4.8 n -0.0137	IFRB: 95.0W SPA-AA/32/1152 SPA-AJ/40/1268
284.0E (76.0W)	21 Feb 81 1981-18-A 12309	USASAT-12C COMSTAR D-4[55] COMSTAR 4	US— Comsat General	FSS 6b/4a	P 1436.1 r_a 35790 r_p 35786 i 3.2 n -0.0201	IFRB: 76.0W AR11/A/123/1615 AR11/C/907/1748 -CORR1/1785
286.0E (74.0W)	22 Sep 83 1983-98-A 14365	USASAT-7A HUGHES GALAXY 2 GALAXY II	US— Hughes Communications	FSS 6b/4a	P 1436.2 r_a 35795 r_p 35780 i 0.0 n -0.0137	IFRB: 74.0W SPA-AA/312/1465 AR11/C/812/1689 -ADD1/1710
286.5E (73.5W)	5 Oct 80 1980-81-A 12003	STATSIONAR-8[9] RADUGA 7[11]	USSR	FSS 6a,6b,8a/4a,7b	P 1436.5 r_a 35765 r_p 35747 i 7.3 n +0.3907	IFRB: 25.0W SPA-AA/95/1197 SPA-AJ/50/1276 SPA-AJ/62/1280 AR11/A/246/1695 AR11/C/918/1752
287.8E (72.2W)	17 Jan 76 1976-4-A 08585	CTS[10,56] CAS-C	Canada	FSS 14a/12a	P 1436.2 r_a 35830 r_p 35746 i 9.4 n -0.0201	
287.9E (72.1W)	8 Sep 83 1983-94-A 14328	USASAT-8B GE SATCOM 2-R SATCOM F2R SATCOM IIR	US— RCA Americom[39]	FSS 6b/4a	P 1436.2 r_a 35800 r_p 35774 i 0.0 n -0.0073	IFRB: 72.0W AR11/A/37/1553 AR11/C/221/1617

TABLE 1. IN-ORBIT GEOSTATIONARY COMMUNICATIONS SATELLITES FOR YEAR-END 1989

SUBSATELLITE LONGITUDE[1] (deg)	LAUNCH DATE/ INTERNATIONAL CATALOG NUMBER[2]	SATELLITE DESIGNATION[3]	COUNTRY OR ORGANIZATION	SERVICE FREQUENCY CODE UP/DOWN-LINK (GHz)	ORBIT PARAMETERS[4]	REGISTRATION SPECIAL SECTION NUMBERS
290.2E (69.8W)	28 Mar 86 1986-26-B 16650	SBTS A2[57] BRAZILSAT A2 SBTS 2	Brazil	FSS 6b/4a	P 1436.2 r_a 35819 r_p 35758 i 0.1 n -0.0265	IFRB: 70.0W AR11/A/16/1526 -ADD1/1558 AR11/C/94/1576 -ADD1/1609
291.0E (69.0W)	10 Nov 84 1984-114-A 15385	USASAT-7C SPACENET-2 GTE SPACENET II SPACENET 2	US— GTE Spacenet	FSS 6b,14a/4a,12a	P 1436.2 r_a 35827 r_p 35748 i 0.0 n -0.0137	IFRB: 69.0W AR11/A/11/1525 -ADD1/1548 AR11/C/835/1699 -ADD1/1710
295.0E (65.0W)	8 Feb 85 1985-15-B 15561	SBTS A1[57] BRAZILSAT A1 SBTS 1	Brazil	FSS 6b/4a	P 1436.2 r_a 35852 r_p 35724 i 0.0 n -0.0201	IFRB: 65.0W AR11/A/17/1526 -ADD1/1558 AR11/C/99/1576 -ADD1/1609
296.0E (64.0W)	22 May 81 1981-49-A 12472	GOES EAST[9] GOES-5[42]	US	MetSat,SRS,EES 0.4b,2/ 0.4g,1.6f,1.6g	P 1435.9 r_a 35790 r_p 35780 i 2.5 n +0.0184	IFRB: 75.0W SPA-AA/28/1147 SPA-AJ/366/1508
300.0E (60.0W)	28 Jan 77 1977-5-A 09785	SATCOM PHASE-3B NATO III-B NATO 3B	NATO	FSS 8a/7b	P 1436.2 r_a 35808 r_p 35770 i 7.0 n -0.0330	IFRB: 60.0W AR11/A/358/1773 -ADD1/1878
307.0E (53.0W)	17 May 88 1988-40-A 19121	INTELSAT 5A CONT1 INTELSAT VA CONT 1 INTELSAT IBS 307E INTELSAT V-A F-13	Intelsat	FSS 6b,14a/ 4a,11, 12a,12c,12d[17]	P 1436.1 r_a 35793 r_p 35782 i 0.0 n -0.0137	IFRB: 53.0W AR11/A/115/1609 -ADD1/1628 -ADD2/1638 AR11/A/128/1617 AR11/C/674/1667 AR11/C/704/1673 -ADD1/1731
314.8E (45.2W)	15 Jun 88 1988-51-C 19217	USASAT-13I PANAMSAT I PAS 1	US— Pan American Satellite	FSS 6b,14a/4a,11,12a	P 1436.1 r_a 35798 r_p 35775 i 0.0 n -0.0009	IFRB: 45.0W AR11/A/199/1675 AR11/C/866/1736
319.2E (40.8W)	13 Mar 89 1989-21-B 19883	TDRS EAST TDRS-4 TDRS-D	US	FSS,SRS 2.1,6b,14f/ 2,2.2,4a,13c	P 1432.2 r_a 35737 r_p 35682 i 0.3 n +0.9879	IFRB: 41.0W SPA-AA/231/1381 AR11/C/46/1568 AR11/C/1183/1802
319.9E (40.1W)	10 Jun 86 1986-44-A 16769	STATSIONAR-25[9] GORIZONT 12	USSR	FSS 6b,14a/4a,11	P 1436.1 r_a 35817 r_p 35758 i 1.5 n -0.0137	IFRB: 37.5W AR11/A/384/1797 -ADD1/1803 -CORR1/1813 AR11/C/1311/1836

TABLE 1. IN-ORBIT GEOSTATIONARY COMMUNICATIONS SATELLITES FOR YEAR-END 1989

SUBSATELLITE LONGITUDE[1] (deg)	LAUNCH DATE/ INTERNATIONAL CATALOG NUMBER[2]	SATELLITE DESIGNATION[3]	COUNTRY OR ORGANIZATION	SERVICE FREQUENCY CODE UP/DOWN-LINK (GHz)	ORBIT PARAMETERS[4]	REGISTRATION SPECIAL SECTION NUMBERS
322.6E (37.4W)	27 Oct 89 1989-87-A 20315	INTELSAT6 335.5 INTELSAT VI ATL 1 INTELSAT VI F-2[58]	Intelsat	FSS 6b,14a/4a,11	P 1436.1 r_a 35833 r_p 35740 i 0.1 n -0.0009	IFRB: 24.5W AR11/A/69/1584 AR11/C/627/1658
325.5E (34.5W)	5 Mar 82 1982-17-A 13083	INTELSAT5 ATL4 INTELSAT V ATL 4 INTELSAT V F-4	Intelsat	FSS 6b,14a/4a,11	P 1436.2 r_a 35802 r_p 35777 i 0.2 n -0.0394	IFRB: 34.5W SPA-AA/121/1232 SPA-AJ/220/1418
328.9E (31.1W)	27 Aug 89 1989-67-A 20193	BSB-1 BSB-R1 MARCO POLO 1	UK— British Satellite Broadcasting	FSS,BSS 14a,17/ 12c,12d,12e	P 1436.2[12] r_a 35798 r_p 35777 i 0.1 n -0.0137	IFRB: 31.0W AR11/A/23/1532 -CORR1/1888 AR11/A/26/1534 AR11/C/173/1605 -ADD1/1655 -ADD2/1801 AR11/C/181/1611 -ADD1/1655 -ADD2/1801 AR11/C/731/1674 -CORR1/1731 -ADD1/1801 AR11/C/1209/1815 -ADD1/1893
331.4E (28.6W)	12 May 77 1977-34-B 10001	USGCSS PH2 ATL[9] DSCS II F-8 DSCS 2-A	US	FSS 8a/7b	P 1437.0 r_a 35817 r_p 35792 i 8.1 n -0.2320	IFRB: 12.0W SPA-AA/128/1242 SPA-AJ/153/1373
332.5E (27.5W)	29 Jun 85 1985-55-A 15873	INTELSAT5A ATL2 INTELSAT VA ATL 2 INTELSAT V-A F-11	Intelsat	FSS 6b,14a/4a,11	P 1436.2 r_a 35799 r_p 35778 i 0.0 n -0.0265	IFRB: 27.5W SPA-AA/335/1478 AR11/C/13/1556 AR11/C/123/1592 AR11/C/815/1694
333.9E (26.1W)	10 Nov 84 1984-114-B 15386	MARECS ATL1 MARECS ATL 1 MARECS B2[59]	ESA	FSS,MMSS 1.6b,6b/1.5b,4a	P 1436.1 r_a 35779 r_p 35779 i 2.8 n +0.0954	IFRB: 26.0W SPA-AA/222/1353 SPA-AJ/244/1432
334.7E (25.3W)	14 Apr 89 1989-30-A 19928	STATSIONAR-8 RADUGA 23	USSR	FSS 6a,6b,8a/4a,7b	P 1436.3 r_a 35794 r_p 35786 i 1.2 n -0.0458	IFRB: 25.0W SPA-AA/95/1197 SPA-AJ/50/1276 SPA-AJ/62/1280 AR11/A/246/1695 AR11/C/918/1752
335.5E (24.5W)	22 Mar 85 1985-25-A 15629	INTELSAT5A ATL1 INTELSAT VA ATL 1 INTELSAT V-A F-10[58]	Intelsat	FSS 6b,14a/4a,11	P 1436.2 r_a 35798 r_p 35778 i 0.0 n -0.0201	IFRB: 24.5W SPA-AA/334/1478 AR11/C/12/1556 AR11/C/122/1592

TABLE 1. IN-ORBIT GEOSTATIONARY COMMUNICATIONS SATELLITES FOR YEAR-END 1989

SUBSATELLITE LONGITUDE[1] (deg)	LAUNCH DATE/ INTERNATIONAL CATALOG NUMBER[2]	SATELLITE DESIGNATION[3]	COUNTRY OR ORGANIZATION	SERVICE FREQUENCY CODE UP/DOWN-LINK (GHz)	ORBIT PARAMETERS[4]	REGISTRATION SPECIAL SECTION NUMBERS
335.5E (24.5W)	27 Oct 89	INTELSAT6 335.5E INTELSAT VI ATL 1 INTELSAT VI F-2[58]	Intelsat	FSS 6b,14a/4a,11	P 1436.1 r_a 35833 r_p 35740 i 0.1 n -0.0009	IFRB: 24.5W AR11/A/69/1584 AR11/C/627/1658
335.6E (24.4W)	28 Oct 87 1987-91-A 18443	STATSIONAR-8 COSMOS 1894[22]	USSR	FSS 6b/4a	P 1436.2 r_a 35794 r_p 35784 i 0.3 n -0.0330	IFRB: 25.0W SPA-AA/95/1197 SPA-AJ/50/1276 SPA-AJ/62/1280
338.4E (21.6W)	18 Jan 80 1980-4-A 11669	FLTSATCOM ATL FLTSATCOM F-3 FLTSATCOM 3 OPS 6393	US	FSS,MSS 0.3a,8a/0.3a,7b	P 1436.1 r_a 35803 r_p 35767 i 5.6 n +0.0184	IFRB: 23.0W SPA-AA/84/1186 SPA-AJ/163/1382 SPA-AJ/164/1382
338.6E (21.4W)	6 Dec 80 1980-98-A 12089	INTELSAT5 CONT4[9,16] INTELSAT V CONT 4 INTELSAT V F-2	Intelsat	FSS 6b,14a/4a,11	P 1437.3 r_a 35819 r_p 35802 i 0.6 n -0.3091	IFRB: 1.0W AR11/A/83/1588 AR11/C/593/1652
339.8E (20.2W)	14 Nov 84 1984-115-A 15391	SATCOM PHASE-3[9] NATO III-D NATO 3D	NATO	FSS 8a/7b	P 1436.6 r_a 35952 r_p 35642 i 2.2 n -0.1357	IFRB: 18.0W SPA-AA/144/1247 SPA-AJ/137/1355
340.8E (19.2W)	28 Oct 88 1988-98-A 19621	TDF-1	France	FSS,BSS 17/12e	P 1436.2 r_a 35800 r_p 35775 i 0.0 n -0.0137	IFRB: 19.0W AR11/A/57/1570 AR11/C/107/1578 AR11/C/124/1592 AR11/C/142/1597 AR11/C/703/1670 AR11/C/741/1674
340.8E (19.2W)	8 Aug 89 1989-62-A 20168	TV-SAT 2	West Germany	FSS,BSS,SRS 20a/2.2,12e	P 1436.2[12] r_a 35806 r_p 35769 i 0.0 n -0.0137	IFRB: 19.0W AR11/A/350/1767 -ADD1/1815 -CORR1/1881 AR11/C/1500/1885
340.9E (19.1W)	12 Jul 89 1989-53-A 20122	L-SAT OLYMPUS 1[60]	ESA	FSS,BSS 13a,14a, 17,20a,30a/ 12c,12e,12f,20b	P 1436.2[12] r_a 35799 r_p 35776 i 0.0 n -0.0137	IFRB: 19.0W SPA-AA/308/1463 SPA-AA/337/1479 AR11/A/32/1544 AR11/A/88/1590 AR11/C/6/1554 AR11/C/124/1592 AR11/C/174/1605 AR11/C/232/1619 AR11/C/782/1682

TABLE 1. IN-ORBIT GEOSTATIONARY COMMUNICATIONS SATELLITES FOR YEAR-END 1989

SUBSATELLITE LONGITUDE[1] (deg)	LAUNCH DATE/ INTERNATIONAL CATALOG NUMBER[2]	SATELLITE DESIGNATION[3]	COUNTRY OR ORGANIZATION	SERVICE FREQUENCY CODE UP/DOWN-LINK (GHz)	ORBIT PARAMETERS[4]	REGISTRATION SPECIAL SECTION NUMBERS
341.5E (18.5W)	19 May 83 1983-47-A 14077	INTELSAT5 ATL2 INTELSAT V ATL 2 INTELSAT MCS ATL A INTELSAT V F-6	Intelsat	FSS,MMSS 1.6b,6b,14a/ 1.5b,4a,11[18]	P 1436.1 r_a 35802 r_p 35773 i 0.0 n -0.0137	IFRB: 18.5W SPA-AA/119/1232 SPA-AA/236/1388 SPA-AJ/175/1389 SPA-AA/240/1390 SPA-AJ/218/1418 AR11/C/1094/1791
342.0E (18.0W)	19 Nov 78 1978-106-A 11115	SATCOM PHASE-3 NATO III-C NATO 3C	NATO	FSS 8a/7b	P 1436.2 r_a 35792 r_p 35783 i 4.1 n -0.0137	IFRB: 18.0W SPA-AA/144/1247 SPA-AJ/137/1355
344.4E (15.6W)	4 Apr 86 1986-27-A 16667	WSDRN[61] COSMOS 1738	USSR	FSS,SRS 14b,14f/11,13c	P 1436.2 r_a 35826 r_p 35750 i 1.8 n -0.0201	IFRB: 16.0W SPA-AA/341/1484 AR11/C/67/1570
344.5E (15.0W)	10 Nov 84 1984-113-C 15384	FLTSATCOM-A ATL SYNCOM IV-1 LEASESAT F-1 LEASAT 1	US— Hughes Communications	FSS,MSS 0.3a,8a/0.3a,7b	P 1436.2 r_a 35873 r_p 35702 i 0.9 n -0.0137	IFRB: 15.0W AR11/A/97/1605 -ADD1/1652 AR11/C/1009/1775
345.1E (14.9W)	19 Feb 76 1976-17-A 08697	MARISAT-ATL[20] MARISAT F-1 MARISAT 1	US— Comsat General	FSS,MSS,MMSS 0.3a,1.6b,6b/ 0.3a,1.5b,4a[21]	P 1436.2 r_a 35794 r_p 35782 i 7.8 n -0.0201	IFRB: 15.0W SPA-AA/4/1101 SPA-AA/7/1101 SPA-AJ/33/1254
345.5E (14.5W)	31 Mar 88 1988-28-A 19017	STATSIONAR-4 GORIZONT 15	Intersputnik	FSS 6b,14a/4a,11	P 1436.2 r_a 35790 r_p 35784 i 0.3 n -0.0073	IFRB: 14.0W SPA-AA/92/1197 AR11/C/765/1677 AR11/C/875/1737 AR11/C/1112/1793 AR11/C/1203/1809
346.3E (13.7W)	1 Aug 88 1988-66-A 19344	STATSIONAR-4 COSMOS 1961[22]	Intersputnik	FSS 6b/4a	P 1436.2 r_a 35793 r_p 35782 i 0.6 n -0.0137	IFRB: 14.0W SPA-AA/92/1197 AR11/C/765/1677 AR11/C/875/1737 AR11/C/1113/1793 AR11/C/1204/1809
348.2E (11.8W)	30 Jun 83 1983-66-A 14160	STATSIONAR-11 GORIZONT 7	USSR	FSS 6b,14a/4a,11	P 1436.1 r_a 35808 r_p 35766 i 4.1 n -0.0073	IFRB: 11.0W SPA-AA/270/1425 SPA-AJ/303/1469 AR11/A/269/1707 -CORR1/1728 AR11/C/877/1737 -CORR1/1743 AR11/C/964/1766 AR11/C/1120/1793 AR11/C/1201/1809

TABLE 1. IN-ORBIT GEOSTATIONARY COMMUNICATIONS SATELLITES FOR YEAR-END 1989

SUBSATELLITE LONGITUDE[1] (deg)	LAUNCH DATE/ INTERNATIONAL CATALOG NUMBER[2]	SATELLITE DESIGNATION[3]	COUNTRY OR ORGANIZATION	SERVICE FREQUENCY CODE UP/DOWN-LINK (GHz)	ORBIT PARAMETERS[4]	REGISTRATION SPECIAL SECTION NUMBERS
349.0E (11.0W)	14 Jun 80 1980-49-A 11841	STATSIONAR-11 GORIZONT 4[11]	USSR	FSS 6b/4a	P 1460.1 r_a 36273 r_p 36236 i 7.2 n -6.0110	IFRB: 11.0W SPA-AA/270/1425 SPA-AJ/303/1469 AR11/C/877/1737 -CORR1/1743 AR11/C/1120/1793
349.2E (10.8W)	19 Jun 81 1981-57-A 12544	METEOSAT S2 METEOSAT-2[62]	ESA	MetSat,SRS,EES 2/1.6f,1.6g,0.4g	P 1436.2 r_a 35794 r_p 35783 i 2.4 n -0.0265	IFRB: 10.0W AR11/A/415/1815 AR11/C/1607/1892
352.0E (8.0W)	4 Aug 84 1984-81-B 15159	TELECOM-1A	France	FSS 6b,8a,14a/ 4a,7b,12c,12d[28]	P 1436.2 r_a 35793 r_p 35781 i 0.0 n -0.0073	IFRB: 8.0W SPA-AA/268/1425 SPA-AJ/299/1461 SPA-AJ/361/1508 SPA-AJ/387/1512 AR11/C/125/1593 -ADD1/1610 AR11/C/184/1611 AR11/C/390/1628
354.9E (5.1W)	15 Jun 88 1988-51-A 19215	METEOSAT[9] METEOSAT-3 METEOSAT-P2	ESA	MetSat,SRS,EES 2/1.6f,1.6g,0.4g	P 1436.3 r_a 35793 r_p 35787 i 0.4 n -0.0458	IFRB: 0.0E AR11/A/413/1815
357.2E (2.8W)	11 Mar 88 1988-18-B 18952	TELECOM-1C	France	FSS 6b,8a,14a/ 4a,7b,12c,12d[28]	P 1436.2 r_a 35794 r_p 35781 i 0.0 n -0.0137	IFRB: 3.0E AR11/A/29/1539 -ADD1/1713 -CORR1/1730 AR11/C/115/1589 -ADD1/1643 AR11/C/131/1594 -ADD1/1643 AR11/C/157/1598 -ADD1/1643
359.0E (1.0W)	31 Dec 89 1990-1-A 20401	SKYNET-4A	UK	FSS,MSS 0.2,0.3a,0.3b, 8a,44/ 0.3a,0.3b,7b	P 1436.2 r_a 35794 r_p 35783 i 3.3 n -0.0265	AR11/A/21/1531 AR11/C/182/1611 -ADD1/1652 -ADD2/1711 AR11/C/588/1652
359.0E (1.0W)	28 Sep 85 1985-87-A 16101	INTELSAT5A CONT4[16] INTELSAT VA CONT 4 INTELSAT V-A F-12	Intelsat	FSS 6b,14a/4a,11	P 1436.2 r_a 35799 r_p 35775 i 0.0 n -0.0073	IFRB: 1.0W AR11/A/117/1609 -ADD1/1628 -ADD2/1638 AR11/C/677/1668

[1] Satellite longitudes are those recorded in the current release of NASA's *Geosynchronous Satellite Report*. For satellites not covered in that report, locations were compiled from the most recent secondary sources available.

[2] International designations are assigned at the time of launch. Object catalog numbers are those used by NORAD, the U.S. Space Command, and NASA.

[3] IFRB satellite network names appear first, followed by common or alternate names.

[4] P = period (min); r_a = apogee (km); r_p = perigee (km); i = inclination (deg); n = drift (deg/day). Negative n indicates westward and positive n indicates eastward drift. Unless otherwise noted, basic elements are compiled from NASA's *Satellite Situation Report* for June 30, 1989.

[5] Orbital Test Satellite. An experimental precursor to the Eutelsat ECS series, OTS-2 is currently maintained in geostationary orbit by means of solar sailing to test subsystem performance.

[6] Shortly after its deployment in the late summer of 1988, ECS 5 was positioned at 10°E. This freed ECS 4, which had been at that location, to move to 13°E where it assumed traffic from ECS 1. The latter was then moved to a new orbital location at 16°E.

[7] Gorizont 11 was initially deployed at Statsionar-5 (53°E), but is currently at Statsionar-27. It is believed to be carrying Ku-band transponders, although no Loutch payload has been registered at this location.

[8] In October 1989, Arabsat agreed to lease 12 transponders on its 1-B satellite to the Indian government. As a result, the system's existing traffic is being transferred to Arabsat 1-A, which had functioned previously as an in-orbit spare. In November it was announced that both satellites would be put into inclined orbit for extended use with the COMSAT Maneuver.

[9] Satellite not currently on-station.

[10] Registration information unavailable.

[11] Believed to be inoperative.

[12] Basic elements compiled from NASA's *Satellite Situation Report* for September 30, 1989.

[13] Gorizont 9 was initially deployed at Statsionar-14 (96.5°E) and subsequently relocated to Statsionar-5 (53°E).

[14] The orbital location 95°E has been established as the central station in the Soviet Satellite Data Relay Network. Cosmos 1700, now at 55.2°E, was previously at that position and was reported to be transmitting messages from ground control center to the Mir Space Station in 1986. At this time, it is thought to be inoperative.

[15] Experimental Ku-band communications satellite.

[16] At 60°E, INTELSAT V-A F-15 replaces INTELSAT V-A F-12, which was previously at that position and which has been relocated to 1°W. At the latter location, F-12 has in turn replaced INTELSAT V F-2, which came to the end of its normal stationkeeping lifetime in September 1989.

[17] INTELSAT V-A F-13 and F-15 each carry Ku-band spot beams designed to enhance their provision of IBS.

[18] INTELSAT V F-5, F-6, F-7, and F-8 each carry a maritime communications subsystem (MCS) for lease by Inmarsat. L-band signals from shipboard terminals are converted to C-band frequencies for relay to coast earth stations.

[19] Raduga 17 was initially deployed at Statsionar-D3 (35°E) and subsequently relocated to Statsionar-20 (70°E). It appears to have been replaced at its previous position by Raduga 22, launched in 1988.

[20] Serves as an in-orbit spare for the Inmarsat system.

[21] The Marisat satellites' UHF channels were leased to the U.S. Navy under the Gapsat program from 1973 until the successful deployment of the first FLTSATCOM satellites, and intermittently thereafter. More recently, the American Mobile Satellite Company in the U.S. and Telesat Mobile in Canada have proposed to purchase the unused capacity on Marisat F-1 on a temporary basis to provide commercial mobile satellite services on the North American continent.

[22] Designation uncertain, but believed to be functionally equivalent to a Gorizont. In the past, emissions have also been detected in Ku-band, indicating the presence of a Loutch transponder on board Cosmos 1540, 1629, and 1888. Currently, only Cosmos 1888, 1894, and 1961 appear to be in operation.

[23] Shiyan Tongxin Weixing. Experimental version of the DFH2 series domsats.

[24] Gorizont 14 was initially deployed at Statsionar-7 (140°E) and subsequently relocated to Statsionar-21 (103°E).

[25] In early 1989, NHK purchased a spare DBS satellite from GE Astro-Space for $130 million, including in-orbit delivery. Originally built for COMSAT's Satellite Television Corporation, the spacecraft was renamed BS-2X and was intended to serve as a backup for BS-2B, which will be nearing the end of its operational lifetime in 1991. BS-2X was subsequently destroyed in an abortive Ariane launch as this log was being compiled, on February 22, 1990. NHK is reportedly seeking a replacement.

[26] Experimental satellite with only one active transponder.

[27] Telecom 1B, previously positioned at 5°W, suffered a malfunction of its on-board attitude control system in January 1988. Although now partially stabilized, it is still not operational.

[28] The X-band transponder is operated by the French Ministry of Defense for the Syracuse network of military communications.

[29] CS-2A and CS-2B were removed from their original orbital positions in 1988 and replaced by second-generation CS-3 satellites.

[30] Engineering Test Satellite. An experimental satellite constructed by NASDA, ETS-5 incorporates a separate maritime mobile satellite project developed by the Japanese Ministry of Transportation. In addition, it carries an aeronautical mobile satellite payload (AMEX) operating at both C- and L-band frequencies.

[31] Geostationary Meteorological Satellite System.

[32] INTELSAT V F-3 served as Intelsat's Atlantic Ocean Region contingency spare at 53°W until May 1988, when it was replaced at that location by INTELSAT V-A F-13.

[33] DSCS II F-12 was originally deployed at approximately 60°E and was until recently operated at that position.

[34] Leasesat F-4 may have been intended to assume the orbital position registered for FLTSATCOM-A W PAC (177°W). However, it was rendered inoperative by a failure of its communications payload which occurred shortly after it reached geosynchronous orbit.

[35] DSCS II F-14 was identified at the time of launch as an in-orbit spare.

[36] Raduga 18 was initially deployed at Statsionar-8 (25°W) and subsequently relocated to Statsionar-D2 (170°W).
[37] Gorizont 10 was initially deployed at Statsionar-13 (80°E) and subsequently relocated to Statsionar-10 (170°W).
[38] Gorizont 6 was initially deployed at Statsionar-7 (140°E). Its closest current station is Statsionar-6.
[39] Acquired by General Electric and renamed GE American Communications.
[40] Disabled by failure of on-board imaging system in early 1989. Not operational.
[41] The DSCS III series of satellites carries an AFSATCOM single-channel UHF transponder in addition to the normal X-band package.
[42] Partially operational.
[43] The FCC has authorized AT&T to relocate Telstar 3D to 123°W.
[44] Acquired by Hughes Communications in July 1989.
[45] All Westar satellites were acquired by Hughes Communications in 1988.
[46] Telesat Canada plans to relocate Anik-D2 to 111°W by year-end 1990.
[47] This satellite is believed to be FLTSATCOM F-7, the first of a series of advanced payloads carrying an experimental EHF channel in addition to the UHF and X-band channels carried on previous FLTSATCOM satellites. Two other satellites in the series—F-6 and F-8—were scheduled to be brought into service in 1987 but were either destroyed or damaged on the launch pad.
[48] SBS-1 and SBS-2 are currently collocated at approximately 99°W. COMSAT has received temporary authority from the FCC to operate these satellites in an inclined orbit by means of the COMSAT Maneuver. It has also been granted permission to move SBS-1 to 97°W, pending a ruling on its request to permanently relocate both satellites to 76°W.
[49] When Satellite Business Systems was dissolved in 1985, three of its in-orbit satellites—SBS-1, SBS-2, and SBS-3—were acquired by MCI. A fourth, SBS-4, was purchased by IBM's subsidiary Satellite Transponder Leasing Corp. Subsequently, in 1987 and 1988, MCI transferred both SBS-1 and SBS-2 to Comsat General, and in July 1989 control of SBS-4 went to Hughes Communications when the latter acquired STLC from IBM.
[50] GOES-7 was originally deployed at the position reserved for GOES EAST (75°W). However, since the failure of GOES-6 it has become the only fully operational weather satellite available to NOAA and is occasionally relocated in order to maximize its coverage.
[51] GSTAR-3 experienced an apogee kick motor failure following launch and was not raised into geostationary orbit until November 1989. Its expected lifetime has been reduced to 5 years.
[52] GSTAR-3 (Geostar R02) and GTE Spacenet 3R (Geostar R01) each carry L-band antennas with receive-only capability for interim reception of signals from Geostar mobile transmitters. These RDSS signals are converted to Ku-band for down-link.

[53] TDRS-1 was originally deployed in the position reserved for TDRS EAST, but was replaced by TDRS-4 in early 1989. It has since been relocated and will be maintained in operation as an in-orbit spare.
[54] S-band antenna believed to be inoperative.
[55] Originally deployed at 95°W, Comstar D-2 has been collocated with Comstar D-4 at 76°W. Beyond their nominal mission lifetimes, both satellites have been placed in inclined orbit and are being maintained in operation by means of the COMSAT Maneuver.
[56] Communications Technology Satellite or Cooperative Applications Satellite. An experimental Ku-band satellite, CTS was a joint project of the Canadian Department of Communications and NASA. Not operational.
[57] Sistema Braziliana de Telecomunicacoes por Satellite.
[58] By April 1990, after initial tests have been completed, INTELSAT VI F-2 will be relocated from its temporary slot at 322°E to replace INTELSAT V-A F-10 at 335.5°E.
[59] Inmarsat has announced plans to establish a fourth "operation region." As a result, it will relocate Marecs B2 from 26°W to 55°W beginning in late September 1990.
[60] Experimental satellite carrying payloads for DBS, Ku- and Ka-band communications, and propagation testing.
[61] Western station in the Soviet Satellite Data Relay Network.
[62] Meteosat-2 ceased routine operations in August 1988 when it was replaced by Meteosat-3. The latter will in turn be replaced by MOP-1 as primary satellite in the Meteosat Operational System, although it will remain in use as an in-orbit spare and its laser-based clock synchronization retroreflector will continue to operate.

TABLE 2. PLANNED GEOSTATIONARY COMMUNICATIONS SATELLITES FOR YEAR-END 1989

SUBSATELLITE LONGITUDE[1] (deg)	IN-USE DATE[2]	SATELLITE DESIGNATION[3]	COUNTRY OR ORGANIZATION	SERVICE FREQUENCY CODE UP/DOWN-LINK (GHz)	PERIOD OF VALIDITY[4] (yr)	SPECIAL SECTION NUMBERS
1.0E	31 Aug 87	GDL-5 ASTRA[5]	Luxembourg–Societe Europeene des Satellites	FSS,BSS 13a,14a/11	25	AR11/A/93/1594 -ADD1/1730 -ADD2/1747 -ADD3/1841 AR11/C/612/1657
1.0E	31 Dec 92	STATSIONAR-22[6]	USSR	FSS 6b/4a	20	AR11/A/410/1806 -CORR1/1822
1.0E	1 Jun 92	TOR-15	USSR	FSS,MSS 43,44/20b,20f	20	AR11/A/372/1790 AR11/C/1418/1862
1.0E	1 Jun 92	VOLNA-21	USSR	MSS 0.3a,0.3b/0.3a	20	AR11/A/375/1793 AR11/C/1581/1887
3.0E	30 Sep 91	TELECOM-2C	France	FSS,SRS 2,6b,8a,14a/ 2.2,4a,7b,12c,12d	10	AR11/A/326/1745 -ADD1/1772 -ADD2/1798 AR11/C/1103/1792 AR11/C/1166/1795 AR11/C/1331/1839
4.0E	1 Jun 91	MILSTAR 13[7]	US	MSS,SRS 0.3a,1.7b,44/ 0.3a,2.2,20f	20	AR11/A/454/1837 AR11/C/1549/1885
5.0E	1 Jun 92	TOR-19	USSR	FSS,MSS 43,44/20b,20f	20	AR11/A/390/1798 AR11/C/1492/1878
7.0E	31 Dec 87	F-SAT 1[8]	France	FSS,SRS 2,6b,30a/ 2.2,4a,20b	10	AR11/A/79/1587 AR11/C/564/1649 AR11/C/568/1649
7.0E	28 Feb 94	EUTELSAT 2-7E EUTELSAT II-F4	Eutelsat	FSS,MSS,MMSS,AMSS 1.6b,1.6c,1.6d,14a/ 1.5b,1.5c,1.5d, 11,12c,12d[9]	20	AR11/A/305/1732 -ADD1/1766 -ADD2/1782 -ADD3/1894 AR11/C/1205/1809 -ADD1/1882
8.0E	30 Aug 90	STATSIONAR-18[6]	USSR	FSS 6b/4a	20	AR11/A/220/1686 AR11/C/911/1749 -ADD1/1756 -ADD2/1877
8.0E	10 Aug 90	TOR-8	USSR	FSS,MSS 43,44/20b,20f	20	AR11/A/285/1710 AR11/C/1361/1851
8.0E	15 Oct 90	VOLNA-15	USSR	MSS,AMSS 0.3a,0.3b,1.6d/ 0.3a,1.5d	20	AR11/A/241/1693 AR11/C/983/1769 -CORR1/1812
10.0E	31 Dec 88	APEX[10]	France	FSS,SRS 2,6b,30a/ 2.2,4a,20b,39,82a	10	AR11/A/62/1578 -ADD1/1611 -ADD2/1716 -ADD3/1730 AR11/C/388/1628 AR11/C/479/1648 AR11/C/582/1651

TABLE 2. PLANNED GEOSTATIONARY COMMUNICATIONS SATELLITES FOR YEAR-END 1989

SUBSATELLITE LONGITUDE[1] (deg)	IN-USE DATE[2]	SATELLITE DESIGNATION[3]	COUNTRY OR ORGANIZATION	SERVICE FREQUENCY CODE UP/DOWN-LINK (GHz)	PERIOD OF VALIDITY[4] (yr)	SPECIAL SECTION NUMBERS
10.0E	28 Feb 94	EUTELSAT 2-10E EUTELSAT II-F2	Eutelsat	FSS,MSS,MMSS,AMSS 1.6b,1.6c,1.6d,14a/ 1.5b,1.5c,1.5d, 11,12c,12d[9]	20	AR11/A/349/1766 -ADD1/1766 -ADD2/1782 -ADD3/1894 AR11/C/1206/1809 -ADD1/1882
12.0E	31 Dec 84	PROGNOZ-2[11]	USSR	SRS,EES 3/2.2	20	SPA-AA/317/1471 SPA-AJ/411/1515 AR11/C/1562/1886
12.0E	1 Jun 92	STATSIONAR-27[6]	USSR	FSS 6b/4a	20	AR11/A/392/1799 -CORR1/1822 AR11/C/1593/1888
12.0E	1 Jun 92	TOR-18	USSR	FSS,MSS 43,44/20b,20f	20	AR11/A/389/1798 AR11/C/1479/1877
12.0E	1 Jun 92	VOLNA-27	USSR	MSS 0.3a,0.3b/0.3a	20	AR11/A/378/1793 AR11/C/1590/1887
13.0E	28 Feb 94	EUTELSAT 2-13E EUTELSAT II-F1	Eutelsat	FSS,MSS,MMSS,AMSS 1.6b,1.6c,1.6d,14a/ 1.5b,1.5c,1.5d, 11,12c,12d[9]	20	AR11/A/306/1732 -ADD1/1766 -ADD2/1782 -ADD3/1894 AR11/C/1207/1809 -ADD1/1882
13.0E	31 Dec 87	ITALSAT	Italy	FSS,SRS 2,30a,48/20b,39[12]	7	AR11/A/157/1633 AR11/C/772/1679 AR11/C/827/1697
15.0E	30 Apr 92	ZENON-B	France	FSS,AMSS,SRS 1.6d,2,6b/ 1.5d,2.2,4a	10	AR11/A/364/1781
15.0E	31 Jul 87	AMS-1	Israel	FSS 6b,14a/4a,11	10	AR11/A/39/1554 -ADD1/1563 AR11/C/816/1695 -ADD1/1708 -ADD2/1803
15.0E	31 Jul 87	AMS-2	Israel	FSS 6b,14a/4a,11	10	AR11/A/39/1554 -ADD1/1563 AR11/C/817/1695 -ADD1/1708 -ADD2/1803
15.0E	31 Dec 90	STATSIONAR-23[6]	USSR	FSS 6b/4a	20	AR11/A/318/1740 -CORR1/1760 AR11/C/1195/1804
15.0E	31 Dec 90	TOR-12	USSR	FSS,MSS 43,44/20b,20f	20	AR11/A/309/1736 AR11/C/1444/1872
15.0E	1 Jun 92	VOLNA-23	USSR	MSS 0.3a,0.3b/0.3a	20	AR11/A/376/1793 AR11/C/1584/1887

TABLE 2. PLANNED GEOSTATIONARY COMMUNICATIONS SATELLITES FOR YEAR-END 1989

SUBSATELLITE LONGITUDE[1] (deg)	IN-USE DATE[2]	SATELLITE DESIGNATION[3]	COUNTRY OR ORGANIZATION	SERVICE FREQUENCY CODE UP/DOWN-LINK (GHz)	PERIOD OF VALIDITY[4] (yr)	SPECIAL SECTION NUMBERS
16.0E	28 Feb 94	EUTELSAT 2-16E EUTELSAT II-F3	Eutelsat	FSS,MSS,MMSS,AMSS 1.6b,1.6c,1.6d,14a/ 1.5b,1.5c,1.5d, 11,12c,12d[9]	20	AR11/A/478/1861 -ADD1/1894 AR11/A/479/1861
16.0E	1987[13]	SICRAL-1A[14]	Italy	FSS,MSS 0.3b,8a,14a,44/ 0.3a,7b,12c,12d,20f	8	AR11/A/44/1557 -ADD1/1588 -ADD2/1652
17.0E	30 Apr 92	SABS[15]	Saudi Arabia	FSS,BSS 14a,14b/11,12e,12f	20	AR11/A/353/1768 -ADD1/1801
17.0E	17 Apr 93	SABS 1-2[15]	Saudi Arabia	FSS,BSS 14a,14b/11,12e,12f	20	AR11/A/125/1616 AR11/C/1212/1815 -CORR1/1830 -CORR2/1862
19.0E	30 Apr 92	ZENON-C	France	FSS,AMSS,SRS 1.6d,2,14a/ 1.5d,2.2,11	10	AR11/A/365/1781
19.0E	1 Mar 93	TOR-26	USSR	FSS,MSS 43,44/20b,20f	20	AR11/A/459/1839
19.0E	1 Feb 91	MILSTAR 9[7]	US	MSS,SRS 0.3a,1.7b,44/ 0.3a,2.2,20f	20	AR11/A/450/1837 AR11/C/1533/1885
19.2E	3 Mar 90	GDL-7 ASTRA 1B[16]	Luxembourg–Societe Europeene des Satellites	FSS,BSS 14a/11	20	AR11/A/472/1860
21.0E	30 Apr 93	BABYLONSAT-3	Iraq	FSS 14a/11	20	AR11/A/441/1832 -ADD1/1875
22.0E	1987[13]	SICRAL-1B[14]	Italy	FSS,MSS 0.3b,8a,14a,44/ 0.3a,7b,12c,12d,20f	8	AR11/A/45/1557 -ADD1/1588 -ADD2/1652
23.0E	1 Aug 90	STATSIONAR-19	USSR	FSS 6a,6b/4a[17]	20	AR11/A/221/1686 AR11/C/916/1752 -CORR1/1756
23.0E	1 Aug 90	TOR-7	USSR	FSS,MSS 43,44/20b,20f	20	AR11/A/284/1710 AR11/C/1356/1851
23.0E	15 Oct 90	VOLNA-17	USSR	MSS,AMSS 0.3a,0.3b,1.6d/ 0.3a,1.5d	20	AR11/A/242/1693 AR11/C/986/1769 -CORR1/1812
26.0E	30 Apr 91	ZOHREH-2	Iran	FSS 14a/11	20	AR11/A/297/1719 -ADD1/1728 -ADD2/1776 AR11/C/1235/1818
27.0E	1 Jun 92	TOR-20	USSR	FSS,MSS 43,44,20b,20f	20	AR11/A/391/1798 AR11/C/1484/1877

TABLE 2. PLANNED GEOSTATIONARY COMMUNICATIONS SATELLITES FOR YEAR-END 1989

Subsatellite Longitude[1] (deg)	In-Use Date[2]	Satellite Designation[3]	Country or Organization	Service Frequency Code Up/Down-Link (GHz)	Period of Validity[4] (yr)	Special Section Numbers
28.5E	30 Nov 89	DFS-2 DFS KOPERNIKUS	West Germany	FSS,SRS 2,13a,14a,30a/ 2.2,11,12c,12d,20b	10	AR11/A/41/1556 -ADD1/1611 -ADD2/1828 AR11/C/698/1670 -ADD1/1877
30.0E	30 Apr 93	BABYLONSAT-1	Iraq	FSS 14a/11	20	AR11/A/439/1832 -ADD1/1875
30.0E	1 Mar 91	MILSTAR 10[7]	US	MSS,SRS 0.3a,1.7b,44/ 0.3a,2.2,20f	20	AR11/A/451/1837 AR11/C/1537/1885
31.0E	1 Jan 91	ARABSAT 1-C ARABSAT F3	Arab League	FSS,BSS 6b/4a	10	AR11/A/345/1764 AR11/C/1366/1854 -CORR1/1875
32.0E	31 Dec 87	VIDEOSAT-1[8]	France	FSS,SRS 2,14a/2.2,12c,12d	10	AR11/A/80/1588 AR11/C/574/1650 AR11/C/580/1650
32.0E	31 Jul 92	TOR-21	USSR	FSS,MSS 43,44/20b,20f	20	AR11/A/416/1815 AR11/C/1568/1886
33.5E	31 Dec 90	DFS-5 DFS KOPERNIKUS	West Germany	FSS,SRS 2,13a,14a,30a/ 2.2,11,12c,12d,20b	10	AR11/A/465/1840 -ADD1/1871
34.0E	30 Apr 91	ZOHREH-1	Iran	FSS 14a/11	20	AR11/A/296/1719 -ADD1/1728 -ADD2/1776 AR11/C/1224/1818
35.0E	31 Dec 84	PROGNOZ-3[11]	USSR	SRS,EES 3/2.2	20	SPA-AA/318/1471 SPA-AJ/412/1515
35.0E	1 Aug 90	TOR-2	USSR	FSS,MSS 43,44/20b,20f	20	AR11/A/279/1710 AR11/C/1299/1832
35.0E	31 Oct 91	VOLNA-11	USSR	MSS,AMSS 0.3a,0.3b,1.6d/ 0.3a,1.5d	20	AR11/A/150/1631 -ADD1/1677 AR11/C/977/1769
36.0E	28 Feb 94	EUTELSAT 2-36E EUTELSAT II-F5	Eutelsat	FSS,MSS,MMSS,AMSS 1.6b,1.6c,1.6d,14a/ 1.5b,1.5c,1.5d, 11,12c,12d[9]	20	AR11/A/307/1732 -ADD1/1766 -ADD2/1782 AR11/C/1208/1809 -ADD1/1882
38.0E	31 Dec 91	PAKSAT-1	Pakistan	FSS,BSS,MetSat 0.4b,14a,14b/ 11,12b,12c,12d, 12g,12h[18]	15	AR11/A/90/1592 -ADD1/1649 -ADD2/1715 AR11/C/1367/1858 -CORR1/1870
40.0E	10 May 84	STATSIONAR-12	USSR	FSS 6b/4a	20	SPA-AA/271/1425 AR11/C/878/1737 AR11/C/1122/1793

TABLE 2. PLANNED GEOSTATIONARY COMMUNICATIONS SATELLITES FOR YEAR-END 1989

SUBSATELLITE LONGITUDE[1] (deg)	IN-USE DATE[2]	SATELLITE DESIGNATION[3]	COUNTRY OR ORGANIZATION	SERVICE FREQUENCY CODE UP/DOWN-LINK (GHz)	PERIOD OF VALIDITY[4] (yr)	SPECIAL SECTION NUMBERS
40.0E	31 Jul 92	TOR-22	USSR	FSS,MSS 43,44/20b,20f	20	AR11/A/417/1815 AR11/C/1563/1886
41.0E	30 Jul 92	ZOHREH-4	Iran	FSS 14a/11	20	AR11/A/394/1800
41.0E	31 Dec 92	PAKSAT-2	Pakistan	FSS,BSS,MetSat 0.4b,14a,14b/ 11,12b,12c,12d, 12g,12h[18]	15	AR11/A/91/1692 -ADD1/1649 -ADD2/1715
45.0E	31 Jul 92	STATSIONAR-9A	USSR	FSS 6b/4a	20	AR11/A/402/1803
45.0E	1 Aug 90	TOR-3	USSR	FSS,MSS 43,44/20b,20f	20	AR11/A/280/1710 AR11/C/1336/1839
45.0E	1980[13]	VOLNA-3	USSR	MSS,MMSS,AMSS 0.3b,1.6b,1.6c,1.6d/ 0.3a,1.5b,1.5c,1.5d	20	SPA-AA/171/1286 SPA-AJ/98/1329
45.0E	1 Dec 90	VOLNA-3M	USSR	MMSS 1.6b/1.5b	20	AR11/A/249/1697 -CORR1/1715 AR11/C/1398/1861
47.0E	30 Apr 91	ZOHREH-3	Iran	FSS 14a/11	20	AR11/A/298/1719 -ADD1/1728 -ADD2/1776 AR11/C/1246/1818
49.0E	1 Jun 92	TOR-16	USSR	FSS,MSS 43,44/20b,20f	20	AR11/A/373/1790 AR11/C/1454/1872
51.0E	30 Apr 93	BABYLONSAT-2	Iraq	FSS 14a/11	20	AR11/A/440/1832 -ADD1/1875
53.0E	31 Jul 90	SKYNET-4C[19]	UK	FSS,MSS 0.3a,8a,44/0.3a,7b	10	AR11/A/84/1588 -ADD1/1597 AR11/C/867/1737
53.0E	1 Sep 90	MORE-53	USSR	FSS,MMSS 1.6b,6b/1.5b,4a	15	AR11/A/185/1662 AR11/C/1088/1791 -CORR1/1883
53.0E	31 Jul 92	TOR-23	USSR	FSS,MSS 43,44/20b,20f	20	AR11/A/418/1815 AR11/C/1573/1886
53.0E	1980[13]	VOLNA-4	USSR	MSS,MMSS,AMSS 1.6b,1.6c,1.6d/ 1.5b,1.5c,1.5d	NA	SPA-AA/172/1286 SPA-AJ/99/1329
55.0E	1 Sep 90	MILSTAR 4[7]	US	MSS,SRS 0.3a,1.7b,44/ 0.3a,2.2,20f	20	AR11/A/445/1837 AR11/C/1513/1885
57.0E	30 Jun 93	USGCSS PH3 INDOC2 DSCS III	US	FSS,SRS 1.7b,8a/2.2,7b	10	AR11/A/490/1875

TABLE 2. PLANNED GEOSTATIONARY COMMUNICATIONS SATELLITES FOR YEAR-END 1989

SUBSATELLITE LONGITUDE[1] (deg)	IN-USE DATE[2]	SATELLITE DESIGNATION[3]	COUNTRY OR ORGANIZATION	SERVICE FREQUENCY CODE UP/DOWN-LINK (GHz)	PERIOD OF VALIDITY[4] (yr)	SPECIAL SECTION NUMBERS
58.0E	31 Dec 90	TOR-13	USSR	FSS,MSS 43,44/20b,20f	20	AR11/A/310/1736 AR11/C/1413/1862
60.0E	31 Dec 89	USGCSS PH3 INDOC DSCS III	US	FSS,SRS 1.7b,8a/2.2,7b	10	AR11/A/267/1706 -ADD1/1730 AR11/C/413/1629 AR11/C/1219/1816 -CORR1/1842
60.0E	1 Oct 90	INTELSAT6 60E INTELSAT VI IND 1 INTELSAT VI F-5	Intelsat	FSS 6b,14a/4a,11	15	AR11/A/71/1584 AR11/C/626/1658 -ADD1/1713 AR11/C/1624/1905
61.5E	1 Nov 92	ACS-7[20]	US	MSS,AMSS 1.6c,1.6d/1.5c,1.5d	15	AR11/A/398/1800
62.0E	31 Jul 92	TOR-24	USSR	FSS,MSS 43,44/20b,20f	20	AR11/A/419/1815 AR11/C/1595/1890
63.0E	1 Nov 90	INTELSAT6 63E INTELSAT VI F-4	Intelsat	FSS 6b,14a/4a,11	15	AR11/A/366/1782 AR11/C/1269/1819 -CORR1/1841 -CORR2/1853
64.5E	1 Jul 89	INMARSAT IOR INMARSAT II[21]	Inmarsat	FSS,MSS,MMSS,AMSS 1.6b,1.6c,1.6d,6b/ 1.5b,1.5c,1.5d,4a	15	AR11/A/178/1644 -ADD1/1760 AR11/C/846/1706 -ADD1/1784
65.0E	31 Jul 92	TOR-25	USSR	FSS,MSS 43,44/20b,20f	20	AR11/A/420/1815 AR11/C/1600/1890
66.5E	31 Jan 90	INMARSAT IOR-2 INMARSAT II[21]	Inmarsat	FSS,MSS,MMSS,AMSS 1.6b,1.6c,1.6d,6b/ 1.5b,1.5c,1.5d,4a	15	AR11/A/293/1713 -ADD1/1760
69.0E	31 Dec 90	TOR-14	USSR	FSS,MSS 43,44/20b,20f	20	AR11/A/311/1736 AR11/C/1449/1872
70.0E	1 Jun 92	TOR-17	USSR	FSS,MSS 43,44/20b,20f	20	AR11/A/37/1790 AR11/C/1474/1877
70.0E	1 Jun 92	VOLNA-19	USSR	MSS 0.3a,0.3b/0.3a	20	AR11/A/374/1793 AR11/C/1578/1887
70.0E	1 Nov 91	USASAT-13N CELESTAR 2	US– McCaw Space Technologies[22]	FSS 14a/11,12c,12d	10	AR11/A/344/1763 AR11/C/1438/1871 -ADD1/1900
72.0E	1 Jan 88	FLTSATCOM-B INDOC[23]	US	MSS 44/20f	10	AR11/A/337/1762 -ADD1/1794 -ADD2/1802
74.0E	31 Jul 90	INSAT-2C	India	FSS,BSS, MetSat,EES 0.4b,6b/4a,4b	20	AR11/A/262/1702 AR11/C/1083/1789 -CORR1/1804

TABLE 2. PLANNED GEOSTATIONARY COMMUNICATIONS SATELLITES FOR YEAR-END 1989

SUBSATELLITE LONGITUDE[1] (deg)	IN-USE DATE[2]	SATELLITE DESIGNATION[3]	COUNTRY OR ORGANIZATION	SERVICE FREQUENCY CODE UP/DOWN-LINK (GHz)	PERIOD OF VALIDITY[4] (yr)	SPECIAL SECTION NUMBERS
76.0E	2 Jul 94	GOMS[24]	USSR	FSS,MetSat 0.4b,8d,30a/7b,20b	20	AR11/A/205/1678 -ADD1/1712 AR11/C/1277/1825
76.0E	31 Dec 90	GOMS-M[24]	USSR	FSS,MetSat,SRS,EES 0.4b,2,2.1,8d,30a/ 0.4g,1.6f,1.6g,7b,20b	15	AR11/A/425/1822
77.0E	17 Oct 89	CSSRD-2[25]	USSR	FSS,SRS 14b,14f/11,12c,13c	20	AR11/A/188/1672 -CORR1/1711
80.0E	30 Dec 82	POTOK-2[26]	USSR	FSS 4b/4a	15	SPA-AA/345/1485 AR11/C/22/1558
80.0E	31 Oct 88	PROGNOZ-4[11]	USSR	SRS,EES 3/2.2	20	SPA-AA/319/1471 SPA-AJ/413/1515 AR11/C/742/1675
81.5E	1 Mar 94	FOTON-2	USSR	FSS 6b/4b	10	AR11/A/236/1692 AR11/C/1015/1776 -CORR1/1790 -CORR2/1881
83.0E	31 Jan 89	INSAT-1D[27]	India	FSS,BSS, MetSat,EES 0.4b,6b/2.5a,4a	15	AR11/A/126/1617 -ADD1/1636 -ADD2/1671 AR11/C/860/1735
83.0E	31 Jan 90	INSAT-2A	India	FSS,BSS, MetSat,EES 0.4b,6b/4a,4b	20	AR11/A/260/1702 AR11/C/1081/1789 -CORR1/1804
85.0E	1 Aug 90	TOR-4	USSR	FSS,MSS 43,44/20b,20f	20	AR11/A/281/1710 AR11/C/1341/1839
85.0E	1980[13]	VOLNA-5	USSR	MSS,MMSS,AMSS 0.3b,1.6b,1.6c,1.6d/ 0.3a,1.5b,1.5c,1.5d	20	SPA-AA/173/1286 SPA-AJ/100/1329
85.0E	1 Dec 90	VOLNA-5M	USSR	MMSS 1.6b/1.5b	20	AR11/A/250/1697 -CORR1/1715 AR11/C/1400/1861
87.5E	15 Dec 92	DFH-3-0C	China	FSS 6b/4a	10	AR11/A/470/1850 -ADD1/1875
90.0E	1 Sep 90	MORE-90	USSR	FSS,MMSS 1.6b,6b/1.5b,4a	15	AR11/A/184/1662 AR11/C/1090/1791 -CORR1/1883
90.0E	1 Oct 90	MILSTAR 5[7]	US	MSS,SRS 0.3a,1.7b,44/ 0.3a,2.2,20f	20	AR11/A/446/1837 AR11/C/1517/1885
93.5E	31 Mar 90	INSAT-2B	India	FSS,BSS, MetSat,EES 0.4b,6b/4a,4b	20	AR11/A/261/1702 AR11/C/1082/1789 -CORR1/1804

TABLE 2. PLANNED GEOSTATIONARY COMMUNICATIONS SATELLITES FOR YEAR-END 1989

SUBSATELLITE LONGITUDE[1] (deg)	IN-USE DATE[2]	SATELLITE DESIGNATION[3]	COUNTRY OR ORGANIZATION	SERVICE FREQUENCY CODE UP/DOWN-LINK (GHz)	PERIOD OF VALIDITY[4] (yr)	SPECIAL SECTION NUMBERS
98.0E	15 Mar 89	CHINASAT-3 DFH2-A3	China	FSS 6b/4a	10	AR11/A/257/1703 -ADD1/1712 AR11/C/1039/1778
103.0E	15 Jun 92	DFH-3-0B	China	FSS 6b/4a	10	AR11/A/469/1850 -ADD1/1875
105.0E	31 Aug 92	FY-2A FENG YUN-2A	China	FSS,SRS, MetSat,EES 0.4b,2,6b/0.4g, 1.6f,1.6g,1.7a,4a	15	AR11/A/492/1877
105.5E	1 Apr 90	ASIASAT-C ASIASAT 1	UK– Asia Satellite Telecommunications[28]	FSS 6b/4a	12	AR11/A/493/1877 AR11/C/1614/1899
105.5E	1 Nov 90	TONGASAT C-5	Tonga– Friendly Islands Satellite Communications[29]	FSS 6b/4a	20	AR11/A/460/1840 -CORR1/1892 AR11/C/1627/1908
110.0E	1 Aug 90	BS-3 YURI 3	Japan	FSS,BSS,SRS 2,14a/ 2.2,12e,12g,12h	20	AR11/A/334/1750 -ADD1/1762 AR11/C/1424/1864
115.5E	1 Nov 90	TONGASAT C-6	Tonga– Friendly Islands Satellite Communications[29]	FSS 6b/4a	20	AR11/A/461/1840 -CORR1/1892 AR11/C/1628/1908
116.0E	30 Sep 90	ASIASAT-B	UK– Asia Satellite Telecommunications[28]	FSS 6b/4a	12	AR11/A/481/1861 AR11/C/1611/1899
118.0E	30 Jun 89	PALAPA-B3[30] PALAPA B-3	Indonesia	FSS 6b/4a	10	AR11/A/157/1637 AR11/C/654/1666
121.5E	1 Nov 90	TONGASAT C-7	Tonga– Friendly Islands Satellite Communications[29]	FSS 6b/4a	20	AR11/A/462/1840 -CORR1/1892 AR11/C/1629/1908
122.0E	1 Sep 90	ASIASAT-A	UK– Asia Satellite Telecommunications[28]	FSS 6b/4a	12	AR11/A/480/1861 AR11/C/1608/1899
125.0E	15 Dec 91	DFH-3-0A	China	FSS 6b/4a	10	AR11/A/468/1850 -ADD1/1875
128.0E	1 Aug 90	TOR-6	USSR	FSS,MSS 43,44/20b,20f	20	AR11/A/283/1710 AR11/C/1315/1838
128.0E	31 Oct 90	VOLNA-9	USSR	MSS,AMSS 0.3a,0.3b,1.6d/ 0.3a,1.5d	20	AR11/A/149/1631 -ADD1/1677 AR11/C/974/1769 -CORR1/1892

TABLE 2. PLANNED GEOSTATIONARY COMMUNICATIONS SATELLITES FOR YEAR-END 1989

Subsatellite Longitude[1] (deg)	In-Use Date[2]	Satellite Designation[3]	Country or Organization	Service Frequency Code Up/Down-Link (GHz)	Period of Validity[4] (yr)	Special Section Numbers
128.0E	1 Dec 90	VOLNA-9M	USSR	MMSS 1.6b/1.5b	20	AR11/A/251/1697 AR11/C/1402/1861
130.0E	1 Jul 90	PROGNOZ-5[11]	USSR	SRS,EES 3/2.2	20	AR11/A/275/1709 AR11/C/938/1763
130.0E	1 Nov 92	TONGASAT AP-1	Tonga–Friendly Islands Satellite Communications[29]	FSS 6b/4a	20	AR11/A/512/1893 AR11/C/1720/1941
130.0E	1 Aug 90	TOR-10	USSR	FSS,MSS 43,44/20b,20f	20	AR11/A/290/1711 AR11/C/1320/1838
131.0E	1 Nov 90	TONGASAT C-8	Tonga–Friendly Islands Satellite Communications[29]	FSS 6b/4a	20	AR11/A/463/1840 -CORR1/1892
133.0E	1 Dec 90	MILSTAR 7[7]	US	MSS,SRS 0.3a,1.7b,44/ 0.3a,2.2,20f	20	AR11/A/448/1837 AR11/C/1525/1885
134.0E	1 Nov 92	TONGASAT AP-2	Tonga–Friendly Islands Satellite Communications[29]	FSS 6b/4a	20	AR11/A/513/1893 AR11/C/1721/1941
134.0E	1 Sep 92	ACS-6[20]	US	MSS,AMSS 1.6c,1.6d/1.5c,1.5d	15	AR11/A/397/1800
140.0E	1 Sep 90	MORE-140	USSR	FSS,MMSS 1.6b,6b/1.5b,4a	15	AR11/A/186/1662 AR11/C/1092/1791 -CORR1/1883
138.0E	1 Nov 92	TONGASAT AP-3	Tonga–Friendly Islands Satellite Communications[29]	FSS 6b/4a	20	AR11/A/514/1893 AR11/C/1722/1941
142.5E	1 Nov 92	TONGASAT AP-4	Tonga–Friendly Islands Satellite Communications[29]	FSS 6b/4a	20	AR11/A/515/1893 AR11/C/1723/1941
145.0E	31 Dec 87	STATSIONAR-16	USSR	FSS 6b/4a	20	AR11/A/76/1586 -ADD1/1593 AR11/C/849/1707 AR11/C/1126/1793
148.0E	1 Nov 93	TONGASAT AP-5	Tonga–Friendly Islands Satellite Communications[29]	FSS 6b/4a	20	AR11/A/516/1893 AR11/C/1724/1941
150.0E	1 Aug 91	MILSTAR 15[7]	US	MSS,SRS 0.3a,1.7b,44/ 0.3a,2.2,20f	20	AR11/A/456/1837 AR11/C/1557/1885

TABLE 2. PLANNED GEOSTATIONARY COMMUNICATIONS SATELLITES FOR YEAR-END 1989

SUBSATELLITE LONGITUDE[1] (deg)	IN-USE DATE[2]	SATELLITE DESIGNATION[3]	COUNTRY OR ORGANIZATION	SERVICE FREQUENCY CODE UP/DOWN-LINK (GHz)	PERIOD OF VALIDITY[4] (yr)	SPECIAL SECTION NUMBERS
151.0E	1 Nov 94	TONGASAT AP-8	Tonga–Friendly Islands Satellite Communications[29]	FSS 6b/4a	20	AR11/A/519/1893 AR11/C/1727/1941
152.0E	1 Apr 91	MILSTAR 11[7]	US	MSS,SRS 0.3a,1.7b,44/ 0.3a,2.2,20f	20	AR11/A/452/1837 AR11/C/1541/1885
154.0E	1 Nov 94	TONGASAT AP-7	Tonga–Friendly Islands Satellite Communications[29]	FSS 6b/4a	20	AR11/A/518/1893 AR11/C/1726/1941
156.0E	29 Feb 92	AUSSAT B2	Australia	FSS,BSS,AMSS,SRS 1.6a,1.6d,14a/ 1.5d,12b,12c, 12d,12g,12h,31[31]	15	AR11/A/361/1779 -ADD1/1790 AR11/A/356/1772 -ADD1/1880 -ADD2/1894 AR11/A/380/1796 AR11/A/435/1828 -ADD1/1894 AR11/A/437/1830 AR11/A/495/1878 -CORR1/1900
157.0E	1 Nov 93	TONGASAT AP-6	Tonga–Friendly Islands Satellite Communications[29]	FSS 6b/4a	20	AR11/A/517/1893 AR11/C/1725/1941
160.0E	1 May 92	ACSAT-1[32]	Australia	FSS 8a/7b	15	AR11/A/393/1799
160.0E	29 Feb 92	AUSSAT B1	Australia	FSS,BSS,AMSS,SRS 1.6a,1.6d,14a/ 1.5d,12b,12c, 12d,12g,12h,31[31]	15	AR11/A/360/1779 -ADD1/1790 AR11/A/355/1772 -ADD1/1880 -ADD2/1894 AR11/A/379/1796 AR11/A/434/1828 -ADD1/1894 AR11/A/436/1830 AR11/A/494/1878 -CORR1/1900
160.0E	1 Dec 92	TONGASAT C-3	Tonga–Friendly Islands Satellite Communications[29]	FSS 6b/4a	20	AR11/A/432/1828 AR11/C/1719/1940 -CORR1/1950
162.0E	1 Jun 89	SUPERBIRD-B[33]	Japan–Space Communications Corporation	FSS 14a,30a/ 12b,12c,20a,20b	13	AR11/A/341/1762 AR11/C/1307/1836 -CORR1/1865
164.0E	31 Dec 92	TONGASAT C-2	Tonga–Friendly Islands Satellite Communications[29]	FSS 6b/4a	20	AR11/A/431/1828 AR11/C/1718/1940 -CORR1/1950

TABLE 2. PLANNED GEOSTATIONARY COMMUNICATIONS SATELLITES FOR YEAR-END 1989

SUBSATELLITE LONGITUDE[1] (deg)	IN-USE DATE[2]	SATELLITE DESIGNATION[3]	COUNTRY OR ORGANIZATION	SERVICE FREQUENCY CODE UP/DOWN-LINK (GHz)	PERIOD OF VALIDITY[4] (yr)	SPECIAL SECTION NUMBERS
166.0E	1 Jun 94	GOMS-2[24]	USSR	FSS,MetSat,SRS,EES 0.4b,2,2.1,8d,30a/ 0.4g,1.6f,1.6g,7b,20b	20	AR11/A/207/1578 -ADD1/1712 AR11/C/1281/1825 -CORR1/1894
166.0E	31 Dec 89	GOMS-2M[24]	USSR	FSS,MetSat,SRS,EES 0.4b,2,2.1,8d,30a/ 0.4g,1.6f,1.6g,7b,20b	15	AR11/A/427/1822
166.0E	1 Jul 90	PROGNOZ-6[11]	USSR	SRS,EES 3/2.2	20	AR11/A/276/1709 AR11/C/940/1763
167.0E	17 Oct 89	VSSRD-2[25]	USSR	FSS,SRS 14b,14f/11,12c,13c	20	AR11/A/187/1672
167.45E	30 Jun 91	PACSTAR-1 PACSTAR A-1	Papua New Guinea– Pacific Satellite[34]	FSS,AMSS 1.6d,6b,14a/ 1.5d,4a,5a,12a,12b,12c	20	AR11/A/200/1676 AR11/A/331/1749 -ADD1/1783 AR11/C/1179/1801 -CORR1/1828 -CORR2/1850 AR11/C/1432/1866
170.0E	1 Oct 91	USASAT-13M CELESTAR 1	US– McCaw Space Technologies[22]	FSS 14a/12a,12c,12d	10	AR11/A/343/1763 AR11/C/1436/1871 -ADD1/1900
170.75E	1 Nov 91	TONGASAT C-1	Tonga– Friendly Islands Satellite Communications[29]	FSS 6b/4a	20	AR11/A/430/1828 AR11/C/1717/1940 -CORR1/1950
171.0E	1 Jul 92	ACS-5[20]	US	MSS,AMSS 1.6c,1.6d/1.5c,1.5d	15	AR11/A/396/1800
172.0E	31 Dec 86	FLTSATCOM-B WEST PAC[23]	US	MSS 44/20f	10	AR11/A/51/1561 -ADD1/1587
175.0E	31 Dec 89	USGCSS PH3 W PAC DSCS III	US	FSS,SRS 1.7b,8a/2.2,7b	10	AR11/A/266/1706 -ADD1/1730 AR11/C/409/1629 AR11/C/1216/1816 -CORR1/1842 AR11/C/1222/1817 -CORR1/1842
177.5E	1 Jul 91	MILSTAR 14[7]	US	MSS,SRS 0.3a,1.7b,44/ 0.3a,2.2,20f	20	AR11/A/455/1837 AR11/C/1553/1885
179.5E	31 Oct 89	INMARSAT POR-I INMARSAT II[21]	Inmarsat	FSS,MSS,MMSS,AMSS 1.6b,1.6c,1.6d,6b/ 1.5b,1.5c,1.5d,4a	15	AR11/A/329/1747
180.0E	31 Dec 92	USGCSS PH3 W PAC-2 DSCS III	US	FSS,SRS 1.7b,8a/2.2,7b	10	AR11/A/408/1806
182.0E (178.0W)	1 Jul 90	USASAT-13K FINANSAT-2	US– Financial Satellite[35]	FSS 6b/4a	10	AR11/A/264/1703 AR11/C/945/1763

TABLE 2. PLANNED GEOSTATIONARY COMMUNICATIONS SATELLITES FOR YEAR-END 1989

SUBSATELLITE LONGITUDE[1] (deg)	IN-USE DATE[2]	SATELLITE DESIGNATION[3]	COUNTRY OR ORGANIZATION	SERVICE FREQUENCY CODE UP/DOWN-LINK (GHz)	PERIOD OF VALIDITY[4] (yr)	SPECIAL SECTION NUMBERS
185.0E (175.0W)	30 Jun 91	PACSTAR-2 PACSTAR A-2	Papua New Guinea–Pacific Satellite[34]	FSS,AMSS 1.6d,6b,14a/ 1.5d,4a,5a,12a,12b,12c	20	AR11/A/201/1676 AR11/C/1180/1801 -CORR1/1804 -CORR2/1828
187.5E (172.5W)	31 Dec 92	TONGASAT C-4	Tonga–Friendly Islands Satellite Communications[29]	FSS 6b/4a	20	AR11/A/433/1828 AR11/C/1697/1928 -CORR1/1952
189.0E (171.0W)	4 Aug 88	TDRS 171W	US	SRS 2,14f/2.2,13c	15	AR11/A/474/1860 -CORR1/1903[36]
189.0E (171.0W)	1 Apr 89	USASAT-14E[37]	US	FSS 6b/4a	10	AR11/A/421/1815 AR11/C/1710/1936
190.0E (170.0W)	31 Jul 92	STATSIONAR-10A[6]	USSR	FSS 6b/4a	20	AR11/A/403/1803
190.0E (170.0W)	1 Aug 90	TOR-5	USSR	FSS,MSS 43,44/20b,20f	20	AR11/A/282/1710 AR11/C/1351/1851
190.0E (170.0W)	1980[13]	VOLNA-7	USSR	MSS,MMSS,AMSS 0.3b,1.6b,1.6c,1.6d/ 0.3a,1.5b,1.5c,1.5d	20	SPA-AA/175/1286 SPA-AJ/102/1329
190.5E (169.5W)	1 Jun 90	FOTON-3	USSR	FSS 6b/4b	10	AR11/A/237/1692
192.0E (168.0W)	Dec 1983[13]	POTOK-3[26]	USSR	FSS 4b/4a	10	SPA-AA/346/1485
195.0E (165.0W)	1 Sep 91	USASAT-13L CCC-1	US–Columbia Communications[38]	FSS 14a/11,12a	10	AR11/A/354/1770
201.0E (159.0W)	1 Jul 90	PROGNOZ-7[11]	USSR	SRS,EES 3/2.2	20	AR11/A/277/1709 AR11/C/942/1763
205.0E (155.0W)	31 Dec 89	STATSIONAR-26	USSR	FSS 6b/4a	20	AR11/A/385/1797 -ADD1/1803 -CORR1/1813 AR11/C/1313/1836
212.0E (148.0W)	1 May 91	MILSTAR 12[7]	US	MSS,SRS 0.3a,1.7b,44/ 0.3a,2.2,20f	20	AR11/A/453/1837 AR11/C/1545/1885
214.0E (146.0W)	Jun 1985[13]	AMIGO-2[39]	Mexico	FSS,BSS 17,20a/12f,12g	10	RES33/A/2/1560
214.0E (146.0W)	15 Nov 90	USASAT-20C[40]	US	FSS 6b/4a	10	AR11/A/259/1702 AR11/C/970/1769
215.0E (145.0W)	30 Jun 92	MORELOS 4 MORELOS IV	Mexico	FSS 6b,14a/4a,12a	10	AR11/A/467/1840
215.0E (145.0W)	1 Dec 90	VOLNA-21M	USSR	MMSS,AMSS 1.6b,1.6d/1.5b,1.5d	20	AR11/A/252/1697

TABLE 2. PLANNED GEOSTATIONARY COMMUNICATIONS SATELLITES FOR YEAR-END 1989

SUBSATELLITE LONGITUDE[1] (deg)	IN-USE DATE[2]	SATELLITE DESIGNATION[3]	COUNTRY OR ORGANIZATION	SERVICE FREQUENCY CODE UP/DOWN-LINK (GHz)	PERIOD OF VALIDITY[4] (yr)	SPECIAL SECTION NUMBERS
215.0E (145.0W)	31 Dec 84	FLTSATCOM-A PAC SYNCOM IV-5[41] LEASESAT F-5 LEASAT 5	US– Hughes Communications	FSS,MSS 0.3a,8a/0.3a,7b	10	AR11/A/181/1652
219.0E (141.0W)	30 Jun 92	MORELOS 3 MORELOS III	Mexico	FSS 6b,14a/4a,12a	10	AR11/A/466/1840
220.0E (140.0W)	31 Dec 89	USASAT-17C[42]	US	FSS 6b/4a	10	AR11/A/228/1687 AR11/C/933/1761
221.0E (139.0W)	1993[13]	ACS-3A[43] AMSC-3	US– American Mobile Satellite[44]	MSS,AMSS 1.6c,1.6d/1.5c,1.5d	15	
221.0E (139.0W)	May 1991[13]	USASAT[43] GE SATCOM C-5 AURORA II[46]	US– Alascom[45]	FSS 6b/4a	10	
223.0E (137.0W)	31 Dec 89	USASAT-17B[47] GE SATCOM C-1[48]	US– GE Americom	FSS 6b/4a	10	AR11/A/227/1687
224.0E (136.0W)	Jun 1985[13]	AMIGO-1[39]	Mexico	FSS,BSS 17,20a/12f,12g	10	RES32/A/1/1560
224.0E (136.0W)	31 Jan 90	USASAT-16D[49]	US	FSS 14a/12a	10	AR11/A/225/1687 AR11/C/1000/1772
225.0E (135.0W)	31 Aug 93	USASAT-21A GE SATCOM C-4	US– GE Americom	FSS 6b/4a	10	AR11/A/483/1864 -ADD1/1883 -CORR1/1935
225.0E (135.0W)	1 Jun 83	USGCSS PH3 E PAC DSCS III	US	FSS,SRS 1.7b,8a/2.2,7b	10	SPA-AA/349/1493 SPA-AJ/344/1499 AR11/C/405/1629
226.0E (134.0W)	31 Jan 90	USASAT-16C COMSTAR K-2[50] COMGEN-B	US– Comsat General	FSS 14a/12a	10	AR11/A/224/1687 AR11/C/1064/1783
227.0E (133.0W)	19 Apr 94	USASAT-22A GALAXY IR	US– Hughes Communications	FSS 6b/4a	12	AR11/A/536/1903 AR11/C/1777 AR11/C/1778–1779
228.0E (132.0W)	15 Mar 87	USASAT-11C WESTAR-B[51]	US– Western Union	FSS 14a/12a	10	AR11/A/111/1609 AR11/C/1063/1782
229.0E (131.0W)	1 Apr 96	USASAT-23B GALAXY B-R[52]	US– Hughes Communications	FSS 14a/12a	12	AR11/A/640/1946
229.0E (131.0W)	31 Dec 94	USASAT-22H[37]	US	FSS 6b/4a	12	AR11/A/600/1920 -CORR1/1945
230.0E (130.0W)	15 Jun 87	USASAT-10D GALAXY-B[52] GALAXY K-2	US– Hughes Communications	FSS 14a/12a	20	AR11/A/108/1609 AR11/C/1057/1781

TABLE 2. PLANNED GEOSTATIONARY COMMUNICATIONS SATELLITES FOR YEAR-END 1989

SUBSATELLITE LONGITUDE[1] (deg)	IN-USE DATE[2]	SATELLITE DESIGNATION[3]	COUNTRY OR ORGANIZATION	SERVICE FREQUENCY CODE UP/DOWN-LINK (GHz)	PERIOD OF VALIDITY[4] (yr)	SPECIAL SECTION NUMBERS
230.0E (130.0W)	10 Sep 90	ACS-3[20]	US	AMSS 1.6d/1.5d	15	AR11/A/303/1723 AR11/C/1110/1792
230.0E (130.0W)	31 Dec 92	USGCSS PH3 E PAC-2 DSCS III	US	FSS,SRS 1.7b,8a/2.2,7b	10	AR11/A/407/1806
230.0E (130.0W)	15 Jun 92	USRDSS WEST[53] GEOSTAR S3	US– Geostar	FSS,AMSS,Radiolocation 1.6a,6b/2.4,5a	10	AR11/A/176/1641 -ADD1/1673 -ADD2/1780
231.0E (129.0W)	18 Jul 94	USASAT-24A CONTELSAT-2	US– Contel ASC	FSS 6b,14a/4a,12a	10	AR11/A/577/1912
233.0E (127.0W)	1993[13]	USASAT-24G[43] SPOTNET-2 NEXSAT-2	US– National Exchange Satellite[54]	FSS 6b,14a/4a,12a	10	
234.0E (126.0W)	15 Sep 87	USASAT-10C MMC-2	US– Martin Marietta[55]	FSS 14a/12a	20	AR11/A/107/1609 AR11/C/989/1769
235.0E (125.0W)	19 Apr 94	USASAT-22B GALAXY V-W	US– Hughes Communications	FSS 6b/4a	12	AR11/A/537/1903 AR11/C/1780 AR11/C/1781–1782
235.0E (125.0W)	18 Jul 94	USASAT-23E GTE GSTAR 4	US– GTE Spacenet	FSS 14a/12a	10	AR11/A/576/1912 AR11/C/1772 AR11/C/1773
236.0E (124.0W)	1 Nov 88	USASAT-10B EXPRESSTAR B	US– Federal Express[56]	FSS 14a/12a	10	AR11/A/106/1609 AR11/C/1054/1781 -CORR1/1811
239.0E (121.0W)	18 Jul 94	USASAT-23C GTE GSTAR 1R	US– GTE Spacenet	FSS 14a/12a	10	AR11/A/575/1912 AR11/C/1759 AR11/C/1760
240.0E (120.0W)	1 Nov 90	MILSTAR 6[7]	US	MSS,SRS 0.3a,1.7b,44/ 0.3a,2.2,20f	20	AR11/A/447/1837 AR11/C/1522/1885
249.5E (110.5W)	1 Dec 90	ANIK E-B[57] TELESAT E-B	Canada– Telesat Canada	FSS 6b,14a/4a,12a	12	AR11/A/323/1744 -ADD1/1765 AR11/C/1293/1832 -CORR1/1861
252.7E (107.3W)	1 May 90	ANIK E-A[57] TELESAT E-A	Canada– Telesat Canada	FSS 6b,14a/4a,12a	12	AR11/A/322/1744 -ADD1/1765 AR11/C/1291/1832 -CORR1/1861
253.5E (106.5W)	5 Oct 89	MSAT[58]	Canada– Telesat Mobile[59]	MSS,LMSS,MMSS, AMSS,SRS 0.8,1.6b,1.6c,1.6d,2/ 0.8,1.5b,1.5c,1.5d,2.2	10	AR11/A/55/1563 -ADD1/1572 -ADD2/1611 -ADD3/1721 AR11/A/300/1723 -CORR1/1731 AR11/C/936/1761 -CORR1/1821

TABLE 2. PLANNED GEOSTATIONARY COMMUNICATIONS SATELLITES FOR YEAR-END 1989

SUBSATELLITE LONGITUDE[1] (deg)	IN-USE DATE[2]	SATELLITE DESIGNATION[3]	COUNTRY OR ORGANIZATION	SERVICE FREQUENCY CODE UP/DOWN-LINK (GHz)	PERIOD OF VALIDITY[4] (yr)	SPECIAL SECTION NUMBERS
254.0E (106.0W)	31 Jul 92	SIMON BOLIVAR 1 CONDOR 1[61]	ASETA[60]	FSS 6b/4a	10	AR11/A/422/1817 -CORR1/1861
257.0E (103.0W)	18 Jul 94	USASAT-24B SPACENET-1R GTE SPACENET IR	US– GTE Spacenet	FSS 6b,14a/4a,12a	10	AR11/A/578/1912 AR11/C/1761 AR11/C/1762–1763
259.0E (101.0W)	1 Jul 90	USASAT-16B USASAT-17A FORDSTAR 1 FORDSAT I	US– Ford Aerospace Satellite Services[62]	FSS 6b,14a/4a,12a	10	AR11/A/223/1687 AR11/A/226/1687 AR11/C/999/1772 AR11/C/931/1755
259.0E (101.0W)	18 Jul 94	USASAT-24C CONTELSAT-1	US– Contel ASC	FSS 6b,14a/4a,12a	10	AR11/A/579/1912
259.0E (101.0W)	1993[13]	ACS-1A[43] AMSC-2	US– American Mobile Satellite[44]	MSS,AMSS 1.6c,1.6d/1.5c,1.5d	15	
260.0E (100.0W)	10 Sep 90	ACS-1[20]	US	AMSS 1.6d/1.5d	15	AR11/A/301/1723 -ADD1/1801 AR11/C/1106/1792
260.0E (100.0W)	15 Jul 90	USRDSS CENTRAL[53] GEOSTAR S2	US– Geostar	FSS,AMSS,Radiolocation 1.6a,6b/2.4,5a	10	AR11/A/175/1641 -ADD1/1663 -ADD2/1780
260.0E (100.0W)	10 Aug 89	ACTS[63]	US	FSS 30a/20b	10	AR11/A/321/1744 -ADD1/1753
261.0E (99.0W)	19 Apr 94	USASAT-22C GALAXY IV-R	US– Hughes Communications	FSS 6b/4a	12	AR11/A/538/1903 AR11/C/1783 AR11/C/1784–1785
261.0E (99.0W)	19 Apr 94	USASAT-23D[43] GALAXY A-R[52]	US– Hughes Communications	FSS 14a/12a	12	AR11/A/605/1921
263.0E (97.0W)	30 Apr 89	STSC-2	Cuba	FSS 6b/4a	10	AR11/A/268/1706 -ADD1/1723
263.0E (97.0W)	19 Apr 94	USASAT-24D TELSTAR 401	US– AT&T	FSS 6b,14a/4a,12a	10	AR11/A/542/1903
265.0E (95.0W)	19 Apr 94	USASAT-22D GALAXY III-R	US– Hughes Communications	FSS 6b/4a	12	AR11/A/539/1903
267.0E (93.0W)	1 Jul 90	USASAT-12D USASAT-16A FORDSTAR 1 FORDSAT I	US– Ford Aerospace Satellite Services[62]	FSS 6b,14a/4a,12a	10	AR11/A/124/1615 AR11/A/221/1687 AR11/C/998/1772
267.0E (93.0W)	1993[13]	USASAT-24I[43] SPOTNET-1 NEXSAT-1	US– National Exchange Satellite[54]	FSS 6b,14a/4a,12a	10	
269.0E (91.0W)	15 Apr 88	WESTAR 6-S[64] WESTAR VIS GALAXY VI	US– Hughes Communications	FSS 6b/4a	10	AR11/A/299/1722 AR11/C/962/1765

TABLE 2. PLANNED GEOSTATIONARY COMMUNICATIONS SATELLITES FOR YEAR-END 1989

SUBSATELLITE LONGITUDE[1] (deg)	IN-USE DATE[2]	SATELLITE DESIGNATION[3]	COUNTRY OR ORGANIZATION	SERVICE FREQUENCY CODE UP/DOWN-LINK (GHz)	PERIOD OF VALIDITY[4] (yr)	SPECIAL SECTION NUMBERS
270.0E (90.0W)	1 Jun 90	MILSTAR 1[7]	US	MSS,SRS 0.3a,1.7b,44/ 0.3a,2.2,20f	20	AR11/A/442/1837 AR11/C/1501/1885
271.0E (89.0W)	19 Apr 94	USASAT-24E TELSTAR 402	US– AT&T	FSS 6b,14a/4a,12a	10	AR11/A/543/1903
271.0E (89.0W)	30 Jun 90	SIMON BOLIVAR-B CONDOR-B[61]	ASETA[60]	FSS 6b/4a	10	AR11/A/209/1679 -CORR1/1861
275.0E (85.0W)	25 Jun 94	NAHUEL-2[65]	Argentina	FSS 6b,14a/4a,12a	10	AR11/A/204/1677 -CORR1/1881
277.0E (83.0W)	Mar 1988[13]	STSC-1	Cuba	FSS 6b/4a	10	AR11/A/58/1578
277.0E (83.0W)	31 Dec 86	USASAT-7D ASC-2[66] CONTEL ASC-2	US– Contel ASC	FSS 6b,14a/4a,12a	10	AR11/A/12/1525 -ADD1/1548 AR11/C/257/1623
279.0E (81.0W)	19 Apr 94	USASAT-22F[43] GALAXY V-E	US– Hughes Communications	FSS 6b/4a	12	AR11/A/541/1903 -CORR1/1935
280.0E (80.0W)	25 Jun 94	NAHUEL-1[65]	Argentina	FSS 6b,14a/4a,12a	10	AR11/A/203/1677 -CORR1/1881
281.0E (79.0W)	31 Jan 87	TDRS-C2	US	SRS 2,14f/2.2,13c	15	AR11/A/265/1704 -ADD1/1713
281.0E (79.0W)	15 Mar 87	USASAT-11A MMC-1	US– Martin Marietta[55]	FSS 14a/12a	10	AR11/A/109/1609 AR11/C/991/1769
281.0E (79.0W)	19 Apr 94	USASAT-24F GE SATCOM H-1 SATCOM HYBRID-1	US– GE Americom	FSS 6b,14a/4a,12a	12	AR11/A/544/1903 AR11/C/1704/1929
282.5E (77.5W)	30 Jun 90	SIMON BOLIVAR-A CONDOR-A[61]	ASETA[60]	FSS 6b/4a	10	AR11/A/208/1679 -CORR1/1861
283.0E (77.0W)	1 Feb 89	USASAT-11B EXPRESSTAR A	US– Federal Express[56]	FSS 14a/12a	10	AR11/A/110/1609 AR11/C/1060/1782
284.6E (75.4W)	1 Mar 93	COLOMBIA 1A[67]	Colombia	FSS 6b/4a	10	AR11/A/428/1825
284.6E (75.4W)	31 Jul 86	SATCOL-1A[67]	Colombia	FSS 6b/4a	10	SPA-AA/338/1479 AR11/C/79/1573 -ADD1/1587
284.6E (75.4W)	31 Jul 86	SATCOL-1B[67]	Colombia	FSS 6b/4a	10	SPA-AA/338/1479 AR11/C/80/1573 -ADD1/1587
285.0E (75.0W)	1 Mar 93	COLOMBIA 2[67]	Colombia	FSS 6b/4a	10	AR11/A/429/1825
285.0E (75.0W)	31 Jul 86	SATCOL-2[67]	Colombia	FSS 6b/4a	10	SPA-AA/338/1479 SPA-AJ/128/1343 AR11/C/81/1573

TABLE 2. PLANNED GEOSTATIONARY COMMUNICATIONS SATELLITES FOR YEAR-END 1989

SUBSATELLITE LONGITUDE[1] (deg)	IN-USE DATE[2]	SATELLITE DESIGNATION[3]	COUNTRY OR ORGANIZATION	SERVICE FREQUENCY CODE UP/DOWN-LINK (GHz)	PERIOD OF VALIDITY[4] (yr)	SPECIAL SECTION NUMBERS
285.0E (75.0W)	31 Jan 90	USASAT-18A COMSTAR K-1[50] COMGEN-A	US– Comsat General	FSS 14a/12a	10	AR11/A/230/1687 AR11/C/1002/1773
286.0E (74.0W)	19 Apr 94	USASAT-22E GALAXY II-R	US– Hughes Communications	FSS 6b/4a	12	AR11/A/540/1903
287.0E (73.0W)	1 Jan 90	USASAT-18B WESTAR-A[51]	US– Western Union	FSS 14a/12a	10	AR11/A/231/1687 AR11/C/1004/1773
288.0E (72.0W)	9 Sep 89	USASAT-15B STLC 3 SBS-6	US– Satellite Transponder Leasing Corp.[68]	FSS 14a/12a	10	AR11/A/163/1637 -ADD1/1673 AR11/C/993/1770
288.0E (72.0W)	30 Jun 90	SIMON BOLIVAR-C CONDOR-C[61]	ASETA[60]	FSS 6b/4a	10	AR11/A/210/1679 -CORR1/1861
288.0E (72.0W)	10 Sep 90	ACS-2[20]	US	AMSS 1.6d/1.5d	15	AR11/A/302/1723 AR11/C/1108/1792
289.0E (71.0W)	31 Jan 90	USASAT-18C GALAXY-A[52] GALAXY K-1	US– Hughes Communications	FSS 14a/12a	20	AR11/A/232/1687 AR11/C/1005/1773
290.0E (70.0W)	31 Dec 89	SATS-1	Brazil	FSS 6b/4a	7	AR11/A/399/1802 AR11/C/1461/1874
290.0E (70.0W)	31 Dec 86	FLTSATCOM-B W ATL[23]	US	MSS 44/20f	10	AR11/A/49/1561 -ADD1/1587
290.0E (70.0W)	15 Jul 91	USRDSS EAST[53] GEOSTAR S1	US– Geostar	FSS,AMSS,Radiolocation 1.6a,6b/2.4,5a	10	AR11/A/174/1641 -ADD1/1673 -ADD2/1780
291.0E (69.0W)	1 Apr 96	USASAT-24H[37]	US	FSS 6b,14a/4a,12a	10	AR11/A/643/1947
292.0E (68.0W)	1 Jan 91	MILSTAR 8[7]	US	MSS,SRS 0.3a,1.7b,44/ 0.3a,2.2,20f	20	AR11/A/449/1837 AR11/C/1529/1885
293.0E (67.0W)	3 Apr 87	USASAT-15D[69] GE SATCOM K-3 SATCOM KU3	US– GE Americom	FSS 14a/12a	10	AR11/A/165/1637 -ADD1/1673 AR11/C/997/1770
293.0E (67.0W)	1 Jan 86	USASAT-8A[70] GE SATCOM C-6	US– GE Americom	FSS 6b/4a	10	AR11/A/36/1553 AR11/C/394/1629
295.0E (65.0W)	31 Dec 89	SATS-2	Brazil	FSS 6b/4a	7	AR11/A/400/1802 AR11/C/1462/1874
295.0E (65.0W)	30 Jun 92	SBTS B2 BRAZILSAT B2	Brazil	FSS 6b/4a	15	AR11/A/367/1785 -ADD1/1796
295.0E (65.0W)	30 Jun 92	SBTS C2 BRAZILSAT C2	Brazil	FSS 14a/12a	15	AR11/A/369/1785 -CORR1/1796

TABLE 2. PLANNED GEOSTATIONARY COMMUNICATIONS SATELLITES FOR YEAR-END 1989

SUBSATELLITE LONGITUDE[1] (deg)	IN-USE DATE[2]	SATELLITE DESIGNATION[3]	COUNTRY OR ORGANIZATION	SERVICE FREQUENCY CODE UP/DOWN-LINK (GHz)	PERIOD OF VALIDITY[4] (yr)	SPECIAL SECTION NUMBERS
296.0E (64.0W)	30 Nov 90	USASAT-14D[71] USASAT-15C ASC-3 CONTEL ASC-3	US– Contel ASC	FSS 6b,14a/4a,12a	10	AR11/A/161/1637 AR11/A/164/1637 -ADD1/1673 AR11/C/930/1755 AR11/C/996/1770
298.0E (62.0W)	30 Jun 89	USASAT-14C[70] GE SATCOM C-7	US– GE Americom	FSS 6b/4a	10	AR11/A/160/1637 AR11/C/929/1755
298.0E (62.0W)	11 Aug 90	TDRS 62W	US	SRS 2,14f/2.2,13c	15	AR11/A/473/1860
298.0E (62.0W)	1 Nov 94	ACS-2A AMSC-1	US– American Mobile Satellite[44]	MSS,AMSS 1.6c,1.6d/ 1.5c,1.5d	15	AR11/A/603/1920
299.0E (61.0W)	30 Jun 92	SBTS B3 BRAZILSAT B3	Brazil	FSS 6b/4a	15	AR11/A/368/1785 -ADD1/1796
299.0E (61.0W)	30 Jun 92	SBTS C3 BRAZILSAT C3	Brazil	FSS 14a/12a	15	AR11/A/370/1785 -CORR1/1796
300.0E (60.0W)	31 Dec 88	USASAT-15A[37]	US	FSS 14a/12a	10	AR11/A/162/1637 -ADD1/1673
300.0E (60.0W)	25 Jun 94	USASAT-26H[37]	US	FSS 14a/11,12a,12c,12d	15	AR11/A/570/1911
300.0E (60.0W)	25 Jun 94	USASAT-25H[37]	US	FSS 6b/4a	15	AR11/A/562/1911
302.0E (58.0W)	15 May 93	USASAT-13E ISI-2	US– International Satellite, Inc.[72]	FSS 14a/11,12a,12c,12d	10	AR11/A/136/1620 AR11/C/702/1670 -CORR1/1945
302.0E (58.0W)	20 Jun 94	USASAT-26G[37]	US	FSS 14a/11,12a,12c,12d	15	AR11/A/569/1911
302.0E (58.0W)	20 Jun 94	USASAT-25G[37]	US	FSS 6b/4a	15	AR11/A/561/1911
303.0E (57.0W)	30 Sep 87	USASAT-13H[73]	US	FSS 6b/4a,11	10	AR11/A/177/1643
304.0E (56.0W)	15 May 93	USASAT-13D ISI-1	US– International Satellite, Inc.[72]	FSS 14a/11,12a,12c,12d	10	AR11/A/135/1620 AR11/C/701/1670 -CORR1/1945
304.0E (56.0W)	15 Jun 94	USASAT-26F[37]	US	FSS 14a/11,12a,12c,12d	15	AR11/A/568/1911
304.0E (56.0W)	15 Jun 94	USASAT-25F[37]	US	FSS 6b/4a	15	AR11/A/560/1911
305.0E (55.0W)	31 Mar 89	INMARSAT AOR -WEST INMARSAT II[21]	Inmarsat	FSS,MSS,MMSS,AMSS 1.6b,1.6c,1.6d,6b/ 1.5b,1.5c,1.5d,4a	15	AR11/A/328/1747

TABLE 2. PLANNED GEOSTATIONARY COMMUNICATIONS SATELLITES FOR YEAR-END 1989

SUBSATELLITE LONGITUDE[1] (deg)	IN-USE DATE[2]	SATELLITE DESIGNATION[3]	COUNTRY OR ORGANIZATION	SERVICE FREQUENCY CODE UP/DOWN-LINK (GHz)	PERIOD OF VALIDITY[4] (yr)	SPECIAL SECTION NUMBERS
305.0E (55.0W)	31 Dec 88	USASAT-14B[37]	US	FSS 6b/4a	10	AR11/A/159/1637
305.5E (54.5W)	31 Jul 89	MARECS ATL4	ESA	FSS,MMSS 1.6b,6b/1.5b,4a	10	AR11/A/477/1860 -ADD1/1889
307.0E (53.0W)	1 Jan 93	INTELSAT6 307E	Intelsat	FSS 6b,14a/4a,11	15	AR11/A/286/1711 -ADD1/1724 AR11/C/1270/1821 -CORR1/1841
307.5E (52.5W)	31 Dec 86	USGCSS PH3 W ATL DSCS III	US	FSS,SRS 1.7b,8a/2.2,7b	10	AR11/A/173/1639 -ADD1/1730 AR11/C/904/1746 -CORR1/1835 AR11/C/1018/1777
310.0E (50.0W)	1 May 93	USASAT-13C	US–Orion Satellite[74]	FSS 14a/11	10	AR11/A/134/1618 AR11/C/748/1675 -CORR1/1945
310.0E (50.0W)	1 Feb 93	INTELSAT6 310E	Intelsat	FSS 6b,14a/4a,11	15	AR11/A/287/1711 -ADD1/1724 AR11/C/1271/1821 -CORR1/1841
313.0E (47.0W)	1 May 93	USASAT-13B ORION-2	US–Orion Satellite[74]	FSS 14a/11,12a,12c,12d	10	AR11/A/133/1618 -ADD1/1716 AP30/A/36/1722 -ADD1/1940 AR11/C/747/1675 AR11/C/1712/1939
313.0E (47.0W)	1 Aug 90	USASAT-13J FINANSAT-1	US–Financial Satellite[35]	FSS 6b/4a	10	AR11/A/263/1703 AR11/C/944/1763
313.0E (47.0W)	10 Jun 94	USASAT-26E[37]	US	FSS 14a/11,12a,12c,12d	15	AR11/A/567/1911
313.0E (47.0W)	10 Jun 94	USASAT-25E[37]	US	FSS 6b/4a	15	AR11/A/559/1911
315.0E (45.0W)	1 Jan 89	USASAT-13F[75]	US	FSS 14a/11,12a,12c,12d	10	AR11/A/154/1635 -ADD1/1714 AR11/C/755/1676 AR11/C/1423/1864
315.0E (45.0W)	5 Jun 94	USASAT-26D[37]	US	FSS 14a/11,12a,12c,12d	15	AR11/A/566/1911
315.0E (45.0W)	5 Jun 94	USASAT-25D[37]	US	FSS 6b/4a	15	AR11/A/558/1911
316.5E (43.5W)	1 Jan 88	VIDEOSAT-3[8]	France	FSS,SRS 2,14a/ 2.2,12a,12b,12c,12d	10	AR11/A/148/1631 -ADD1/1638 AR11/C/766/1678

TABLE 2. PLANNED GEOSTATIONARY COMMUNICATIONS SATELLITES FOR YEAR-END 1989

SUBSATELLITE LONGITUDE[1] (deg)	IN-USE DATE[2]	SATELLITE DESIGNATION[3]	COUNTRY OR ORGANIZATION	SERVICE FREQUENCY CODE UP/DOWN-LINK (GHz)	PERIOD OF VALIDITY[4] (yr)	SPECIAL SECTION NUMBERS
317.0E (43.0W)	1 Jun 88	USASAT-13G PANAMSAT II PAS 2	US– Pan American Satellite	FSS 14a/11,12a,12c,12d	10	AR11/A/155/1635 AR11/C/756/1676
317.0E (43.0W)	30 May 94	USASAT-26C[37]	US	FSS 14a/11,12a,12c,12d	15	AR11/A/565/1911
317.0E (43.0W)	30 May 94	USASAT-25C[37]	US	FSS 6b/4a	15	AR11/A/557/1911
317.5E (42.5W)	31 Dec 86	USGCSS PH3 MID-ATL DSCS III	US	FSS,SRS 1.7b,8a/2.2,7b	10	AR11/A/140/1622 -ADD1/1638 -ADD2/1730
319.0E (41.0W)	1 Dec 89	USASAT-14A[37]	US	FSS 6b/4a	10	AR11/A/158/1637 -ADD1/1815 AR11/C/891/1743 -ADD1/1936
319.0E (41.0W)	25 May 94	USASAT-26B[37]	US	FSS 14a/11,12a,12c,12d	15	AR11/A/564/1911
319.0E (41.0W)	25 May 94	USASAT-25B[37]	US	FSS 6b/4a	15	AR11/A/556/1911
322.5E (37.5W)	31 Dec 87	VIDEOSAT-2[8]	France	FSS,SRS 2,14a/ 2.2,12a,12b,12c,12d	10	AR11/A/86/1598 -ADD1/1630 AR11/C/575/1650 AR11/C/727/1673 -CORR1/1678
322.5E (37.5W)	20 May 94	USASAT-26A[37]	US	FSS 14a/11,12a,12c,12d	15	AR11/A/563/1911
322.5E (37.5W)	20 May 94	USASAT-25A[37]	US	FSS 6b/4a	15	AR11/A/555/1911
322.5E (37.5W)	31 Dec 89	STATSIONAR-25	USSR	FSS 6b/4a	20	AR11/A/384/1797 -ADD1/1803 AR11/C/1311/1836
322.5E (37.5W)	1 May 93	USASAT-13A ORION-1	US– Orion Satellite[74]	FSS 14a/11,12a,12c,12d	10	AR11/A/132/1618 -ADD1/1716 AP30/A/35/1722 -ADD1/1940 AR11/C/746/1675 AR11/C/1711/1939
325.5E (34.5W)	15 Oct 91	INTELSAT6 325.5E INTELSAT VI F-1	Intelsat	FSS 6b,14a/4a,11	15	AR11/A/288/1711 -ADD1/1724 AR11/C/1272/1821 -CORR1/1841
326.0E (34.0W)	30 Nov 88	INMARSAT AOR -CENT 1A INMARSAT II[21]	Inmarsat	FSS,MSS,MMSS,AMSS 1.6b,1.6c,1.6d,6b/ 1.5b,1.5c,1.5d,4a	15	AR11/A/351/1767

TABLE 2. PLANNED GEOSTATIONARY COMMUNICATIONS SATELLITES FOR YEAR-END 1989

SUBSATELLITE LONGITUDE[1] (deg)	IN-USE DATE[2]	SATELLITE DESIGNATION[3]	COUNTRY OR ORGANIZATION	SERVICE FREQUENCY CODE UP/DOWN-LINK (GHz)	PERIOD OF VALIDITY[4] (yr)	SPECIAL SECTION NUMBERS
327.0E (33.0W)	30 Nov 91	SKYNET-4D	UK	FSS,MSS 0.3a,8a,44/0.3a,7b	10	AR11/A/333/1749
327.5E (32.5W)	31 Jul 89	MARECS ATL3	ESA	FSS,MMSS 1.6b,6b/1.5b,4a	10	AR11/A/476/1860 -ADD1/1889
328.0E (32.0W)	30 Nov 88	INMARSAT AOR -CENT 2A INMARSAT II[21]	Inmarsat	FSS,MSS,MMSS,AMSS 1.6b,1.6c,1.6d,6b/ 1.5b,1.5c,1.5d,4a	15	AR11/A/352/1767
329.0E (31.0W)	1 Dec 91	HISPASAT-1[76]	Spain	FSS,BSS 8a,13a,14a/ 7b,11,12a,12c,12d 12e,12f,12g	20	AR11/A/487/1871 -ADD1/1929 AR11/C/1707/1936
329.0E (31.0W)	31 Mar 90	EIRESAT-1	Ireland– Atlantic Satellites[77]	FSS,BSS 13a,17/11	15	AR11/A/182/1656 -ADD1/1794 -ADD2/1803 AR11/C/1349/1850
332.5E (27.5W)	1 Jul 90	INTELSAT6 332.5E[78] INTELSAT VI F-3	Intelsat	FSS 6b,14a/4a,11	15	AR11/A/70/1584 AR11/C/628/1658 -ADD1/1713
333.5E (26.5W)	30 Jun 88	STATSIONAR-D1[6]	USSR	FSS 6b/4a	20	AR11/A/193/1675 AR11/C/1168/1796
333.5E (26.5W)	1 Aug 90	TOR-1	USSR	FSS,MSS 43,44/20b,20f	20	AR11/A/278/1710 AR11/C/1295/1832
334.0E (26.0W)	31 Aug 88	INMARSAT AOR -CENT INMARSAT II[21]	Inmarsat	FSS,MSS,MMSS,AMSS 1.6b,1.6c,1.6d,6b/ 1.5b,1.5c,1.5d,4a	15	AR11/A/152/1634 -ADD1/1760 AR11/C/843/1706 -ADD1/1784
335.0E (25.0W)	1 Aug 90	TOR-9	USSR	FSS,MSS 43,44/20b,20f	20	AR11/A/289/1711 AR11/C/1440/1872
335.0E (25.0W)	1 Mar 91	VOLNA-1A	USSR	MSS,AMSS 0.3a,0.3b,1.6d/ 0.3a,1.5d	20	AR11/A/291/1712 -CORR1/1812
335.0E (25.0W)	1 Dec 90	VOLNA-1M	USSR	MMSS 1.6b/1.5b	20	AR11/A/248/1697 -CORR1/1715 AR11/C/1396/1861 -CORR1/1872
336.0E (24.0W)	31 Dec 88	INMARSAT AOR -CENT2 INMARSAT II[21]	Inmarsat	FSS,MSS,MMSS,AMSS 1.6b,1.6c,1.6d,6b/ 1.5b,1.5c,1.5d,4a	15	AR11/A/292/1713 -ADD1/1760
336.0E (24.0W)	31 Dec 84	PROGNOZ-1[11]	USSR	SRS,EES 3/2.2	20	SPA-AA/316/1471 SPA-AJ/410/1515 AR11/C/1561/1886
337.0E (23.0W)	31 Dec 86	FLTSATCOM-B EAST ATL[23]	US	MSS 44/20f	10	AR11/A/48/1561 -ADD1/1587

TABLE 2. PLANNED GEOSTATIONARY COMMUNICATIONS SATELLITES FOR YEAR-END 1989

SUBSATELLITE LONGITUDE[1] (deg)	IN-USE DATE[2]	SATELLITE DESIGNATION[3]	COUNTRY OR ORGANIZATION	SERVICE FREQUENCY CODE UP/DOWN-LINK (GHz)	PERIOD OF VALIDITY[4] (yr)	SPECIAL SECTION NUMBERS
338.5E (21.5W)	1 Jan 92	INTELSAT K[79]	Intelsat	FSS,BSS 14a/11,12a,12c,12d, 12e,12f,12g	15	AR11/A/614/1923
340.0E (20.0W)	31 Jan 89	GDL-4 ASTRA[5]	Luxembourg–Societe Europeene des Satellites	FSS,BSS 6b,14a/11	25	AR11/A/92/1594 -ADD1/1747 -ADD2/1802 -ADD3/1841 AR11/C/610/1657 -CORR1/1744
340.0E (20.0W)	1 May 92	ACS-4[20]	US	MSS,AMSS 1.6c,1.6d/1.5c,1.5d	15	AR11/A/395/1800
341.0E (19.0W)	31 Dec 88	TDF-2	France	FSS,BSS,SRS 2,11,17/2.2,12f	10	AR11/A/216/1684 AR11/C/1346/1839
341.0E (19.0W)	31 Mar 91	SARIT[80]	Italy	FSS,BSS,SRS 2,13a,30a/2.2,20b	7	SPA-AA/371/1457 AR11/A/294/1716 AR11/C/1334/1839
341.0E (19.0W)	1986[13]	LUX-SAT[81]	Luxembourg	FSS,BSS 17,20a/12e,12f	10	AR11/A/20/1529
341.0E (19.0W)	1986[13]	SUI-19W/1[82] HELVESAT 1	Switzerland	FSS,BSS,SRS 2,20a/12e,12f	10	SPA-AA/356/1500
342.0E (18.0W)	1 Jul 90	GOMS-1M[24]	USSR	FSS,MetSat,SRS,EES 0.4b,2,2.1,8d,30a/ 0.4g,1.6f,1.6g,7b,20b	15	AR11/A/426/1822
342.2E (17.8W)	1 Sep 90	SATCOM-4	NATO	FSS,MSS 0.3a,8a,44/0.3a,7b	20	AR11/A/342/1762 AR11/C/1288/1832 -CORR1/1852
344.0E (16.0W)	1 Aug 92	ZSSRD-2[25]	USSR	FSS,SRS 14b,14f/11,12c,13c	20	AR11/A/189/1672 -CORR1/1711 AR11/C/880/1740 -CORR1/1881
344.0E (16.0W)	1 Aug 90	MILSTAR 3[7]	US	MSS,SRS 0.3a,1.7b,44/ 0.3a,2.2,20f	20	AR11/A/444/1837 AR11/C/1509/1885
345.0E (15.0W)	1 Aug 88	INMARSAT AOR-EAST INMARSAT II[21]	Inmarsat	FSS,MSS,MMSS,AMSS 1.6b,1.6c,1.6d,6b/ 1.5b,1.5c,1.5d,4a	15	AR11/A/153/1634 -ADD1/1760 AR11/C/840/1706 -ADD1/1784 -CORR1/1883
345.0E (15.0W)	1 Jun 90	FOTON-1	USSR	FSS 6b/4b	10	AR11/A/235/1692
346.0E (14.0W)	2 Jul 94	GOMS-1[24]	USSR	FSS,MetSat,SRS,EES 0.4b,2,2.1,8d,30a/ 0.4g,1.6f,1.6g,7b,20b	20	AR11/A/206/1578 -ADD1/1712 AR11/C/1273/1825 -CORR1/1894
346.0E (14.0W)	1 Sep 90	MORE-14	USSR	FSS,MMSS 1.6b,6b/1.5b,4a	15	AR11/A/183/1662 AR11/C/1086/1791 -CORR1/1883

TABLE 2. PLANNED GEOSTATIONARY COMMUNICATIONS SATELLITES FOR YEAR-END 1989

SUBSATELLITE LONGITUDE[1] (deg)	IN-USE DATE[2]	SATELLITE DESIGNATION[3]	COUNTRY OR ORGANIZATION	SERVICE FREQUENCY CODE UP/DOWN-LINK (GHz)	PERIOD OF VALIDITY[4] (yr)	SPECIAL SECTION NUMBERS
346.0E (14.0W)	1980[13]	VOLNA-2	USSR	MSS,MMSS,AMSS 1.6b,1.6c,1.6d/ 1.5b,1.5c,1.5d	10	SPA-AA/170/1286 SPA-AJ/97/1329
346.5E (13.5W)	30 Dec 82	POTOK-1[26]	USSR	FSS 4b/4a	15	SPA-AA/344/1485 AR11/C/18/1557
348.0E (12.0W)	31 Jul 84	USGCSS PH3 ATL DSCS III	US	FSS,SRS 1.7b,8a/2.2,7b	10	SPA-AA/250/1413 SPA-AA/351/1493 SPA-AJ/287/1451 AR11/C/403/1629
349.0E (11.0W)	31 Dec 87	F-SAT 2[8]	France	FSS,SRS 2,14a,30a/ 2.2,12c,12d,20b	10	AR11/A/73/1586 AR11/C/466/1647
351.0E (9.0W)	1 Jul 90	MILSTAR 2[7]	US	MSS,SRS 0.3a,1.7b,44/ 0.3a,2.2,20f	20	AR11/A/443/1837 AR11/C/1505/1885
352.0E (8.0W)	30 Sep 91	TELECOM-2A	France	FSS,SRS 2,6b,8a,14a/ 2.2,4a,7b,12c,12d	10	AR11/A/324/1745 -ADD1/1772 AR11/C/1097/1792 AR11/C/1162/1795 AR11/C/1325/1839
352.0E (8.0W)	30 Apr 92	ZENON-A	France	FSS,AMSS,SRS 1.6d,2,14a/ 1.5d,2.2,11	10	AR11/A/363/1781
355.0E (5.0W)	30 Sep 91	TELECOM-2B	France	FSS,SRS 2,6b,8a,14a/ 2.2,4a,7b,12c,12d	10	AR11/A/325/1745 -ADD1/1772 AR11/C/1100/1792 AR11/C/1164/1795 AR11/C/1328/1839
357.0E (3.0W)	31 Dec 90	TOR-11	USSR	FSS,MSS 43,44/20b,20f	20	AR11/A/308/1736 AR11/C/1408/1862

[1] Satellite longitudes are those recorded in the July 1989 release of the IFRB's *List of Geostationary Space Stations.*

[2] In-use dates are taken from the notifying administration's most recent IFRB filing and do not necessarily indicate the date of launch.

[3] IFRB satellite network names appear first, followed by common or alternate names.

[4] Period of validity refers to the number of years for which frequency assignments are to be in use.

[5] SES officials announced in January 1990 that procurement of a third Astra satellite is a "strong possibility." It would be located at either 1°E or 20°W.

[6] An X-band (Gals) payload has also been registered at this location, suggesting that the station is intended for a Raduga satellite.

[7] The Milstar satellites, originally intended for deployment in both geosynchronous and highly inclined polar orbits, are designed to combine the functions of proposed follow-on satellites for the FLTSATCOM and AFSATCOM programs. Lockheed Corporation is the prime contractor for the series.

[8] First announced in 1983, F-Sat and Videosat are each designed to provide for fixed satellite traffic between France and its overseas departments. Neither project has received much publicity in recent years and some sources suggest that they have since been superseded by the Telecom II series.

[9] Eutelsat announced in 1989 that it is considering modifying some of its second-generation satellites to operate a pan-European land mobile satellite service in the L-band.

[10] Apex is intended to transmit television and telephony signals between France and its overseas departments, as well as part of the African continent. In addition to its C- and Ka-band transponder, it will carry three beacons in the 20-, 40-, and 80-GHz frequency ranges for conducting propagation experiments.

[11] Prognoz, or "Forecast," is a remote-sensing satellite designed to study atmospheric processes and monitor the depletion of natural resources. Earlier satellites in this series collected data on solar radiation and were launched into highly eccentric orbits.

[12] In addition to its Ka-band payload for domestic telecommunications, Italsat will be equipped to carry out propagation experiments in the 40/50-GHz range. It is currently scheduled for launch in September 1990.

[13] No other date given.

[14] The Sicral network is designed to offer coverage of all Italian territories, including Italian flag ships in the Mediterranean and the North Atlantic.

[15] Saudi Arabian Broadcasting Satellite System. Intended to provide DBS and to facilitate networking among medium-wave broadcasting stations.

[16] In June 1989, SES acquired a GE 5000 satellite that was originally built for Crimson Satellite Associates, GE's failed joint venture with HBO. Renamed Astra 1B, it will be collocated with the in-orbit Astra 1A.

[17] Transmits in the earth-to-space direction in the 5.725- to 6.275-GHz frequency band.

[18] In addition to telephony and television broadcasting services, Paksat-1 and Paksat-2 will be used to collect meteorological and hydrological data.

[19] According to the British Ministry of Defense, Skynet 4C is to serve as an in-orbit spare for the system's operational satellites at 6°E and 1°W. In the event of a failure of either Skynet 4A or 4B, it would be relocated to one of the latter positions.

[20] Orbital positions at 61.5°E, 134°E, 171°E, 130°W, 100°W, 72°W, and 20°W have been designated for a U.S.-based mobile satellite system. A global AMSS network, composed of six operational satellites and an in-orbit spare, was proposed by Aeronautical Radio, Inc. (Arinc) in 1987. The so-called AvSat system would have occupied similar locations but would have utilized both C- and L-band frequencies. The FCC subsequently rejected Arinc's application, in part because it conflicted with the commission's previously announced frequency allocation plan, and in part because Arinc failed to demonstrate adequate financial backing. Some of the ACS slots have since been assigned to American Mobile Satellite Corporation (see Footnote 44).

[21] The INMARSAT II launch schedule has been revised several times, with the result that launch options originally secured with Arianespace for 1989 were never used. Current plans call for the first INMARSAT II satellite to be launched in June 1990, and the second in February 1991. Flight numbers had not been assigned at the time of publication.

[22] McCaw Space Technologies filed an application with the FCC in 1986 for an international separate satellite system consisting of two in-orbit satellite serving India, China, Southeast Asia, and the Pacific Rim. The Celestar network would provide Ku-band capacity for transpacific communications and would offer connections to the TPC-3 fiber optic cable.

[23] Possibly reserved for FLTSATCOM F-6 or F-8, which were destroyed in launch pad accidents (see Table 1, Footnote 46). These satellites were each equipped with an experimental EHF transponder and were thought to be precursors to the Milstar series.

[24] Intended to join the U.S. GOES and Japanese GMS satellites as part of the World Meteorological Organization's World Weather Watch Program, the first of the GOMS satellites was originally scheduled for deployment in the early 1980s. Introduction of the series has since been delayed several times.

[25] The Soviet SSRD system is designed to retransmit space research data by means of low earth orbit satellites known as subscribers. The latter are to be arranged in three regional networks, each served by a geostationary repeater satellite located at central (CSSRD), western (ZSSRD), and eastern (VSSRD) orbital stations.

[26] Designed to facilitate the transmission of digital data between central and peripheral earth stations, the Potok system has been registered for nearly a decade. It has yet to be officially implemented, although observers speculate that several of the recent geostationary Cosmos satellites may have functioned as experimental Potok prototypes.

[27] Insat-1D was to have been launched in July 1989, but was damaged by a crane while still on the launch pad. It has been returned to its manufacturer, Ford Aerospace, for repairs and will be rescheduled for launch in 1990.

[28] Asia Satellite Telecommunications is a joint venture company owned by Cable & Wireless, Hutchison Whampoa, and the China International Trust (CITIC). It is intended to provide domestic telecommunications, television programming distribution, and private network services for the countries of Southeast Asia, South Korea, Taiwan, and China. Current plans envision the use of one in-orbit satellite, the refurbished Westar VI, which is scheduled for launch in April 1990. AsiaSat has applied for three orbital positions—105.5°E, 116°E, and 122°E—although company officials have indicated a preference for 105.5°E.

[29] A private company formed at the behest of the Tongan government, Friendly Islands Satellite Communications has reserved 16 orbital slots over the Pacific. A company spokesman has predicted that four of these will be occupied by Tongan domestic satellites by 1993, while the remaining slots may be leased to operators of separate satellite systems such as Finansat or Pacstar.

[30] Palapa B-3 will be preceded at this location by Palapa B-2R, which was successfully launched into orbit as this table was being compiled, on April 13, 1990. Palapa B-2R was originally launched in 1984 as B-2, but failed to achieve geosynchronous orbit. It was subsequently recovered by the Space Shuttle, refurbished, and repurchased by the Indonesian government.

[31] The second-generation Aussat B satellites will carry several specialized payloads in addition to their standard Ku-band package. These include an L-band transponder for mobile satellite services, an experimental Ka-band beacon, and a retroreflector mirror for ranging experiments. Additionally, as many as eight transponders on each satellite can be reconfigured to provide coverage of New Zealand.

[32] ACSAT is intended to provide government communications services.

[33] Superbird-B, launched February 22, 1990, as this table was being compiled, was destroyed when the Ariane rocket carrying it exploded shortly after lift-off. A replacement is under construction and is tentatively scheduled for launch in late 1991.

[34] Pacific Satellite, Inc., is owned principally by PacifiCorp subsidiary TRT Telecommunications. Its proposed Pacstar system, composed of two hybrid satellites operating in the C- and Ku-bands, is intended to provide domestic services to Papua New Guinea and other island nations in the Pacific Basin. By incorporating high-power spot beams into its satellite design, PSI hopes to facilitate the use of smaller earth stations, including VSATs. In addition, the Pacstar payload will carry an L-band transponder for AMSS.

[35] Originally conceived as a global network linking banks and other financial institutions in the U.S., Europe, and Asia, the Finansat system would consist of two C-band satellites. Each would utilize spread-spectrum technology and would be accessible via VSAT. Granted a conditional authorization by the FCC, Financial Satellite Corporation has received two 1-year extensions of the time limit set for demonstrating permanent financial qualifications. In January 1990 it requested a third extension.

[36] Cancels information contained in preceding advance publication.

[37] Unassigned.

[38] Columbia Communications Corporation has received conditional authorization from the FCC to establish a separate system providing Ku-band capacity and transpacific private line services. It has yet to place a contract for a satellite at this location. In a related development in 1989, Columbia became the highest bidder for the right to lease excess C-band transponders on NASA's TDRS satellites.

[39] The Amigo satellites are intended to provide domestic DBS in the 14/12-GHz band.

[40] Originally assigned to Alascom for use by its Aurora II satellite, this location was relinquished by that operator in 1988 when Aurora II was reassigned to 139°W.

[41] The fifth and final satellite in the Leasat series, Syncom IV-5, was launched as this table was being compiled in January 1990. It is intended to serve the Pacific Ocean Region and may be earmarked to replace the aging FLTSATCOM F-1 at 177°W.

[42] Originally assigned to Hughes Communications for use by its Galaxy IV satellite, this location was relinquished by that operator in 1988 when Galaxy IV was reassigned to 99°W.

[43] This network is newly registered with the IFRB. As of year-end 1989, advance publication information was still not available.

[44] A consortium of eight U.S. companies, the American Mobile Satellite Corporation was made necessary by the FCC's decision in 1986 to license only one mobile satellite system. This decision was based on the commission's concerns that the existing spectrum allocated to MSS was insufficient and could not be equitably divided among what were then a total of 12 individual applicants.

Eight of these original applicants—Hughes Communications, McCaw Space Technologies, MTel, Mobile Satellite Corporation, North American Mobile Satellite, Satellite Mobile Telephone Company, Skylink, and Transit Communications—contributed $5 million each to finance the corporation's startup costs. AMSC's network will consist of three in-orbit satellites, the first of which is scheduled for launch in late 1993. The consortium plans to offer a variety of thin-route and mobile communications services, and the system will be operated in conjunction with Telesat Canada's MSAT program to ensure continental coverage.

[45] Alascom's follow-on satellite will be operated by GE Americom, with the latter marketing 10 of 24 transponders.

[46] In its November 1988 Domsat Order, the FCC assigned Aurora II to 137°W and GE's Satcom C-1 to 139°W. Both operators subsequently requested to exchange orbital locations and this was authorized in January 1990.

[47] The network name USASAT-17B was previously associated with the proposed GTE Spacenet 4, which has since been withdrawn. This orbital slot is now assigned to GE Americom, and a new designation is expected from the IFRB.

[48] Designated as an in-orbit spare for GE's Satcom fleet.

[49] This location was originally assigned to GTE Spacenet for use by its GStar III satellite (launched September 8, 1988), but was subsequently relinquished by that operator when GStar III was reassigned to 93°W.

[50] A proposed domestic satellite system for the provision of Ku-band services, the Comstar K program was authorized by the FCC in 1985 to occupy orbital positions at 75°W and 134°W. The operator has since relinquished these assignments.

[51] Western Union's planned Ku-band system, consisting of two in-orbit satellites, has been cancelled. The existing Westar fleet was purchased by Hughes Communications in 1988.

[52] Hughes Communications was authorized by the FCC in 1985 to construct and launch two Ku-band satellites, to be launched at 71°W and 130°W. Hughes allowed these authorizations to lapse and instead sought permission to place its satellites at 99°W and 131°W. The changes were approved by the FCC in its 1988 Domsat Order.

[53] The orbital locations 70°W, 100°W, and 130°W have been designated by the FCC for the United States Radiodetermination Satellite System. Geostar Corporation, which is currently offering its radiolocation and navigational services through the use of leased transponders on-board the in-orbit GStar III and GTE Spacenet 3R satellites, has applied for use of these slots for its proposed RDSS network. Geostar's System 3.0 dedicated satellites will broadcast a continuous timing and interrogation signal from the operator's central earth station. These signals will in turn be encoded and retransmitted by individual mobile transceivers for relay back to the earth station via each of the three operational satellites, thus allowing for an accurate position fix.

[54] National Exchange, Inc., owned primarily by the Burlington Northern Railroad, has been authorized by the FCC to operate two hybrid satellites. The Spotnet communications package incorporates multiple spot beam coverage patterns, reuse of orbital frequencies, and high e.i.r.p. ratings to maximize its compatibility with small customer-premise earth stations.

[55] One of several prospective domsat operators to apply for FCC approval in 1983, Martin Marietta Communications Systems had intended to operate a network of high-power satellites in the Ku-band for the provision of specialized business communications and private networks. It later abandoned the venture.

[56] The Expresstar system was devised in the early 1980s to provide a variety of electronic mail, facsimile, and other high-speed data communications—marketed collectively under the trade name Zapmail. The new courier services suffered from a lack of consumer interest, and in 1987 Federal Express cancelled the project.

[57] The Anik E series comprises two hybrid satellites operating in both C- and Ku-bands. It is intended to replace the in-orbit Anik C and Anik D spacecraft.

[58] The MSAT system, operating at UHF and EHF frequencies, was first proposed in 1983. It was originally designed to provide rural telephone links and land and maritime mobile communications via transportable earth stations. Later, in 1986, an L-band payload was added to incorporate AMSS. The program is being developed in cooperation with AMSC, and both companies have issued Requests for Proposals for their respective satellites. In the interim, they plan to offer initial services using space segment leased from Inmarsat, including transponders on Marisat F-1 (14.0°W), Marecs B2 (26.1°W), and INTELSAT MCS Pacific-A (180.0°E).

[59] Fifty percent of Telesat Mobile's stock is owned by its parent company, Telesat Canada. The remainder has been purchased by Canadian Pacific Ltd., Cable & Wireless, and a bloc of Japanese investors led by C. Itoh.

[60] The Association of State Telecommunication Undertakings of the Andean Sub-Regional Agreement (ASETA) is a joint body created by the nations of Bolivia, Colombia, Ecuador, Peru, and Venezuela. It is entrusted with building and operating a regional satellite system for the provision of domestic and transborder telecommunications services.

[61] The designation Condor was officially changed in 1988 to Simon Bolivar.

[62] Ford Aerospace Satellite Services Corporation (FASSC), a subsidiary of Ford Motor Company, was created in 1983 and received authorization from the FCC 2 years later to build and launch a pair of hybrid satellites. The Fordstar satellites, based on the design used for the INTELSAT V series, were to have been launched in 1987 and were intended to provide capacity for satellite newsgathering, video distribution, VSAT networks, and other specialized applications. But although Ford began construction in 1986, the project lagged behind schedule. Following speculation that FASSC had failed to generate much interest among potential end users, the division was sold to AT&T, which had expressed a desire to obtain its orbital slots.

[63] Advanced Communications Technology Satellite. Sponsored by NASA, the ACTS program is intended to develop a satellite compatible with the demands of an intelligent network. Its principal innovations will consist of on-board switching capabilities and the use of multiple spot beams in flexible "scanning" configurations.

[64] Westar VI was acquired by Hughes Communications in 1988, together with the rest of the Westar fleet. It will be added to the Hughes Galaxy network and has been renamed. Launch is tentatively scheduled for June 1990.

[65] Argentina's Nahuel network, consisting of two in-orbit satellites, is intended to provide domestic services, including DBS and low-speed data transmissions.

[66] Contel ASC-2 was constructed by RCA between 1983 and 1984 under Contel's initial order for two satellites. It had been slated to be brought into service shortly after the deployment of ASC-1, but the launch date was indefinitely postponed as a result of the Challenger disaster. In 1988, the satellite's initial assignment of 81°W was changed to 83°W. Contel appealed the decision, requesting reassignment to 99°W, but the FCC denied that petition. In 1989, Contel again requested reassignment, this time to 101°W—a slot assigned to its proposed follow-on, Contelsat-1.

[67] Since 1982, the Colombian government has intermittently discussed the possibility of establishing a domestic satellite system. Under the original Satcol proposal, it went so far as to solicit bids for three spacecraft, but never placed a contract. That project, like the more recent "Colombia" satellites which have been registered at the same orbital locations, has been postponed indefinitely. Colombia is instead cooperating with other Andean governments in the establishment of ASETA's proposed regional satellite network.

[68] Pending FCC approval, ownership of all STLC satellites, including SBS VI (tentatively scheduled for launch in 1991), will pass to Hughes Communications as a result of the latter's offer to acquire the IBM subsidiary in 1989.

[69] GE Americom, which was authorized to deploy its Satcom K-3 satellite at 67°W, relinquished this assignment in 1989. This action followed an unsuccessful attempt to secure FCC approval for modifications to both K-3 and the ground spare, K-4, so as to offer high-power services (including domestic DBS) through Crimson Associates, GE's joint venture with HBO. In denying GE Americom's petition, which was opposed by neighboring domsat operators, the FCC created a special bifurcated high-power-density arc with eastern (75°W–79°W) and western (132°W–136°W) segments.

[70] GE Americom has not pursued its predecessor RCA's plans for a Satcom C-6 and Satcom C-7. It has relinquished its assignments for these satellites.

[71] Contel has relinquished its assignment at 64°W. Its proposed ASC-3 satellite has been superseded by the follow-on Contelsat-1 and Contelsat-2.

[72] International Satellite, Inc., received conditional authorization from the FCC in 1985 to begin work on its proposed separate satellite system. It has since been granted two extensions and is seeking a third. ISI's original plans envisioned a network of two in-orbit satellites, each with spot beams covering CONUS and the major western European countries. The design is intended to facilitate the use of customer-premise earth stations for the transmission of video programming and high-speed data communica-

tions and would ensure single-hop capability between any point in the U.S. and terminals in Europe. The company is a partnership between TRT Telecommunications and other smaller investors, including Satellite Syndicated Systems and Kansas City Southern Industries.

[73] Originally assigned to PanAmSat, the orbital position 56°W has been abandoned by that operator in favor of 43°W.

[74] Orion Satellite, a subsidiary of Orion Network Systems and the first of several start-up ventures to apply for FCC authorization as a separate system, completed the Intelsat coordination process in July 1989. It has since finalized a contract for two satellites with British Aerospace, a minority shareholder. The operator intends to offer private line services, including teleconferencing, facsimile, and high-speed data communications, beginning in 1992. It has also discussed the possibility of offering leased domestic services to several West African countries. Although at one time Orion was considering a network of three satellites at 37.5°W, 47°W, and 50°W, it does not currently intend to deploy a satellite at the latter location.

[75] Originally assigned to Cygnus Satellite Corporation, an early U.S. applicant for separate system licensing, the orbital location 45°W was relinquished by that operator when it was acquired by PanAmSat in 1987. Also in the course of that acquisition, PanAmSat gained the rights to Cygnus' assignment at 43°W—the position currently proposed for its second satellite, PAS-2.

[76] The Hispasat network is based on a design incorporating multiple payloads. It will offer DBS capabilities in addition to providing long-distance telephony and television distribution services. The presence of an X-band transponder indicates future military applications as well. Although only advance publication data were available for Hispasat-1 at the time of compilation, the Hispasat system will ultimately consist of two in-orbit satellites.

[77] Atlantic Satellites Ltd., owned principally by Hughes Communications, is licensed by the Irish government to build and operate a system capable of providing DBS services to the U.K. and Western Europe. It is also considering transatlantic private line services in the fixed satellite service.

[78] INTELSAT VI F-3 was launched on March 14, 1990, as this table was being compiled, but was stranded in low earth orbit after the Martin Marietta booster rocket on which it was mounted failed to properly disengage. The satellite was not damaged, although some of its stationkeeping fuel was expended in subsequent maneuvers intended to free it from its booster and raise it to a higher orbit. Plans are being considered to retrieve it using the Space Shuttle.

[79] INTELSAT K, the organization's first all-Ku-band satellite and the first Intelsat satellite to be purchased off the shelf without design competition, was acquired from GE Astro-Space in June 1989. It was originally built as Satcom K4 and was intended for use by the now-defunct Crimson Associates. After modifications, it will be collocated at 338.5°E with INTELSAT V F-6, currently located at 341.5°E. INTELSAT K will primarily handle video and business communications and is considered a precursor to the planned INTELSAT VII series. ITU registration information was not available at the time of publication.

[80] Satellite di Radiodiffusione Italiano. A proposed DBS system for Italian programming, Sarit is expected to be modeled after Olympus 1 and will carry additional transponders for data communications.

[81] Luxembourg's first foray into the DBS market, the Luxsat project was centered around a high-power satellite capable of broadcasting into neighboring countries. It was intended to compete with France's TDF and West Germany's TV-Sat networks, but it was abandoned in 1983 in favor of the medium-power GDL system now being pursued by SES.

[82] Helvesat is the project devised by Switzerland for its own DBS system. Few details are known about the program, although it would probably be used to develop transborder broadcasting capabilities for the Swiss Broadcasting Corporation. The Swiss government solicited proposals from satellite manufacturers in 1986 for the purpose of conducting a feasibility study.

TABLE 3. FREQUENCY CODES FOR ALLOCATED BANDS, SERVICES, AND ITU REGIONS

Code	Service	Link Direction ITU Region[1]		Allocated Frequency Band (GHz)
0.1a	MSS[2]	Up[3]1, 2, 3		0.12145 – 0.12155
0.1b	AMSS (sec[4])	Up 1, 2, 3	Down 1, 2, 3	0.117975 – 0.137
0.1c	MetSat[5], SRS[6]		Down[7]1, 2, 3	0.136 – 0.138
0.1d	SRS (sec)		Down 1[8], 2, 3	0.138 – 0.1436
0.1e	SRS		Down 1, 2, 3	0.1436 – 0.14365
0.1f	SRS (sec)		Down 1[8], 2, 3	0.14365 – 0.144
0.1g	RNS[9]		Down 1, 2, 3	0.1499 – 0.15005
0.1h	SRS		Down 3[10]	0.174 – 0.184
0.2	MSS	Up[3]1, 2, 3		0.24295 – 0.24305
0.3a	MSS	Up 1, 2, 3	Down 1, 2, 3	0.235 – 0.322
0.3b	MSS	Up 1, 2, 3	Down 1, 2, 3	0.3354 – 0.3999
0.3c	RNS		Down 1, 2, 3	0.3999 – 0.40005
0.4a	MetSat, SRS		Down 1, 2, 3	0.40015 – 0.401
0.4b	MetSat (sec) EES[11] (sec)	Up 1, 2, 3		0.401 – 0.403
0.4c	LMSS, MMSS	Up 2[12]		0.4055 – 0.406
0.4d	MSS	Up[3]1, 2, 3		0.406 – 0.4061
0.4e	LMSS, MMSS	Up 2[12]		0.4061 – 0.410
0.4f	SRS	Up 1, 2, 3		0.450 – 0.460
0.4g	MetSat (sec)[13] EES (sec)		Down 1, 2, 3	0.460 – 0.470
0.4h	SRS		Down 3[10]	0.470 – 0.485
0.6	LMSS (sec) MMSS (sec)	Up 2		0.608 – 0.614
0.7	BSS (CR[14])		Down 1, 2, 3	0.620 – 0.790
0.8	LMSS[15], MMSS[15]	Up 1[16], 2, 3	Down 1[16], 2, 3	0.806 – 0.890
0.9	LMSS[15], MMSS[15]	Up 1[16], 3	Down 1[16], 3	0.942 – 0.960
1.2a	RNS		Down 1, 2, 3	1.215 – 1.260
1.2b	SRS (sec) EES (sec)	Passive 1, 2, 3		1.215 – 1.300
1.3	SRS (sec) EES (sec)	Passive 1, 2, 3		1.370 – 1.400
1.5a	EES (sec)	Passive 1, 2, 3		1.525 – 1.530
1.5b	MMSS		Down[17]1, 2, 3	1.530 – 1.544
1.5c	MSS		Down[18]1, 2, 3	1.544 – 1.545
1.5d	AMSS		Down[19]1, 2, 3	1.545 – 1.559

TABLE 3. FREQUENCY CODES FOR ALLOCATED BANDS, SERVICES, AND ITU REGIONS (CONT'D)

Code	Service	Link Direction ITU Region[1]		Allocated Frequency Band (GHz)
1.5e	RNS		Down 1, 2, 3	1.559 – 1.610
1.6a	AMSS	Up 1, 2, 3	Down 1, 2, 3	1.610 – 1.6265
1.6b	MMSS	Up 1, 2, 3		1.6265 – 1.6455
1.6c	MSS	Up[18] 1, 2, 3		1.6455 – 1.6465
1.6d	AMSS	Up[19] 1, 2, 3		1.6465 – 1.6605
1.6e	SRS	Passive 1, 2, 3		1.6605 – 1.6684
1.6f	MetSat		Down 1, 2, 3	1.670 – 1.690
1.6g	MetSat, EES		Down 1, 2, 3	1.690 – 1.710
1.7a	SRS		Down 3[20]	1.700 – 1.710
1.7b	SRS	Up 2, 3[21]		1.750 – 1.850
1.7c	MetSat	Up[22]1, 2, 3	Down[22]1, 2, 3	1.770 – 1.790
2	SRS, EES	Up 1, 2, 3	Down 1, 2, 3	2.025 – 2.110
2.1	SRS	Up 1, 2, 3		2.110 – 2.120
2.2	SRS		Down 1, 2, 3	2.200 – 2.300
2.4	Radiolocation	Passive 1, 2, 3		2.450 – 2.500
2.5a	BSS (CR)		Down 1, 2, 3	2.500 – 2.690
2.5b	FSS		Down[23] 2, 3	2.500 – 2.535
2.5c	FSS		Down[23] 2	2.535 – 2.655
2.6a	SRS (sec) EES (sec)	Passive 1, 2, 3		2.640 – 2.655
2.6b	SRS (sec)	Passive 1, 2, 3		2.655 – 2.690
2.6c	FSS	Up[23] 2, 3	Down[23] 2	2.655 – 2.690
2.6d	SRS, EES	Passive 1, 2, 3		2.690 – 2.700
3	SRS (sec) EES (sec)	Passive 1, 2, 3		3.100 – 3.400
4a	FSS		Down 1, 2, 3	3.400 – 4.200
4b	FSS		Down[24]1, 2, 3	4.500 – 4.800
4c	SRS (sec) EES (sec)	Passive 1, 2, 3		4.950 – 4.990
4d	SRS (sec)	Passive 1, 2, 3		4.990 – 5.000
5a	AMSS	Up 1, 2, 3	Down 1, 2, 3	5.000 – 5.250
5b	SRS (sec) EES (sec)	Passive 1, 2, 3		5.250 – 5.350
6a	FSS	Up 1		5.725 – 5.850
6b	FSS	Up[24]1, 2, 3		5.850 – 7.075
7a	SRS	Up 1, 2, 3		7.145 – 7.235

TABLE 3. FREQUENCY CODES FOR ALLOCATED BANDS, SERVICES, AND ITU REGIONS (CONT'D)

CODE	SERVICE	LINK DIRECTION ITU REGION[1]	ALLOCATED FREQUENCY BAND (GHz)
7b	FSS	Down 1, 2, 3	7.250 – 7.750
7c	MSS	Down 1, 2, 3	7.250 – 7.375
8a	FSS	Up 1, 2, 3	7.900 – 8.400
8b	MSS	Up 1, 2, 3	7.900 – 8.025
8c	EES (sec)[25]	Down 1, 2, 3	8.025 – 8.400
8d	MetSat	Up 1, 2, 3	8.175 – 8.215
8e	SRS[26]	Down 1, 2, 3	8.400 – 8.500
8f	SRS (sec) EES (sec)	Passive 1, 2, 3	8.550 – 8.650
9a	SRS (sec) EES (sec)	Passive 1, 2, 3	9.500 – 9.800
9b	MetSat (sec)	Down 1, 2, 3	9.975 – 10.025
10	SRS, EES	Passive 1, 2, 3	10.600 – 10.700
11	FSS	Up[24] 1[27] Down[24] 1[27], 2, 3	10.700 – 11.700
12a	FSS	Down 2[28]	11.700 – 12.300
12b	FSS	Down 3[29]	12.200 – 12.500
12c	FSS	Up 1 Down 1, 3	12.500 – 12.700
12d	FSS	Up 1, 2 Down 1, 3	12.700 – 12.750
12e	BSS	Down 1, 2[28,30] 3	11.700 – 12.200
12f	BSS	Down 1, 2[28]	12.200 – 12.500
12g	BSS	Down 2[28], 3[31]	12.500 – 12.700
12h	BSS	Down 3[31]	12.700 – 12.750
13a	FSS	Up[24] 1, 2, 3	12.750 – 13.250
13b	SRS (sec)	Up 1, 2, 3	13.250 – 13.400
13c	SRS (sec) EES (sec)	Passive 1, 2, 3	13.400 – 14.000
14a	FSS	Up[32] 1, 2, 3	14.000 – 14.500
14b	FSS	Up[32] 1, 2, 3	14.500 – 14.800
14c	LMSS (sec)	Up 1, 2, 3	14.000 – 14.500
14d	RNS (sec)	Down 1, 2, 3	14.300 – 14.400
14e	SRS (sec)	Down 1, 2, 3	14.400 – 14.470
14f	SRS (sec)	Passive 1, 2, 3	14.800 – 15.350
15a	EES (sec)	Passive 1, 2, 3	15.200 – 15.350
15b	SRS, EES	Passive 1, 2, 3	15.350 – 15.400
15c	AMSS	Up 1, 2, 3 Down 1, 2, 3	15.400 – 15.700
17	FSS	Up[33] 1, 2, 3	17.300 – 17.700

TABLE 3. FREQUENCY CODES FOR ALLOCATED BANDS, SERVICES, AND ITU REGIONS (CONT'D)

CODE	SERVICE	LINK DIRECTION ITU REGION[1]	ALLOCATED FREQUENCY BAND (GHz)
20a	FSS	Up[33] 1, 2, 3 Down 1, 2, 3	17.700 – 18.100
20b	FSS	Down 1, 2, 3	18.100 – 21.200
20c	MetSat	Down 1, 2, 3	18.100 – 18.300
20d	SRS (sec)[34] EES (sec)[34]	Passive 1, 2, 3	18.600 – 18.800
20e	MSS (sec)	Down 1, 2, 3	19.700 – 20.200
20f	MSS	Down 1, 2, 3	20.200 – 21.200
21	SRS, EES	Passive 1, 2, 3	21.200 – 21.400
22	SRS, EES	Passive 1, 2, 3	22.210 – 22.500
23	BSS	Down 2, 3	22.500 – 23.000
24	SRS, EES	Passive 1, 2, 3	23.600 – 24.000
27	FSS	Up 2, 3	27.000 – 27.500
30a	FSS	Up 1, 2, 3	27.500 – 31.000
30b	MSS (sec)	Up 1, 2, 3	29.500 – 30.000
30c	MSS	Up 1, 2, 3	30.000 – 31.000
31	SRS, EES	Passive 1, 2, 3	31.300 – 31.800
33	FSS	Down 3[35]	31.800 – 33.800
36	SRS, EES	Passive 1, 2, 3	36.000 – 37.000
37	FSS	Up 3[35]	37.000 – 39.000
39	FSS	Down 1, 2, 3	37.500 – 40.500
40	MSS	Down 1, 2, 3	39.500 – 40.500
42	BSS	Down 1, 2, 3	40.500 – 42.500
43	FSS	Up 1, 2, 3	42.500 – 43.500
44	MSS, RNS	Up 1, 2, 3 Down 1, 2, 3	43.500 – 47.000
48	FSS	Up 1, 2, 3	47.200 – 50.200
50a	SRS, EES	Passive 1, 2, 3	50.200 – 50.400
50b	FSS	Up 1, 2, 3	50.400 – 51.400
50c	MSS (sec)	Up 1, 2, 3	50.400 – 51.400
58	SRS, EES	Passive 1, 2, 3	51.400 – 59.000
65	SRS, EES	Passive 1, 2, 3	64.000 – 66.000
66	MSS, RNS	Up 1, 2, 3 Down 1, 2, 3	66.000 – 71.000
72a	MSS	Up 1, 2, 3	71.000 – 74.000
72b	FSS	Up 1, 2, 3	71.000 – 75.500
82a	FSS	Down 1, 2, 3	81.000 – 84.000
82b	MSS	Down 1, 2, 3	81.000 – 84.000
84	BSS	Down 1, 2, 3	84.000 – 86.000

[1] Numbers placed after the link direction refer to the ITU Regions for which the allocation applies.
[2] In all cases, MSS includes LMSS, MMSS, and AMSS.
[3] For emissions of emergency position—indicating radiobeacons only. See footnote 592 in the ITU *Table of Frequency Allocations.* (All footnotes cited hereafter refer to this publication.)
[4] sec = secondary allocation.
[5] Meteorological Satellite Service.
[6] Space Research Service.
[7] The band 0.136–0.137 was allocated to the Meteorological Satellite Service and the Space Research Service on a primary basis only until January 1, 1990. After that date it is allocated to those services on a secondary basis (fn. 595).
[8] In Region 1, the bands 0.138–0.1436 and 0.14365–0.144 are allocated to the Space Research Service on a secondary basis only in the following countries: West Germany, Austria, Belgium, France, Israel, Italy,Liechtenstein, Luxembourg, the U.K., Sweden, Switzerland, and Czechoslovakia (fn. 600).
[9] Radionavigation Satellite Service.
[10] China only (fns. 619 and 673).
[11] Earth Exploration Satellite Service.
[12] Canada only (fn. 648).
[13] Allocation to the Meteorological Satellite Service is on a primary basis in the following countries: Afghanistan, Bulgaria, China, Cuba, Hungary, Japan, Mongolia, Poland, Czechoslovakia, and the USSR (fn. 672).
[14] CR = community reception, TV only (fns. 693 and 757).
[15] Use of these services in the designated bands is limited to operation within national boundaries (fns. 699, 700, and 701).
[16] Norway and Sweden only (fn. 699).
[17] The allocation to the Maritime Mobile Satellite Service in the band 1.530–1.535 became effective January 1, 1990 (fn. 726).
[18] Use of this service in the designated band is limited to distress and safety operations (fn. 728).
[19] Transmissions in the bands 1.545–1.559 and 1.6465–1.6605 from terrestrial aeronautical stations directly to aircraft stations are also authorized when such transmissions are used to extend or supplement the satellite-to-aircraft links (fn. 729).
[20] India, Indonesia, Japan, and Thailand only (fn. 743).
[21] Afghanistan, Australia, India, Indonesia, Japan, and Thailand only (fn. 745).
[22] Bulgaria, Cuba, Hungary, Mali, Mongolia, Poland, East Germany, Roumania, Czechoslovakia, and the USSR only (fn. 746).
[23] Use of this service in the designated bands is limited to national and regional systems (fn. 761).
[24] Use of this band is subject, in whole or in part, to the provisions and associated plan of national allotments as adopted by the Second Session of the World Administrative Radio Conference on the "Use of the Geostationary Satellite Orbit and the Planning of Space Services Utilizing It."

[25] Allocation to the Earth Exploration Satellite Service is on a primary basis in Region 2 and in the following countries: Bangladesh, Benin, Cameroon, China, the Central African Republic, the Ivory Coast, Egypt, France, Guinea, Upper Volta, India, Iran, Israel, Italy, Japan, Kenya, Libya, Mali, Niger, Pakistan, Senegal, Somalia, Sudan, Sweden, Tanzania, Zaire, and Zambia (fn. 815).
[26] Allocation to the Space Research Service is on a secondary basis in the following countries: Belgium, Israel, Luxembourg, Malaysia, Singapore, and Sri Lanka (fn. 817).
[27] Use of this service in Region 1 is limited to feeder links for the Broadcasting Satellite Service (fn. 835).
[28] Use of this service in the designated bands in Region 2 is limited to national and subregional systems (fn. 839).
[29] Use of this service in the designated bands in Region 3 is limited to national and subregional systems (fn. 845).
[30] In Region 2, transponders on satellites in the Fixed Satellite Service in the band 11.7–12.1 may also be used for transmissions in the Broadcasting Satellite Service. Such transmissions are limited to a maximum e.i.r.p. of 53 dBW per television channel (fn. 836).
[31] Use of this service in the designated bands in Region 3 is limited to community reception (fn. 847).
[32] For countries outside of Europe and for Malta, the band 14.5–14.8 is reserved solely for feeder links for the Broadcasting Satellite Service. Similarly, the band 14–14.5 may also be used for this purpose, subject to coordination with other networks in the Fixed Satellite Service (fns. 858 and 863).
[33] Use of the band 17.3–18.1 is limited to feeder links for the Broadcasting Satellite Service (fn. 869).
[34] Allocation to the Space Research Service and the Earth Exploration Satellite Service is on a primary basis in Region 2.
[35] Japan only (fns. 892 and 899).

operación de un conmutador delantero/trasero. Las memorias intermedias basculantes proporcionan la separación de las distintas velocidades para cada corriente de datos entrantes, y los bitios de justificación compensan las variaciones debidas al corrimiento Doppler y la variación del oscilador local. Las corrientes del multiplejador por distribución en el tiempo (TDM) consisten en una palabra única de sincronización para sincronizar las tramas, y las palabras de control asociadas a cada ráfaga de datos para identificar la presencia o ausencia de un bitio de justificación. Se describen trayectos de datos redundantes para las corrientes de datos de ida y de retorno.

Pruebas de laboratorio y ensayos de campo transatlánticos con un modem COPSK de 140 Mbitios/s

D. H. LAYER, J. M. KAPPES Y C. B. COTNER

Abstracto

Se presentan los resultados de las pruebas de laboratorio y los ensayos de campo transatlánticos realizados con un módem de modulación por desplazamiento de fase octal (COPSK) codificada a una velocidad de información de 140 Mbitios/s. Las pruebas en el laboratorio incluyeron el rendimiento de la tasa de errores en los bitios (BER) del módem como una función del nivel de la frecuencia intermedia (IF) de recepción y de las variaciones en la frecuencia, introduciéndose una pendiente lineal de IF, retardo de grupo parabólico y distorsión de amplitud lineal. Estas pruebas se hicieron por medio de canales adosados y no lineales (simulador de satélite). Bajo condiciones nominales, el sistema COPSK de 140 Mbitios/s proporcionó una BER de 1×10^{-6} a una relación E_b/N_o más baja de lo que se requeriría de un módem con modulación por desplazamiento de fase cuadrivalente (QPSK) no codificada de 120 Mbitios/s. Los resultados de las pruebas de laboratorio también demostraron que este sistema es más sensible a las distorsiones del canal que la QPSK no codificada de 120 Mbitios/s; sin embargo, el funcionamiento mejora considerablemente cuando se utiliza un igualador transversal.

Los ensayos de campo se realizaron entre estaciones terrenas tipo A de INTELSAT situadas en Francia, los Estados Unidos y el Reino Unido, utilizando transpondedores de haz de zona de un satélite INTELSAT V-A ubicado a 332,5° de longitud este. Se describe el método empleado para acondicionar las estaciones terrenas y establecer los puntos de funcionamiento óptimo de sus amplificadores de alta potencia y los transpondedores del satélite, y se presentan los resultados de esa labor. Se comparan las mediciones de la BER con el rendimiento previsto, y los resultados demuestran un funcionamiento acorde con las actuales recomendaciones del CCIR. Estas pruebas son de notable importancia histórica, pues representan la primera transmisión digital transoceánica jamás realizada a una velocidad de información de 140 Mbitios/s por cualquier medio.

Author Index, CTR 1989

The following is a cross-referenced index of articles that appeared in the *COMSAT Technical Review* in 1989. The code number at the end of each entry is to be used for ordering reprints from: Corporate Records, COMSAT Corporation, 22300 Comsat Drive, Clarksburg, MD 20871-9475.

Index of 1989 Publications by COMSAT Authors

The following is a cross-referenced list of 1989 publications by authors at COMSAT Corporation. Copies may be obtained by contacting the COMSAT authors at: COMSAT Corporation, 22300 Comsat Drive, Clarksburg, MD 20871-9475.

*INTELSAT author.

CHITRE, D. M., "Network Architectures for Satellite ISDN," 8th International Conference on Digital Satellite Communications, Guadeloupe (ICDSC8), FWI, April 1989, *Proc.*, pp. 721–727.

CHITRE, D. M., and R. Kohli, "Performance Modeling and Analysis of VSAT Networks," 8th International Conference on Digital Satellite Communications (ICDSC8), Guadeloupe, FWI, April 1989, *Proc.*, pp. 215–221.

CLINE, P., see Geller, B.

CORNFELD, A. B., see Hegazi, G.; Metze, G. M. (two papers)

COTNER, C., and W. Carver, "Bringing INTELSAT Down to Earth for Military Users of the 1990s," 4th Annual Pacific International Defense Electronics Conference and Exposition, Honolulu, HI, December 1989, *Proc.*, Paper No. 11.

COTNER, C. B., see Russo, A. A.

CROCKETT, B., "The Changing Role of Satellites in Telecommunications," *Telecommunications Magazine*, Vol. 23, No. 6, June 1989, pp. 37–46.

CROCKETT, B. L., and S. S. Skjei, "Comparative Economics of Advanced Satellites and Cables," 8th International Conference on Digital Satellite Communications (ICDSC8), Guadeloupe, FWI, April 1989, *Proc.*, pp. 435–438.

DAHROOGE, G., see Metze, G. M. (two papers)

DAS, A. K.,* A. Mukhopadhyay,* A. Paul,* and D. K. Paul, "Optimum Fusion Splicing Condition of Optical Fibers," Conference on Fiber Optics Reliability: Benign and Adverse Environments III, Boston, MA, September 1988, *Proc. SPIE*, Vol. 1174, pp. 358–368, D. K. Paul and R. A. Greenwell, eds.

DIMOLITSAS, S., "An Adaptive IIR Filter Based on the Hurwitz Stability Properties and a Chebychev System Function Approximation," *Signal Processing*, Vol. 17, No. 1, May 1989, pp. 39–50.

DIMOLITSAS, S., "Objective Speech Distortion Measures and Their Relevance to Speech Quality Assessment," *Proc. IEE*, Part I: Communications, Speech and Vision, Vol. 136, No. 5, October 1989, pp. 317–324.

DUNLOP, J., see Earl, M.

EARL, M., J. Dunlop, R. Beauchamp,* and J. Sindorf,* "Design and Development of an Aerospace CPV Ni/H_2 Battery," 24th Intersociety Energy Conversion Engineering Conference, Washington, DC, August 1989, *Proc.*, Vol. 3, Electrochemical Storage and Conversion, pp. 1395–1400.

EVANS, J. V., and C. E. Mahle, "Research Into Advanced Satellite Technology at COMSAT Laboratories," 8th International Conference on Digital Satellite Communications (ICDSC8), Guadeloupe, FWI, April 1989, *Proc.*, pp. 593–600.

FARIS, F., see Pontano, B. A.

GELLER, B., F. Assal, R. Gupta, and P. Cline, "A Technique for the Maintenance of FET Power Amplifier Efficiency Under Backoff," IEEE MTT-S International Microwave Symposium, Long Beach, CA, June 1989, *Digest*, pp. 949–952.

*Non-COMSAT author.

GOURLEY, S., S. Siddiqi, J. Potukuchi, F. Assal, R. Gupta, and R. Mott, "An Ultra-Broadband Linear Phase Shift Module for Phased-Array Applications," SBMO International Microwave Symposium, Brazil, July 1989, *Proc.*, pp. 53–58.

GREENWELL, R. A.,* and D. K. Paul, eds., *Proc. SPIE*, Vol. 1174, Conference on Fiber Optics Reliability: Benign and Adverse Environments III, Boston, MA, September 1988.

GUPTA, R., see Geller, B.; Gourley, S.; Nakamura, A. M.

HEGAZI, G., H-L. A. Hung, J. L. Singer, F. R. Phelleps, A. B. Cornfeld, T. Smith, J. F. Bass, H. E. Carlson, and H. C. Huang, "GaAs Molecular Beam Epitaxy Monolithic Power Amplifiers at U-Band," IEEE Microwave and Millimeter-Wave Monolithic Circuits Symposium, Long Beach, CA, June 1989, *Digest*, pp. 209–213.

HEMMATI, F., "Closest Coset Decoding of | u | u + v | Codes," *IEEE Transactions on Selected Areas in Communications*, Vol. 7, No. 6, August 1989, pp. 982–988.

HUANG, H. C., see Hegazi, G.; Hung, H-L. A. (two papers); Peterson, K. E.

HULLEY, M., and J. Stevenson,** "Multiple-Stress Testing in the Screening of Space TWTAs," ESA/ESTEC International Workshop on Requirements for Space TWTAs in the 1990s, Noordwijk, The Netherlands, May 1989, *Proc.*, pp. 295–302.

HUNG, H-L. A., T. T. Lee, P. Polak-Dingels,* E. Chauchard,* K. Webb,* C. H. Lee,* and H. C. Huang, "Characterization of GaAs Monolithic Integrated Circuits by Optical Techniques," SPIE Symposium on Optical Applications of Microwaves, *Proc.*, Vol. 1102, March 1989, pp. 98–106.

HUNG, H-L. A., P. Polak-Dingels,* K. J. Webb,* T. Smith, H. C. Huang, C. H. Lee,* "Millimeter-Wave Monolithic Integrated Circuit Characterization by a Picosecond Optoelectronic Technique," *IEEE Transactions on Microwave Theory and Techniques*, Vol. 37, No. 8, August 1989, pp. 1223–1231.

HUNG, H-L. A., see Hegazi, G.; Metze, G. M. (two papers); Peterson, K. E.; Webb, K. J.

KING, C., see Lunsford, J.

KIRKENDALL, T., see Metze, G. M.

KLOPER, D., see Agarwal, A.

KNIGHT, I. N., "Satellite Compatible ISDN—An Experiment in Global Customer Assessment of Voice and Packet Switched Data Services," 8th International Conference on Digital Satellite Communications (ICDSC8), Guadeloupe, FWI, April 1989, *Proc.*, pp. 863–866.

KOHLI, R., see Chitre, D. M.

KROLL, R. T., see Zaghloul, A. I.

LEE, T. T., see Hung, H-L. A.; Metze, G. M. (two papers)

LEE, Y. S., "Utility Analysis of Fiber Optic Networks in Milsatcom Architecture," IEEE Military Communications Conference (MILCOM 89), Boston, MA, October 1989, *Conf. Rec.*, Vol. 1, pp. 251–257.

*Non-COMSAT author.
**INTELSAT author.

LIN, K. T., see Rogers, D. V.

LUNSFORD, J.,* P. Roach,** T. Mizuike,* C. King, and P. Trusty, "Network Configuration and Control Selection in the INTELSAT Satellite Switched TDMA System," 8th International Conference on Digital Satellite Communications (ICDSC8), Guadeloupe, FWI, April 1989, *Proc.*, pp. 59–66.

MAHLE, C. E., see Evans, J. V.

MAURER, R. H.,* G. A. Herbert,* J. D. Kinnison,* and A. Meulenberg, "Gallium Arsenide Solar Cell Radiation Damage Study," *IEEE Transactions on Nuclear Science*, Vol. 36, No. 6, December 1989, pp. 2083–2091.

METZE, G. M., A. Cornfeld, E. Carlson, G. Dahrooge, E. Chang, J. Singer, J. Bass, H-L. Hung, and T. Lee, "60-GHz Pseudomorphic-MODFET Low-Noise MMIC Amplifiers," *IEEE Electron Device Letters*, Vol. EDL-10, No. 4, April 1989, pp. 165–167.

METZE, G., A. Cornfeld, J. Singer, H. Carlson, E. Chang, T. Kirkendall, G. Dahrooge, J. Bass, H-L. Hung, and T. Lee, "Monolithic V-Band Pseudomorphic-MODFET Low-Noise Amplifiers," IEEE Microwave and Millimeter-Wave Monolithic Circuits Symposium, Long Beach, CA, June 1989, *Digest*, pp. 199–204.

MEULENBERG, A., see Maurer, R. H.

MOTT, R. C., see Gourley, S.; Zaghloul, A. I.

NAKAMURA, A. M.,* R. K. Gupta, F. T. Assal, J. N. Narayanan, and L. A. Argyle,* "Integration and Testing of the Satellite Switched TDMA (SS-TDMA) Subsystem for the INTELSAT-VI Spacecraft," 8th International Conference on Digital Satellite Communications (ICDSC8), Guadeloupe, FWI, April 1989, *Proc.*, pp. 49–57.

NARAYANAN, J. N., see Nakamura, A. M.

NEIBERT, M. T., "International Packet Switched Connection Performance Measurements," IEEE International Conference on Communications, Boston, MA, June 1989, *Conf. Rec.*, Vol. 1, pp. 3.6.1–3.6.3.

NOBLE, T. F., see Peterson, K. E.

OSPINA, S., "Project CONDOR, The Andean Regional Satellite System: When Will This Bird Fly?" Pacific Telecommunications Council (PTC89), Honolulu, HI, January 1989, *Proc.*, pp. 117–126.

OSPINA, S., "Regional Satellite Systems: Legal and Economic Implications," Satellite 8 Conference, Washington, DC, April 1989, *Proc.*

OSPINA, S., "Whither Project CONDOR?" *Via Satellite*, Vol. 4, No. 6, July 1989, pp. 34–36.

OSPINA, S., "Project CONDOR, The Andean Regional Satellite System: Key Legal Considerations," *Space Communication and Broadcasting*, Vol. 6, Elsevier, North Holland, 1989, pp. 367–377.

OSPINA, S., "Third World Countries' Challenges and Contributions to Space Law," 31st Colloquium on the Law of Outer Space, International Institute of Space Law, Bangalore, India, *Proc.*, pp. 135–142. Published by AIAA, 1989.

*Non-COMSAT author.
**INTELSAT author.

PALMER, L. C., "A Perspective on Satellite On-Board Processing," U. S. Army Communications Electronics Command Symposium on Space—Supporting the Soldier, Asbury Park, NJ, June 1989, *Proc.*, pp. III-48–III-53.

PALMER, L. C., and L. W. White, "An Evaluation of Two Error Detection Codes Used With a Particular Convolutional Coder/ML Decoder," 8th International Conference on Digital Satellite Communications (ICDSC8), Guadeloupe, FWI, April 1989, *Proc.*, pp. 241–248.

PAUL, D. K., see Das, A. K.; Greenwell, R. A.; Pontano, B. A.

PETERSON, K. E., H-L. A. Hung, F. R. Phelleps, T. F. Noble, and H. C. Huang, "Monolithic High-Voltage FET Power Amplifiers," IEEE MTT-S International Microwave Symposium, Long Beach, CA, June 1989, *Digest*, pp. 945–948.

PHELLEPS, F. R., see Hegazi, G.; Peterson, K. E.

PONTANO, B. A., L. White, F. Faris, and D. K. Paul, "Cost-Effective Satellite Systems for International Communications," 8th International Conference on Digital Satellite Communications (ICDSC8), Guadeloupe, FWI, April 1989, *Proc.*, pp. 427–434.

POTUKUCHI, J. R., see Gourley, S.; Zaghloul, A. I.

RHODES, S. A., and S. I. Sayegh, "Digital On-Board Demodulator for Reception of an Up-Link Group of TDMA/QPSK Channels," 8th International Conference on Digital Satellite Communications (ICDSC8), Guadeloupe, FWI, April 1989, *Proc.*, pp. 845–852.

RIESER, J. H., see Campanella, S. J.

ROGERS, D. V., C. Zaks, and K. T. Lin, "Up-Link Power Control Experiments at 14/11 GHz," 6th International Conference on Antennas and Propagation, University of Warwick, Coventry, U. K., April 1989, *IEE Conference Publication No. 301*, Pt. 2, pp. 206–210.

ROGERS, D. V., see Allnutt, J. E.

RUSSO, A. A., and C. B. Cotner, "Analysis of Measured Performance of a 2.048 Mbps International Digital Route (IDR) Carrier," 8th International Conference on Digital Satellite Communications (ICDSC8), Guadeloupe, FWI, April 1989, *Proc.*, pp. 777–783.

SANDRIN, W. A., and L. N. Nguyen,* "Computing the Performance of Digital Satellite Links on a System-Wide Basis," 8th International Conference on Digital Satellite Communications (ICDSC8), Guadeloupe, FWI, April 1989, *Proc.*, pp. 747–754.

SAYEGH, S. I., see Rhodes, S. A.

SEN, A., "INAM—An Expert System for Intelligent Network-Alarm Management," 8th International Conference on Digital Satellite Communications (ICDSC8), Guadeloupe, FWI, April 1989, *Proc.*, pp. 509–519.

SIDDIQI, S., see Gourley, S.

SINGER, J. L., see Hegazi, G.; Metze, G. M. (two papers)

*INTELSAT author.

SKJEI, S. S., see Crockett, B. L.

SMITH, T., see Hegazi, G.; Hung, H-L. A.; Webb, K. J.

SORBELLO, R. M., and A. I. Zaghloul, "Wideband, High-Efficiency, Circularly Polarized Slot Elements," IEEE International Symposium on Antennas and Propagation, San Jose, California, June 1989, *Proc.*, pp. 1473–1476.

TRUSTY, P., see Lunsford, J.

TZENG, F., "Near-Toll-Quality Real-Time Speech Coding at 4.8 kbit/s for Mobile Satellite Communications," 8th International Conference on Digital Satellite Communications (ICDSC8), Guadeloupe, FWI, April 1989, *Proc.*, pp. 93–98.

TZENG, F., "Performance Improvement and Complexity Reduction for a High-Quality 4.8-kbps Speech Coder" (Abstract), IEEE Workshop on Speech Coding for Telecommunications, Vancouver, British Columbia, September 1989, *Program and Abstracts*, p. 5.

TZENG, F., "Analysis-by-Synthesis Linear Predictive Speech Coding at 2.4 kbit/s," IEEE Global Telecommunications Conference, Dallas, TX, November 1989, *Proc.*, pp. 34.4.1–34.4.5.

VAIDYANATHAN, H., "Effect of Design Variables on the Cycling Characteristics of $Ni\text{-}H_2$ Cells," 24th Intersociety Energy Conversion Engineering Conference, Washington, DC, August 1989, *Proc.*, pp. 1405–1409.

WEBB, K. J.,* E. P. Chauchard,* P. Polak-Dingels,* C. H. Lee,* H-L. Hung, and T. Smith, "A Time-Domain Network Analyzer Which Uses Optoelectronic Techniques," IEEE MTT-S International Microwave Symposium, Long Beach, CA, June 1989, *Digest*, pp. 217–220.

WHITE, L. W., see Palmer, L. C.; Pontano, B. A.

WILLIAMS, A. E., see Bonetti, R. R. (two papers).

ZAGHLOUL, A. I., J. R. Potukuchi, R. C. Mott, and R. T. Kroll, "Analysis and Measurement of Tolerances in MMIC Active Phased Arrays," 19th European Microwave Conference, London, September 1989, *Digest*, pp. 966–971.

ZAGHLOUL, A. I., see Sorbello, R. M.

ZAKI, K. A., see Chen, S.

ZAKS, C., see Rogers, D. V.

---

*Non-COMSAT author.